

University Library

Author/Filing Title .....TED, HUE.....

Class Mark .....T.....

Please note that fines are charged on ALL  
overdue items.

FOR REFERENCE ONLY

0403177111



**RECOVERY OF DILUTE ACETIC ACID  
THROUGH ESTERIFICATION  
IN A  
REACTIVE DISTILLATION COLUMN**

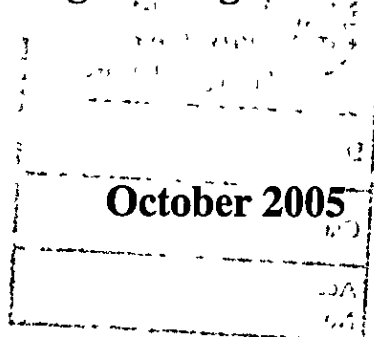
**By**

**Hue Tat Ronnie Teo**


**A Doctoral Thesis**

**Submitted in partial fulfilment of the requirements for the award of**

**Doctor of Philosophy  
of  
Loughborough University**



**© Hue Tat Ronnie Teo, 2005**

 <b>Loughborough University</b> Pilkington Library
Date JAN 2006
Class T
Acc No. 0403177111

*to my family...  
especially to my Dad and Mum for their fantastic support and encouragement  
throughout my studies*

## ACKNOWLEDGEMENTS

I wish to express my sincerest gratitude to my supervisor, Dr. Basu Saha, for his invaluable guidance, time and encouragement over the years of this research.

I would also like to thank EPSRC for the financial backing towards this project. Acknowledgement is also extended to Dr. Jim Dale of Purolite for kindly supplying the catalysts and to the Department of Pure and Applied Chemistry of the University of Strathclyde for the elemental analysis measurements.

I would also like to extend my thanks to the following people:

- Chris Manning and Dr. Paul Russell for their assistance towards the development of the reactive distillation column.
- The technical staff of the Chemical Engineering Department (Tony Eyre, Dave Smith, Andy Milne, Terry Neale, Sean Creedon, Graham Moody, Kim Winfer and Dave Barker) for rendering their assistance.
- The administrative staff of the Chemical Engineering Department (Anne Cage, Anna Temple, Yasmin Kosar and Janey Briers) for catering to all administrative needs.
- Paul Izzard for IT support.
- All my friends for extending their unconditional friendship and support.

## ABSTRACT

With ever-growing environmental concerns, petrochemical and fine chemical industries face an omnipresent issue in recovering acetic acid from its aqueous solutions. The recovery of acetic acid through the esterification process is a very viable option. However, esterification reactions are typically restricted by equilibrium limitations, and face challenges with product purification. Reactive distillation is an emerging technology that has an extremely attractive potential as a process alternative for carrying out equilibrium limited chemical reactions. Although the reactive distillation process has been successfully commercialised for the manufacture of high commodity chemicals e.g. methyl tertiary butyl ether (MTBE) and methyl acetate, its potential as a separation tool for the recovery of acetic acid using *iso*-amyl alcohol has not been exploited.

The physical and chemical characterisation of different ion exchange resin catalysts in the form of scanning electron microscopy, Brunauer-Emmett-Teller (BET) surface area measurement, pore size distribution, elemental analysis and particle size distribution were carried out to assess the catalysts' performance for the esterification reaction. In the investigation of the kinetics of esterification reactions of acetic acid with *iso*-amyl alcohol to produce a value added ester in the form of *iso*-amyl acetate, the effects of various parameters including speed of agitation, catalyst particle size, reaction temperature, catalyst loading, feed mole ratio, acetic acid concentration, catalyst reusability and catalyst type were studied to optimise the reaction conditions under batch conditions. The non-ideality of each species in the reacting mixture was accounted for by using the activity coefficient via the use of the UNIFAC group contribution method. The kinetic data were correlated with different kinetic models which are the Langmuir-Hinshelwood-Hougen-Watson (LHHW), Eley-Rideal (E-R), Quasi-Homogeneous (Q-H) and Modified LHHW (M-L) kinetic models. The LHHW model gave the best representation of the kinetic data.

The feasibility of reactive distillation for the recovery of acetic acid using *iso*-amyl alcohol was evaluated through a systematic procedure of residue curve map (RCM). RCM provides information to a design engineer of the existence of separation boundaries imposed by the singular points corresponding to the reactive/non-reactive azeotropes, and thereby provides an insight into the feasibility of reactive distillation for this purpose.

A laboratory scale packed reactive distillation column (RDC) was designed and constructed. The experiments were subsequently conducted with the objective of achieving optimum process conditions and column configurations for the recovery of acetic acid and synthesis of *iso*-amyl acetate in an RDC through the variation of the RDC set-up including feed mole ratio, reflux ratio, location of feed points, reflux configuration and acetic acid concentrations.

**Keywords:** Acetic acid recovery, esterification, reactive distillation, ion exchange resins, *iso*-amyl acetate, kinetic modelling, residue curve map.

# TABLE OF CONTENTS

<b>1.</b>	<b>INTRODUCTION</b>	<b>1</b>
1.1	GENERAL INTRODUCTION	1
1.2	RESEARCH OBJECTIVES	11
<b>2.</b>	<b>LITERATURE REVIEW</b>	<b>13</b>
2.1	INTRODUCTION	13
2.2	APPLICATIONS OF REACTIVE DISTILLATION	13
	2.2.1 Etherification: MTBE, ETBE, TAME and other processes	14
	2.2.2 Esterification: methyl acetate and other esters	16
	2.2.3 Recovery and purification of chemicals	21
	2.2.4 Hydrogenation/hydrodesulfurisation/hydrocracking/dehydrogenation	22
	2.2.5 Other processes	23
2.3	ADVANTAGES AND DISADVANTAGES OF REACTIVE DISTILLATION	32
	2.3.1 Advantages of reactive distillation	32
	2.3.2 Disadvantages of reactive distillation	36
2.4	CATALYSIS	37
	2.4.1 Catalysis by ion exchange resins	40
	2.4.2 Commercial applications of ion exchange resins as catalysts	46
	2.4.3 Advantages and disadvantages of ion-exchange resins as catalysts	47
2.5	KINETIC RATE EXPRESSIONS	51
<b>3.</b>	<b>CATALYST CHARACTERISATION AND BATCH KINETIC STUDIES</b>	<b>55</b>
3.1	INTRODUCTION	55
3.2	EXPERIMENTAL	55
	3.2.1 Materials	55
	3.2.1.1 Chemicals	55
	3.2.1.2 Catalysts	56

3.2.1.2.1	Catalyst characterisation	57
3.2.1.2.1.1	Scanning electron microscopy	57
3.2.1.2.1.2	Surface area, pore volume and pore size distribution	61
3.2.1.2.1.3	Elemental analysis	66
3.2.1.2.1.4	Particle size distribution	67
3.2.1.2.1.5	True density	69
3.2.2	Method of analysis	
3.2.2.1	Calibration curves	70
3.2.2.2	Internal standardisation	75
3.2.3	Experimental set-up and procedure for batch kinetic studies	77
3.3	MECHANISM OF REACTION	78
3.4	RESULTS AND DISCUSSION OF BATCH KINETIC STUDIES	80
3.4.1	Elimination of mass transfer resistances	80
3.4.2	Effect of reaction temperature	84
3.4.3	Effect of catalyst loading	87
3.4.4	Effect of feed mole ratio	90
3.4.5	Effect of acetic acid concentration	92
3.4.6	Effect of catalyst reusability	94
3.4.7	Comparison of different catalysts	95
3.5	CONCLUSIONS	96
4.	KINETIC MODELLING	98
4.1	INTRODUCTION	98
4.2	THE KINETIC MODELS	98
4.2.1	Langmuir-Hinshelwood-Hougen-Watson model	108
4.2.2	Eley-Rideal model	118
4.2.3	Modified Langmuir-Hinshelwood-Hougen-Watson model	127
4.2.4	Quasi-Homogeneous model	127
4.2.5	Criteria for acceptance of kinetic models	129
4.3	RESULTS AND DISCUSSION OF BATCH KINETIC MODEL	129
4.4	CONCLUSIONS	137

<b>5.</b>	<b>RESIDUE CURVE MAP DETERMINATION</b>	<b>138</b>
5.1	INTRODUCTION	138
5.2	THEORY	138
5.3	EXPERIMENTAL	142
	5.3.1 Materials	142
	5.3.1.1 Chemicals	142
	5.3.1.2 Catalyst	142
	5.3.2 Experimental set-up	142
	5.3.3 Method of analysis	144
5.4	RESULTS AND DISCUSSION OF THE DEVELOPMENT OF RESIDUE CURVE MAP	144
5.5	CONCLUSIONS	152
 <b>6.</b>	 <b>PILOT PLANT STUDIES (REACTIVE DISTILLATION COLUMN)</b>	 <b>153</b>
6.1	INTRODUCTION	153
6.2	EXPERIMENTAL	153
	6.2.1 Materials	153
	6.2.1.1 Chemicals	153
	6.2.1.2 Catalyst	153
	6.2.2 Experimental set-up	154
	6.2.3 Method of analysis	159
6.3	RESULTS AND DISCUSSION OF REACTIVE DISTILLATION COLUMN EXPERIMENTS	160
	6.3.1 Effect of feed mole ratio of reactants	160
	6.3.2 Effect of reflux ratio	164
	6.3.3 Effect of acid feed position	167
	6.3.4 Effect of reflux configuration	171
	6.3.5 Effect of acetic acid concentration in the feed stream	174
6.4	CONCLUSIONS	177
 <b>7.</b>	 <b>CONCLUSIONS AND FUTURE WORK</b>	 <b>179</b>
7.1	CONCLUSIONS	179
7.2	FUTURE WORK	180
 <b>8.</b>	 <b>REFERENCES</b>	 <b>182</b>

## LIST OF FIGURES

Figure 1.1. Worldwide use of acetic acid for various industrial application	2
Figure 1.2. Schematic of a reactive distillation column	8
Figure 2.1. Conventional processing schemes for carrying out the esterification reaction $\text{HOAc} + \text{MeOH} \leftrightarrow \text{MeOAc} + \text{H}_2\text{O}$ , consisting of one reactor followed by nine distillation columns (Krishna, 2002)	17
Figure 2.2. Eastman's process of methyl acetate synthesis (Schoenmakers and Bessling, 2003)	18
Figure 2.3. Reaction schemes in a heterogeneous catalysed process.	38
Figure 2.4. Various catalyst envelope "tea-bag" configurations (Taylor and Krishna, 2000)	43
Figure 2.5. Horizontally disposed wire mesh (a) wire gauze gutters and (b) wire gauze tubes containing catalyst (Taylor and Krishna, 2000)	43
Figure 2.6. Catalyst bales as licensed by Chemical Research and Licensing (Taylor and Krishna, 2000)	44
Figure 2.7. Structured catalyst sandwiches (Taylor and Krishna, 2000)	44
Figure 2.8. Catalytically active packing (Taylor and Krishna, 2000)	45
Figure 2.9. Catalyst envelopes placed along the liquid flow paths (Taylor and Krishna, 2000)	45
Figure 2.10. Counter-current vapour-liquid-catalyst contacting in trayed columns (Taylor and Krishna, 2000)	46
Figure 3.1. Scanning electron microscopy image of Purolite® CT-175 ion exchange resin catalyst	58
Figure 3.2. Scanning electron microscopy image of Purolite® CT-275 ion exchange resin catalyst	59
Figure 3.3. Scanning electron microscopy image of Purolite® CT-124 ion exchange resin catalyst	59
Figure 3.4. Scanning electron microscopy image of Purolite® CT-151 ion exchange resin catalyst	60
Figure 3.5. BET surface area of Purolite® CT-151, Purolite® CT-175 and Purolite® CT-275 ion exchange resin catalysts	62
Figure 3.6. Pore volume of Purolite® CT-151, Purolite® CT-175 and Purolite® CT-275 ion exchange resin catalysts	62

Figure 3.7. Surface area/ pore volume ratio of Purolite® CT-151, Purolite® CT-175 and Purolite® CT-275 ion exchange resin catalysts	63
Figure 3.8. Pore size distribution of Purolite® CT-151 ion exchange resin catalyst	64
Figure 3.9. Pore size distribution of Purolite® CT-175 ion exchange resin catalyst	65
Figure 3.10. Pore size distribution of Purolite® CT-275 ion exchange resin catalyst	65
Figure 3.11. Comparison of pore size distribution of different ion exchange resin catalysts	66
Figure 3.12. Particle size distribution of Purolite® CT-124 catalyst	68
Figure 3.13. Particle size distribution of Purolite® CT-151 catalyst	68
Figure 3.14. Particle size distribution of Purolite® CT-175 catalyst	69
Figure 3.15. Particle size distribution of Purolite® CT-275 catalyst	69
Figure 3.16. <i>iso</i> -amyl alcohol - acetic acid calibration curve	74
Figure 3.17. <i>iso</i> -amyl alcohol – <i>iso</i> -amyl acetate calibration curve	74
Figure 3.18. <i>iso</i> -amyl alcohol – water calibration curve	75
Figure 3.19. Experimental set-up for batch kinetic studies	77
Figure 3.20. Mechanism of ion exchange resin catalysed reaction of acetic acid with <i>iso</i> -amyl alcohol	80
Figure 3.21. Effect of stirrer speed on conversion of 30% (w/w) acetic acid at a catalyst loading of 5% (w/w); feed mole ratio ( <i>iso</i> -amyl alcohol to acetic acid), 2:1; temperature, 358 K; catalyst, CT-275	82
Figure 3.22. Effect of stirrer speed on conversion of concentrated acetic acid at a catalyst loading of 2.5% (w/w); feed mole ratio ( <i>iso</i> -amyl alcohol to acetic acid), 2:1; temperature, 358 K; catalyst, CT-275	82
Figure 3.23. Effect of catalyst particle size on conversion of 30% (w/w) acetic acid at a catalyst loading of 5% (w/w); feed mole ratio ( <i>iso</i> -amyl alcohol to acetic acid), 2:1; temperature, 358 K; catalyst, CT-275; stirrer speed, 500 rpm	84
Figure 3.24. Effect of temperature on conversion of 30% (w/w) acetic acid at a catalyst loading of 5% (w/w); feed mole ratio ( <i>iso</i> -amyl alcohol to acetic acid), 2:1; catalyst, CT-175; stirrer speed, 500 rpm	85

- Figure 3.25. Effect of temperature on conversion of 30% (w/w) acetic acid at a catalyst loading of 5% (w/w); feed mole ratio (*iso*-amyl alcohol to acetic acid), 2:1; catalyst, CT-275; stirrer speed, 500 rpm 86
- Figure 3.26. Effect of temperature on conversion of concentrated acetic acid at a catalyst loading of 5% (w/w); feed mole ratio (*iso*-amyl alcohol to acetic acid), 2:1; catalyst, CT-175; stirrer speed, 500 rpm 86
- Figure 3.27. Effect of catalyst loading on conversion of 30% (w/w) acetic acid at temperature of 358 K; feed mole ratio (*iso*-amyl alcohol to acetic acid), 2:1; catalyst, CT-175; stirrer speed, 500 rpm 88
- Figure 3.28. Effect of catalyst loading on conversion of 30% (w/w) acetic acid at temperature of 358 K; feed mole ratio (*iso*-amyl alcohol to acetic acid), 2:1; catalyst, CT-275; stirrer speed, 500 rpm 89
- Figure 3.29. Effect of catalyst loading on conversion of concentrated acetic acid at 358 K; feed mole ratio (*iso*-amyl alcohol to acetic acid), 2:1; catalyst, CT-175; stirrer speed, 500 rpm 89
- Figure 3.30. Effect of feed mole ratio (*iso*-amyl alcohol to acetic acid) on conversion of 30% (w/w) acetic acid at a catalyst loading of 5% (w/w); temperature, 358 K; catalyst, CT-175; stirrer speed, 500 rpm 91
- Figure 3.31. Effect of feed mole ratio (*iso*-amyl alcohol to acetic acid) on conversion of 30% (w/w) acetic acid at a catalyst loading of 5% (w/w); temperature, 358 K; catalyst, CT-275; stirrer speed, 500 rpm 91
- Figure 3.32. Effect of feed mole ratio (*iso*-amyl alcohol to acetic acid) on conversion of concentrated acetic acid at a catalyst loading of 5% (w/w); temperature, 343 K; catalyst, CT-175; stirrer speed 500 rpm. 92
- Figure 3.33. Effect of acetic acid concentration on conversion of acetic acid at a catalyst loading of 5% (w/w); temperature, 358 K; feed mole ratio (*iso*-amyl alcohol to acetic acid), 2:1; catalyst, CT-275; stirrer speed, 500 rpm 94
- Figure 3.34. Effect of catalyst reusability on conversion of 30% (w/w) acetic acid at a catalyst loading of 10% (w/w); temperature, 358 K; feed mole ratio (*iso*-amyl alcohol to acetic acid), 2:1; catalyst, CT-175; stirrer speed, 500 rpm 95
- Figure 3.35. Effect of catalyst type on conversion of concentrated acetic acid at a catalyst loading of 5% (w/w); temperature, 358 K; feed mole ratio (*iso*-amyl alcohol to acetic acid), 2:1; stirrer speed 500 rpm 96

Figure 4.1. Illustration of the LHHW mechanism	116
Figure 4.2. Illustration of the Eley-Rideal mechanism	126
Figure 4.3. Conversion <i>versus</i> time for the esterification of concentrated acetic acid with <i>iso</i> -amyl alcohol at a catalyst loading of 5% (w/w); feed mole ratio ( <i>iso</i> -amyl alcohol to acetic acid), 2:1, temperature, 333 K; stirrer speed, 500 rpm; catalyst, Purolite® CT-175	133
Figure 4.4. Conversion <i>versus</i> time for the esterification of concentrated acetic acid with <i>iso</i> -amyl alcohol at a catalyst loading of 5% (w/w); feed mole ratio ( <i>iso</i> -amyl alcohol to acetic acid), 2:1, temperature, 343 K; stirrer speed, 500 rpm; catalyst, Purolite® CT-175	134
Figure 4.5. Conversion <i>versus</i> time for the esterification of concentrated acetic acid with <i>iso</i> -amyl alcohol at a catalyst loading of 5% (w/w); feed mole ratio ( <i>iso</i> -amyl alcohol to acetic acid), 2:1; temperature, 358 K; stirrer speed, 500 rpm; catalyst, Purolite® CT-175	134
Figure 4.6. Conversion <i>versus</i> time for the esterification of concentrated acetic acid with <i>iso</i> -amyl alcohol at different temperatures over a catalyst loading of 5% (w/w); feed mole ratio ( <i>iso</i> -amyl alcohol to acetic acid), 2:1; stirrer speed, 500 rpm; catalyst, Purolite® CT-175	135
Figure 4.7. Conversion <i>versus</i> time for the esterification of concentrated acetic acid with <i>iso</i> -amyl alcohol at a catalyst loading of 2.5% (w/w); feed mole ratio ( <i>iso</i> -amyl alcohol to acetic acid), 2:1; temperature, 358 K; stirrer speed, 500 rpm; catalyst, Purolite® CT-175	135
Figure 4.8. Conversion <i>versus</i> time for the esterification of concentrated acetic acid with <i>iso</i> -amyl alcohol at a catalyst loading of 10.0 % (w/w); feed mole ratio ( <i>iso</i> -amyl alcohol to acetic acid), 2:1; temperature, 358 K; stirrer speed, 500 rpm; catalyst, Purolite® CT-175	136
Figure 4.9. Conversion <i>versus</i> time for the esterification of 30 wt% acetic acid with <i>iso</i> -amyl alcohol at a catalyst loading of 10 % (w/w); feed mole ratio ( <i>iso</i> -amyl alcohol to acetic acid), 2:1, temperature, 358 K; stirrer speed, 500 rpm; catalyst, Purolite® CT-175	136
Figure 4.10. Conversion <i>versus</i> time for the esterification of 30 wt% acetic acid with <i>iso</i> -amyl alcohol at a catalyst loading of 5% (w/w); feed mole ratio ( <i>iso</i> -amyl alcohol to acetic acid), 1:1, temperature, 358 K; stirrer speed, 500 rpm; catalyst, Purolite® CT-175	137

Figure 5.1. A simple batch still	139
Figure 5.2. Classification of singular points in a residue curve map	141
Figure 5.3. Experimental set-up for the measurement of residue curve map	143
Figure 5.4. Residue curve for acetic acid- <i>iso</i> -amyl alcohol- <i>iso</i> -amyl acetate-water reacting system with initial feed mole ratio ( <i>iso</i> -amyl alcohol/acetic acid), 0.5:1 at 1 atm	145
Figure 5.5. Residue curve for acetic acid- <i>iso</i> -amyl alcohol- <i>iso</i> -amyl acetate-water reacting system with initial feed mole ratio ( <i>iso</i> -amyl alcohol/acetic acid), 0.7:1 at 1 atm	146
Figure 5.6. Residue curve for acetic acid- <i>iso</i> -amyl alcohol- <i>iso</i> -amyl acetate-water reacting system with initial feed mole ratio ( <i>iso</i> -amyl alcohol/acetic acid), 0.9:1 at 1 atm	146
Figure 5.7. Residue curve for acetic acid- <i>iso</i> -amyl alcohol- <i>iso</i> -amyl acetate-water reacting system with initial feed mole ratio ( <i>iso</i> -amyl alcohol/acetic acid), 1:1 at 1 atm	147
Figure 5.8. Residue curve for acetic acid- <i>iso</i> -amyl alcohol- <i>iso</i> -amyl acetate-water reacting system with initial feed mole ratio ( <i>iso</i> -amyl alcohol/acetic acid), 1.3:1 at 1 atm	147
Figure 5.9. Residue curve for acetic acid- <i>iso</i> -amyl alcohol- <i>iso</i> -amyl acetate-water reacting system with initial feed mole ratio ( <i>iso</i> -amyl alcohol/acetic acid), 1.5:1 at 1 atm	148
Figure 5.10. Residue curve for acetic acid- <i>iso</i> -amyl alcohol- <i>iso</i> -amyl acetate-water reacting system with initial feed mole ratio ( <i>iso</i> -amyl alcohol/acetic acid), 2:1 at 1 atm	148
Figure 5.11. Residue curve for acetic acid- <i>iso</i> -amyl alcohol- <i>iso</i> -amyl acetate-water reacting system with initial feed mole ratio ( <i>iso</i> -amyl alcohol/acetic acid), 3:1 at 1 atm	149
Figure 5.12. Residue curve for acetic acid- <i>iso</i> -amyl alcohol- <i>iso</i> -amyl acetate-water reacting system with initial feed mole ratio ( <i>iso</i> -amyl alcohol/acetic acid), 8:1 at 1 atm	149
Figure 5.13. Residue curve map for acetic acid- <i>iso</i> -amyl alcohol- <i>iso</i> -amyl acetate-water reacting system at 1 atm	152
Figure 6.1. Diagram of reactive distillation column	155
Figure 6.2. Different sections of RDC used for present work	156/157

Figure 6.3. Katamax <sup>®</sup> packing (Kulprathipanja, 2001)	158
Figure 6.4. Effect of feed mole ratio (acetic acid to <i>iso</i> -amyl alcohol) on conversion of acetic acid	162
Figure 6.5. Effect of feed mole ratio (acetic acid to <i>iso</i> -amyl alcohol) on composition of top product (aqueous) in a reactive distillation column	162
Figure 6.6. Effect of feed mole ratio (acetic acid to <i>iso</i> -amyl alcohol) on composition of top product (organic) in a reactive distillation column	163
Figure 6.7. Effect of feed mole ratio (acetic acid to <i>iso</i> -amyl alcohol) on composition of bottom product in a reactive distillation column	163
Figure 6.8. Effect of reflux ratio on conversion of acetic acid	165
Figure 6.9. Effect of reflux ratio on composition of top product (aqueous) in a reactive distillation column	165
Figure 6.10. Effect of reflux ratio of composition of top product (organic) in a reactive distillation column	166
Figure 6.11. Effect of reflux ratio of composition of bottom product in a reactive distillation column	166
Figure 6.12. Effect of acid feed position on conversion of acetic acid	169
Figure 6.13. Effect of acid feed position on composition of top product (aqueous) in a reactive distillation column	170
Figure 6.14. Effect of acid feed position on composition of top product (organic) in a reactive distillation column	170
Figure 6.15. Effect of acid feed position on composition of bottom product in a reactive distillation column	171
Figure 6.16. Effect of reflux position on conversion of acetic acid	172
Figure 6.17. Effect of reflux position on composition of top product (aqueous) in a reactive distillation column	172
Figure 6.18. Effect of reflux position on composition of top product (organic) in a reactive distillation column	173
Figure 6.19. Effect of reflux position on composition of bottom product in a reactive distillation column	173
Figure 6.20. Effect of acetic acid concentration on conversion of acetic acid	175
Figure 6.21. Effect of acetic acid concentration on composition of top product (aqueous) in a reactive distillation column	175

Figure 6.22. Effect of acetic acid concentration on composition of top product (organic) in a reactive distillation column 176

Figure 6.23. Effect of acetic acid concentration on composition of bottom product in a reactive distillation column 176

## LIST OF TABLES

Table 1.1. Different types of esters formed from acetic acid with different alcohols.	7
Table 2.1. Industrially important reactions (Sharma and Mahajani, 2003)	26
Table 2.2. Phase combinations for heterogeneous catalysis (Bond, 1987)	38
Table 3.1. Characteristics of ion exchange resin catalysts	57
Table 3.2. Elemental analysis results of different ion exchange resins	67
Table 3.3. Parameters for calibration curves	71
Table 3.4. Preparation of reaction mixture	93
Table 4.1. The volume and area parameters $R_k$ and $Q_k$ of the UNIFAC group for the acetic acid/ <i>iso</i> -amyl alcohol/ <i>iso</i> -amyl acetate/water system. (Skjold-Jørgensen <i>et al.</i> , 1979)	100
Table 4.2. The interaction parameters, $a_{mn}$ , of the UNIFAC group (m,n) for the acetic acid/ <i>iso</i> -amyl alcohol/ <i>iso</i> -amyl acetate/water system (Gmehling <i>et al.</i> , 1982)	101
Table 4.3. Values of $e_{ki}$	103
Table 4.4(i) Values of $\tau_{mk}$	103
Table 4.4(ii) Values of $\tau_{mk}$	104
Table 4.5. Values of $\beta_{ik}$	104
Table 4.6. Values of $\theta_i$ and $S_i$	105
Table 4.7. Values of $J_i$ and $L_i$	106
Table 4.8. Values of $\ln\gamma_i^C$ and $\ln\gamma_i^R$	106
Table 4.9. Activity coefficient values at 333 K as calculated by UNIFAC group contribution method	107
Table 4.10. Values of parameters for the kinetic equations based on mechanisms A and B	130
Table 4.11. Adjustable parameters of the kinetic models for the catalysed esterification of acetic acid with <i>iso</i> -amyl alcohol	132
Table 5.1. Azeotropes for non-reacting system at 1 atm (Horsley, 1952)	144
Table 6.1. Key features of the reactive distillation column	159

## NOMENCLATURE

$a_i$	activity of component $i$
$a_{mn}$	interaction parameter of the UNIFAC group
A,B, C, D	acetic acid, <i>iso</i> -amyl alcohol, <i>iso</i> -amyl acetate and water respectively
$C_{AO}$	initial concentration of acetic acid ( $\text{mol cm}^{-3}$ )
$c_{i-s}$	concentration of component $i$ at the catalyst site ( $\text{mol cm}^{-3}$ ) (Equation 4.41)
$c_s$	concentration of vacant site on the catalyst surface ( $\text{mol cm}^{-3}$ ) (Equation 4.41)
$e_{ki}$	UNIFAC property of component (Equation 4.5)
$J_i$	UNIFAC property of component (Equations 4.10, 4.12)
$k_i$	adsorption coefficient of component $i$ (Equation 4.41)
$k$	reaction rate constant
$K_{eq}$	equilibrium constant of the reaction
$L_i$	UNIFAC property of component (Equations 4.10, 4.13)
MRD	mean relative deviation (Equation 4.72)
$N$	all samples (Equations 4.71,4.72)
$N_{AO}$	initial number of moles of acetic acid (Equation 4.1)
$Q_k$	area parameter of UNIFAC group (Equation 4.4)
$q_i$	UNIFAC property of component (Equation 4.4)
$-r_A$	reaction rate of acetic acid ( $\text{mol g}^{-1}\text{min}^{-1}$ )
$r_i$	UNIFAC property of component (Equation 4.3)
$R$	universal gas constant ( $8.314472 \text{ J K}^{-1} \text{ mol}^{-1}$ )
$R_k$	volume parameter of UNIFAC group (Equation 4.3)
$S$	vacant active catalyst site (Equations 4.22, 4.51)
$S_i$	concentration of sites occupied by species $i$ (Equations 4.22, 4.50)
$S_0$	total concentration of active catalytic sites (Equations 4.22, 4.50, 4.51)
$s_k$	UNIFAC property of component (Equation 4.9)
SRS	minimum sum of residual squares resulting from the fitting procedure (Equation 4.71)

$T$	temperature (K)
$t$	time (min)
$W$	weight (g)
$x_i$	liquid mole fraction of component $i$
$X$	transformed mole composition (Equations 5.1, 5.2, 5.3)
$X_A$	conversion of acetic acid

### ***Greek Symbols***

$\alpha$	empirical constant introduced in M-L kinetic model (Equation 4.57)
$\beta_{ik}$	UNIFAC property of component (Equation 4.7)
$\gamma$	activity coefficient
$\gamma_i^C$	combinatorial activity coefficient (Equation 4.2)
$\gamma_i^R$	residual activity coefficient (Equation 4.2)
$\theta_{BO}$	feed mole ratio ( <i>iso</i> -amyl alcohol to acetic acid)
$\theta_k$	UNIFAC property of component (Equation 4.8)
$\theta_i$	catalytic sites occupied by component $i$
$\theta_{total}$	total coverage of the catalytic sites (Equation 4.31)
$\tau_{mk}$	UNIFAC property of component (Equation 4.6)
$v_k^1$	number of each subgroup in component $i$

### ***Subscripts***

calc	calculated values
exp	experimental values
eq	equilibrium
$j$	dummy index running over all components (Equation 4.8)
$k$	subgroup number
$m$	dummy index running over all subgroups (Equation 4.9)

### ***Superscript***

$i$	component
-----	-----------

# 1. INTRODUCTION

## 1.1 GENERAL INTRODUCTION

Acetic acid is an important industrial chemical of which the production was about 7.835 billion pounds in the United States alone in 2002 (Shi *et al.*, 2005). As one of the most widely used carboxylic acids, acetic acid is often used as a raw material for many key petrochemical intermediates and products including vinyl acetate monomer (VAM), purified terephthalic acid (PTA), dimethyl terephthalate (DMT), acetate esters, cellulose acetate, acetic anhydride and monochloroacetic acid (MCA). The production of ethyl acetate by British Petroleum (BP) Amoco, United Kingdom is 250,000 tonnes annually ([www.chemicals-technology.com](http://www.chemicals-technology.com)). This high production figure makes it the largest producer of ethyl acetate in the world. The breakdown of the uses of acetic acid world production is illustrated in Figure 1.1. Dilute aqueous acetic acid solution in waste streams is the unwanted product as a result of these processes. The end uses for VAM include paints, adhesives, textiles, papers, films and chewing gums. The production of PTA is the fastest growing sector in Asia fuelled by the strong demand for polyethylene terephthalate (PET) bottles and polyester fibres used in the manufacture of clothing. DMT and PTA are also used for making PET solid state resins and films. Acetic anhydride is used in the manufacture of plastics, coatings and pesticides. Acetate esters e.g. ethyl acetate and butyl acetate are used primarily in paints and coatings. The remaining portion of acetic acid production is utilised by chloroacetic acid, moving downstream to end uses in di-ketene production for pharmaceutical applications. Another important application of acetic acid is to serve as a solvent to facilitate the manufacture of pharmaceutical products. Moreover, reactions involving the use of acetic anhydride as a reagent e.g. acetylation or as a solvent e.g. nitration can produce a vast amount of acetic acid containing waste (Neumann and Sasson, 1984). Saha *et al.* (2000) reported that the recovery of dilute acetic acid from its dilute aqueous solution possesses a major problem in both the petrochemical and fine chemical industries. Saha *et al.* (2000) further reported that the process for the manufacture of cellulose acetate is typically associated with a 35% (w/w)

aqueous solution of acetic acid as a waste stream, the process for the synthesis of glyoxal from acetaldehyde and nitric acid produces 13-20% (w/w) of acetic acid in the waste stream, and the wood distillate process contains 1-8% (w/w) of acetic acid in water. In addition, the terephthalic acid process involves concentrations of up to 65% (w/w) of acetic acid in water (Van Brunt, 1992). Xu and Chuang (1996) stated that the low concentration of acetic acid in the water produced from these processes should be removed or recovered before the water is reused or discharged into the environment. This is set so as to protect the environment from being more polluted, which would have an adverse effect on the ecological system.

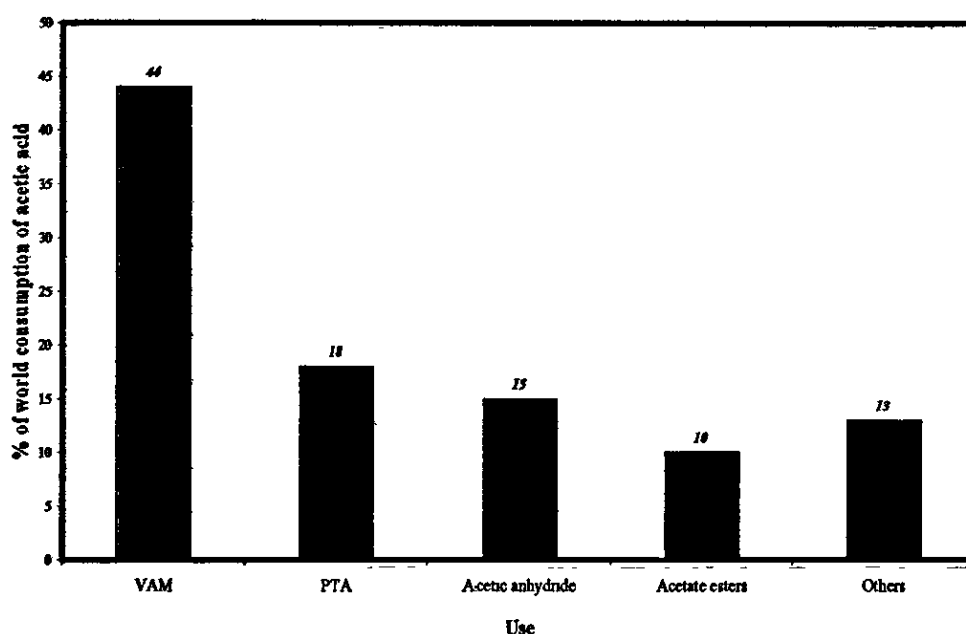


**Figure 1.1.** Worldwide uses of acetic acid for various industrial applications (www.icisl.or.com).

McKetta (1976) and Neumann and Sasson (1984) highlighted that the major methods for recovering acetic acid are simple fractional distillation, azeotropic distillation (Kirk and Othmer, 1980), and solvent extraction (Vermijs and Kramer, 1954; Wainwright, 1949; Ricker *et al.*, 1980). In more recent times, a number of methods have been proposed to recover the acetic acid. Kuo *et al.* (1987) suggested the use of solid adsorbents for the recovery of acetic acid from aqueous solutions. O'Brien and Senske (1989) looked at the separation and recovery of acetic acid, amongst other acids (acrylic acid, lactic acid and

propionic acid), resulting from whey fermentation source by emulsion liquid membranes (ELMs). They defined ELM as a water immiscible phase which separates two aqueous phases, thus preventing direct contact of the aqueous phases. Ho (2002) described an ELM as an emulsion that acts as a liquid membrane for the separation of the target species, in this instance acetic acid, from a feed solution. An ELM is created by forming a stable emulsion, such as a water-in-oil emulsion, between two immiscible phases, followed by dispersion of the emulsion into a third, continuous phase by agitation for extraction. The membrane phase is the oil phase that separates the encapsulated, internal aqueous droplets in the emulsion from the external, continuous phase. The acetic acid-extracting agent is contained in the membrane phase, and the stripping agent is contained in the internal aqueous droplets. Emulsions formed from these two phases are stabilised by the use of a surfactant. The external, continuous phase is the feed solution containing the acetic acid. The acetic acid is subsequently extracted from the aqueous feed solution into the membrane phase and then stripped into the aqueous droplets in the emulsion. The acetic acid can then be recovered from the internal aqueous phase by breaking the emulsion, typically via electrostatic coalescence, followed by electroplating or precipitation. Althouse and Tavlarides (1992) stated the use of different organic extractant systems and addressed the selection of the optimum extractant for the removal of acetic acid from aqueous streams. This work was driven by the need to produce a de-icing alternative in the form of calcium magnesium acetate, which is more environmentally friendly, and less corrosive to metal and concrete as compared to the more common de-icing salt, sodium chloride (Wise and Augenstein, 1988) without the use of unnecessary thermal operations and expensive intermediates. The conventional method of producing calcium magnesium acetate is very expensive because it involves a costly distillation operation to concentrate the glacial acetic acid, which is used as an intermediate in the manufacture of calcium magnesium acetate. The alternative method proposed involved the extraction of acetic acid from aqueous streams by a suitable organic extractant, e.g. an amine extractant with the raffinate being recycled to the fermenter. The organic extractant was thereafter stripped of the acetic acid with an aqueous slurry of a basic calcium

magnesium salt to produce a closely saturated solution of calcium magnesium acetate. The only thermally driven operation in the proposed process was to evaporate the water from the almost saturated solution to yield the salt. Ingale and Mahajani (1994) investigated on the recovery of acetic acid from aqueous waste streams using pure phosphate as an extractant. Reisinger and King (1995) investigated on the use of amine and ammonium extractants, and solid sorbents towards the recovery of acetic acid whilst forming calcium magnesium acetate. The calcium magnesium acetate was made by recovering the acetic acid with a separating agent, either that of an extractant or a solid sorbent, followed by the removal of acetic acid from the separating agent with a basic calcium/magnesium compound. Water can then be removed and isolated from the aqueous solution of calcium magnesium acetate through evaporation and spray drying. Cloete and Marais (1995) suggested the use of basic ion exchange resins for the recovery of very dilute acetic acid. This method works on the basis of the neutralisation of an acid by a base. Any non-acids adsorbed could be removed from the ion exchange resin by washing with water, whilst the acids could be eluted from the resin by raising the pH. The acids could be subsequently separated by using distillations. An advantage of this technique is that the ion exchanger is insoluble, and there is no release of toxic solvents which might cause problems further downstream. Yu *et al.* (2000) proposed and described the use of bipolar membrane electrodialysis for the recovery of acetic acid from dilute wastewater. The space between the anion exchange membrane and the anion exchange layer of the bipolar membrane is known as the Dilute Solution Chamber (DSC). The space between the anion exchange membrane and the cation exchange layer of the bipolar membrane is the Concentrated Solution Chamber (CSC). The wastewater containing the acetic acid is introduced into the DSC. When an electric field is imposed, the anion group of the acetic acid ( $\text{Ac}^-$ ) is transferred from the DSC through the anion exchange membrane into the CSC. The hydroxyl ions generated by the bipolar membrane through the splitting of water neutralises the hydrogen ions remaining after  $\text{Ac}^-$  ions removal. The wastewater in the DSC is gradually cleaned, and its pH value gradually rises to 7. In the CSC, the  $\text{Ac}^-$  ions combine with the hydrogen ions generated by the bipolar membrane, and thus concentrated acetic acid can be obtained. The

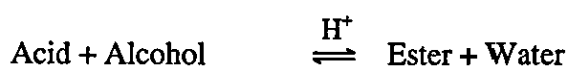
concentrated acetic acid could subsequently be removed for further treatment undertaken by distillation or extraction. Shi *et al.* (2005) proposed the recovery of acetic acid from the anaerobic fermentation broth with a sulphur dioxide stream. This proposal arose from sourcing a promising alternative towards the production of acetic acid. In this case, the cost-effective alternative was to produce acetic acid using biomass materials instead of basing the production on the non-renewable natural gas resource solely (Agreda and Zoeller, 1993). The major problems faced with the recovery of acetic acid involve the separation of minute amounts of acetic acid from relatively large amounts of water. The major drawback of the conventional distillation process is that it is an energy intensive procedure and consequently uneconomic because of the excessive costs in vapourising the high volumes of water which possesses a large latent heat of vaporisation ( $2260 \text{ kJkg}^{-1}$ ). Moreover, with an increase in the concentration of acetic acid towards the bottom half of the distillation column, the solution becomes more corrosive. Expensive materials of construction must be acquired to cope with this corrosion problem. As such, the capital and maintenance costs associated with conventional distillation for the recovery of acetic acid are extremely high. Solvent extraction is limited by phase separation and distribution of the components involved in the reacting system. Xu and Chuang (1997) reported that it is very energy consuming to remove acetic acid from water by azeotropic distillation because of the higher boiling point of acetic acid as compared to water.

In view of the constraints associated with the conventional separation methods, alternative methods should be looked at with regards to the treatment of the dilute acetic acid stream and more specifically for the recovery of acetic acid from its contents. Reactive distillation is a potentially feasible method of separation for the recovery of acetic acid.

Sundmacher and Kienle (2003) defined reactive distillation as an integration of chemical reaction and separation of the end products via distillation within a single operation unit. It can be used to conduct processes that would be prohibitively complicated if handled in a conventional process consisting

mainly of many individual single-operation units (Krishna, 2002). This can lead on to substantial savings in the energy and equipment costs. Xu and Chuang (1997) stated that implementation of reactive distillation can provide energy savings of up to 80% as compared to conventional separation methods. Reactive distillation is an attractive method for improving process efficiency. Implementing reactive distillation by conducting reaction and distillation simultaneously allows reaction to overcome the limitations of distillation by circumventing azeotropes as well as bringing reactions to near completion (Malone and Doherty, 2000). For equilibrium limited chemical reactions such as esterification processes, the conversion of acetic acid could be increased far beyond chemical equilibrium conversion due to the continuous removal of reaction products from the reactive zone. This is in accordance with Le Chatelier's Principle, which states that if a system is placed under stress, it will act so as to relieve the stress. In the application to chemical reactions, it means that if a product or by-product is removed from the system, the equilibrium of the reacting system will be upset, and the reaction will produce more products to make up for the loss. As such, since the products are simultaneously separated from the reaction mixture, no chemical equilibrium can be established, and therefore the reaction velocity is maintained at a high rate. Other advantages include utilising the heat of reaction for the desired heat of reaction for distillation on the condition that the reaction is exothermic in nature, as well as suppressing any side reactions occurring by separating the desired products from further reaction as they are formed, thereby leading to improved product selectivity.

Though reactive distillation has been successfully commercialised for the manufacture of high commodity chemicals, its potential as a separation and recovery tool has not been exploited in depth. The catalytic reactive distillation method involves the addition of a certain amount of alcohol to the acid in a catalytic distillation column. In general, the alcohol reacts with the acid to form the corresponding ester and water as products.



The type of ester formed depends on the alcohol that is being used. Table 1.1 presents some of the different types of esters that could be formed in various esterification reactions with acetic acid (Carey, 1996).

**Table 1.1.** Different types of esters formed from acetic acid with different alcohols.

Alcohol	Group R (R-OH)	Ester
Methyl alcohol	- CH <sub>3</sub>	Methyl acetate
Ethyl alcohol	- CH <sub>2</sub> CH <sub>3</sub>	Ethyl acetate
<i>n</i> -Propyl alcohol	- CH <sub>2</sub> CH <sub>2</sub> CH <sub>3</sub>	<i>n</i> -Propyl acetate
<i>n</i> -Butyl alcohol	- CH <sub>2</sub> CH <sub>2</sub> CH <sub>2</sub> CH <sub>3</sub>	<i>n</i> -Butyl acetate
Allyl	- CH <sub>2</sub> CH=CH <sub>2</sub>	Allyl acetate
<i>iso</i> -Propyl	- CH(CH <sub>3</sub> ) <sub>2</sub>	<i>iso</i> -Propyl acetate
3-Pentanol	- CH(CH <sub>2</sub> CH <sub>3</sub> ) <sub>2</sub>	3-Pentyl acetate
<i>tert</i> -Butyl	- C(CH <sub>3</sub> ) <sub>3</sub>	<i>tert</i> -Butyl acetate
Phenol	- C <sub>6</sub> H <sub>5</sub>	Phenyl acetate
<i>iso</i> -Amyl alcohol	- C <sub>5</sub> H <sub>11</sub>	<i>iso</i> -Amyl acetate

A popular commercialised reactive distillation system for the esterification process is the manufacture of methyl acetate. This method was first put to invention and patented by Agreda and Partin (1984), and subsequently commercialised by Eastman Kodak Chemical Company in the production of high purity methyl acetate (Agreda *et al.*, 1990). Sirola (1995) reported five times lower investment and five times lower energy use for the Eastman process.

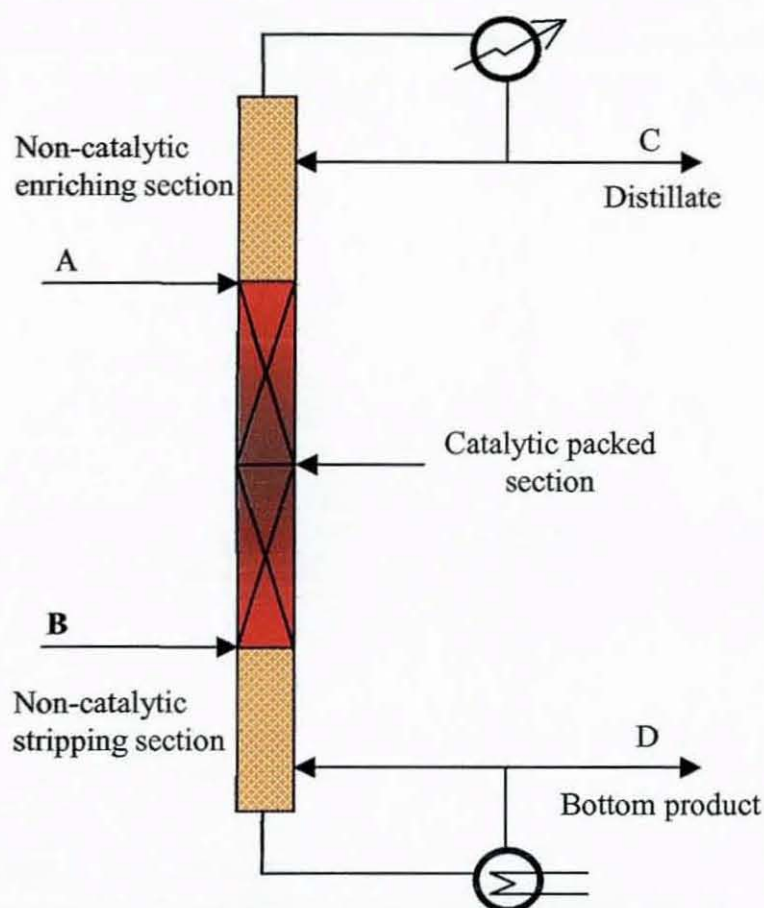


**Figure 1.2.** Schematic of a reactive distillation column (RDC)

Most of the previous literatures dealt with the esterification reaction in batch operation using 98-100% acetic acid as one of the reactants. The use of dilute acetic acid, which is more applicable in the industries as far as the recovery process is concerned, has received little attention. No systematic study has been previously carried out in a continuous reactive distillation column for the recovery of an aqueous solution of acetic acid by esterification with *iso*-amyl alcohol using cation exchange resins as catalysts.

Leyes and Othmer (1945) investigated the kinetics of the reaction between butanol and acetic acid using sulphuric acid as catalyst. Neumann and Sasson (1984) looked at the recovery of acetic acid from 20 to 60% (w/w) acetic acid solution through esterification reaction with methanol in a chemo-rectification column packed using an acidic organic polymer catalyst to produce methyl acetate. The result was a high acetic acid conversion of 70 to 80%.

column packed using an acidic organic polymer catalyst to produce methyl acetate. The result was a high acetic acid conversion of 70 to 80%.

Xu and Chuang (1996) investigated the kinetics of the reaction of methanol with dilute acetic acid solutions using ion exchange resin catalyst, Amberlyst 15. The effects of stirrer speed, reaction temperature, reactant concentration and catalyst loading on the reaction rate were studied. A complete kinetic equation describing the reaction catalysed by the Amberlyst 15 catalyst was also developed in the study.

Saha *et al.* (2000) worked towards the esterification of dilute acetic acid with *n*-butanol in a reactive distillation column using macroporous ion-exchange resin, Indion 130, as a catalyst bed. The aim of their work was directed towards the recovery of 30% (w/w) acetic acid.

In addition to the advantages offered by reactive distillation over the other techniques, a value added ester in the form of *iso*-amyl acetate is produced during the recovery of acetic acid by esterification with *iso*-amyl alcohol. *iso*-Amyl acetate is used in large quantities as solvents for gums, resins, plastics and lacquers. In addition, *iso*-amyl acetate has also found applications as artificial flavouring for banana-flavoured bubble gum, as preservatives in sodas and soft drinks as well as in artificially pear flavoured food articles because of its strong smell and flavouring characteristics (Teo and Saha, 2004). Other useful applications of the ester include being used as an artificial scent to cover unpleasant odours, as perfume in shoe polish, though rare but can be found as an additive in american cigarettes, as swelling agent in bath sponges as well as being used in the manufacture of artificial silk, photographic films and metallic paints.

In view of the appreciable value and usefulness of this ester, coupled with the drawbacks associated with the use of the other physical separation methods (conventional distillation, solvent extraction, etc.), it is apparent that the application of reactive distillation on the esterification process between *iso*-amyl alcohol and acetic acid could be very advantageous.

For the purpose of process development, a vital understanding of the reactive distillation process is required. Moreover, a reliable kinetic model is needed to represent accurately the kinetic behaviour of the reacting system between *iso*-amyl alcohol and acetic acid.

To accelerate the reaction rate, catalysts are always employed in a liquid phase esterification. Both homogenous and heterogeneous catalysts can be used in reactive distillation columns (Saha *et al.*, 2000). In homogeneously catalysed processes, sulphuric acid is generally used. Despite a strong catalytic effect, the use of a homogenous catalysts suffer from several drawbacks such as the existence of possible side reactions, corrosion of equipment as well as the need to deal and treat the acid-containing waste, amongst others. In recent years, the use of solid acid catalysts has received greater attention to redress the problems of using homogenous catalysts. Among the many solid acid catalysts, ion exchange resins are the most commonly used and have proved to be effective in liquid phase esterification (Chakrabati and Sharma, 1993; Sharma, 1995; Harmer and Sun, 2001). In heterogeneously catalysed reactions, acidic polymeric catalysts such as ion-exchange resins in various forms (e.g. Dowex, Amberlyst 15, Amberlyst 35 and Indion 130) had been previously used (Xu and Chuang, 1996; Lee *et al.*, 2000; Saha *et al.*, 2000; Lee *et al.*, 2001; Lee *et al.*, 2002). For the present research, Purolite<sup>®</sup> CT-124, Purolite<sup>®</sup> CT-151, Purolite<sup>®</sup> CT-175 and Purolite<sup>®</sup> CT-275 catalysts have been employed.

There were no adequate systems in assessing the suitability and feasibility of reactive distillation on a given reacting system prior to the work of Song *et al.* (1998) on residue curve maps. The residue curve map allows one to identify the existence of any thermodynamic constraints that may impose restrictions on the implementation of reactive distillation.

## 1.2 RESEARCH OBJECTIVES

The kinetic behaviour of the heterogeneously catalysed esterification of acetic acid with *iso*-amyl alcohol has been carried out with different types of catalysts in the form of ion exchange resins. The ion exchange resins used in this work were supplied by Purolite International Limited, United Kingdom. The emphasis was placed towards optimising the reaction conditions under batch conditions. Different kinetic models have been tested, and a reliable kinetic model has been used to express the kinetics of the reaction over a range of operating conditions.

Subsequently, the feasibility of the reactive distillation process has been accessed through a systematic procedure of residue curve maps. A residue curve map provides a design engineer with the information of the existence of separation boundaries imposed by the singular points corresponding to the reactive or kinetic azeotropes, and thereby providing an insight into the feasibility of the reactive distillation operation. The residue curve maps have been generated under different conditions to elucidate the feasibility of the reactive distillation operation.

The overall objective of this research is to develop a reactive distillation column for the recovery of acetic acid from aqueous streams. A laboratory scale packed reactive distillation has been built and preliminary experiments have been carried out. Various operation variables including feed mole ratio of reactants, reflux ratio, location of the feed points, reflux configuration, and concentration of acetic acid have been investigated with the aim of optimising the reactive distillation column configurations.

The objectives of this research work are summarised as follow:

- Understanding of the reactive distillation process for the recovery of dilute acetic acid.
- Understanding the chemistry of the reaction.
- Optimising the reaction conditions for the reaction between acetic acid and *iso*-amyl alcohol under batch conditions.
- Correlation of the batch kinetic data by conventional theoretical kinetic models.
- Evaluation of the techno-feasibility of the reactive distillation operation for the reacting system between acetic acid and *iso*-amyl alcohol through a systematic procedure of residue curve maps (RCMs).
- Design and development of a reactive distillation column (RDC).
- Establishment of experimental methodology for the evaluation of reactive distillation strategies in terms of optimising the process conditions and the column configurations.

## 2. LITERATURE REVIEW

### 2.1 INTRODUCTION

The uses of reactive distillation for the different applications, especially for etherification have been well documented in the literature, but the potential for reactive distillation as a separation and recovery tool has received far less attention. This chapter summarises the considerable amount of work to date on the various applications of reactive distillation as well as the advantages and disadvantages through the implementation of reactive distillation.

The catalysts used in this research are mainly commercial ion exchange resins. This chapter further looks at the definition, classification and properties of ion exchange resins, and the applications of different ion exchange resins that have been employed in various reactive distillation processes.

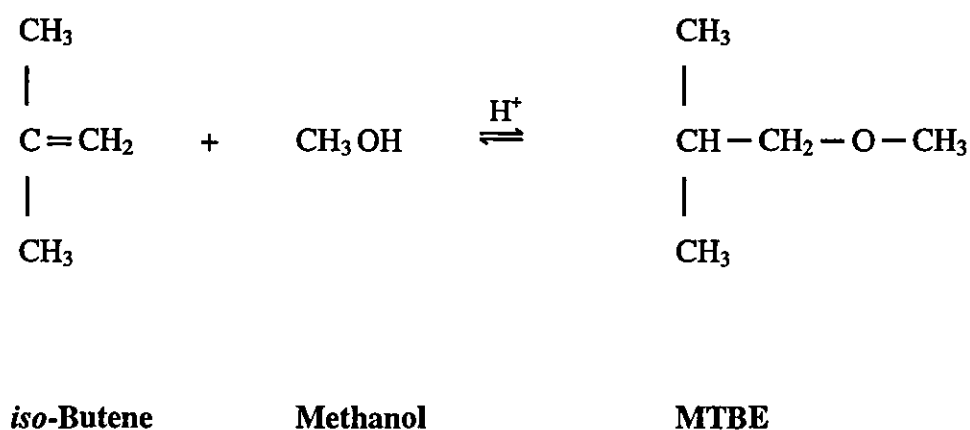
### 2.2 APPLICATIONS OF REACTIVE DISTILLATION

Reactive distillation is a state of the art technology that combines reaction and distillation within a single operation unit. The first patents on reactive separation processes dated back to the 1920s by Backhaus (1921, 1922 and 1923). The patents described the process and apparatus used for the production of high grade esters. However, the industrial applications of reactive distillation did not take place before the 1980s (Agreda *et al.*, 1990).

Towler and Frey (2000) and Taylor and Krishna (2000) reported that it is essential to meet some of the practical issues in order to implement a reactive distillation application. These issues include good liquid/vapour contacting in the reactive zone, efficient contacting of the liquid with the catalyst particles, sufficient liquid hold-up in the reactive section, low pressure drop through the catalytically packed reactive section as well as easy installation and removal of the reactive distillation equipment and that of the catalyst.

### 2.2.1 Etherification: MTBE, ETBE, TAME and other processes

Hiwale *et al.* (2004) highlighted that etherification processes, and especially that for the synthesis of methyl *tert*-butyl ether (MTBE) has been probably the most studied reacting system in reactive distillation as evident from the previous reviews (Taylor and Krishna, 2000; Sharma and Mahajani, 2003). Sharma and Mahajani (2003) reported that it is due to the enormous demand for MTBE that the reactive distillation process gained prominent status as a promising multifunctional reactor and separator. The demand was driven by the implementation of the Clean Air Act in the United States of America in the late 1970s which led to a boost of MTBE and other fuel ethers' (ethyl *tert*-butyl ether, ETBE; *tert*-amyl methyl ether, TAME) production to higher levels in the 1980s. MTBE was advantageous as a fuel additive because of its antiknock property, enhancing the fuel octane number, improving the water tolerance limit of the fuel and having a higher calorific value than other additives such as methanol. Sharma and Mahajani (2003) further reported that the pioneering work to commercialise reactive distillation for etherification was performed by Smith from the Chemical Research and Licensing Company, and several patents have been awarded for different catalyst structures, internal column design and flow schemes (Smith, 1980, 1981, 1990). Taylor and Krishna (2000) highlighted that for the acid catalysed reaction between *iso*-butene and methanol to form MTBE, the conventional reactor followed by distillation concept is particularly complex because the reaction mixture leaving the reactor forms minimum boiling azeotropes. The reaction is as represented:



The implementation of reactive distillation requires only one column to which the butanes feed (consisting of a mixture of *n*-butene, which is non-reactive, and *isobutene* which is reactive) and methanol are fed near the bottom of the reactive section. The reactive distillation concept is capable of achieving close to 100% conversion of *iso*-butene and methanol, along with the suppression of the formation of the unwanted side-products in the form of dimethyl ether, water, *tert*-butanol and *di-iso*-butene (Isla and Irazoqui, 1996).

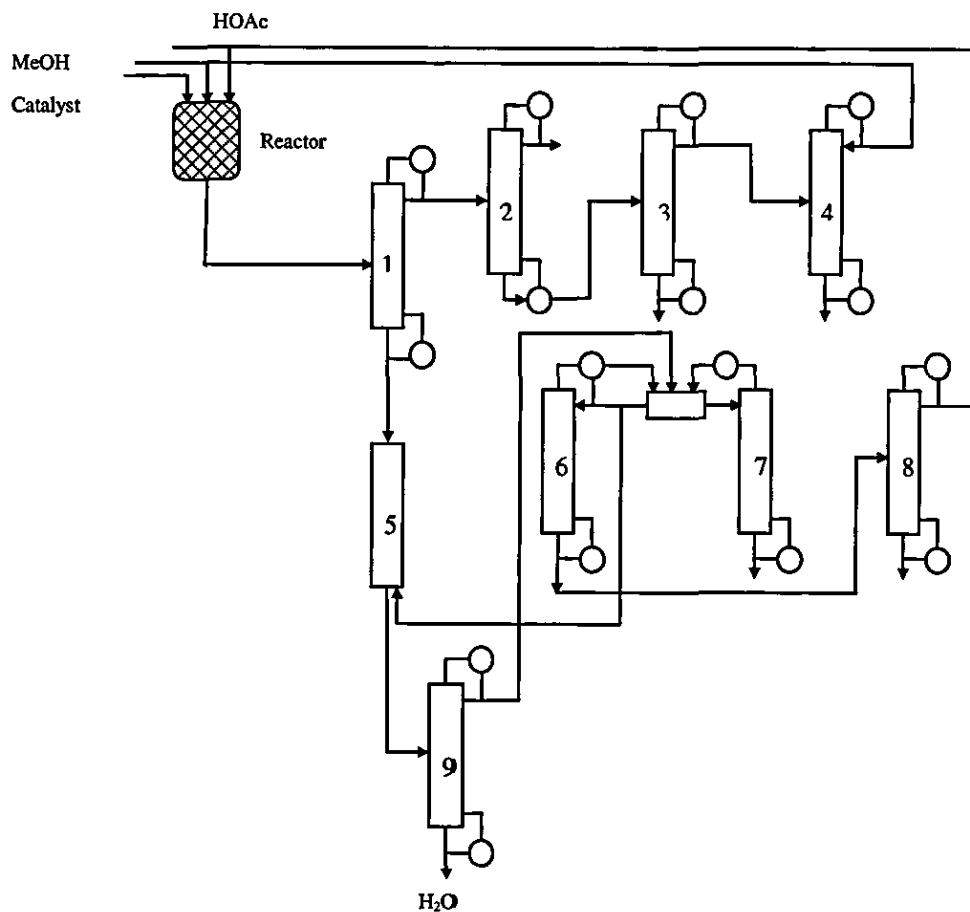
Sharma and Mahajani (2003) reported that the decision to ban MTBE state-wide in California (the biggest consumer among the different states) imposed in March 2002 and enforced by December 2003 because of pollution issues have forced refiners to look for alternative fuel additives. However, MTBE has been mainly responsible for the many research activities carried out in relations to reactive distillation. The work carried out for MTBE production alone using reactive distillation has been intensively carried out by many researchers (Isla and Irazoqui, 1996; Sundmacher and Hoffman, 1996; Tejero *et al.*, 1996; Hauan *et al.*, 1997; Thiel *et al.*, 1997; Espinosa *et al.*, 1999; Higler *et al.*, 1999; Baur *et al.*, 2000; Chen *et al.*, 2000; Tadé and Tian, 2000; Lee and Westerberg, 2001; Yadav and Joshi, 2001; Bao *et al.*, 2002; Beckmann *et al.*, 2002; Li *et al.*, 2002; Noeres *et al.*, 2003; Wang *et al.*, 2003). Several investigations on the ETBE process have also been presented (Thiel *et al.*, 1997; Sneesby and Tadé, 2000; Tadé and Tian, 2000; Bisowarno and Tadé, 2002; Tian *et al.*, 2003; Bisowarno *et al.*, 2004; Wang *et al.*, 2005). The production of TAME using reactive distillation has been looked at as well by several researchers (Thiel *et al.*, 1997; Baur and Krishna, 2002; Peng *et al.*, 2002; Baur *et al.*, 2003). Rihko-Struckmann *et al.* (2004) reported on the etherification of isobutylene dimer and methanol for the production of 2-methoxy-2,4,4-trimethylpentane, which can be used as a fuel additive due to its low solubility in water and high octane value.

Baur *et al.* (2001) explored the possibility of using etherification as a separation tool for the C<sub>4</sub> stream (1-butene, 2-butene, *n*-butane, butadiene and *iso*-butene) by reacting methanol with *iso*-butene to form MTBE which then

separates the *iso*-butene from the other components. A second column is used to split the MTBE back into methanol and *iso*-butene, after which the methanol is recycled back to the MTBE formation column while *iso*-butene is obtained as a pure product. It is of importance that the outlet of the splitting column be separated before recycling as the presence of side products such as *di-iso*-butene, dimethyl ether and water would affect the purity of the methanol.

### 2.2.2 Esterification: methyl acetate and other esters

Keyes (1932) reported various chemical processes and equipment associated with esterification before reactive distillation was implemented for the esterification process. Amongst the processes highlighted were the ethyl acetate process, the ethyl lactate process, butyl acetate process, methyl acetate process, etc. High purity methyl acetate is used in large amounts as an intermediate in the manufacture of a variety of polyesters such as cellulose acetate and photographic film base. Baur and Krishna (2004) stated that there were a lot of difficulties faced with the manufacturing process of high purity methyl acetate. This is mainly attributed to the equilibrium limitation in the reaction of methanol and acetic acid. Moreover, there is the presence of minimum boiling azeotropes between methyl acetate and methanol, as well as that of methyl acetate and water (Agreda *et al.*, 1990). Conventional processes use multiple reactors with the use of a large excess of methanol to achieve a high conversion of the acetic acid to form the methyl acetate ester. Krishna (2002) reported that a conventional separation system would require a reactor and a train of nine distillation columns (Figure 2.1). As a result, this process carried out through the conventional way requires a huge capital investment, high energy costs and a large inventory of chemicals.



Column 1: Distillation column

Column 2: Extractive distillation column

Column 3: Solvent recovery column

Column 4: Methanol recovery column

Column 5: Extraction unit column

Column 6: Azeotropic distillation column

Column 7: Entrainer recovery column

Column 8: Distillation column

Column 9: Distillation column

**Figure 2.1.** Conventional processing schemes for carrying out the esterification reaction  $\text{HOAc} + \text{MeOH} \leftrightarrow \text{MeOAc} + \text{H}_2\text{O}$ , consisting of one reactor followed by nine distillation columns (Krishna, 2002)

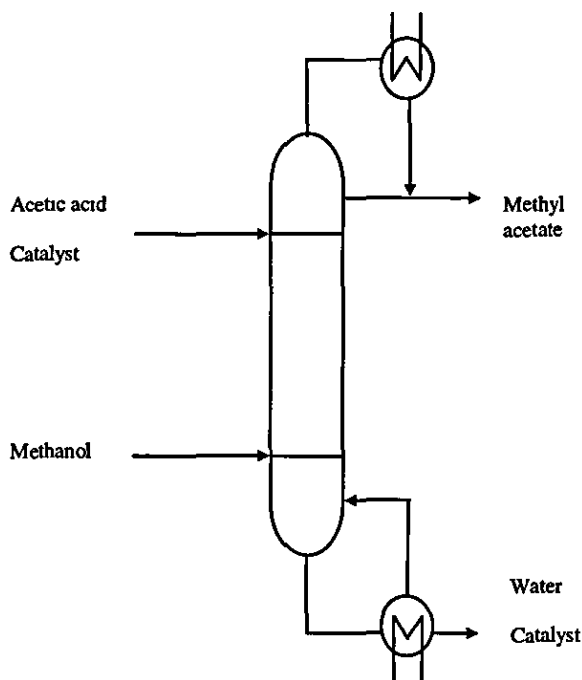


**Figure 2.2.** Eastman's process of methyl acetate synthesis (Schoenmakers and Bessling, 2003)

A reactive distillation process with stoichiometrically balanced feeds was invented by Agreda and Partin (1984) and commercialised by Eastman Chemical Company as represented in Figure 2.2. Most of the reaction takes place in the middle section of the column below the sulphuric acid catalyst feed point. The lower section of the column, below the methanol feed, is mostly a methanol-water separation to get high purity water as bottom product. The top sections of the column, above the sulphuric acid catalyst feed point, refine the methyl acetate to give high purity product. The column, which integrates an entire chemical plant in one unit, produces 400 million lb of high purity methyl acetate products per year (Mayfield and Agreda, 1986). In this single column, methyl acetate can be made without additional purification steps and with no unconverted reactant streams to be recovered. Fernholz *et al.* (2000) commented that the implementation of reactive distillation for methyl acetate synthesis overcame the limitations of raw material conversion and product purity caused by azeotropes, and the reaction equilibrium through the removal of methyl acetate as the product as well as

the consumption of methanol by the reaction. Agreda and Lilly (1990) came out with an invention with a variation on this process developed in 1984 that was capable of producing ultra-high methyl acetate. They proposed that the reactants (i.e. methanol and acetic acid) should flow counter current in a sequence of flashing reactors whereby the high concentration of reactants at opposite ends would ensure the high conversion of both acetic acid and methanol at the opposite ends of the series of flashing reactors. Siirola (1995) reported that the implementation of reactive distillation for the synthesis of methyl acetate gave a reduction in the investment and energy costs by a factor of five.

Hiwale *et al.* (2004) stated that the synthesis of methyl acetate has been and is still being used as a model reaction for various experimental and modelling studies on reactive distillation. Other authors described the optimisation for the operation of a reactive distillation column towards the synthesis of methyl acetate through a process model (Fernholz *et al.*, 2000) the synthesis and hydrolysis of methyl acetate using structured catalytic packings (Pöpkén *et al.*, 2001), the characterisation of MULTIPAK<sup>®</sup> catalyst packing used while synthesising methyl acetate in a reactive distillation column (Kolodziej *et al.*, 2001) and the investigation of the control of a reactive distillation column for the synthesis of methyl acetate (Al-Arfaj and Luyben, 2002).

Reactive distillation is not limited to the synthesis of methyl acetate for the esterification process. Sharma and Mahajan (2003) reported that reactive distillation could also be used for the production of other esters including ethyl acetate (Lee and Westerberg, 2001; Kenig *et al.*, 2001; Okur and Bayramoglu, 2001; Vora and Daoutidis, 2001), *iso*-propyl acetate (Lee and Kuo, 1996) and butyl acetate (Leyes and Othmer, 1945; Yang *et al.*, 1998; Hanika *et al.*, 1999; Venimadhavan *et al.*, 1999; Steinigeweg and Gmehling, 2002; Cardona *et al.*, 2004). Moreover, Saha and Sharma (1996) worked towards the synthesis of cyclohexyl formate, cyclohexyl acrylate and cyclohexyl methacrylate through the reaction of cyclohexene with the respective acids (formic acid, acrylic acid and methacrylic acid) using different types of ion exchange resins (Amberlyst-15, Indion-130, Amberlite

IR-120). Furthermore, Smejkal *et al.* (2001), Hanika *et al.* (2001), and Yadav and Thathagar (2002) reported works towards the synthesis of methyl *iso*-propyl acetate and *di*-ethyl maleate using the reactive distillation technology. The former ester is widely used as solvents in the chemical industry whereby it finds applications as an extracting agent, paint solvents and adhesives based on its ability to dissolve both polar and non-polar compounds. Moreover, methyl isopropyl acetate has a lower impact on the environment as compared to the aromatics solvents. The latter ester, *di*-ethyl maleate, is an important intermediate that is used in the polymer industry. Venimadhavan *et al.* (1999), Hanika *et al.* (1999), Jiménez *et al.* (2002), Gangadwala *et al.* (2003) and Singh *et al.* (2005) studied on the reactive distillation process for the production of butyl acetate from the reaction of butanol with acetic acid, with Jiménez *et al.* (2002) claiming that an extractive agent in the form of *o*-xylene must be added to the reactive distillation column. However, it meant that the entrainer must be recovered in a subsequent column, and there was also the unpreventable contamination of the desired products with small amounts of the entrainer occurring. In addition, Adams *et al.* (2003) patented the reactive distillation process for the manufacture of vinyl acetate from acetic acid and ethylene. Schmitt *et al.* (2004) worked on the synthesis of *n*-hexyl acetate using reactive distillation and subsequently reported on the synthesis of the same reacting system using modified internals (Schmitt *et al.*, 2005).

Reactive distillation has also been extended towards the esterification of fatty acids, with the fatty acid esters having important uses as surfactants and lubricants, and intermediates used in the manufacture of cosmetics and detergents. Bock *et al.* (1997) investigated on the esterification of myristic acid with 2-propanol in a tray column. Steinigeweg and Gmehling (2003) worked on the esterification of decanoic acid with methanol using a heterogeneous catalyst in the form of the strong acidic ion exchange resin, Amberlyst 15. Other works related to the esterification of fatty acid were done by Omota *et al.* (2003a, b) and Dimian *et al.* (2004). Omota *et al.* (2003a,b) worked on the feasibility of a continuous process for fatty acid esterification using reactive distillation with sulphated zirconia as the solid

acid catalyst. Dimian *et al.* (2004) investigated the use of an entrainer in the reactive distillation column for the esterification of fatty acid, which would allow for quantitative removal of water by liquid-liquid separation and gave a final product of acceptable impurity. Moreover, the addition of the entrainer enhances the reaction rate through higher reactant concentration in the reaction space, and offered better protection of catalyst against deactivation.

### 2.2.3 Recovery and purification of chemicals

The use of reactive distillation for the recovery of chemicals was first put to invention through the recovery of lactic acid (Schopmeyer and Arnold, 1944). They described that the process was carried out by the reaction of crude lactic acid with methanol in the presence of a homogenous catalyst in the form of sulphuric acid. The conventional recovery process of distillation followed by the hydrolysis of lactate ester was complex, and uneconomical because of the high costs of equipment and low purity of the recovered lactic acid. Doherty and Buzad (1992) investigated the reactive distillation technology for the recovery of pure lactic acid. Choi and Hong (1999) developed a batch reactive distillation system using acidic cation exchange resins for the recovery of lactic acid.

Kolah and Sharma (1995) and Chopade and Sharma (1997a, b) worked towards the removal of formaldehyde from aqueous solutions using reactive distillation using methanol or ethanol with ethylene glycol. This method not only solves the problem of reducing the environmentally damaging formaldehyde concentration in the aqueous streams to parts per million (ppm) levels but also produce useful acetal products. Bock *et al.* (1997) investigated the recovery of myristic acid using isopropanol. Xu *et al.* (1999) looked at the recovery of acetic acid using ion exchange resins in the form of Amberlyst 15 enclosed in catalyst baskets, and obtained results of more than 50% recovery in a 1.5 m high column. Saha *et al.* (2000) worked towards the recovery of acetic acid from their aqueous solutions through the reaction with *n*-butanol in a reactive distillation column. Mahajani (2000) reported that glyoxylic acid could potentially be recovered from its aqueous solutions through the formation of their esters and acetals. Chopade *et al.* (2003) used the reactive

distillation process for the recovery of ethylene and propylene glycol from a mixed polyol aqueous solutions resulting from the hydrogenolysis of sugars. Bianchi *et al.* (2003) proposed to clean industrial water from acetic acid by reacting with *n*-butanol and 2-ethyl-1-hexanol.

Sharma (1995) described the use of reactive distillation for the purification of phenol, which is used as a raw material for the reaction with acetone to produce high purity bisphenols. Bisphenols are industrially important intermediates used in the manufacture of epoxy resins and polycarbonates. The purity requirement of the phenol raw material is very high, of which the main impurities of acetone, mesityl oxide and hydrotropaldehyde have to be reduced to very low levels (less than 10 ppm).

### 2.2.4 Hydrogenation/hydrodesulfurisation/hydrocracking/dehydrogenation

The dual advantages of removing benzene as an undesirable carcinogenic impurity in gasoline (Sharma and Mahajani, 2003) and the alternative production of cyclohexane to meet its increasing demand as a main precursor for the manufacture of nylon products (Hiwale *et al.*, 2004), have made reactive distillation towards the production of cyclohexane through the hydrogenation of benzene a very desirable process. Gildert (2001) patented the invention of this process. High conversions of benzene (90%) and almost 100 % selectivity of cyclohexane have been reported with the use of reactive distillation. Gildert and Loescher (2001) patented the hydrogenation of diisobutene in a reactive distillation column towards the synthesis of isooctane. Kolah *et al.* (2001) stated that the isooctane product could be an alternative fuel additive for MTBE. Saayman *et al.* (2003) patented the use of reactive distillation for the production of methyl *iso*-butyl ketone (MIBK) through the hydrogenation of acetone via mesityl oxide.

Podrebarac *et al.* (2001) and Groten and Loescher (2002) patented the reactive distillation method in removing organic sulphur compounds from petroleum distillate streams with very promising results of the sulphur content being less than 50 ppm (Hiwale *et al.*, 2004). Tung (2002) patented a modification in reactive distillation technology through the implementation of

a stripped reactive distillation column to overcome the problem of the undesirable cracking of the recycled lighter compounds during the cracking of heavy petroleum in a reactive distillation column (Mukherjee and Louie, 2003). The modification prevented the re-entry of the lighter product in the reactive zone and hence the undesirable cracking. Vargas-Villamil *et al.* (2004) implemented catalytic distillation for the light gas oil hydrodesulphurisation process, during which the catalytic distillation process produced diesel with a lower concentration of sulphur compounds than the traditional reaction/separation process. Viveros-García *et al.* (2005) worked towards achieving the higher demands of producing ultra-low sulphur diesel through the implementation of reactive distillation, with the European Union agreeing that the maximum permissible sulphur content in diesel should be reduced from 350 parts per million by weight (wppm) to 50 wppm from the year 2005.

A very interesting work was proposed by Shinya *et al.* (2003) and Shinohara *et al.* (2004) which involved the generation of hydrogen for fuel cells under reactive distillation conditions in the presence of carbon supported platinum-based catalysts. The hydrogen source for the fuel cell was obtained through the dehydrogenation of decalin, after which the naphthalene product as a result of dehydrogenation could be removed from the vehicle for off board hydrogenation. Preliminary studies carried out have shown much higher hydrogen evolution rates and conversions under relatively milder temperature conditions for the fuel cells.

### 2.2.5 Other processes

Fuchigami (1990), Pöpkén *et al.* (2001) and Xiao *et al.* (2001) reported that reactive distillation could be used for the hydrolysis of methyl acetate, which is produced in great amounts as a by product from purified terephthalic acid and polyvinyl alcohol plants. Xiao *et al.* (2001) reported an estimated figure of 1.5-1.7 tons of methyl acetate for every ton of polyvinyl alcohol produced. As methyl acetate is a low cost commodity chemical, the purpose is to produce more valuable methanol and acetic acid from the hydrolysis process.

The hydration of ethylene oxide by reactive distillation to produce ethylene glycol had been looked at by several researchers (Ciric and Miao, 1994; Ciric and Gu, 1994; Monroy-Loerena and Alvarez-Ramirez, 1999; Liu *et al.*, 2002). Frank *et al.* (2002) and Zhang *et al.* (2002) investigated the synthesis of cyclohexanol through the hydration of cyclohexene by reactive distillation because the conventional distillation process involves the difficult separation of close boiling components in the form of benzene, cyclohexene and cyclohexane (Hiwale *et al.* 2004). Sharma and Mahajani (2003) reported that reactive distillation could also be extended for the hydration of olefins such as isobutylene, propylene, isoamylene and cyclohexene (Smith, 1980, 1993; Gonzalez and Fair, 1997). Knifton *et al.* (1998), Abella *et al.* (1999) and Gotze *et al.* (2001) reported on the dehydration of *tert*-butanol in a reactive distillation column.

Podrebarac *et al.* (1998) and Huang *et al.* (2000) developed a catalytic distillation process for the aldol condensation of acetone to produce diacetone alcohol, which could subsequently be dehydrated to produce mesityl oxide. Chopade (1999) investigated on the use of reactive distillation with the integration of molecular sieve for the ketalization of acetone with diols to produce cyclic ketals. Tustin *et al.* (2000) proposed the use of reactive distillation for the synthesis of vinyl acetate monomer. This was done through the carbonylation of *di*-methyl ether to acetic anhydride, which was followed by the reaction of the acetic anhydride with acetaldehyde in a reactive distillation column to produce vinyl acetate monomer and acetic acid. The acetaldehyde required in the reactive distillation column was formed from the hydrogenation of the co-produced acetic acid. Luo and Xiao (2001) reported the use of reactive distillation for the carbonylation process of ethanol with dimethyl carbonate to produce diethyl carbonate. Fang and Xiao (2004) and Steinigeweg and Gmehling (2004) investigated the transesterification process for the synthesis of dimethyl carbonate and *n*-butyl acetate using reactive distillation respectively, with the latter work involving pervaporation. Dirk-Faitakis and Chuang (2004) proposed the removal of water from ethanol by reacting the near azeotropic ethanol-water mixture with isobutylene in a catalytic distillation column to form *tert*-butyl alcohol, with a portion of the

ethanol reacting to form ETBE. Both *tert*-butyl alcohol and ETBE could be used as oxygenated fuel additives.

Several other patents for different production processes have also arisen because of the immense potential that the reactive distillation process holds. Shoemaker and Jones (1987) reported on the production of cumene through the alkylation of benzene with propylene via the use of catalytic distillation. Feathers and Mansell (1992) patented on the use of catalytic distillation for the chlorination of benzene to produce the chlorinated products. DiGuilio and McKinney (2000) patented the production of ethanolamines through the reaction of ethylene oxide and aqueous ammonia using reactive distillation. Voss (2001) patented the invention of producing acetic acid by reactive distillation based on the carbonylation of dimethyl ether and methanol. The reacting system, through the implementation of reactive distillation, allows for the simultaneous removal of acetic acid and the unconverted carbon monoxide. Netzer (2001) patented the invention of using reactive distillation for the alkylation of benzene with ethylene to produce ethyl benzene. Reactive distillation could also be used for the production of polymer products. Leemann *et al.* (2002) patented the production of polyamides by reactive distillation whilst Cohen *et al.* (2002) patented the production of nylon-6 through reactive distillation. The conventional pipeline reactor for the conversion of 6-aminocapronitrile to nylon-6 requires long residence time which leads to the nylon product degradation. Sharma and Mahajani (2003) reported that the implementation of reactive distillation enhance the conversion and produce good quality polymer in the process. Levin and Santiesteban (2002) patented the use of reactive distillation for the production of phenol. Gelbein (2002) described the epoxidation of propylene to propylene oxide using reactive distillation. Knifton *et al.* (2003) reported the use of reactive distillation to produce linear alkyl benzenes, which is a basic starting material for the manufacture of detergents.

Table 2.1 lists reactions that have been investigated using the reactive distillation technology. These are industrially important reactions that are either carried out on a commercial scale or on a laboratory scale. Besides the

more common esterification and etherification reactions, oligomerisation, isomerisation, hydrogenation and hydrodesulphurisation are some of the more unconventional processes to which reactive distillation has been successfully implemented on a commercial scale. Sharma and Mahajani (2003) and Hiwale *et al.* (2004) reported that some other processes including acetalisation, alkylation and transesterification have also been identified as processes with immense potential for the implementation of reactive distillation.

**Table 2.1.** Industrially important reactions (Sharma and Mahajani, 2003)

Reaction	Catalyst/column internals
<b>Acetalisation</b>	
Methanol + aqueous formaldehyde $\rightarrow$ Methylal + water	Ion-exchange resins, zeolites
Ethanol + aqueous formaldehyde $\rightarrow$ Ethylal + water	Ion-exchange resins
Ethylene glycol + formaldehyde $\rightarrow$ Acetal + water	Ion-exchange resins
<b>Addition of amines to aldehydes/ketones</b>	
Primary amine + mesityl oxide $\rightarrow$ Acetone + imine	Mineral acid
Acroelin + substituted anilines $\rightarrow$ Schiffs base	Mineral acid
<b>Alcoholysis</b>	
Diacetate ester of polytetramethylene ether + alkanol $\rightarrow$ Polytetramethylene ether glycol (PTMEG) + alkanol acetate ester	Alkali metal oxide or alkaline earth metal oxide in the presence of hot methanol

Table 2.1 (Continued)

Reaction	Catalyst/ Column internals
<b>Dimerisation/Oligomerisation</b>	
Oligomerisation of C <sub>4</sub> <i>iso</i> -olefins	Solid phosphoric acid, cation exchange resins
Oligomerisation of linear butanes	Acid catalyst, nickel based catalyst
<b>Esterification with alcohols/olefins</b>	
Acetic acid + methanol → Methyl acetate + water	Dowex 50W X-8, Amberlyst-15, Katamax packing, Sulphuric acid
Acetic acid + butanol → Butyl acetate + water	Cation exchange resin
Acetic acid + 2-methyl propanol → 2-methyl propyl acetate	Katapak-S
Lactic acid + methanol → Methyl lactate + water	Dowex 50-W
Myristic acid + <i>iso</i> -propanol → <i>iso</i> -propyl myristate + water	Dowex 50-W

Table 2.1 (Continued)

Reaction	Catalyst/column internals
<b>Aldol condensation followed by dehydration</b> Acetone $\rightarrow$ <i>di</i> -acetone alcohol (DAA) and mesityl oxide  <i>n</i> -Butaraldehyde $\rightarrow$ 2-ethyl hexenal	Anion exchange resin  Aqueous alkaline solution
<b>Alkylation/trans-alkylation/dealkylation</b> Benzene + propylene $\rightarrow$ cumene  <i>m</i> -Xylene (MX) + di- <i>tert</i> -butyl benzene (TBB) $\rightarrow$ <i>tert</i> butyl <i>m</i> -xylene (TBMX) + <i>tert</i> -butyl benzene  MX + TBB $\rightarrow$ TBMX + benzene  Benzene + ethylene/propylene $\rightarrow$ alkyl benzene  <i>iso</i> -Butane + propylene/butylenes $\rightarrow$ highly branched paraffins	Union carbide-LZY-82 molecular sieves  Zeolite- $\beta$  Zeolite- $\beta$  Zeolite- $\beta$  Lewis acid promoted inorganic oxide catalyst
<b>Amination</b> Alcohols + ammonia $\rightarrow$ amine + water	Hydrogen and hydrogenation catalyst
<b>Carbonylation</b> Methanol/ <i>di</i> -methyl ether + CO $\rightarrow$ acetic acid	Homogenous system

Table 2.1 (Continued)

Reaction	Catalyst/ Column internals
<b>Condensation of aldehydes</b> Formaldehyde $\rightarrow$ trioxane	ZSM-5
<b>Etherification</b> Methanol + <i>iso</i> -butene $\rightarrow$ methyl <i>tert</i> butyl ether (MTBE)	Amberlyst-15
Methanol + <i>iso</i> -amylene $\rightarrow$ <i>tert</i> amyl methyl ether (TAME)	Ion-exchange resin
Ethanol/bioethanol + <i>tert</i> butyl alcohol $\rightarrow$ ethyl <i>tert</i> butyl ether (ETBE) + water	Amberlyst-15
<i>Iso</i> -propanol + propylene $\rightarrow$ <i>di-iso</i> -propyl ether (DIPE)	ZSM 12, Amberlyst-36, Zeolite
<b>Hydration/dehydration</b> Ethylene oxide + water $\rightarrow$ ethylene glycol	Cationic/anionic exchange resins
Isobutene + water $\rightarrow$ <i>tert</i> - butyl ether	Cationic exchange resins
Hydration of propylene $\rightarrow$ <i>iso</i> -propanol	Cationic exchange resins
Hydration of <i>iso</i> -amylene $\rightarrow$ <i>tert</i> -amyl alcohol	Amberlyst-15
Hydration of cyclohexene $\rightarrow$ cyclohexanol	SiO <sub>2</sub> /Ga <sub>2</sub> O <sub>3</sub>

Table 2.1 (Continued)

Reaction	Catalyst/column internals
<b>Hydrolysis</b> Methyl acetate + water $\rightarrow$ methanol + acetic acid  Acrylonitrile $\rightarrow$ acrylamide	Ion-exchange resin bags fluidized RD  Cation exchanger on inert copper oxide catalyst
<b>Hydrogenation/hydrodesulphurisation/ dehydrogenation</b> Hydrogenation of alkyl anthraquinone  Hydrogenation of benzene to cyclohexane  Hydrogenation of mesityl oxide to methyl <i>iso</i> -butyl ketone (MIBK)  Hydrodesulphurisation of vacuum gas oil  Hydrogenation of butadiene	Alumina supported nickel catalyst  Alumina supported nickel catalyst  Bifunctional catalyst: cation exchange resin with palladium/nickel  Hydrogenation catalyst with acidic support  Alumina supported palladium oxide

Table 2.1 (Continued)

Reaction	Catalyst/column internals
<b>Hydrogenation/hydrodesulphurisation/ Dehydrogenation</b>  Methanol from synthesis gas	Copper/zinc/alumina in the presence of inert solvent (C <sub>7</sub> - C <sub>12</sub> )
<b>Isomerisation</b> $\alpha$ -Isophorone $\rightarrow$ $\beta$ -isophorone  But-2-ene $\rightarrow$ but-1-ene  But-1-ene $\rightarrow$ but-2-ene  <i>n</i> -Paraffin to <i>iso</i> -paraffins	Adipic acid, ZSM-S, alumina  Alumina supported palladium oxide  Standard hydrogenation catalyst  Chlorinated alumina catalyst
<b>Metathesis/ disproportionation</b> But-1-ene $\rightarrow$ propylene + pentene  But-1-ene $\rightarrow$ ethylene + <i>trans</i> - hex-2-ene	Activated metal oxide  Activated metal oxide

Table 2.1 (Continued)

Reaction	Catalyst/column internals
<b>Neutralisation (protonation of organic bases)</b> Pyridines + carboxylic acids $\rightarrow$ pyridinium salts	Alkali catalyst (NaOH)
Propylene oxide from propylene chlorohydrin	Alkali catalyst (NaOH)
<b>Production of <i>di</i>-ethanol amine</b> Monoethanolamine + ethylene oxide $\rightarrow$ <i>di</i> -ethanol amine	No catalyst or ion exchange resins
<b>Transesterification</b> Polytetramethylene glycol diacetate + methanol = polytetramethylene glycol + methyl acetate	lead, zeolites, phenol as entrainer
Diakyl carbonate + phenol/ethanol $\rightarrow$ diaryl carbonate + alcohol	lead, zeolites, phenol as entrainer
Acetic acid + vinyl stearate $\rightarrow$ stearic acid + vinyl acetate	lead, zeolites, phenol as entrainer

## 2.3 ADVANTAGES AND DISADVANTAGES OF REACTIVE DISTILLATION

### 2.3.1 Advantages of reactive distillation

Malone and Doherty (2000) highlighted that the reactive distillation method has received a great deal of attention in recent years because of its demonstrated potential for capital productivity improvements (by overcoming very low reaction equilibrium constants, and by avoiding or eliminating difficult separations). Taylor and Krishna (2000) and Tischmeyer and Arlt (2004) highlighted several advantages through the application of reactive distillation. First and foremost, the simplification and elimination of the

separation system can lead to significant capital cost savings. One process step alongside the associated pumps, piping and instrumentation are eliminated by carrying out the chemical reaction and distillation in the same vessel (Malone and Doherty, 2000). Okur and Bayramoglu (2001) reported that the flow sheets of reactive distillation tend to be much simpler and have fewer recycle streams as compared to those of conventional technology. Voss (2001) stated that the implementation of reactive distillation for the carbonylation of *di*-methyl ether/methanol has led to a replacement of several operation units carried out through the conventional scheme. Chiang *et al.* (2002) presented a comparison between a coupled reactor/column and reactive distillation for the synthesis of amyl acetate, and found that reactive distillation is four times more efficient than the former configuration in terms of the total annual cost. Vargas-Villamil *et al.* (2004) highlighted that the light gas oil hydrodesulphurisation process via catalytic distillation was operated at a lower cost than the traditional reaction/separation process, in addition to the advantage of producing diesel with a lower concentration of sulphur compounds. Luyben *et al.* (2004) made comparisons between the conventional and reactive distillation processes for the production of butyl acetate, and found that the reactive distillation process had a 20% lower total annual cost. DeGarmo *et al.* (1992) stated that the implementation of reactive distillation processes overcame limitations due to reaction equilibria and azeotropes by removing products from the reaction zone and by consuming azeotrope forming components in the reaction. There was an improved conversion of reactants with the application of reactive distillation resulting from the direct removal of products or intermediates formed (Steinigeweg and Gmehling, 2003). This increase in conversion gave a benefit in reduced recycle costs. Subawalla and Fair (1999) reported that there was also improved selectivity of the desired products such that removing one of the products from the reaction mixture can lead to the reduction of the rates of any side reactions and formation of side products that may occur. As a result, the reaction can proceed to a much higher level of conversion with reactive distillation than without separation. Isla and Irazoqui (1996) reported that higher yields could also be attained by the continuous recycling of unconverted reactants into the reaction section with the enriched liquid reflux

stream. Gildert *et al.* (1998) reported a highly selective separation in the hydrogenation of benzene to cyclohexane using reactive distillation. Abella *et al.* (1999) and Gotze *et al.* (2001) reported enhanced conversions of *tert*-butanol with the implementation of reactive distillation. Shoemaker and Jones (1987) highlighted that the catalytic distillation process produced cumene of extremely high purity with a range of feed purities. It was reported that catalytic distillation gave the same high conversions and yields with the propylene feed concentration ranging from 30 to 99% (w/w). There was also a reduction in excess raw material usage. Liu *et al.* (2002) and Hiwale *et al.* (2004) reported that the mole proportion of water to ethylene oxide for the hydration of ethylene oxide to ethylene glycol may be reduced from 20:1 to 3:1 with the use of reactive distillation. Moreover, reactive distillation allows for the suppression of the decrease in the activity of the catalyst (Netzer, 2001). Cohen *et al.* (2002) reported that the implementation of reactive distillation for the production of nylon-6 overcame the limitation of long residence time associated with the conventional production process, which would have led to the nylon product degradation. In addition, with the application of reactive distillation, there is an avoidance of azeotropes because the reactive distillation conditions can allow the azeotropes to be "reacted away" in a single vessel. Fernholz *et al.* (2000) reported that reactive distillation is also beneficial such that if the reaction is exothermic, the heat of reaction can be used to facilitate the heat of vaporisation and hence reduce the reboiler duty. DeGarmo *et al.* (1992) reported that some chemical reactions have significant heats of reaction which may be exothermic or endothermic. This may lead to a dramatic change in the temperature of the reaction mixture as the reaction progresses in an adiabatic reactor. This marked temperature change will shift the chemical equilibrium unfavourably, lower the conversion, reduce the selectivity and possibly detrimentally affect the catalyst stability. The capital cost of the equipment for such reactions in a conventional process would go up because good design would have to accommodate for interstage cooling for exothermic reactions and inter-stage heating for endothermic reactions, with the provision of heat transfer area inside the reactor as an alternative. However, if the same reactions were carried out using reactive distillation technology, the heat of reaction in a

reactive distillation will not affect the temperature and the reaction equilibrium in turn. The exothermic heat would not affect the catalyst stability. The heat of reaction promotes additional mass transfer between the liquid and vapour phases, over and above the level of mass transfer that would occur for the distillation process alone. The temperature of the phase where the reaction occurs will be the bubble (or dew) point temperature at its composition, and will be uniform and constant across the cross-section of the reactive distillation column. As a result, there is no need for interstage heat transfer equipment to remove or supply the heat of reaction and a substantial reduction in energy use, leading to significantly lower investment and operational costs (Tuchlenski *et al.*, 2001; Steinigeweg and Ghemling, 2002). Shoemaker and Jones (1987) reported an effective utilisation of the reaction exotherm with the application of reactive distillation for the alkylation of benzene with propylene to form cumene. Their studies showed a net high-level heat requirement was  $223.41 \text{ kJmol}^{-1}$  of cumene produced with the implementation of reactive distillation whereas another non-reactive distillation process would have required a net heat input of  $335.24 \text{ kJmol}^{-1}$  of cumene produced. Ciric and Miao (1994) and Liu *et al.* (2002) stated that the hydration process of ethylene oxide to ethylene glycol is exothermic and the heat could be utilised effectively to provide the boil-up for fractionation. Levin and Santiesteban (2002) reported that the use of reactive distillation for the production of phenol substantially reduces the reboiler duty because of the exothermic nature of the reaction, thus making the process cost effective.

Other advantages associated with the implementation of reactive distillation were reported. Gildert *et al.* (1998) reported that the implementation of reactive distillation for the hydrogenation of benzene to cyclohexane allows for efficient contact of hydrogen and benzene and the *in-situ* washing of the nickel catalyst by reducing polymer build-up and coking, which increases the catalyst's life. Subawalla and Fair (1999) stated that reactive distillation was advantageous because the removal of the desired product also reduces the chances of product degradation. Voss (2001) reported that catalyst deactivation, precipitation and losses are prevented through the elimination of flash vaporization with the implementation of reactive distillation for the

carbonylation process towards the synthesis of acetic acid. Knifton *et al.* (2003) stated that the continuous removal of aqueous product from the reaction system producing linear alkyl benzenes through reactive distillation ensures long catalyst life. Qi and Zhang (2004) demonstrated through experiments guided by modelling work that the implementation of reactive distillation for the alkylation of benzene with ethylene would allow for a longer catalyst life. This was based on simulation results that predicted a very low liquid composition of ethylene in most of the catalyst bed, which was a contributing factor towards the heavy deactivation of the catalyst through the conventional method.

### 2.3.2 Disadvantages of reactive distillation

Despite the advantages associated with the application of reactive distillation, Towler and Frey (2000) highlighted some constraints associated with the use of this separation technique. The reagents and the products must have suitable volatility to maintain high concentrations of reactants and low concentrations of products in the reaction zone. Moreover, it would be uneconomical to implement reactive distillation if the residence time for the reaction is long. A long residence time would require a large column size as well as large tray hold-ups; it would be more economical then to use a conventional reactor-separator arrangement. Furthermore, it is difficult to design reactive distillation processes for very large flow rates because of liquid distribution problems in packed reactive distillation columns. In addition, there may be a mismatch of process conditions for reaction and distillation because reactive distillation is an integration of both processes i.e. the two operations occur simultaneously in a reactive distillation column. The optimum conditions of temperature and pressure for distillation may be far from optimal for reaction and *vice versa*. DeGarmo *et al.* (1992) stated that a chemical/catalyst system for which the distillation and reaction temperature overlap is very ideally suited for the implementation of reactive distillation. Luyben (2000) stated that reactive distillation columns are occasionally operated with an excess of one of the reactants, for which the disadvantage would be the requirement of recovering and recycling of the excess reactant, usually through the installation of a second recovery column.

## 2.4 CATALYSIS

A catalyst is defined as a substance which is capable of increasing the rate of a reaction without itself undergoing a permanent chemical change. DeGarmo *et al.* (1992) stated that a chemical/catalyst system in which the preferred temperature range of the catalyst either matches or substantially overlaps that for the distillation would be a very suitable choice of catalyst for reactive distillation. Catalysts can be classified as homogenous (e.g. sulphuric acid), heterogeneous (e.g. porous solid resins) or biological (e.g. enzymes). Bond (1987) defined homogenous catalysis occurring when the catalyst is in the same phase as the reactants and no phase boundary is existent. A phase is defined as a boundary between two components, even if they may exist in the same physical state e.g. a mixture of oil and water consist of two phases. In homogenous catalysis, a small catalyst molecule or ion is consumed in an early reaction step and is restored in a later step. Homogenous catalysis can take place either in the liquid phase e.g. acids and bases catalysing the mutarotation of glucose or in the gas phase e.g. nitrogen oxide catalysing the oxidation of sulphur dioxide. Heterogeneous catalysis is defined as catalysis occurring when a phase boundary separates the catalyst from the reactants. In heterogeneous catalysis, one or more reactants are adsorbed or immobilised at the active catalytic sites on the surface of the catalyst. An active site is a part of the catalyst surface which is particularly good at adsorbing molecules and helping the reactant molecules to react. However, this might involve an actual reaction with the catalyst surface, during which the forces active at the solid catalyst surface distort or even dissociate an adsorbed reactant molecule, and hence increase the rate of reaction. Table 2.2 is an illustration of the possible phase combinations for heterogeneous catalysis.

**Table 2.2.** Phase combinations for heterogeneous catalysis (Bond, 1987)

Catalyst	Reactant	Example
Solid	Liquid	Decomposition of hydrogen peroxide catalysed by gold
Solid	Gas	Ammonia synthesis catalysed by iron
Liquid	Gas	Polymerization of alkenes catalysed by phosphoric acid
Solid	Liquid + Gas	Hydrogenation of nitrobenzene to aniline catalysed by palladium

A reaction catalysed by a heterogeneous catalyst can be represented by a flow chart as illustrated in Figure 2.3.

Step 1	Reactant + Catalyst
Step 2	Reactant/Catalyst complex
Step 3	Product/Catalyst complex
Step 4	Product + Catalyst

**Figure 2.3.** Reaction schemes in a heterogeneous catalysed process.

DeGarmo *et al.* (1992) highlighted that the reactive distillation technique was first applied in the 1920s to accelerate esterification processes using homogenous catalysts. Although mineral acids such as sulphuric acids have been used in previous esterification reactions (Sawistowski and Pilavakis, 1979, 1988; Agreda *et al.*, 1990; Backhaus 1921; Agreda and Partin, 1984), such mineral acids could not be used in the process ideally because they would contaminate the water leaving the reactive distillation column. In industrial applications, the quantity of mineral acid used as a catalyst is limited because a high acid concentration would give rise to an increased

corrosion of equipment and poses separation problems as well. Moreover, problems would arise with waste disposal with the use of homogenous catalyst. It was almost fifty years later that the invention of employing reactive distillation for reactions relying on a solid heterogeneous catalyst was patented (Sennewald *et al.*, 1971). Fernholz *et al.* (2000) stated that the synthesis of methyl acetate could be carried out by homogenous catalysis via the use of sulfonic acid or by heterogeneous catalysis whilst using a solid catalyst. Hiwale *et al.* (2004) reported that the recovery of lactic acid was difficult to apply on the industrial level because of corrosion and separation problems together with the occurrence of side reactions associated with the use of homogeneous catalysts. Heterogeneous catalysis systems have become increasingly popular since they have been introduced. This is partly due to heterogeneous catalysis systems being able to overcome some of the shortfalls that are related to the use of homogenous catalysis systems. Amongst the advantages of heterogeneous catalysis are being regenerable, having a non-toxic nature, ease with handling, safe to store, long lifetime, high tolerance towards a wide range of temperatures and pressures as well as safe disposal. In addition, Steinigeweg and Ghemling (2003) reported that size and location of the reactive section can be chosen, and corrosion problems could be minimised with the use of heterogeneous catalysts. In industrial processes, heterogeneous catalysis dominates strongly with an overwhelming 85% of all known catalytic processes conducted in this manner. The main reason for its dominance is subsequent catalyst separation after its use. In industrial applications, the amount of mineral acids used as catalyst is limited because a high acid concentration will give rise to an increased corrosion of the equipment. There is the added issue of recovering the liquid catalysts which is usually very expensive (Noeres *et al.*, 2004). Harmer and Sun (2001) highlighted that the advantages of the use of a solid acid catalysts such as ion exchange resins include reduced equipment corrosion, ease of product separation (e.g. by filtration or centrifugation), less potential contamination in the waste streams as well as recycle of the catalyst. Sharma and Mahajani (2003) reported that the use of a solid catalyst offers non-corrosive operating conditions so that a less expensive material of construction could be used. If heterogeneous catalysts are used, the catalytic

capacity can be increased dramatically by increasing the amount of catalyst without worrying about environmental concerns that are associated with the disposal of corrosive mineral acids. Furthermore, heterogeneous catalysts such as ion exchange resins could be tailored to suit specific operational requirements in terms of particle size, pore volume, surface area and swelling capability in solvents. Sharma (1995) stated that the drive for clean, safe and selective processes will lead to more extensive adoption of cationic exchange resins as catalyst for small, medium and large scale production for a wide variety of speciality and bulk chemicals e.g. the manufacture of methyl tertiary butyl ether (MTBE), ethyl tertiary butyl ether (ETBE) and tertiary amyl methyl ether (TAME). Saha *et al.* (2000) stated that ion exchange resins find good applications in reactive distillation columns whereby they play a dual role of catalyst as well as being a form of tower packing.

However, homogenous catalysis systems are still employed in some industrial processes as the choice of heterogeneous catalysis systems has a significant impact on the mechanical design and operation of the reactive distillation column. The main advantage of a homogenous catalysis system is that the catalyst can be added or withdrawn at any one time. However, in the case of the use of a heterogeneous catalyst, there is a need for special mechanical design to accommodate for the replenishment of the catalyst. Otherwise, the catalyst would have to possess a long sustainability in order to avoid constant maintenance.

### 2.4.1 Catalysis by ion exchange resins

The structure of the polymer matrix plays a key role in the catalytic activity of the ion exchange resin. Charkrabati and Sharma (1993) stated that the ion exchange resins can be divided into two groups with major structural differences, namely the gel and "macroreticular" resins. The ion exchange resins are broadly classified according to the amount of divinylbenzene that is used in the resin preparation.

The gelular ion exchange resins are rigid, transparent and spherical beads. Gelular resins are characterized by divinylbenzene content below 12%. A

typical resin bead is a three dimensional homogenous structure with no discontinuities in the pore system. In cases when the gelular beads are totally dry, the polymeric structure collapses and the polystyrene chains will be as close as atomic forces will allow for. The catalytic activity of the gelular resins is negligible unless the reactant is capable of swelling the matrix. This limits the use of gelular resins in a non-swelling medium. Hence, the swelling ability of the reactants is an important prerequisite for catalysis by the use of gelular resins. Furthermore, the swelling of the gelular resins is also dependant on the degree of cross linking within the matrix structure, and the swelling decreases with a higher cross linking density. This leads to poor catalytic activity. Moreover, gelular resins have got poor mechanical strength and are prone to attrition losses during reaction at higher speeds of agitation.

The limitation of the gelular resins was overcome with the advent of the “macroporous” ion exchange resins (Corte *et al.*, 1957). These resins are prepared by polymerisation with high divinylbenzene content in the region of 5-60% in the presence of diluents. During the polymerisation process, phase separation occurs, and after the extraction of the diluents and drying, permanent pores of various sizes are created. When the amount of divinylbenzene is increased, the nuclei are less fused and the surface area is increased. Hence, the reactants can permeate easily into these pores regardless of whether the matrix is swollen by the reacting medium. Since the “macroporous” resins have a fixed pore structure, the reactants can enter the matrix through the macropores and interact with the large number of sulfonic acid sites. The “macroporous” ion exchange resins also show far greater resistance to attrition as compared to gelular resins. Chakrabati and Sharma (1993) stated that the significant difference between gelular and macroporous resins is whereas gel resins can only function in a swelling medium, macroporous resins can function in both swelling and non-swelling solvents.

Taylor and Krishna (2000) highlighted that for heterogeneously catalysed processes, hardware design poses considerable challenges. The catalyst particle sizes used in such operations are usually in the 1-3 mm range. However, larger particle sizes may lead to intra-particle diffusion limitations.

To overcome the limitations of flooding within the column, the catalyst particles have to be enveloped within wire gauze envelopes. The most common practice is that the catalyst envelopes are packed inside the column. Several catalyst envelopes of almost every conceivable shape has been patented and some of these structures are exemplified as follow (Taylor and Krishna, 2000):

- (i) Porous spheres filled with catalyst (Buchholz *et al.*, 1995; Johnson, 1993) (Figure 2.4a)
- (ii) Cylindrical shaped envelopes with catalysts inside them (Johnson, 1993) (Figure 2.4b)
- (iii) Wire gauze envelopes with various shapes: spheres, tablets, doughnuts, *et al.* (Smith, 1984) (Figure 2.4c)
- (iv) Horizontally disposed wire-mesh “gutters”, filled with catalyst (Figure 2.5a)
- (v) Horizontally disposed wire-mesh tubes containing catalyst (Buchholz *et al.*, 1995; Groten *et al.*, 1998; Hearn, 1993) (Figure 2.5b)
- (vi) Catalyst particles enclosed in cloth wrapped in the form of bales (Johnson and Dallas, 1994; Smith, 1985) (Figure 2.6)

Figure 2.6 shows the configuration as adopted by Chemical Research and Licensing in their reactive distillation technology for the etherification, hydrogenation and alkylation of aromatic compounds (Shoemaker and Jones, 1987).

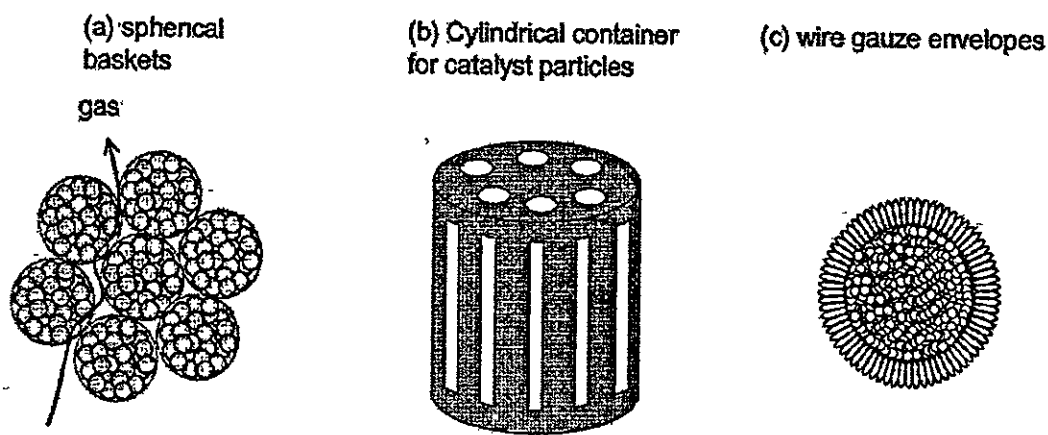


**Figure 2.4.** Various catalyst envelope "tea-bag" configuration (Taylor and Krishna, 2000).

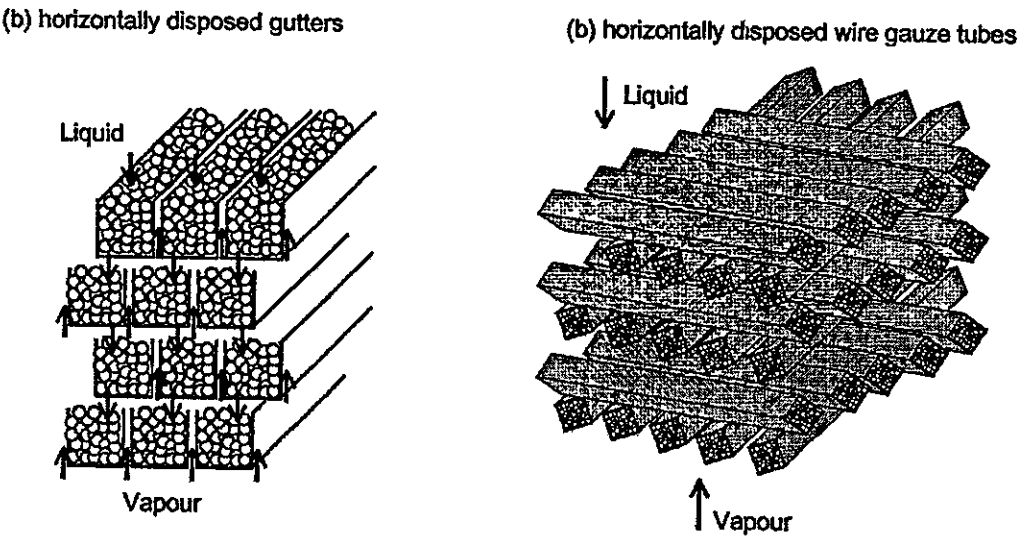


**Figure 2.5.** Horizontally disposed wire-mesh (a) wire gauze gutters and (b) wire gauze tubes containing catalyst (Taylor and Krishna, 2000).

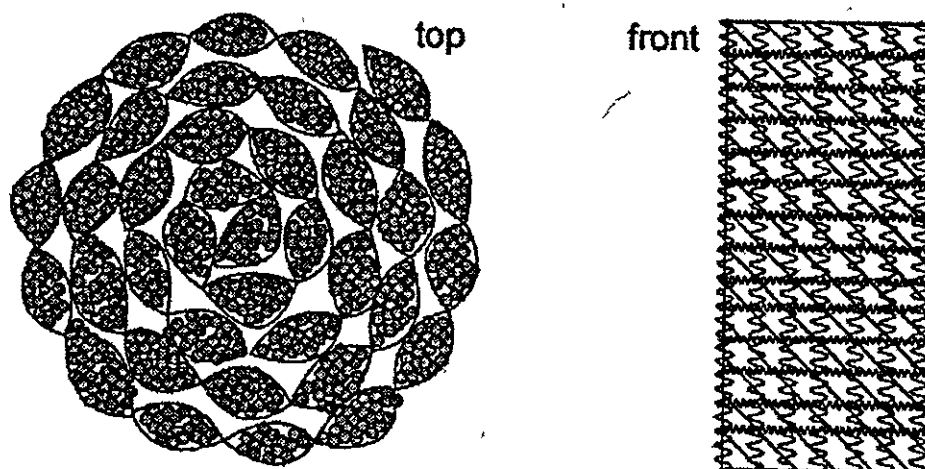


Figure 2.6. Catalyst bales as licensed by Chemical Research and Licensing (Taylor and Krishna, 2000)

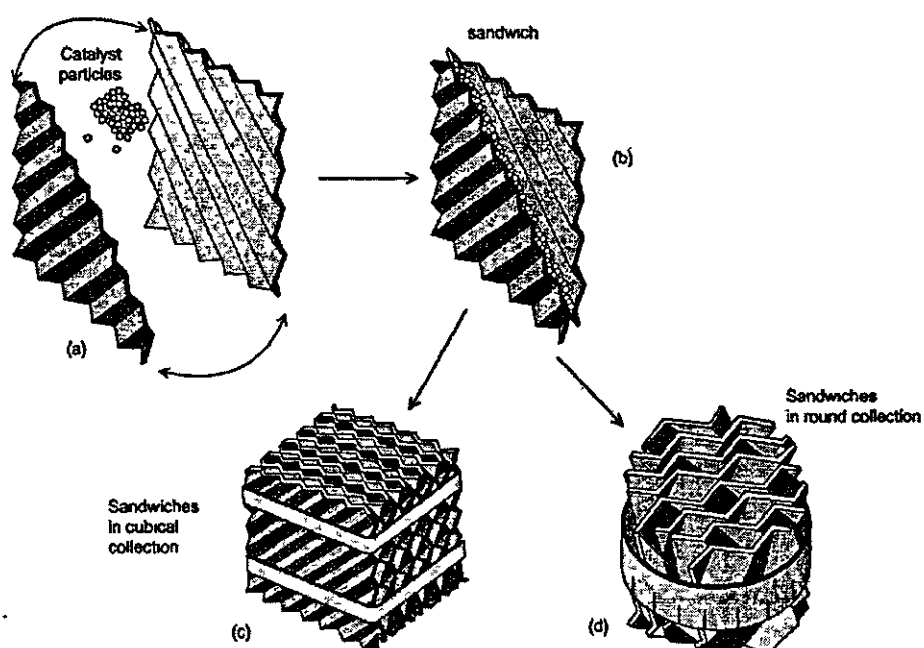
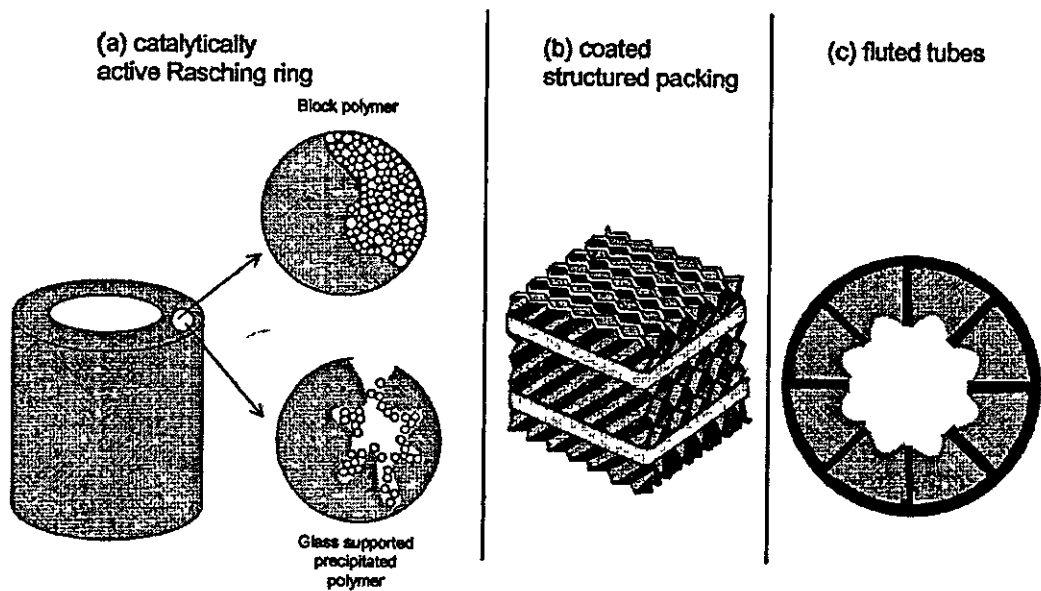
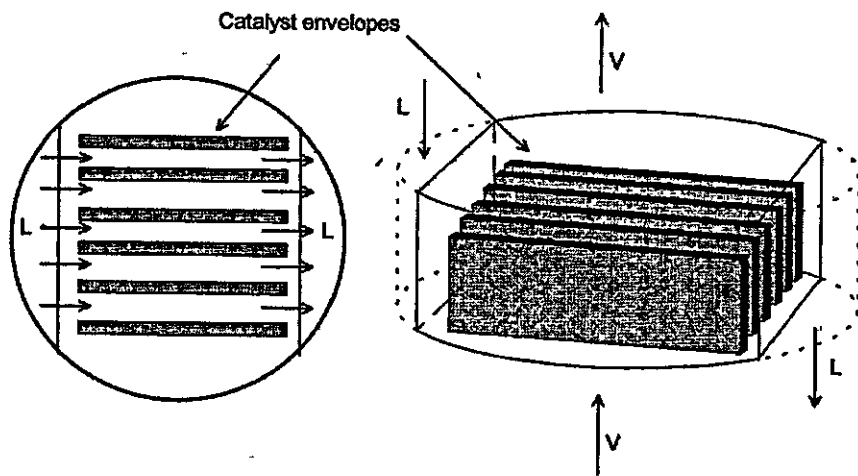


Figure 2.7. Structured catalyst-sandwiches. (a) Catalyst sandwiched between two corrugated wire gauze sheets. (b) The wire gauze sheets are joined together and sewn on all four sides. (c) The sandwich elements arranged into a cubical collection. (d) The sandwich elements arranged in a round collection (Taylor and Krishna, 2000).



**Figure 2.8.** Catalytically active packing. (a) Catalytically active Raschig ring. (b) Structured packing coated with catalyst. (c) Fluted catalyst monolith tubes (Taylor and Krishna, 2000).



**Figure 2.9.** Catalyst envelopes placed along the liquid flow path (Taylor and Krishna, 2000).

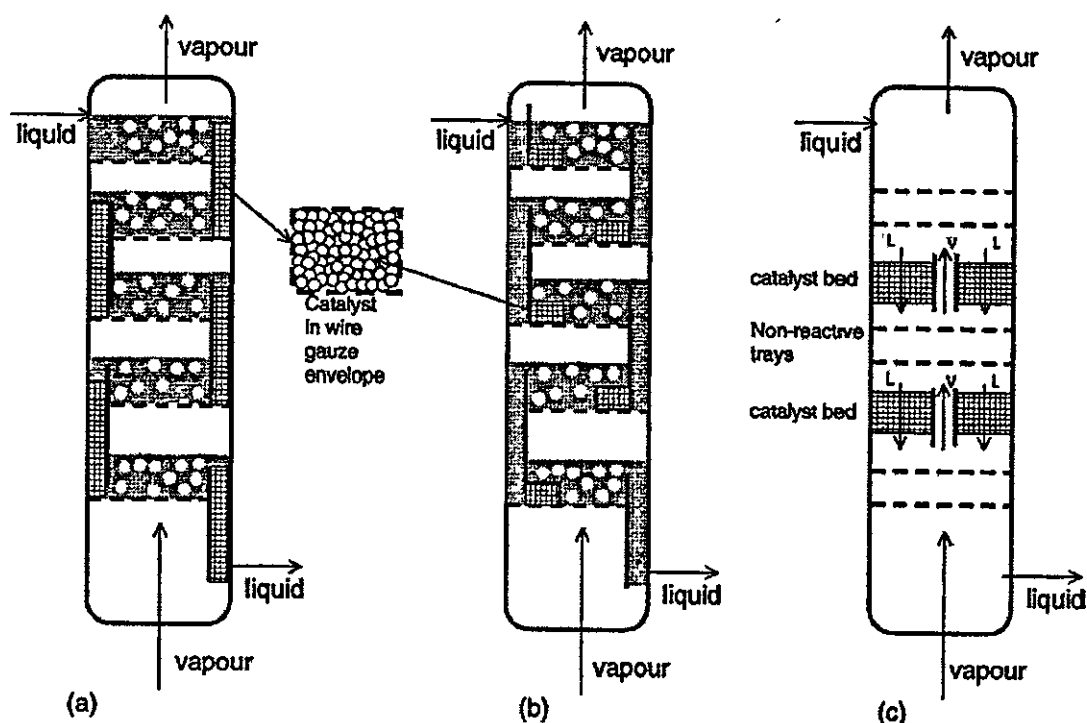


**Figure 2.10.** Counter-current vapor-liquid-catalyst contacting in trayed columns. (a) catalyst in envelopes inside downcomers, (b) tray contacting with catalyst placed in wire gauze envelopes near the liquid exit from the downcomers and (c) alternating packed layers of catalyst and trays (Taylor and Krishna, 2000).

#### 2.4.2 Commercial applications of ion-exchange resins as catalysts

Harmer and Sun (2001) and Gelbard (2005) presented a wide range of applications of the ion-exchange resins as catalysts. Among some of the useful applications are:

- (i) The etherification of olefins with alcohols e.g. the coupling of *iso*-butene with methanol to form methyl *tert*-butyl ether (MTBE). At present, it is the largest volume application of acidic ion-exchange resin in catalysis. Unfortunately, due to the growing concern of water contamination and air pollution caused by MTBE, MTBE is slowly being phased out in the United States. This will lead to a significant increase in the demand for paraffinic alkylates as the octane enhancers (Qi *et al.*, 2002).
- (ii) Ester hydrolysis (Choi and Hong, 1999; Saari *et al.*, 2002).

- (iii) Manufacture of bisphenol-A (an annual turnout of 2 billion) from phenol and acetone through a condensation reaction (Mendiratta, 1983; Kissinger, 1989; Furumoto and Jimi, 1993; Lundquist and Bigwood, 1995; Sugawara et al., 1995; Iwahara, 2001; Banno *et al.*, 2002; Hayashi, 2002; Kissinger *et al.*, 2002; Lundquist, 2002; Webb, 2003).
- (iv) Alkylation of phenols to alkyl phenols (Ito and Ishikawa, 2004).
- (v) Dehydration of alcohols to olefins or ethers e.g. *tert*-butanol dehydration to form *iso*-butene (Abella *et al.*, 1999).
- (vi) Hydration of *iso*-butene to *tert*-butanol (Armor, 1991).

#### 2.4.3 Advantages and disadvantages of ion-exchange resins as catalysts

Chakrabati and Sharma (1993) published a general overview on the use of cationic ion exchange resins as catalysts. Sharma (1995), Harmer and Sun (2001) and Gelbard (2005) reported on the many different types of ion exchange resins being used as catalysts in a reactive distillation column.

The use of ion exchange resins as catalysts offers several advantages. Lorette *et al.* (1959) stated that the reaction rates for the reaction of linear ketones and alcohols to give ketals were higher with the use of acidic ion exchange resins as compared with the use of soluble acids. Sharma (1995) reported that the waste disposal problem through the production of bad effluents associated with the use of homogenous catalysts was eliminated because no washing of the homogenous acid was required. The ion exchange resin matrix, particularly that of the macroporous variety, allows for reactions to be conducted in aqueous as well as non-aqueous, polar or non-polar media. Charkrabati and Sharma (1993) reported that hydrophobic systems could be catalysed by dry macrorecticular resins. It is not feasible to use acid-activated clays in aqueous medium. Moreover, the capital and processing costs are significantly reduced by eliminating the steps and equipment required for catalyst removal. The use of ion exchange resins offer far less corrosive conditions so that a less expensive material of construction could be used. This is due to the heterogeneous nature of the ion exchange resin which meant that the number of acid groups at the surface of the resin bead in

contact with the equipment constitutes a small percentage of the total number of acid groups present and hence obviating the problem of corrosion (Charkrabati and Sharma, 1993). In addition, there is the advantage of higher product purity and yield with lower by-product formation. Kim and Lee (1993) reported that the alkylation of 2-methyl hydroquinone with isobutylene using Amberlyst-15 gave 2-methyl-5-*tert*-butyl-hydroquinone with 93.8% selectivity using ion exchange resins as compared to 82.2% selectivity whilst using sulphuric acid. Helfferich (1962) reported that ion exchange resin catalyst could lead to high selectivity and yields of the desired products in reactions as compared to catalysis by dissolved electrolytes, and this selectivity could be exploited for the separation of close boiling point mixtures. Charkrabati and Sharma (1993) stated that the use of ion exchange resins with the equivalent strength of a strong mineral acid allows for safer handling. Furthermore, the ion exchange resins could often be used in hundreds of catalytic cycles without the need for regeneration, and hence making the catalyst cost (through the use of heterogeneous catalysts) far lower than their homogenous counterparts.

The properties of some of the commercially available ion exchange resins (e.g. Amberlyst, Indion 130, Lewatit, Diaion and Dowex) were included in the review by Sharma (1995). The temperature stability for most of the ion exchange resins is 393 K. In the case of macrorecticular resins, operation at temperatures higher than 423 K for a prolonged period of time may cause desulfonation leading to a release of the sulfonic acid as well as a drop in the catalyst activity. The low thermal stability of ion exchange resins is a limitation towards the use of them as catalysts. However, perfluorinated ion exchange resins such as Nafion can withstand temperatures up to 473 K, but the drawback is that they are very expensive.

The prominence of ion exchange resins have prompted many researchers to carry out various research activities for different chemical processes. Dassy *et al.* (1994) looked at the kinetics of the liquid phase synthesis and hydrolysis of butyl lactate catalysed by the use of cation exchange resin, Amberlyst-15. Rihko and Krause (1995) prompted the investigations for the kinetics of

TAME reactions catalysed by Amberlyst-16. Saha and Sharma (1996) investigated on the esterification of formic acid/ acrylic acid/ methacrylic acid with cyclohexene using macroporous cation-exchange resins, Indion 130 and Amberlyst-15, as catalysts. Kolah *et al.* (1996) looked at the production of methylal by acetalization of formaldehyde with methanol in both batch and continuous reactive distillation columns in the presence of a cation-exchange resin, Indion 130. Xu and Chuang (1996) carried out a detailed study on the kinetics of acetic acid esterification over Amberlyst-15, with subsequent work carried out towards the investigation of the effect of internal diffusion on the same reaction using the same catalyst (Xu and Chuang, 1997). Saha and Sharma (1997) worked on the reaction of dicyclopentadiene with formic acid and chloroacetic acid using different ion exchange resins (Indion 130, Amberlyst-15 and Amberlite IR-120). Chopade and Sharma (1997a) investigated the reaction of aqueous ethanol and aqueous formaldehyde to produce diethoxymethane in the presence of cation-exchange resin, Indion 130, in a reactive distillation column (in both batch and continuous modes). Chopade and Sharma (1997b) used the same catalyst i.e. Indion 130, to prepare 1,3-Dioxolane through the acetalisation of ethylene glycol with formaldehyde.

Ion exchange catalyst in the form of Amberlyst-15 was used by Xu *et al.* (1999) for the recovery of acetic acid by esterification with methanol in a reactive distillation column. Saha *et al.* (2000) looked at the recovery of dilute acetic acid by using ion exchange resins, Indion 130, in stainless steel wire cages. Pöppen *et al.* (2000) used acidic ion exchange resins in the form of Amberlyst-15 sandwiched between Katapak-S structured catalytic packing for the synthesis and hydrolysis of methyl acetate. Cunill *et al.* (2000) looked at the conversion, selectivity and kinetics towards the production of *iso*-propyl *tert*-butyl ether (IPTBE) through the etherification of propanol and *iso*-butene using a macroporous ion exchange resin in the form of Bayer K2631. Mahajan (2000) investigated the recovery of glyoxylic acid from its dilute aqueous solution through esterification with different aliphatic alcohols (namely methanol, *n*-butanol, *iso*-amyl alcohol and 2-ethyl hexanol) using both gelular and macroporous ion exchange resins as catalysts in a reactive

distillation column. The catalysts used in the investigation were Indion-130, Amberlyst-15 and Amberlite IR-120. Lee *et al.* (2000) used the acidic ion exchange resin, Dowex, for their investigation of the kinetics for the esterification process of acetic acid and amyl alcohol, and Amberlyst-15 for the same reaction (Lee *et al.*, 2001)

Liu and Tan (2001) and Lee *et al.* (2002) both investigated the kinetics of the catalytic esterification of propionic acid and *n*-butanol over different acidic cation exchange resins, with the latter using Amberlyst-35 in their investigations and the former using Amberlyst-15, Amberlyst-35, Amberlyst-39 and HZSM-5 pellets. Liu and Tan (2001) found that the Amberlyst series of ion exchange resins was effective for the esterification between propionic acid and *n*-butanol. Steinigeweg and Ghemling (2002) studied on the reactive distillation process for the production of decanoic acid methyl esters through the esterification of fatty acid (decanoic acid) with methanol using Amberlyst-15 as catalysts. Sanz *et al.* (2002) used four different ion exchange resins (Dowex 50W8x, Dowex 50W2x, Amberlyst-15 and Amberlyst-36) for their investigation towards the esterification kinetics of lactic acid with methanol. Yadav and Thathagar (2002) carried out work towards the esterification of maleic acid with ethanol using several heterogeneous catalysts such as Amberlyst-15, Amberlyst-36, Indion-170, Amberlite IRA 120 and 20% DTP/K-10 (dodecatungstophosphoric acid supported on K-10 clay), with the former three catalysts being the more effective amongst the catalysts investigated.

Altıokka and Cıtaç (2003) investigated the esterification of acetic acid with *iso*-butanol in the presence of Amberlite IR-120 catalyst. Gangadwala *et al.* (2003) looked at the esterification kinetics of acetic acid with *n*-butanol in the presence of Amberlyst-15 catalysts.

Schmitt *et al.* (2004) used Amberlyst CSP-2 in their work towards the synthesis of *n*-hexyl acetate. Teo and Saha (2004) investigated the recovery of acetic acid using *iso*-amyl alcohol in the presence of a macroporous ion exchange resin in the form of Purolite® CT-175. Zhang *et al.* (2004) worked

on the esterification of lactic acid with ethanol with various catalysts, with Amberlyst-15 among them.

Cunill *et al.* (2005) studied the dehydration of 1-pentanol to *di-n*-pentyl ether using a gelular type ion exchange resin in the form of Purolite® CT-224. Toukoniitty *et al.* (2005) investigated the esterification of propionic acid with ethyl alcohol over Amberlyst-15 under microwave dielectric heating conditions.

### 2.5. KINETIC RATE EXPRESSIONS

Although it has been previously highlighted that catalysis systems can be classified as either homogenous or heterogeneous systems, this classification is not as clearly defined when ion exchange resins are used as catalysts (Helfferich and Hwang, 1988). There are a few ways of defining the classification of ion exchange resins according to various literatures, and several models have also been proposed for correlating the kinetic data.

Chakrabarti and Sharma (1993) expressed that most resin-catalysed reactions could be classified as either quasi-homogenous (e.g. hydrolysis of sucrose and carboxylic acid) or quasi-heterogeneous (e.g. benzene propylation and isobutene oligomerisation). A simple pseudohomogenous model could be used in the absence of any intraparticle diffusion limitation. This model treats the catalysis by ion exchange resins as homogenous catalysts confined within the resin volume. The pseudohomogenous model has been successfully used for the hydration of olefins (Petrus *et al.*, 1984, 1986) and the dehydration of alcohols (Gates, 1992). Furthermore, Subramaniam and Bhatia (1987) have used the pseudohomogenous kinetic model to correlate the experimental kinetic data of MTBE synthesis satisfactorily. However, the Langmuir-Hinshelwood Hougen Watson (LHHW) or Eley Rideal (E-R) kinetic models have been more widely used for kinetic data correlation (Rehfinger and Hoffmann, 1990; Sundmacher and Hoffmann, 1992; Ancillotti *et al.*, 1977; Gicquel and Torck, 1983; Gates and Johanson, 1969; Cunill *et al.*, 1989), and the application of the kinetic models could be extended over a wider range of concentrations.

Neumann and Sasson (1984) found that the reaction order for the heterogeneous esterification is second order in acetic acid and zero order in methanol, while the kinetics showed that the reaction to be of the intermediate type whereby both diffusion and chemical reaction were controlling partially.

Lee *et al.* (2000) stated that the rate of a heterogeneous reaction is often dependent and related to the external/ internal diffusion, adsorption/ desorption, surface reaction and the non-ideality of the reacting mixtures. Depending on the type of phenomenon occurring, various models have been developed to represent the kinetic behaviours of the heterogeneous esterification. The quasi-homogenous (Q-H) model, which is in the same form as the power law model for homogenous reactions, has commonly been adopted to generate residue curve maps for the design of reactive distillation columns (Venimadhavan *et al.*, 1994). The Q-H model can be derived on the basis of the L-H formalism by assuming that the surface reaction is the controlling step and the adsorption is weak for all components (Xu and Chuang, 1996). However, as the adsorption of the reacting species in the system is appreciable, the adsorption effects should be taken into consideration in the derivation of the kinetic model. Whenever the rate-limiting step is the surface reaction between two adsorbed molecules, the LHHW model is to be used to correlate with the kinetic data. However, the E-R model is applicable if the rate-determining step is the surface reaction between one adsorbed species and one non-adsorbed reactant from the liquid phase (Lee *et al.*, 2000).

Gonzalez and Fair (1997) modified the LHHW formalism (M-L) by introducing an empirical exponent to the activity of water in the rate expression. This was to account for the non-linear distribution of water between the gelular phase of the catalyst and the bulk liquid phase.

Kinetic rate expressions used in reactive distillation models are best written in terms of activities as opposed to the more familiar concentration based rate expression (Venimadhavan *et al.*, 1994). Rihko *et al.* (1997), Lee *et al.* (2000), Sanz *et al.* (2002) and Zhang *et al.* (2004) were amongst many

researchers who expressed their kinetic equations in terms of the activities of the components. Pópken *et al.* (2000) highlighted that the use of activities in the kinetic model instead of the mole fractions resulted in a much smaller residual error. For the esterification system, the rate expression in terms of activities is strongly preferred because the high polarity of water and alcohol compared to the ester product leads to strong non-ideal liquid behaviour. The behaviour of liquid mixtures in the liquid phase reactions may deviate greatly from that of the ideal solution. The non-ideality is particularly significant in aqueous mixtures. The activity coefficients are used to represent this non-ideality of the species in the liquid solutions. Because of the non-ideality of the reaction mixture, the UNIFAC group contribution method has been adopted to determine the activity of the components. Okur and Bayramoglu (2001), Sanz *et al.* (2002) and Zhang *et al.* (2004) used the UNIFAC group contribution method to determine the activity of the components in their work. Okur and Bayramoglu (2001) reported that UNIFAC was well suited for the simulation of ethyl acetate production by reactive distillation.

Xu and Chuang (1996) developed a kinetic equation based on the Q-H mechanism whilst investigating the kinetics of acetic acid with methanol over Amberlyst-15. They developed a kinetic equation which they claimed to be able to be used in the design of a catalytic distillation column to remove low concentrations of acetic acid from wastewater. Rihko *et al.* (1997) developed a kinetic model which was based on the E-R kinetic mechanism for the etherification of *iso*-amylenes with methanol.

Besides Gonzalez and Fair (1997) who first introduced the M-L model to account for the non-linear distribution of water in the catalyst and bulk liquid phase, Lee *et al.* (2000) correlated their experimental data with different kinetic models (LHHW, E-R, Q-H and M-L) and reported that the M-L kinetic model (with an empirical constant value of 3) best represented the kinetic behaviour of the reaction between acetic acid and amyl alcohol using Dowex over wide ranges of temperature and feed composition. Lee *et al.* (2001) reported an empirical constant value of 4 for the M-L kinetic model in representation of the kinetic data for the same reacting system using

Amberlyst-15 as the catalyst. Gangadwala *et al.* (2003) reported that the M-L kinetic model with an empirical constant value of 2 was the best kinetic model that fitted the experimental data for the esterification of acetic acid with butanol. They further reported that the kinetic model gave a slightly better fit to the experimental data if the empirical constant was set as a model parameter. The value of the empirical constant reported was 1.48.

Liu and Tan (2001) correlated their isothermal data with several kinetic models, including the LHHW and E-R models for the esterification of propionic acid with *n*-butanol. The E-R kinetic model gave the best representation of the kinetic data, and the values of the kinetic parameters were reported at different temperatures. However, it was reported that the results could be difficult to apply directly in the simulation and design of a reactive distillation unit, in which the reaction temperatures may differ with the experimental conditions. Lee *et al.* (2002) investigated on the kinetics for the esterification process of propionic acid with *n*-butanol, and found that the LHHW kinetic model best represented the kinetic behaviour of the liquid-solid catalytic esterification over Amberlyst-35.

Yadav and Thathagar (2002) studied the esterification kinetics of maleic acid with ethanol over cation-exchange resin catalysts, and developed a Q-H kinetic model to represent their experimental data. Sanz *et al.* (2002) used different kinetic models (LHHW, E-R and Q-H) and found that the Q-H kinetic model best represented the kinetic data for the reaction between lactic acid and methanol using Amberlyst-15 as catalyst. Altıokka and Cıtak (2003) investigated the esterification of acetic acid with *iso*-butanol in the presence of Amberlite IR-120 catalyst, and found that the E-R kinetic model gave the best representation of the kinetic data for this reaction.

Different kinetic models, including the LHHW, E-R, Q-H and M-L models were tested as part of this work in finding the best kinetic model to represent the behaviour of the heterogeneously catalysed esterification reaction between acetic acid and *iso*-amyl alcohol (see Chapter 4).

### 3. CATALYST CHARACTERISATION AND BATCH KINETIC STUDIES

#### 3.1 INTRODUCTION

The characteristics of ion exchange resins provide the basis for many processes of practical interest involving separations and catalytic reactions. The first part of this chapter presents results on the porous nature of the ion exchange resins (Purolite® CT-124, Purolite® CT-151, Purolite® CT-175 and Purolite® CT-275) through the Density Functional Theory (DFT) model based on nitrogen adsorption, scanning electron microscopy (SEM), elemental analysis, particle size distribution and the determination of the true density.

The optimal design and operation of catalytic processes require a good understanding of the equilibrium behaviour of the multi-component liquid mixtures in contact with sulphonic acid ( $-\text{SO}_3\text{H}$ ) cross-linked polymeric ion exchange resins over a wide range of operating conditions. In addition, an understanding of the reaction kinetics of the catalysed esterification process provides the basis towards determining the nature of the reaction mechanism which is controlling the catalytic process. This work is also directed towards understanding the chemistry of the heterogeneously catalysed reaction. The second part of this chapter presents the batch kinetic results of the catalysed esterification of acetic acid with *iso*-amyl alcohol over a wide range of experimental conditions using Purolite® CT-175 and Purolite® CT-275 ion exchange resins as catalysts along with the detailed descriptions of the analytical methods for the quantitative analysis.

#### 3.2 EXPERIMENTAL

##### 3.2.1 Materials

###### 3.2.1.1 Chemicals

*iso*-Amyl alcohol (99%) was purchased from Aldrich Chemical Company, Inc. Acetic acid (99.8%) and *iso*-amyl acetate (>99% purity) were purchased from Fisher Scientific, United Kingdom. The purity of the chemicals was verified

by gas chromatographic analysis and they were used without further purification.

#### 3.2.1.2 Catalysts

The catalysts used for the tests were ion exchange resins, Purolite® CT-124, Purolite® CT-151, Purolite® CT-175 and Purolite® CT-275 (supplied courtesy of Purolite, United Kingdom). The typical physical and chemical properties of the catalysts are listed in Table 3.1.

The catalyst was pre-treated by first washing several times with water until the supernatant liquid was colourless to remove impurities. The catalyst was subsequently washed with methanol to remove any water sorbed on the catalyst resin. This step aids in avoiding the collapse of the resin pore structure in the subsequent drying process. The washed catalyst was dried in a vacuum oven at 373K for 6 hours. Drying at higher temperatures involves the risk of losing sulfonic acid sites in the form of  $\text{SO}_3$  because of desulfonation of the polystyrene matrix of the catalyst (Teo and Saha, 2004). The dried catalyst was stored in a desiccator prior to further use.

**Table 3.1.** Characteristics of ion exchange resin catalysts.

	CT-124	CT-151	CT-175	CT-275
Polymer matrix structure	Gel styrene divinylbenzene	Macroporous	Macroporous	Macroporous
Moisture retention (H%)	56-61	56-58	52-57	53-57
Specific surface area (m <sup>2</sup> /g)	<i>a</i>	15-25	20-40	20-35
Median pore diameter (Å)	<i>a</i>	250-450	600-700	600-750
Pore volume (ml/g)	<i>a</i>	0.15-0.30	0.4-0.6	0.4-0.6
Total capacity H (eq/L)	1.15	1.7	1.8	<i>a</i>
Screen analysis (microns)	+1000 < 5% -350 < 6%	+1200 < 2% - 425 < 2%	+1190 < 2% - 425 < 2%	+1190 < 2% - 425 < 2%
Temperature limit (K)	418	418	418	418

<sup>a</sup> Data not available

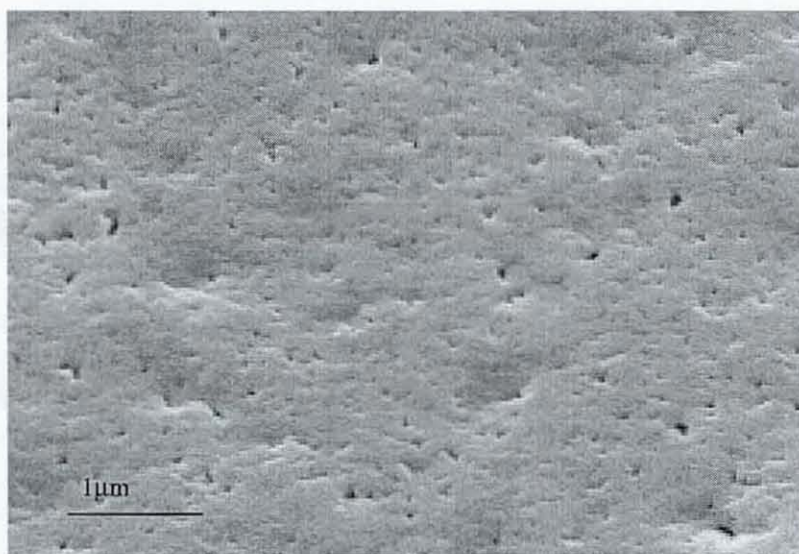
### 3.2.1.2.1 Catalyst Characterisation

#### 3.2.1.2.1.1 Scanning electron microscopy (SEM)

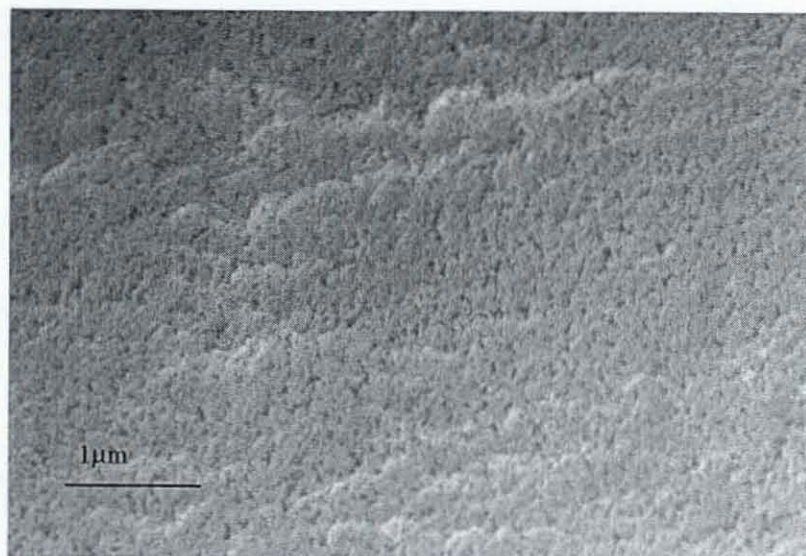
A Carl Zeiss 1530 field emission microscope was used to take the scanning electron micrographs of the different ion exchange resins at room temperature.

The normal secondary electron mode and in-lens detector were used, with the accelerating voltage set at 5 kV.

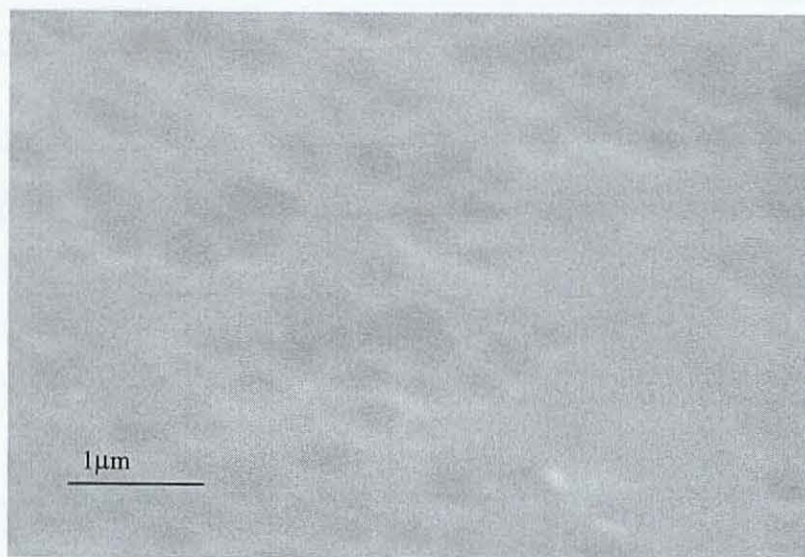
Prior to being analysed, the catalyst sample was dried in a vacuum oven at room temperature, and subsequently mounted on an aluminium platform using polyvinyl acetate (PVA) glue. Since the SEM uses electrons to produce an image, it is a prerequisite for the samples to be electrically conductive. In order to conform to this requirement of the sample being electrically conductive, the sample is coated with gold using a sputter coater. The SEMs of the different ion exchange resins employed for the present research are illustrated in Figures 3.1 to 3.4.



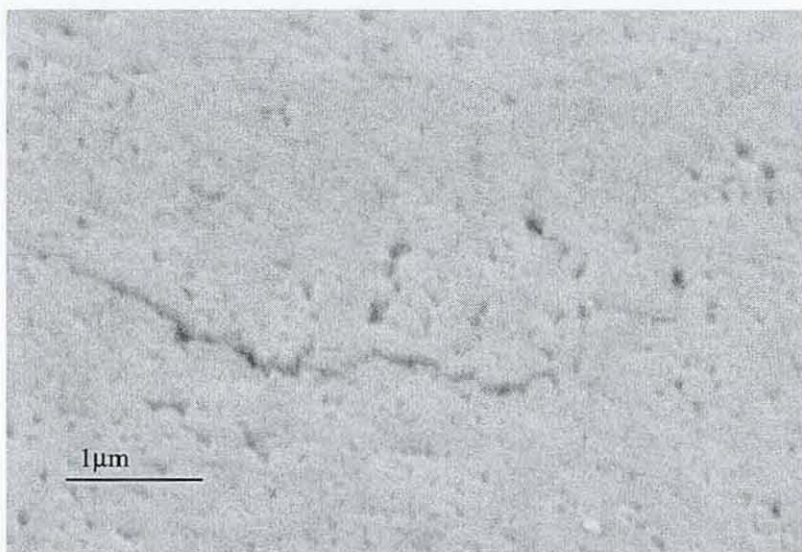
**Figure 3.1.** Scanning electron microscopy image of Purolite® CT-175 ion exchange resin catalyst.



**Figure 3.2.** Scanning electron microscopy image of Purolite® CT-275 ion exchange resin catalyst.



**Figure 3.3.** Scanning electron microscopy image of Purolite® CT-124 ion exchange resin catalyst.



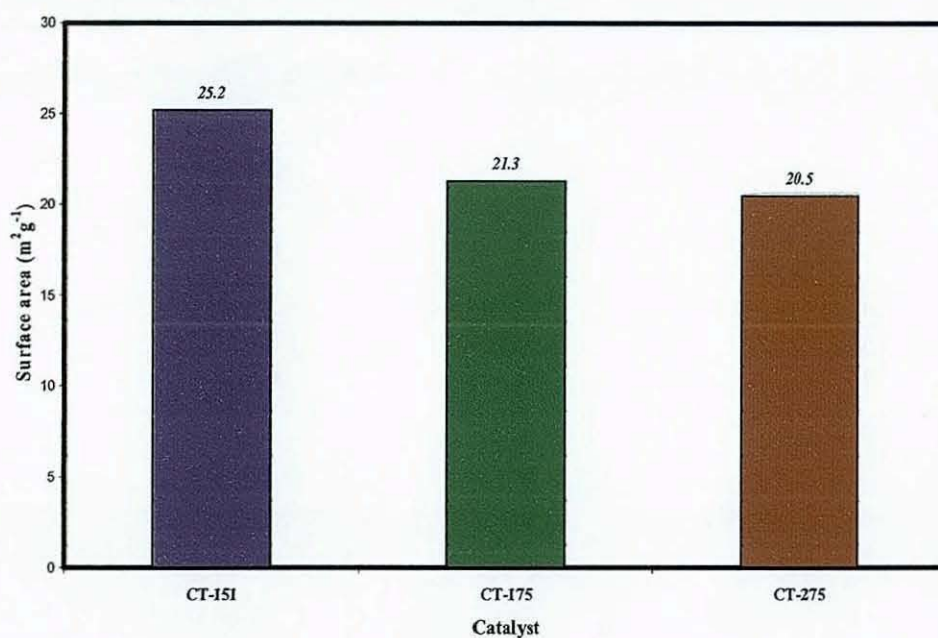
**Figure 3.4.** Scanning electron microscopy image of Purolite® CT-151 ion exchange resin catalyst.

Figure 3.1 presents the microscopic examination of the surface morphology of the Purolite® CT-175 ion exchange resin. It shows agglomerates of microspheres which look like cauliflowers, and smaller nuclei (10-30 nm) more or less fused together are observed within each microsphere. Intermediate pores (20-50 nm), known as mesopores, are accountable for the moderate surface areas. Large pores (50-1000 nm), otherwise known as macropores, are responsible for the pore volume of the catalyst. These large pores allow the reactants to permeate easily into the catalyst structure, regardless of whether the microspheres are swollen by the reactants. Figure 3.2 illustrates the surface morphology of the Purolite® CT-275 ion exchange resin. The figure shows that Purolite® CT-275 ion exchange resin are agglomerates of smaller beads. Figures 3.3 and 3.4 further illustrate the electron micrographs of both Purolite® CT-124 and Purolite® CT-151 ion exchange resins, respectively. Figure 3.3 shows that the surface of Purolite® CT-124 is very smooth and gel-like which corresponds well with its gelular polymer matrix structure as shown in Table 3.1. Figure 3.4 shows that the surface of Purolite® CT-151 has much more cracks than the other ion exchange resins analysed.

### 3.2.1.2.1.2 Surface area, pore volume and pore size distribution

The surface area and pore size distribution of the ion exchange resins were measured by nitrogen adsorption and desorption method using a Micromeritics Accelerated Surface Area and Porosimetry (ASAP) 2010 surface analyser. The weighed catalyst was prepared by being out-gassed at 373.15 K for a minimum period of 24 hours on the de-gas port of the analyser. Surface area was measured for linear relative pressure range between 0.05 and 0.15. Surface area and pore size distribution analysis for all samples were carried out by N<sub>2</sub> adsorption/desorption method at 77 K.

The surface area and pore volume results of the ion exchange resins used in this study are illustrated in Figure 3.5 and Figure 3.6 respectively. Figure 3.5 shows that Purolite® CT-151 has the largest surface area ( $25.2 \text{ m}^2 \text{ g}^{-1}$ ) among the ion exchange resin catalysts analysed while both Purolite® CT-175 and Purolite® CT-275 show almost similar surface area values, with Purolite® CT-175 having a Brunauer-Emmett-Teller (BET) surface area of  $21.3 \text{ m}^2 \text{ g}^{-1}$  while the BET surface area of Purolite® CT-275 sample is  $20.5 \text{ m}^2 \text{ g}^{-1}$ . Furthermore, Figure 3.6 shows that Purolite® CT-175 has the highest pore volume ( $0.31 \text{ cm}^3 \text{ g}^{-1}$ ) among the ion exchange resins analysed. Purolite® CT-275 exhibited a pore volume of  $0.24 \text{ cm}^3 \text{ g}^{-1}$  whilst Purolite® CT-151 showed a pore volume of  $0.17 \text{ cm}^3 \text{ g}^{-1}$ . Figure 3.7 illustrates the surface area to pore volume ratio of the ion exchange resin catalysts.



**Figure 3.5.** BET surface area of Purolite<sup>®</sup> CT-151, Purolite<sup>®</sup> CT-175 and Purolite<sup>®</sup> CT-275 ion exchange resin catalysts.

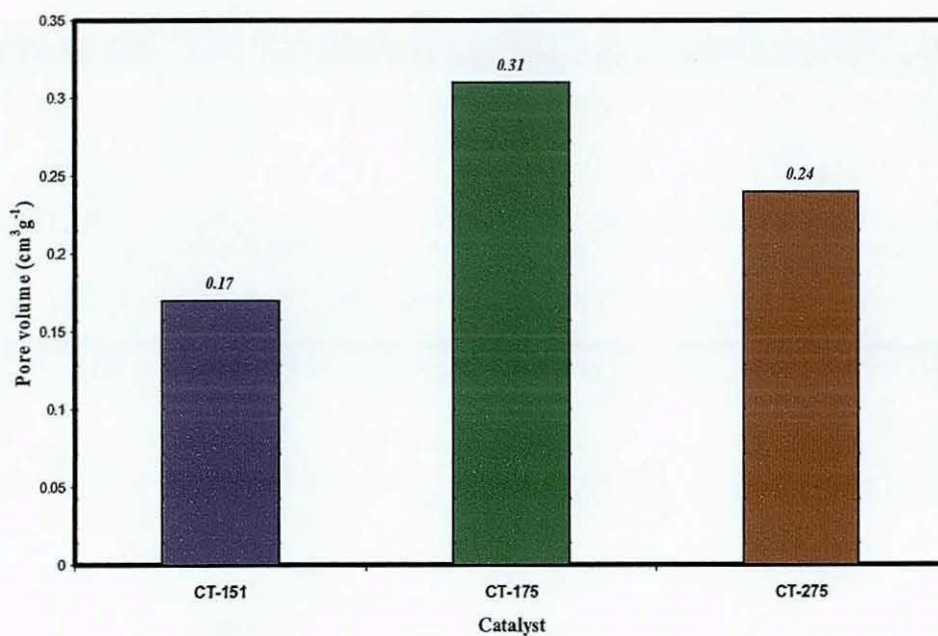


**Figure 3.6.** Pore volume of Purolite<sup>®</sup> CT-151, Purolite<sup>®</sup> CT-175 and Purolite<sup>®</sup> CT-275 ion exchange resin catalysts.

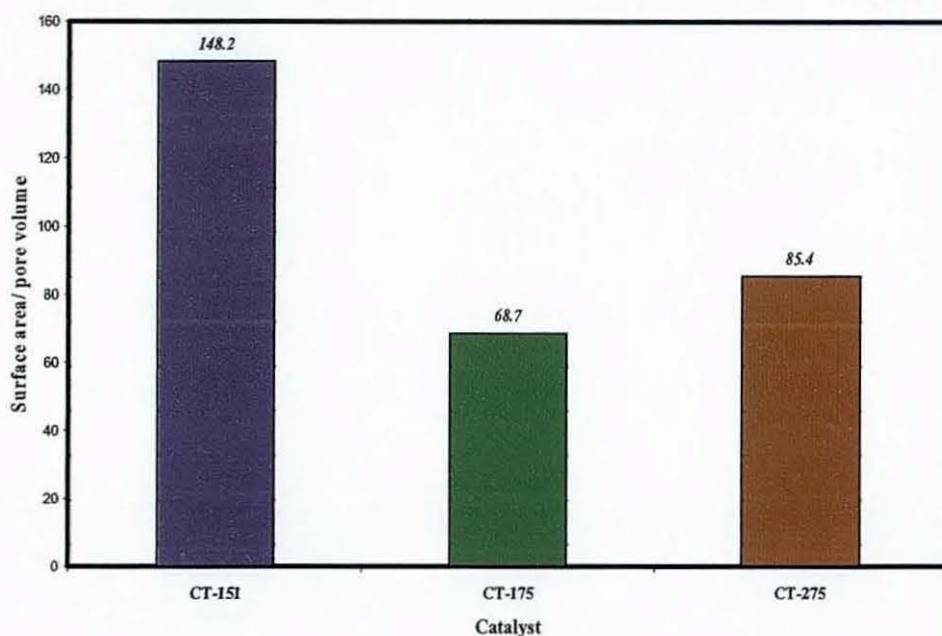


**Figure 3.7.** Surface area/ pore volume ratio of Purolite<sup>®</sup> CT-151, Purolite<sup>®</sup> CT-175 and Purolite<sup>®</sup> CT-275 ion exchange resin catalysts.

The pore size distribution of the ion exchange resins were measured through the Density Functional Theory (DFT) model based on nitrogen adsorption assuming slit pore geometry. The DFT model has been recognised as a powerful tool for the study of inhomogeneous fluids (Olivier, 1998; Saha *et al.*, 2000). The modelled system consists of a single pore represented by two parallel walls separated by a specific distance. The pore is considered to be open and immersed in a single-component fluid at a fixed temperature and pressure. The fluid responds to the walls and reaches an equilibrium under such conditions. The chemical potential at every point equals the chemical potential of the bulk fluid. The bulk fluid is a homogeneous system of constant density and its chemical potential is determined by the pressure of the system using standard equations. The fluid near the walls is not of constant density and its chemical potential is composed of several position-dependent contributions that must total at every point to the same value as the chemical potential of the bulk fluid. At equilibrium, the entire system has a minimum Helmholtz free energy, which is thermodynamically known as the grand potential energy. DFT describes the grand potential energy as a function of the

single particle density distribution and therefore calculates the density profile that minimises the grand potential energy, leading on to the yield of the equilibrium density profile.

Purolite<sup>®</sup> CT-151, Purolite<sup>®</sup> CT-175 and Purolite<sup>®</sup> CT-275 are macroreticular sulphonated styrene divinylbenzene polymeric resins. Figures 3.8-3.10 are representations of the individual pore size distribution for each of the ion exchange resin catalysts. Figure 3.11 shows a comparison of the pore size distribution results for the different ion exchange resin catalysts. Figure 3.11 shows that all the ion exchange resin catalysts are macroporous. The ion exchange resins exhibited significant pore volume in the macroporous regions. However, more prominent access pores are observed in Purolite<sup>®</sup> CT-175 as compared to Purolite<sup>®</sup> CT-151 and Purolite<sup>®</sup> CT-275 which exhibit much less prominent catalyst access pores. It was not possible to obtain the pore size distribution for Purolite<sup>®</sup> CT-124 as the gelular matrix structure collapsed during the course of the analysis.

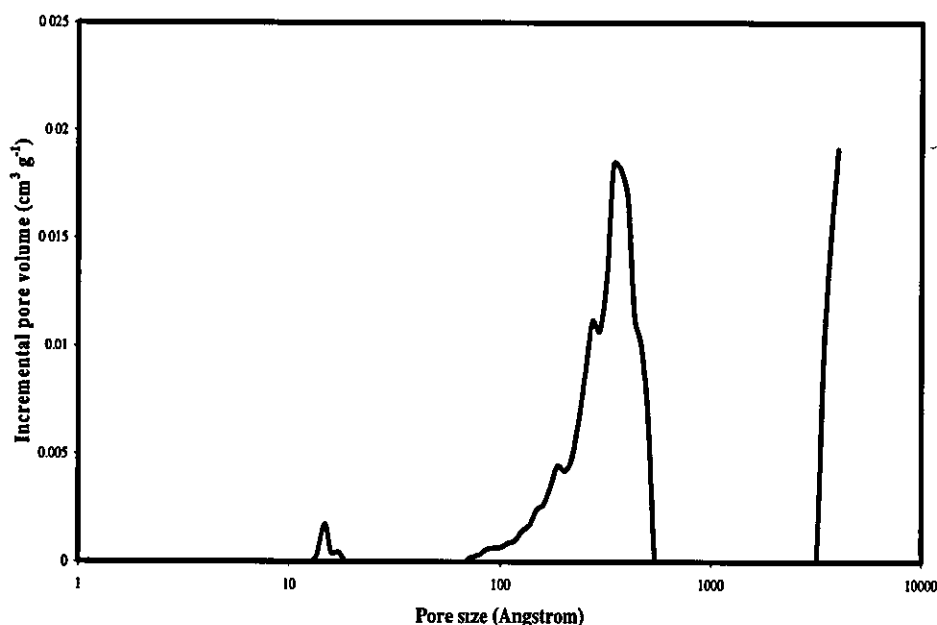


**Figure 3.8.** Pore size distribution of Purolite<sup>®</sup> CT-151 ion exchange resin catalysts.

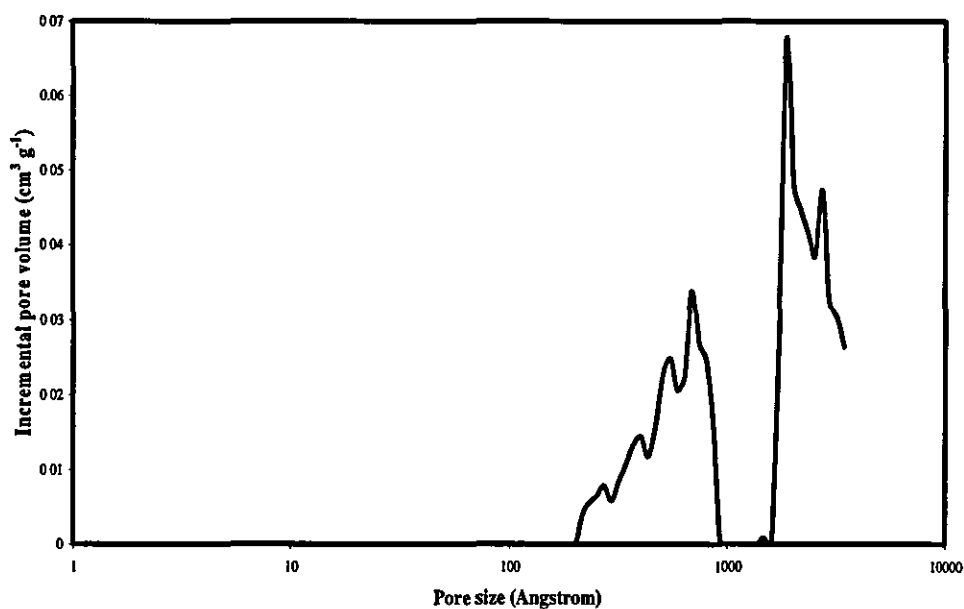


Figure 3.9. Pore size distribution of Purolite® CT-175 ion exchange resin catalysts.

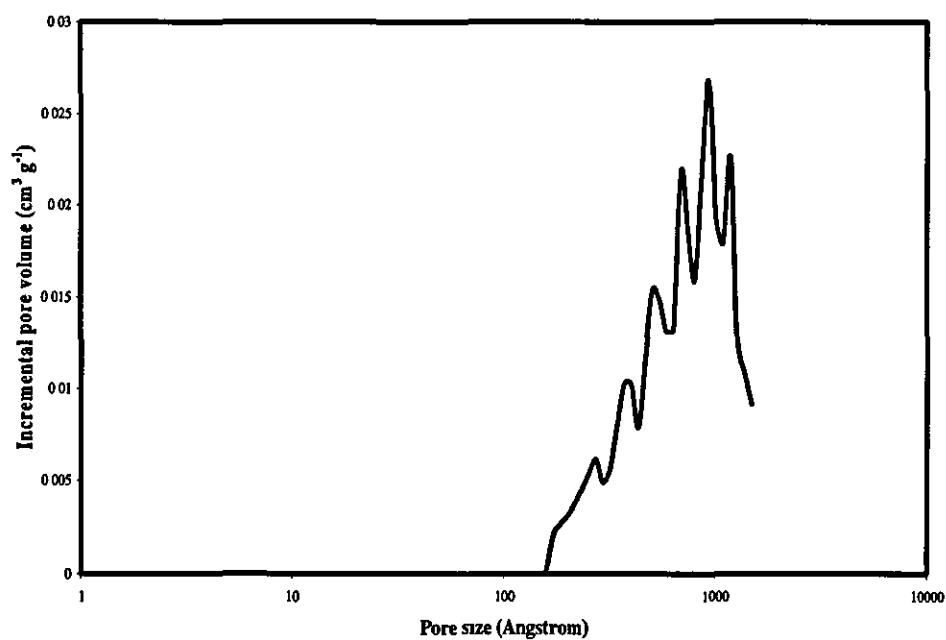


Figure 3.10. Pore size distribution of Purolite® CT-275 ion exchange resin catalysts.

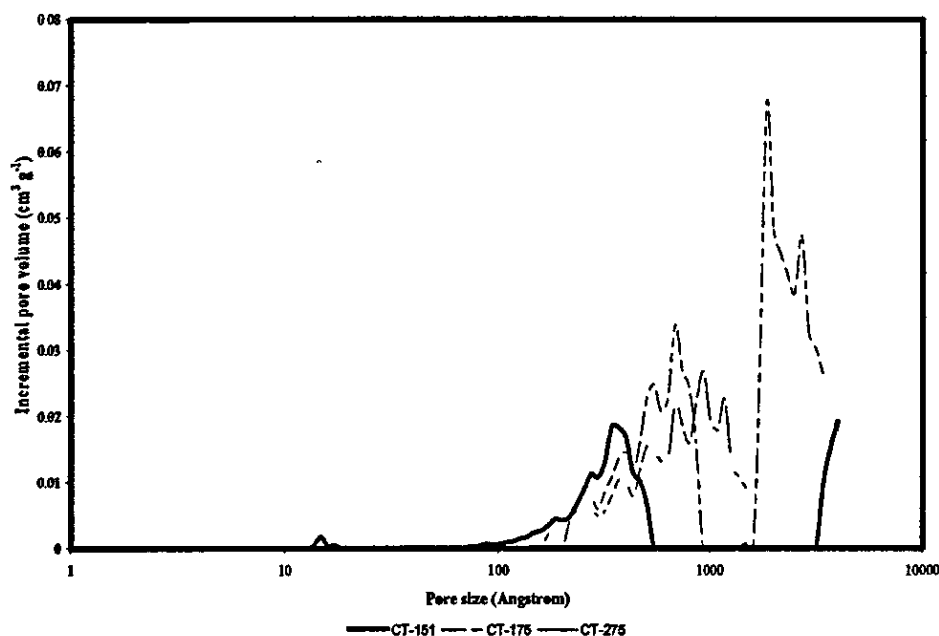


Figure 3.11. Comparison of pore size distribution of different ion exchange resin catalysts.

### 3.2.1.2.1.3 Elemental analysis

The elemental analysis of the polymeric resin samples was performed in the Department of Pure and Applied Chemistry of the University of Strathclyde, Glasgow, United Kingdom. The analysis involved weighing the catalyst samples accurately on an aluminium foil and then inserting the samples into the Perkin Elmer 2400 Elemental Analyser instrument. Prior to the flash combustion process, the system was purged with helium carrier gas. Flash combustion was then performed at 2073 K, and the gaseous combustion products were quantified using a thermal conductivity detector. The results were obtained as weight percentages of carbon, hydrogen, sulphur and (Table 3.2). Nitrogen was not detected in the ion exchange resins. The resin samples appeared to be homogenous. Nitrogen was not detected during the elemental analysis of the ion exchange resin catalysts. The oxygen content presented in Table 3.2 was not inferred directly from the elemental analysis but was determined by the difference from the weight percentage compositions of the other elements.

**Table 3.2.** Elemental analysis results of different ion exchange resins.

Catalyst	Weight (%)			
	C	H	S	O
CT-124	37.13	6.59	12.46	43.82
CT-151	41.04	5.96	13.78	39.22
CT-175	44.57	5.64	15.07	34.72
CT-275	49.89	4.47	17.50	28.14

#### 3.2.1.2.1.4 Particle size distribution

The particle size distribution of the catalysts were determined using standard sized sieves. Prior to sieving the catalyst, every individual sieve was cleaned, weighed and arranged in decreasing sieve diameters. A known amount of the ion exchange resin catalyst was accurately weighed and placed in the top sieve. The catalyst was then sieved down through the tower of sieves with the aid of a mechanical shaker. The weight of each sieve was subsequently measured, after which the weight of ion exchange resin catalyst collected on each sieve was determined. This procedure was repeated several times to ensure reproducibility. The particle size distribution results of different ion exchange resin catalysts are presented in Figures 3.12 to 3.15. Figure 3.12 shows that Purolite® CT-124 has a wide range of size distribution, with the majority of the ion exchange resin catalysts (~82%) falling within the size range of 300-600 µm. The particle size distribution result of Purolite® CT-151 (Figure 3.13) shows that almost 74% (w/w) of the resin catalyst falls within the size range of 500-600 µm. Both Purolite® CT-124 and Purolite® CT-151 exhibit similar quantities (~16.5%) of catalysts particles in the size range of 850-1400 µm. The result from Figure 3.14 shows that about 97% (w/w) of the Purolite® CT-175 catalyst particles are within the size range of 600-850 µm while the remainder i.e. 3% (w/w) of the catalyst particles are within the size range of 180-500 µm. The result from Figure 3.15 shows that Purolite® CT-275 catalyst has got a wider particle size distribution as compared to Purolite® CT-175 catalyst. The majority of Purolite® CT-275 catalyst i.e. 92% (w/w)

falls within the size range of 420-710  $\mu\text{m}$ . The remaining of the catalyst particles are within the size range of 180-355  $\mu\text{m}$  and >850  $\mu\text{m}$ .

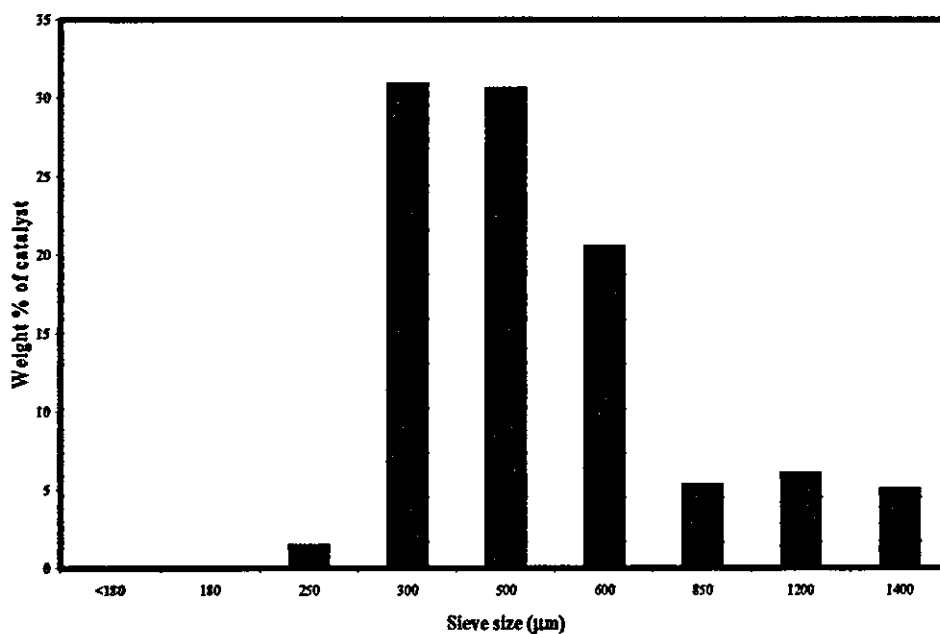


**Figure 3.12.** Particle size distribution of Purolite® CT-124 catalyst.

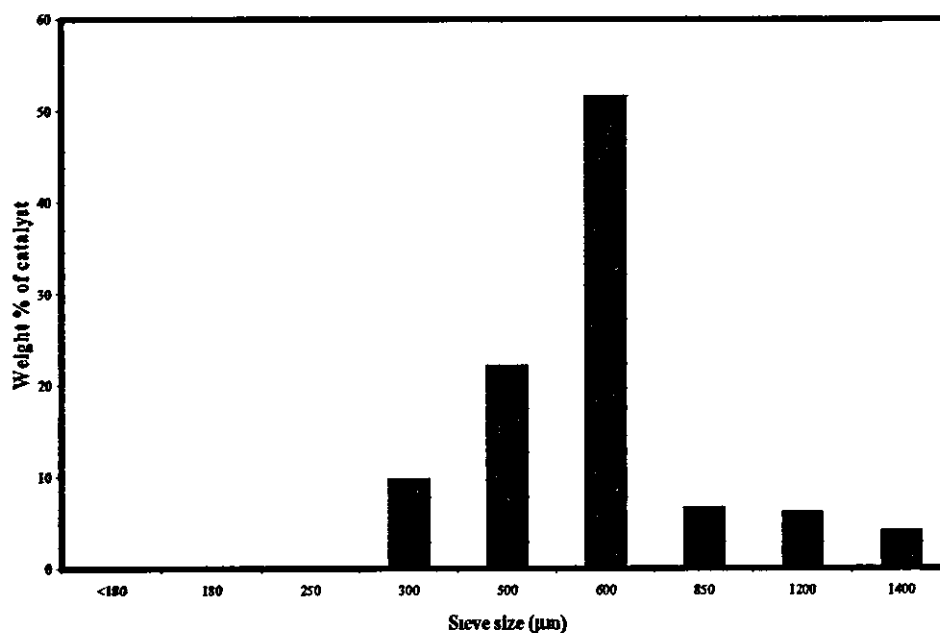


**Figure 3.13.** Particle size distribution of Purolite® CT-151 catalyst

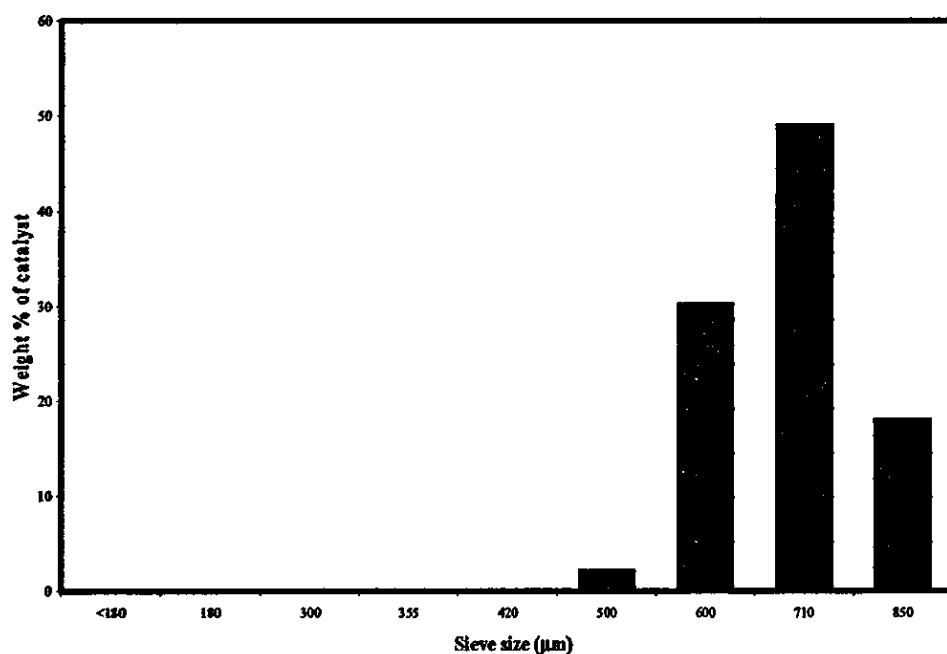


**Figure 3.14.** Particle size distribution of Purolite® CT-175 catalyst

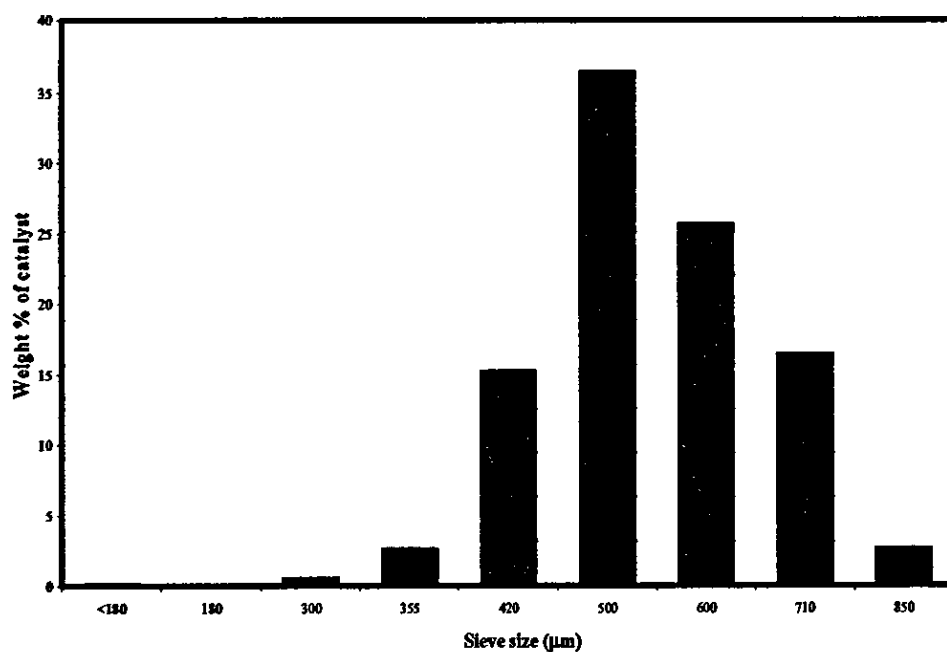


**Figure 3.15.** Particle size distribution of Purolite® CT-275 catalyst.

#### 3.2.1.2.1.5 True density

The true density of the ion exchange resin catalysts was measured using a density bottle. The density bottle of known volume was initially weighed with

methanol in it. After that, a known weight of the catalyst was carefully added into the density bottle and reweighed. The volume of methanol displaced by the catalyst would be known, and the true density of the catalyst was determined. The measured true density of Purolite® CT-124, Purolite® CT-151, Purolite® CT-175 and Purolite® CT-275 catalysts are 1.43 g/cm<sup>3</sup>, 1.38g/cm<sup>3</sup>, 1.95 g/cm<sup>3</sup> and 1.66 g/cm<sup>3</sup> respectively.

#### 3.2.2 Method of analysis

A Pye Unicam 104 gas chromatograph (GC) equipped with a thermal conductivity detector was used to analyse the composition of the samples from the liquid phase of the reacting mixture. The sample size for each gas chromatograph injection was 1 µL. Both the oven and detector port temperatures were set isothermally at 523 K. The GC column was packed with Porapak Q, which was used to separate water, acetic acid, *iso*-amyl alcohol and *iso*-amyl acetate. The length and diameter of the column were 2.5 m and 0.00635 m respectively. High purity (> 98%) helium gas was used as a carrier gas. The flow rate of the helium gas was 50 ml/min (measured using a calibrated flowmeter), and a complete GC run took about 12 minutes.

##### 3.2.2.1 Calibration curves

With reference to the works of Lee *et al.* (1996) which included the determination of liquid mole fraction in a ternary mixture, the same concept was applied to determine the mole fraction of each constituent component in the quaternary mixture of *iso*-amyl alcohol - acetic acid – *iso*-amyl acetate-water for the batch kinetic experiments with concentrated acetic acid.

The composition of a quaternary mixture was calculated from the mathematical relationship between the mole fraction and the peak area fraction developed by the calibration curves of the binary pair. The detailed calibration procedure is presented as follows:

Table 3.3. Parameters for calibration curves.

Component	<i>iso</i> -Amyl alcohol	Acetic acid	<i>iso</i> -Amyl acetate	Water
Peak area	A <sub>1</sub>	A <sub>2</sub>	A <sub>3</sub>	A <sub>4</sub>
Mole fraction	x <sub>1</sub>	x <sub>2</sub>	x <sub>3</sub>	x <sub>4</sub>

$$x_1 + x_2 + x_3 + x_4 = 1 \quad \text{Eq. 3.1}$$

The value of  $A_1/(A_1+A_2)$  and the calibration curve of *iso*-amyl alcohol and acetic acid gives  $x_1/(x_1+x_2)$ ; the value of  $A_1/(A_1+A_3)$  and the calibration curve of *iso*-amyl alcohol and *iso*-amyl acetate gives  $x_1/(x_1+x_3)$ , and the value of  $A_1/(A_1+A_4)$  and the calibration curve of *iso*-amyl alcohol-acetic acid gives  $x_1/(x_1+x_4)$ .

Letting

$$x_1/(x_1+x_2) = a \quad \text{Eq. 3.1a}$$

$$x_1/(x_1+x_3) = b \quad \text{Eq. 3.1b}$$

$$x_1/(x_1+x_4) = c \quad \text{Eq. 3.1c}$$

From Eq. 3.1a,

$$x_1 = (x_1+x_2)a$$

$$= x_1a + x_2a$$

$$x_2a = x_1 - x_1a$$

$$= x_1(1-a)$$

$$\therefore x_2 = \frac{x_1(1-a)}{a}$$

From Eq. 3.1b,

$$\begin{aligned} x_1 &= (x_1+x_3)b \\ &= x_1a + x_3b \end{aligned}$$

$$\begin{aligned} x_3b &= x_1 - x_1b \\ &= x_1(1-b) \end{aligned}$$

$$\therefore x_3 = \frac{x_1(1-b)}{b}$$

From Eq. 3.1c,

$$\begin{aligned} x_1 &= (x_1+x_4)c \\ &= x_1a + x_4c \end{aligned}$$

$$\begin{aligned} x_4c &= x_1 - x_1c \\ &= x_1(1-c) \end{aligned}$$

$$\therefore x_4 = \frac{x_1(1-c)}{c}$$

Substituting  $x_2$ ,  $x_3$  and  $x_4$  into Eq. 3.1,

$$x_1 + \frac{x_1(1-a)}{a} + \frac{x_1(1-b)}{b} + \frac{x_1(1-c)}{c} = 1$$

Solving the above equation give

$$x_1 = \frac{abc}{[bc(1-2a) + a(b+c)]} \quad \text{Eq. 3.2}$$

$$x_2 = \frac{x_1(1-a)}{a} = \frac{bc(1-a)}{[bc(1-2a) + a(b+c)]} \quad \text{Eq. 3.3}$$

$$\therefore x_3 = \frac{x_1(1-b)}{b} = \frac{ac(1-b)}{[bc(1-2a) + a(b+c)]} \quad \text{Eq. 3.4}$$

$$\therefore x_4 = \frac{x_1(1-c)}{c} = \frac{ab(1-c)}{[bc(1-2a) + a(b+c)]} \quad \text{Eq. 3.5}$$

The calibration curves of the binary mixtures of *iso*-amyl alcohol - acetic acid, *iso*-amyl alcohol - *iso*-amyl acetate and *iso*-amyl alcohol - water were determined experimentally and plotted. Each calibration curve was a regression of a set of solutions of known compositions, and the peak area fraction of the selected component with *iso*-amyl alcohol. A representative set of the calibration curves and the polynomial equations for each binary pair mixture are shown in Figures 3.16, 3.17 and 3.18:

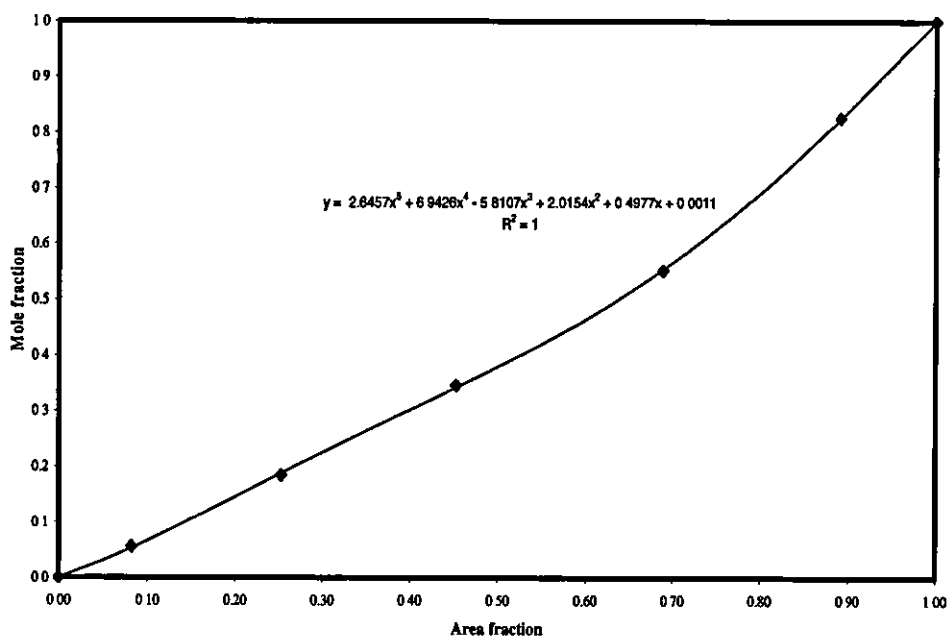


Figure 3.16. *iso*-amyl alcohol – acetic acid calibration curve

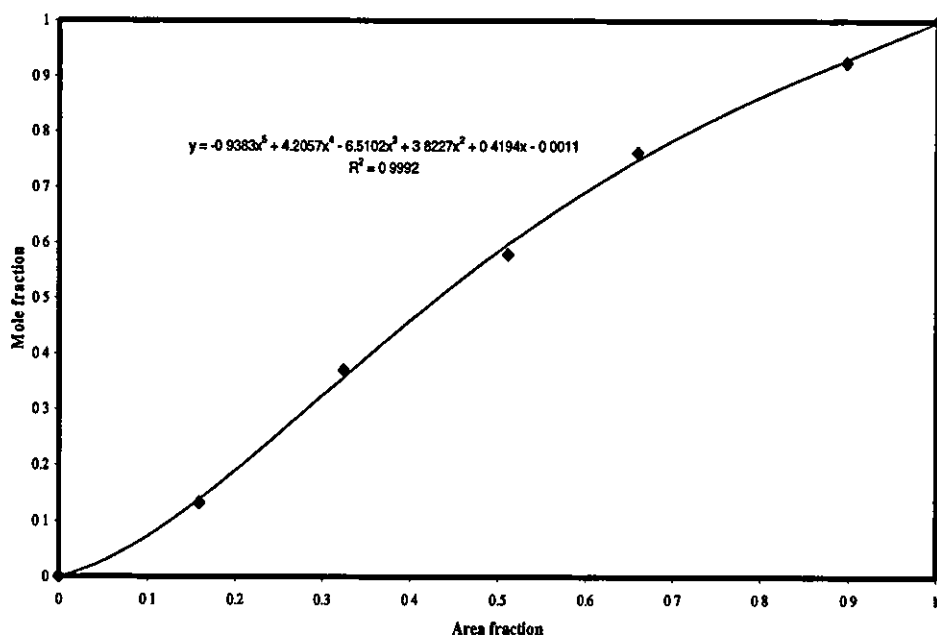


Figure 3.17. *iso*-amyl alcohol- *iso*-amyl acetate calibration curve

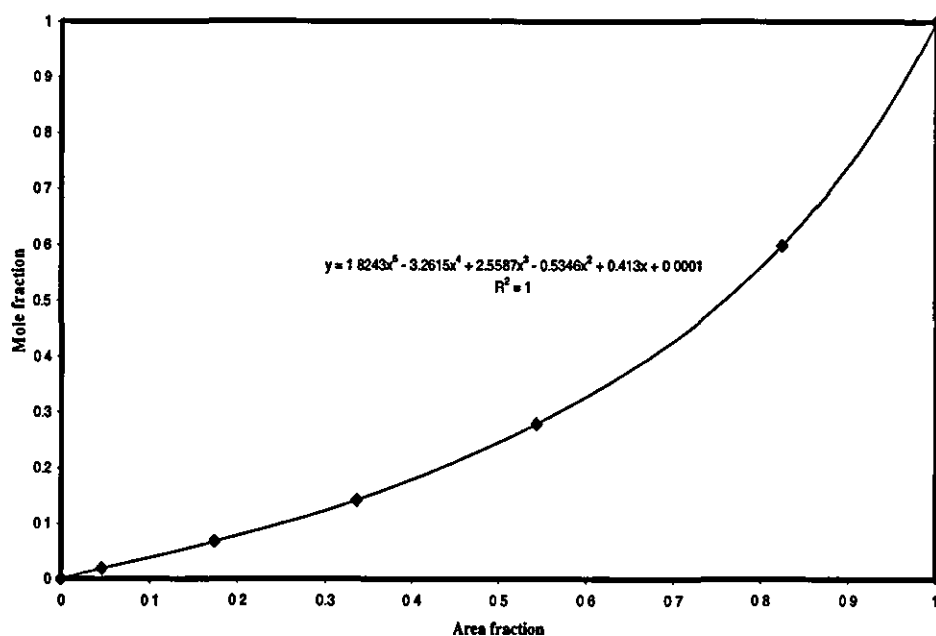


Figure 3.18. *iso*-amyl alcohol- water calibration curve

### 3.2.2.2 Internal standardisation

Internal standardisation was used as the choice method of analysis to determine the composition of each constituent component in the quaternary mixture of *iso*-amyl alcohol - acetic acid - *iso*-amyl acetate - water for the batch kinetic experiments with diluted acetic acid. A summary of other quantitative analysis is listed in Appendix B. Grob (1995) defined the internal standardisation technique as a technique that combines the sample and standard into one injection.

The advantages of the internal standardisation technique are given below:

- (i) The result is expressed as an absolute concentration i.e. if the units of concentration for the internal standard ( $\text{Conc}_{\text{IS}}$ ) for both calibration and analysis are the same, then the final answer is expressed in the concentration units of calibration ( $\text{Conc}_i$ ). If the units for both  $\text{Conc}_i$  and  $\text{Conc}_{\text{IS}}$  for the calibration are identical, then the response factor is dimensionless, and it is possible to obtain the final answer in any desired units by simply adjusting the units of  $\text{Conc}_i$  for the analysis.

- (ii) Allowance is made for the response of each component to the detector.
- (iii) The result of each injection is independent of the injection volume.

The disadvantages associated with using the internal standardisation technique are as follow:

- (i) The technique is not readily usable with gaseous samples.
- (ii) There is a need to select a suitable internal standard.

The prerequisites for an internal standard are as follow:

- (i) The internal standard must be miscible with the sample being analysed.
- (ii) The internal standard must elute from the column and adequately separated from all sample components i.e. during the GC analysis, the internal standard should give only one peak which must be well resolved from the peaks of the sample components.
- (iii) The internal standard must elute as near as possible to the desired components and ideally before the last sample peak so that the analysis time is not increased.
- (iv) The internal standard should preferably be similar in functional group type to the component(s) of interest. If such a compound is not readily available, an appropriate hydrocarbon should be substituted.
- (v) The internal standard must be stable under the required analytical conditions and must not react with any of the components or solvents present in the sample.
- (vi) The internal standard must be sufficiently non-volatile to make allowance for storage of standard solutions for significant periods of time.

In consideration of the prerequisites towards the selection of the internal standard as outlined above, *n*-butanol was chosen as the choice of internal standard for the analysis of the present system.

### 3.2.3 Experimental set-up and procedure for batch kinetic studies

A continuously stirred batch reactor as shown in Figure 3.19 was used for the kinetic experiments. The reactor was made of glass with a capacity of 500 cm<sup>3</sup>. The four-necked jacketed reactor was connected to a thermocouple and a reflux condenser. The other two outlets were capped with glass stoppers, one of which was utilised as the sampling port. The thermocouple was placed in the reactor to monitor the temperature of the reactants. The reflux condenser was used to avoid the loss of volatile compounds. The desired temperature of the reactants in the reactor was maintained by adjusting the thermal stirrer's temperature accordingly. The temperature of the reactants in the reactor was kept within  $\pm 0.5$  K of the desired temperature condition. The ion exchange resin catalyst particles were suspended in the reaction mixture by continuous stirring through the use of a paddle shaft, which was powered by a stirrer motor (IKA-WERKE).

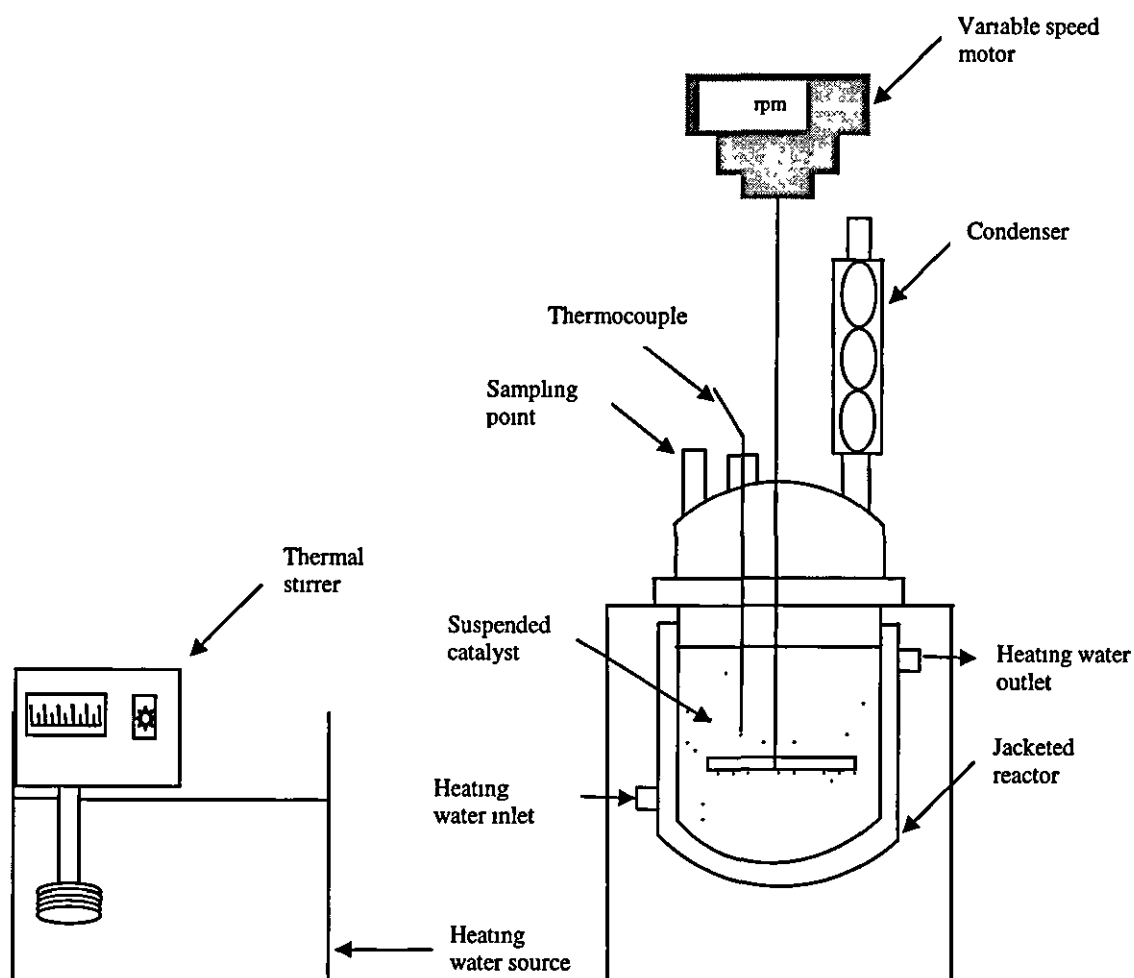
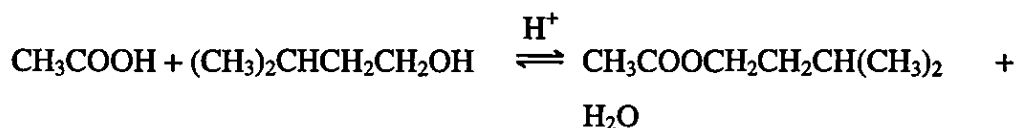


Figure 3.19. Experimental set-up for batch kinetic studies.

The reactor was initially charged with a measured amount of acetic acid and *iso*-amyl alcohol for the batch kinetic studies using concentrated acetic acid. For the batch kinetic studies using diluted acetic acid, a measured weight amount of distilled water was added on. When the reacting mixture reached the desired temperature, the first sample was withdrawn, after which the measured amount of catalyst was added to the mixture in the reactor through the sampling port. This was considered as the starting time of the reaction. The timing of the experimental run was started after the catalyst was added to the reacting mixture. Samples of the reaction mixture were withdrawn at regular time intervals whilst the reaction mixture was being stirred, and subsequently analysed for their composition using the gas chromatography (GC) analysis. The change in composition with respect to time was noted. The reactions were performed under reflux conditions. The batch kinetic experiments were carried out in duplicates to ensure result reproducibility. The experimental errors for the results is  $\pm 3\%$ . The duplicate experimental results obtained always fall within this error range. Experimental runs under different reacting conditions were performed to validate the kinetic models and its parameters (see Chapter 4).

### 3.3 MECHANISM OF REACTION

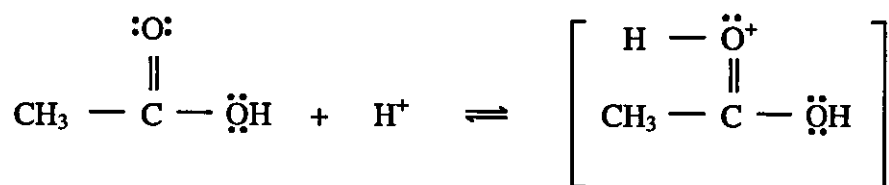
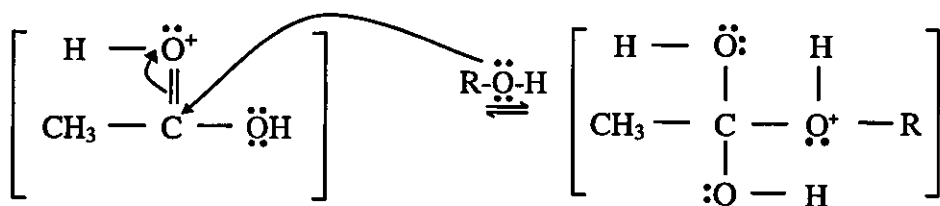
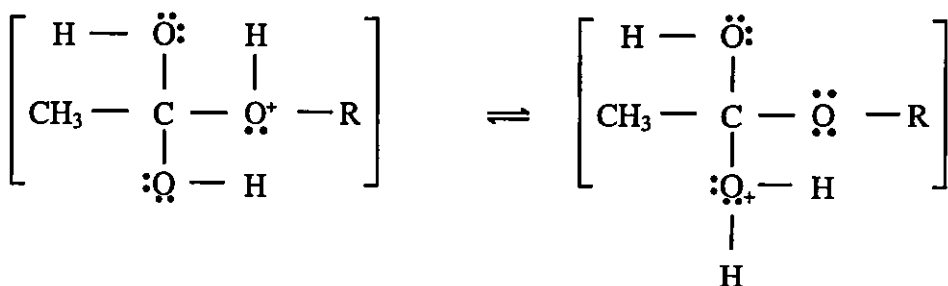
Acetic acid reacts with *iso*-amyl alcohol in the presence of ion exchange resins to produce the ester product in the form of *iso*-amyl acetate. It is proposed that the ion exchange resin catalysed (heterogeneous) esterification follows the same mechanistic steps of the homogeneously acid catalysed reaction (Solomons and Fryhle, 2000). This esterification reaction (Equation 3.6) is an equilibrium-limited chemical reaction.



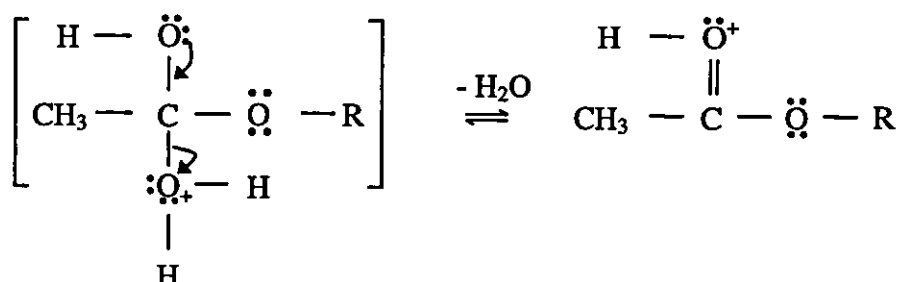
Eq. 3.6

The proposed reaction mechanism is shown in Figure 3.20. In the first step, acetic acid molecule accepts a proton from the strong acid cation exchanger (Step 1). After the proton transfer, the acetic acid is prone to a nucleophilic

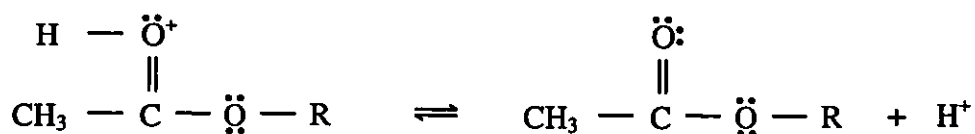
attack from the hydroxyl group of the alcohol (*iso*-amyl alcohol). The *iso*-amyl alcohol molecule reacts with the protonated carbonyl group of acetic acid to give a tetrahedral intermediate (Step 2). In the next step, a proton is lost at one oxygen atom and gained at another oxygen atom to form another intermediate (Step 3). This is followed by the loss of a molecule of water to give a protonated ester (Step 4). In the final step, a proton is transferred to a water molecule to give the ester product, *iso*-amyl acetate (Step 5). All of these steps in the reaction mechanism are reversible.

**Step 1:****Step 2:****Step 3:**

Step 4:



Step 5:



where  $\text{R} = \text{CH}_3(\text{CH})\text{CH}_3\text{CH}_2\text{CH}_2-$

Figure 3.20. Mechanism of ion exchange resin catalysed reaction of acetic acid with *iso*-amyl alcohol.

### 3.4 RESULTS AND DISCUSSION OF BATCH KINETIC STUDIES

#### 3.4.1 Elimination of mass transfer resistances

There exists two types of mass transfer resistances in this reaction, one of which exists across the solid-liquid interface while the other exists in the intraparticle space of the catalyst (Gangadawla *et al.*, 2003). To determine the influence of external mass transfer on the reaction rate, the kinetic experiments were carried out at different stirrer speeds (Saha and Sharma, 1996; Xu and Chuang, 1996; Sanz *et al.*, 2002; Gangadwala *et al.*, 2003; Cunill *et al.*, 2005). In the study towards the elimination of external mass transfer with the use of diluted acetic acid, the experiments were carried out at 358 K, using 30% (w/w) acetic acid with a feed mole ratio (*iso*-amyl alcohol to acetic acid)

of 2:1 and at a catalyst loading of 5% (w/w). The stirrer speed of the reaction was varied between 300 revolutions per minute (rpm) and 800 rpm while keeping the rest of the reaction conditions constant. The experimental results are shown in Figure 3.21. There was a slight difference in reaction rates between 300 and 500/800 rpm in the initial stages of reaction. However, there was no distinct effect of the mass transfer resistance as caused by the variation in stirrer speed after six hours of reaction between 300 and 800 rpm as similar results of about 37% conversion of acetic acid were achieved. In the study towards the elimination of mass transfer resistances with the use of concentrated acetic acid (99.8%), the experiments were carried out at 358 K with a feed mole ratio of 2:1 (*iso*-amyl alcohol to acetic acid) and at a catalyst loading of 2.5% (w/w). The effect of stirrer speed was investigated by using stirrer speed of the reaction at 240 rpm and 500 rpm while keeping the other reaction conditions constant. The experimental results are shown in Figure 3.22. There was no distinct effect of the mass transfer resistance as caused by the variation in stirrer speeds of 240 rpm and 500 rpm. Similar rates of reaction and conversions of about 65% were obtained for both stirrer speeds after six hours of operation. Both sets of results using concentrated and diluted acetic acid suggest that external mass transfer caused by stirrer speed is not a controlling mechanism in the rate of reaction. Similar observations were made by Chakrabati and Sharma (1993), Saha and Sharma (1996) and Sanz *et al.* (2002) who all indicated that external mass transfer resistance does not usually control the overall rate in the reactions catalysed by ion exchange resins unless the agitation speed is very low or the reaction mixture is very viscous. Moreover, there was a possibility of attrition of catalyst particles at higher speeds of agitation (i.e. >800 rpm). Consequently, the effect of external mass transfer resistance for the reaction was eliminated by carrying out all further kinetic experiments at a stirrer speed of 500 rpm. It was confirmed that there was no attrition of the catalyst particles under the experimental conditions investigated for this work.

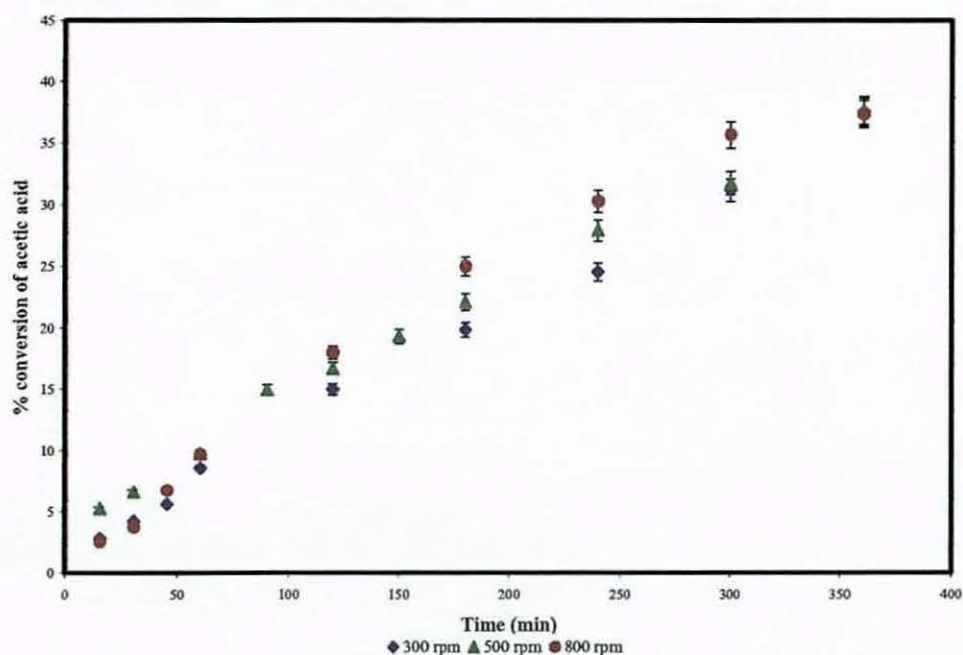


**Figure 3.21.** Effect of stirrer speed on conversion of 30% (w/w) acetic acid at a catalyst loading of 5% (w/w); feed mole ratio (*iso*-amyl alcohol to acetic acid), 2:1; temperature, 358 K; catalyst, CT-275.

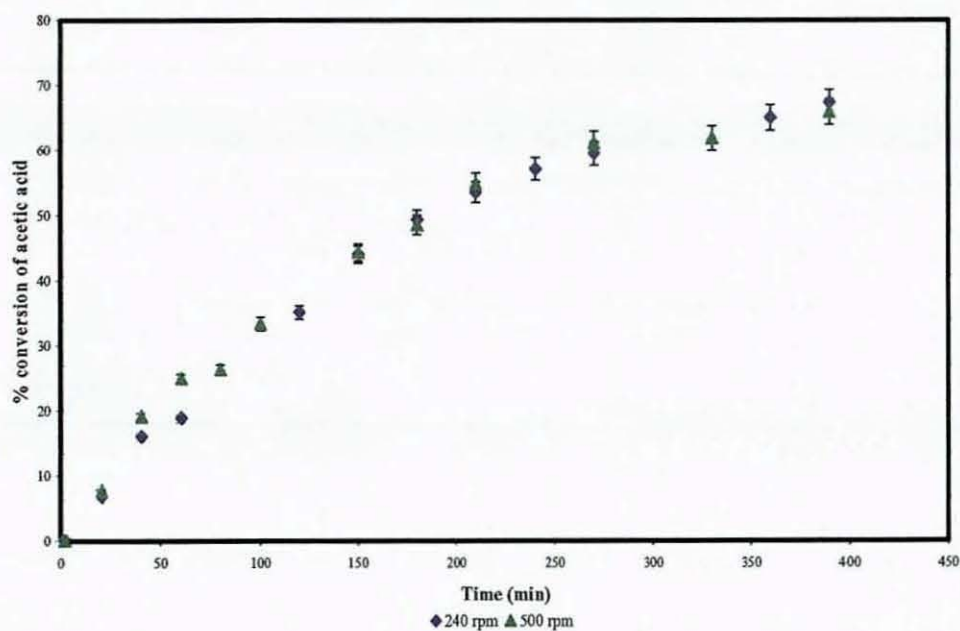


**Figure 3.22.** Effect of stirrer speed on conversion of concentrated acetic acid at a catalyst loading of 2.5% (w/w); feed mole ratio (*iso*-amyl alcohol to acetic acid), 2:1; temperature, 358 K; catalyst, CT-275.

Xu and Chuang (1996) stated that for the macroporous ion exchange catalyst without external mass transfer resistance, the rate controlling steps can be the reaction at the micro-particle surface or diffusion within the macropores. The possible influence of internal mass transfer resistance was investigated by carrying out the kinetic experiments with different particle sizes (Rihko and Krause, 1995; Saha and Sharma, 1996; Xu and Chuang, 1996; Gonzalez and Fair, 1997; Sanz *et al.*, 2002; Gangadwala *et al.*, 2003). This was done by screening the catalyst particles into different size fractions using sieves. For the investigation of the effect of particle sizes using diluted acetic acid, the kinetic experiments were carried out at 358 K, using 30% (w/w) acetic acid with a feed mole ratio (*iso*-amyl alcohol to acetic acid) of 2:1, at a catalyst loading of 5% (w/w) and utilising a stirrer speed of 500 rpm. Different runs were carried out with each of the particle size fractions obtained under otherwise identical reaction conditions. Figure 3.23 shows the effect of particle size on the conversion of acetic acid. It can be derived from the results that the conversion of acetic acid is not influenced by the wide range of catalyst particle sizes used, as similar reaction rates and conversion results of about 37% conversion of acetic acid were achieved after six hours of reaction. The results were an indication that the mass transfer resistance due to intraparticle diffusion was insignificant. As such, all further kinetic experiments were carried out with the ion exchange resin catalysts in the supplied form for Purolite<sup>®</sup> CT-175 (Teo and Saha, 2004) and Purolite<sup>®</sup> CT-275 (Saha *et al.*, 2005b) as Purolite<sup>®</sup> CT-124 and Purolite<sup>®</sup> CT-151 did not show as promising results for the reaction between acetic acid and *iso*-amyl alcohol, both Purolite<sup>®</sup> CT-124 and Purolite<sup>®</sup> CT-151 ion exchange resin catalysts have been excluded from further experimental investigations.

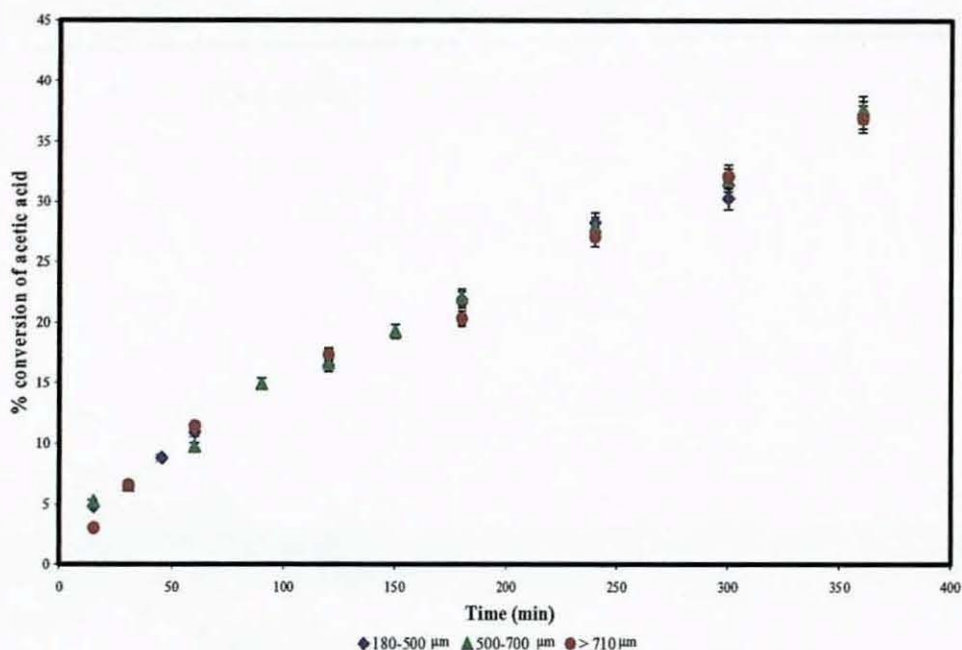


**Figure 3.23.** Effect of catalyst particle size on conversion of 30% (w/w) acetic acid at a catalyst loading of 5% (w/w); feed mole ratio (*iso*-amyl alcohol to acetic acid), 2:1; temperature, 358 K; catalyst, CT-275; stirrer speed, 500 rpm.

### 3.4.2 Effect of reaction temperature

The study on the effect of temperature on the reaction kinetics is very important for a heterogeneously catalysed reaction as the information would be useful for calculating the activation energy for the catalysed reaction of acetic acid with *iso*-amyl alcohol. Moreover, the intrinsic rate constants are strong functions of temperatures. Figure 3.24 presents the variation of conversion of acetic acid with contact time for the reaction taking place using 30% (w/w) acetic acid at a catalyst loading of 5% (w/w), at a feed mole ratio (*iso*-amyl alcohol to acetic acid) of 2:1, Purolite<sup>®</sup> CT-175 catalyst and at a stirrer speed of 500 rpm over a temperature range of 338 K to 358 K. It can be seen from Figure 3.24 that the acetic acid conversion was 16.1% at a reaction temperature of 338 K and 39.1% at a reaction temperature of 358 K after six hours of operation. Figure 3.25 shows the variation of conversion of acetic acid with contact time under similar experimental conditions whilst using Purolite<sup>®</sup> CT-275 catalyst over a temperature range of 338 - 363 K. After six hours of operation, about 43.4% conversion of acetic acid was achieved at a reaction temperature of 363 K. The minimum acetic conversion using

Purolite<sup>®</sup> CT-275 catalyst was 11.5% at a reaction temperature of 338 K after six hours of operation.

Figure 3.26 illustrates the conversion of concentrated acetic acid by varying the reaction temperatures in the range of 333 - 358 K at a catalyst loading of 5% (w/w) Purolite<sup>®</sup> CT-175 catalyst using a feed mole ratio (*iso*-amyl alcohol to acetic acid) of 2:1 and utilising a reaction stirrer speed of 500 rpm. The equilibrium conversions for reactions carried out at the temperatures of 343 K and 358 K were nearly equal (~ 82 % conversion). All the results show that the higher reaction temperature yields a greater conversion of acetic acid at a fixed contact time. Choi *et al.* (1996) and Sanz *et al.* (2002) found similar results of the reaction rate being enhanced with increasing reaction temperatures. Increasing the reaction temperature is favourable for the acceleration of the forward reaction. In general, the equilibrium constant is dependent on the temperature according to the Van't Hoff Equation. However, Simons (1983) reported that the heat of reaction for many esterification reactions is very small or even zero and hence, the equilibrium constant is essentially temperature independent.

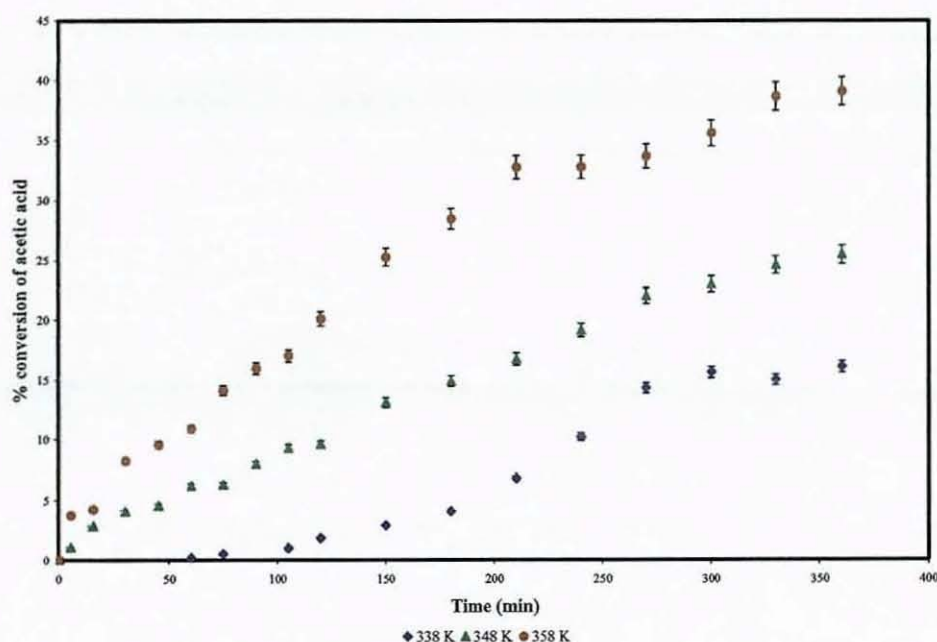


**Figure 3.24.** Effect of temperature on conversion of 30% (w/w) acetic acid at a catalyst loading of 5% (w/w); feed mole ratio (*iso*-amyl alcohol to acetic acid), 2:1; catalyst, CT-175; stirrer speed, 500 rpm.

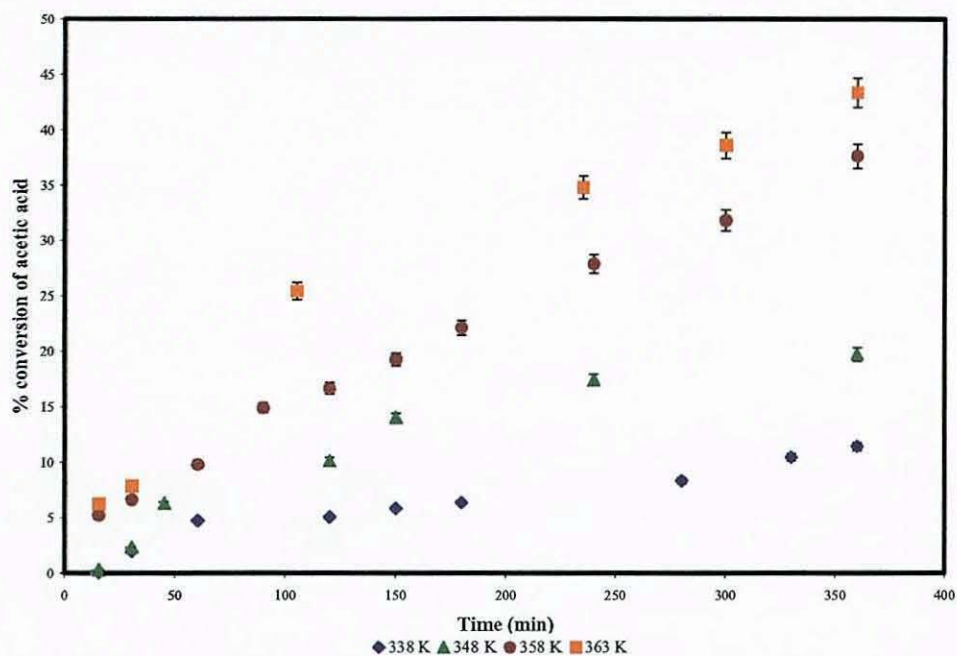


**Figure 3.25.** Effect of temperature on conversion of 30% (w/w) acetic acid at a catalyst loading of 5% (w/w); feed mole ratio (*iso*-amyl alcohol to acetic acid), 2:1; catalyst, CT-275; stirrer speed, 500 rpm.

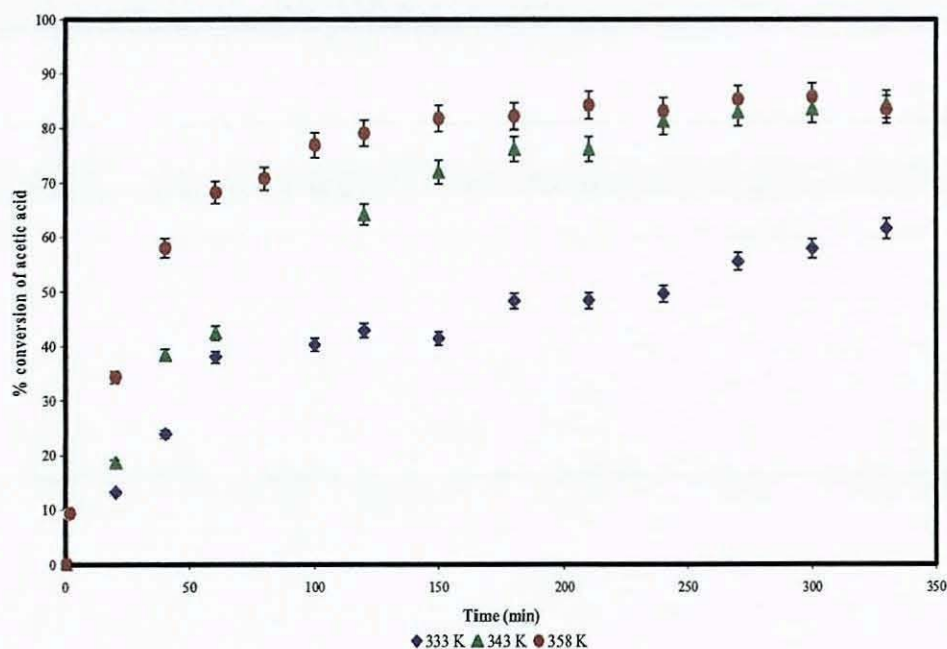


**Figure 3.26.** Effect of temperature on conversion of concentrated acetic acid at a catalyst loading of 5% (w/w); feed mole ratio (*iso*-amyl alcohol to acetic acid), 2:1; catalyst, CT-175; stirrer speed, 500 rpm.

### 3.4.3 Effect of catalyst loading

Figures 3.27 and 3.28 show the effect of catalyst loading using Purolite® CT-175 and Purolite® CT-275 catalysts, respectively. The reactions were carried out using 30% (w/w) acetic acid at a reaction temperature of 358 K, feed mole ratio (*iso*-amyl alcohol to acetic acid) of 2:1, and at a stirrer speed of 500 rpm. The catalyst loading was varied from 2.5 to 10% (w/w) (w/w: weight of catalyst over the total weight of reactants). The results from Figures 3.27 and 3.28 show that a higher catalyst loading promotes a faster reaction rate. This is because of the increase in the total number of acid sites i.e. more sulphonic acid groups, are available for the reaction. For 10% (w/w) catalyst loading of Purolite CT-175® (Figure 3.27), the equilibrium acetic acid conversion of ~ 52% was reached after 270 minutes, whereas the conversions of acetic acid were still increasing for 2.5% (w/w) and 5% (w/w) catalyst loadings at the same stage of the respective experimental runs. For the kinetic experiments carried out using Purolite® CT-275 (Figure 3.28), the conversion of acetic acid was 49.9% and 25.7% without reaching equilibrium whilst using 10% (w/w) and 2.5% (w/w) catalyst loading, respectively.

In the investigation of catalyst loading towards the esterification between acetic acid and *iso*-amyl alcohol using concentrated acetic acid, the catalyst loading was varied between 2.5% and 10% (w/w) at a reaction temperature of 358 K, feed mole ratio (*iso*-amyl alcohol to acetic acid) of 2:1 and utilising a stirrer speed of 500 rpm. Figure 3.29 depicts that for a catalyst loading of 10% (w/w), the equilibrium conversion of acetic acid was reached within 90 minutes of reaction; whereas for a catalyst loading of 2.5% (w/w), it took nearly 360 minutes for the reaction to reach its near stationary state. The results showed that the equilibrium conversion of acetic acid was independent of catalyst loading (after 6 hours of chemical reaction).

All the results obtained towards the investigation of the effect of catalyst loading showed that a higher catalyst loading promoted a faster reaction rate. In the case of using concentrated acetic acid, it meant a faster reaction rate towards reaching equilibrium. The results as obtained were because of the increase in the total number of available active catalytic sites for the reaction.

As the catalyst loading increases, the number of active sites per volume of reactants increase in proportion leading to an increase in the rate of reaction. For reactions catalysed by heterogeneous catalysts in batch kinetic experiments, it was impractical to use more than 10% (w/w) catalyst loading. Hence it was concluded from the experimental findings that the optimum catalyst loading was 10% (w/w) for the reacting system between acetic acid and *iso*-amyl alcohol whilst employing both Purolite® CT-175 and Purolite® CT-275 as catalysts.

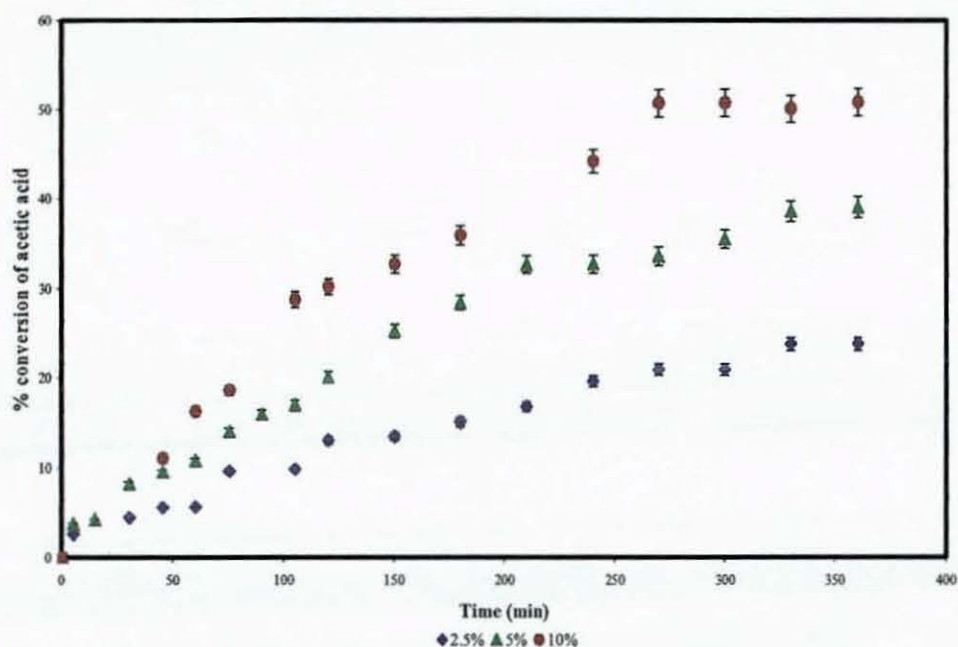


**Figure 3.27.** Effect of catalyst loading on conversion of 30% (w/w) acetic acid at temperature of 358 K; feed mole ratio (*iso*-amyl alcohol to acetic acid), 2:1; catalyst, CT-175; stirrer speed, 500 rpm.

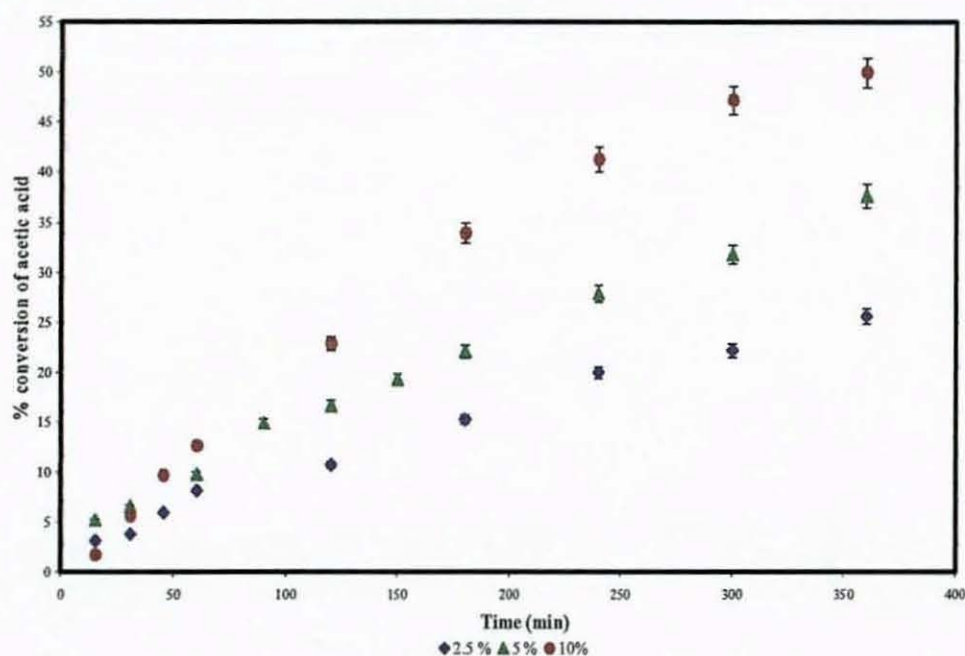


**Figure 3.28.** Effect of catalyst loading on conversion of 30% (w/w) acetic acid at temperature of 358 K; feed mole ratio (*iso*-amyl alcohol to acetic acid), 2:1; catalyst, CT-275; stirrer speed, 500 rpm.

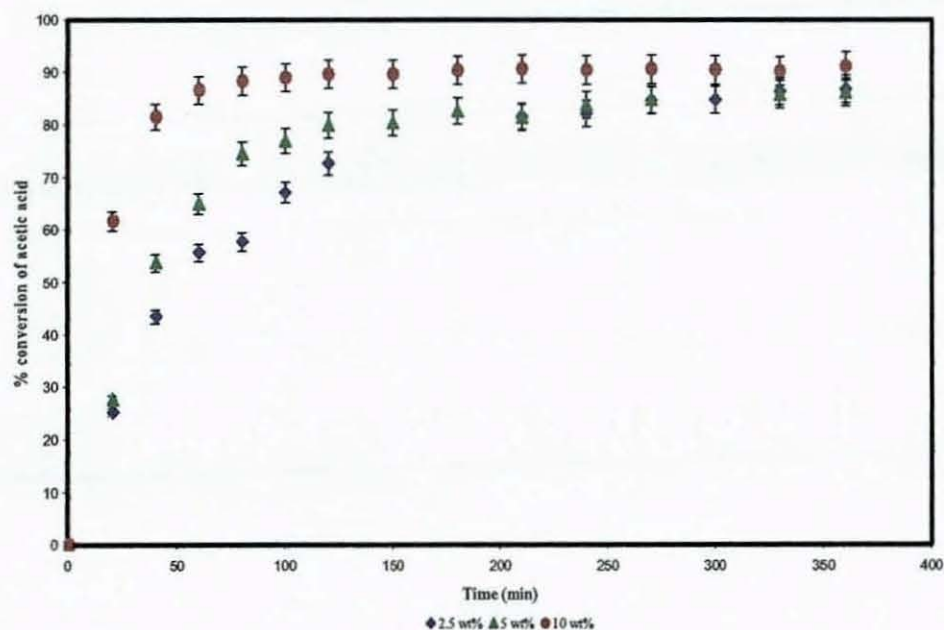


**Figure 3.29.** Effect of catalyst loading on conversion of concentrated acetic acid at 358 K; feed mole ratio (*iso*-amyl alcohol to acetic acid), 2:1; catalyst, CT-175; stirrer speed, 500 rpm.

### 3.4.4. Effect of feed mole ratio

The esterification of acetic acid with *iso*-amyl alcohol is an equilibrium-limited chemical reaction and because the position of equilibrium is a controlling factor towards the amount of ester formed, the use of excess *iso*-amyl alcohol increases the rate of acetic acid conversion. For the investigation of the effect of feed mole ratio using diluted acetic acid, the kinetic experiments were carried out at a reaction temperature of 358 K using 30% (w/w) acetic acid at a catalyst loading of 5% (w/w) and utilising a stirrer speed of 500 rpm. The effect of feed mole ratio was investigated by varying the initial feed molar ratio *iso*-amyl alcohol to diluted acetic acid from 1:1 to 2:1 (Purolite® CT-175) and 1:1 to 4:1 (Purolite® CT-275) while keeping the rest of the reaction conditions constant. Figures 3.30 and 3.31 both show that the reaction rate increases slightly with an increase in the feed molar ratio of *iso*-amyl alcohol to diluted acetic acid.

The results from the experiments using concentrated acetic acid with different initial feed molar ratios of *iso*-amyl alcohol to acetic acid (2:1, 5:1 and 10:1) at 343 K over 5% (w/w) Purolite® CT-175 at a stirrer speed of 500 rpm are compared in Figure 3.32. The results show that the conversion of acetic acid is higher at a fixed contact time with an excess of *iso*-amyl alcohol in the reacting system. The conversion of acetic acid after 4 hours of reaction increased from 81% at a feed mole ratio (*iso*-amyl alcohol to acetic acid) of 2:1 to 98 % at a feed mole ratio (*iso*-amyl alcohol to acetic acid) of 10:1.

All the experimental results using both diluted acetic acid and concentrated acetic acid in the investigation of the effect of feed mole ratio showed that a higher feed mole ratio resulted in a higher conversion of acetic acid at a fixed contact time. This was because a higher amount of *iso*-amyl alcohol in the reacting system would result in a higher adsorption of *iso*-amyl alcohol on the catalyst resin, and hence leading to a higher conversion of acetic acid. Similar behaviour was previously observed in the lactic acid esterification with butanol (Dassy *et al.*, 1994), the lactic acid esterification with methanol (Sanz *et al.*, 2002) the propionic acid esterification with *n*-butanol (Lee *et al.*, 2002) and the maleic acid esterification with ethanol (Yadav and Thathagar, 2002).

Lee *et al.*, 2002 reported that the equilibrium conversion of propionic acid decreased from 0.870 to 0.390 when the feed mole ratio (*n*-butanol to propionic acid) decreased from 2 to 0.5 at 373 K.

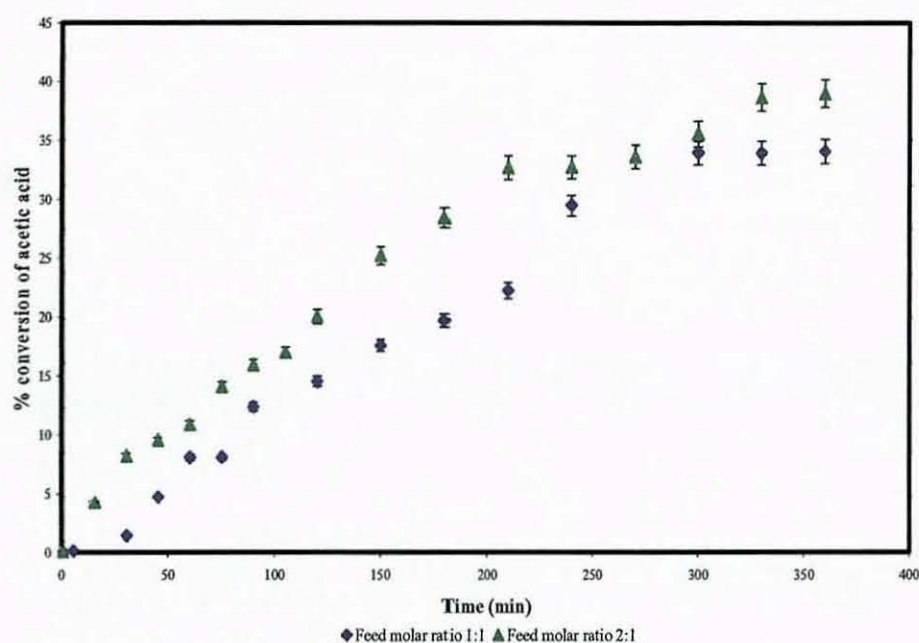


**Figure 3.30.** Effect of feed mole ratio (*iso*-amyl alcohol to acetic acid) on conversion of 30% (w/w) acetic acid at a catalyst loading of 5% (w/w); temperature, 358 K; catalyst, CT-175; stirrer speed, 500 rpm.

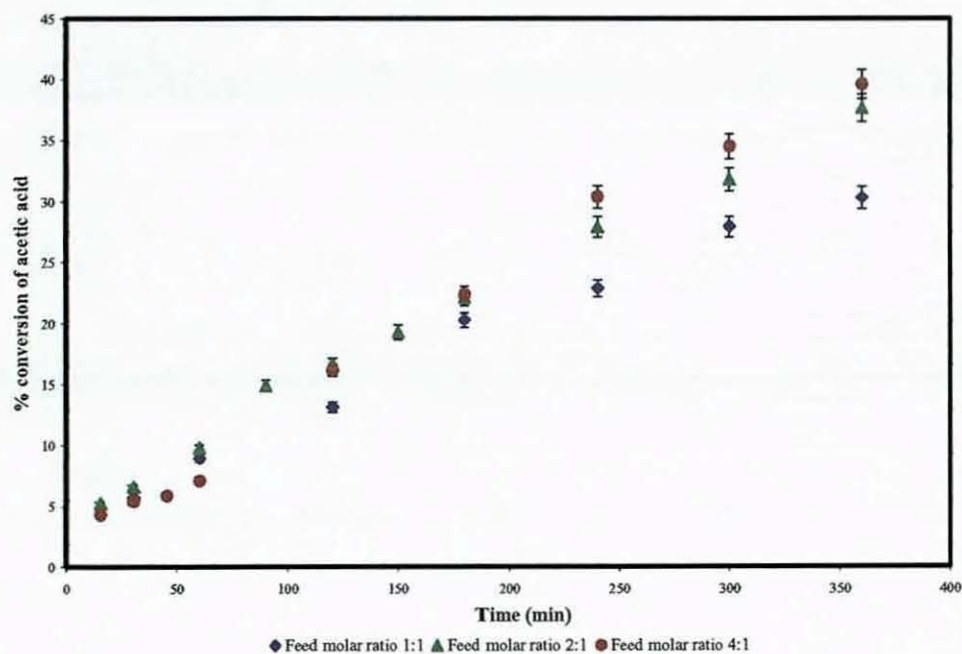


**Figure 3.31.** Effect of feed mole ratio (*iso*-amyl alcohol to acetic acid) on conversion of 30% (w/w) acetic acid at a catalyst loading of 5% (w/w); temperature, 358 K; catalyst, CT-275; stirrer speed, 500 rpm.

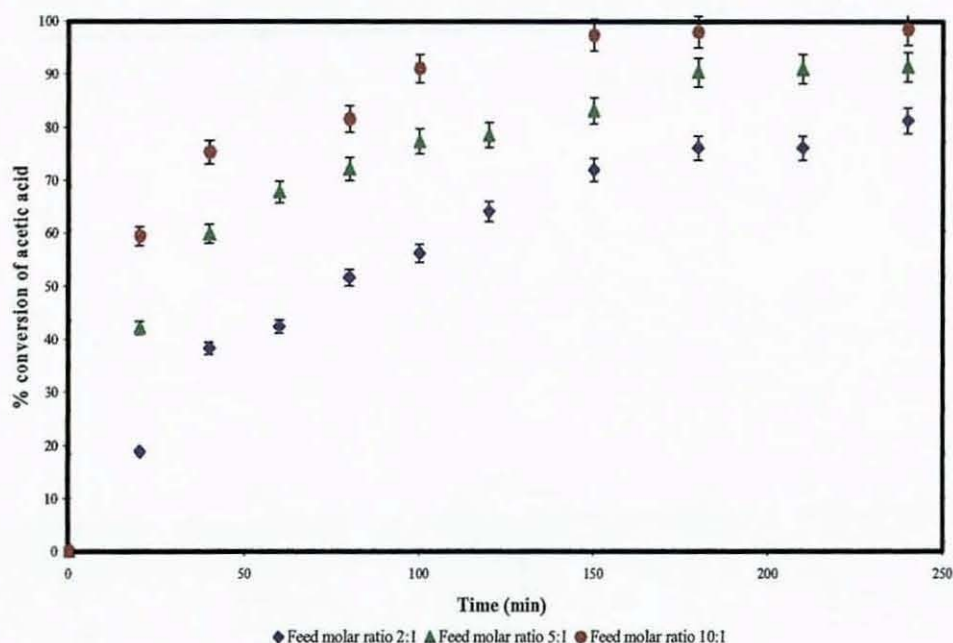


**Figure 3.32.** Effect of feed mole ratio (*iso*-amyl alcohol to acetic acid) on conversion of concentrated acetic acid at a catalyst loading of 5% (w/w); temperature, 343 K; catalyst, CT-175; stirrer speed 500 rpm.

### 3.4.5. Effect of acetic acid concentration

In the investigation of the effect of acetic acid concentration, the experiments were carried out at 358 K, using a feed mole ratio (*iso*-amyl alcohol to acetic acid) of 2:1, at a catalyst loading of 5% (w/w) and utilising a stirrer speed of 500 rpm. The acetic acid concentrations were varied between 10% and 99.8% (w/w).

The reaction mixture was prepared using the following procedure. First, the number of moles of acetic acid and *iso*-amyl alcohol used in the reacting system were defined. With this knowledge, the weight of acetic acid and *iso*-amyl alcohol were determined from the molecular weights of acetic acid and *iso*-amyl alcohol respectively. Since the acetic acid concentration defined in this work was in terms of % (w/w) acetic acid to water, the amount of water subsequently added would then be dependent upon the acetic acid concentration being investigated. An example for an acid concentration, 10% (w/w) acetic acid, using a feed molar ratio of *iso*-amyl alcohol to acetic acid of 2:1 is given as follows:

**Table 3.4.** Preparation of reaction mixture.

Component	No. of Moles	Mass (g)	Volume (cm <sup>3</sup> )	Density (g/cm <sup>3</sup> )	Molecular weight
Acetic acid	0.25	15.01	14.33	1.048	60.053
<i>iso</i> -Amyl Alcohol	0.50	44.08	54.28	0.812	88.15
Water	7.5	135.12	135.12	1.000	18.02

Figure 3.33 shows that both the reaction rate and conversion of acetic acid increase with an increase in acetic acid concentration. The conversion of acetic acid increased from 33% to 88% when the concentration of acetic acid was increased from 10%-99.8% (w/w). The results further showed that the equilibrium conversion was only reached when 99.8% (w/w) concentrated acid was used. More time was required for the other experimental runs for the reactions to reach equilibrium. Zundel (1969) reported that in the presence of water molecules, four sulphonic acid groups of the ion exchange resin are attached to one water molecule. Thus, the availability of the active sites decreases, which leads to a decrease in the catalytic activity of the ion exchange resin, which then further results in a sharp decrease in the rate of reaction. With a decrease in the concentration of acetic acid, the concentration of water increases. The increasing presence of water in the more diluted concentrations of acetic acid hindered the forward progression of the chemical reaction in batch mode of operation.

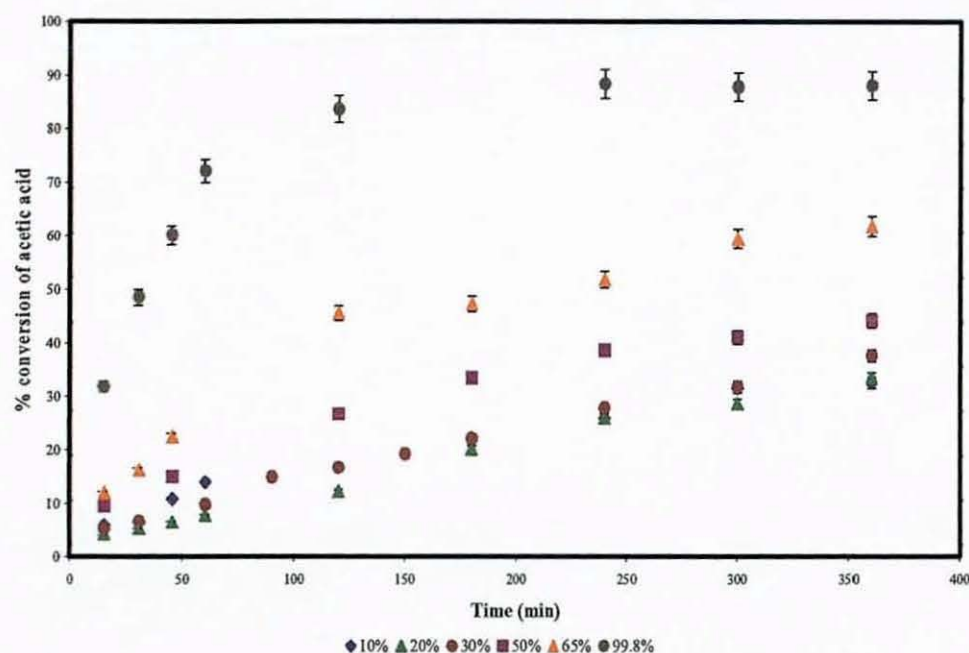


**Figure 3.33.** Effect of acetic acid concentration on conversion of acetic acid at a catalyst loading of 5% (w/w); temperature, 358 K; feed mole ratio (*iso*-amyl alcohol to acetic acid), 2:1; catalyst, CT-275; stirrer speed, 500 rpm.

### 3.4.6. Effect of catalyst reusability

Neier (1991) reported that ion exchange resins could be deactivated by hydrolysis of functional groups, blocking of active sites as a result of polymerisation/polycondensation products, depolymerisation, and release of oligomeric sulphonic acids due to oxygen sensitivity and desulphonation. Desulphonation leads to thermal degradation of the resins, and takes place significantly above 380 K. Fang (1964) investigated on the thermal stability of Amberlyst-15 in the temperature range between 373 - 438 K and found that at up to 413 K, partial desulphonation occurred and a shrinkage of the three-dimensional network took place at higher temperatures, resulting in a hindrance for the access of reactant molecules to the active catalytic sites. Pertrus *et al.* (1981) looked at the mechanism and kinetics of desulphonation. The desulphonation rate was found to be dependent on the temperature, acid concentration and charge density on the sulphonic acid group. In the investigation of catalyst reusability, the macroporous ion exchange resin, Purolite® CT-175, was reused for up to three experimental runs, with each experimental run lasting six hours. The reused catalyst was soaked in

deionised water for 24 hours, washed with methanol and kept in a vacuum oven at 373 K for 6 hours to remove moisture completely. Figure 3.34 shows that there was no significant change in the conversion of acetic acid with the reused catalysts. The results show that Purolite<sup>®</sup> CT-175 ion exchange resins can be used repeatedly for this chemical reaction without foregoing catalytic activity. In order to ensure the consistency of experimental conditions for the batch kinetic studies, fresh ion exchange resins were used for each individual experimental run. According to the manufacturer's specifications, the lifetime of the ion exchange resin is normally about 6,000-10,000 operating hours, even when used at elevated temperatures.

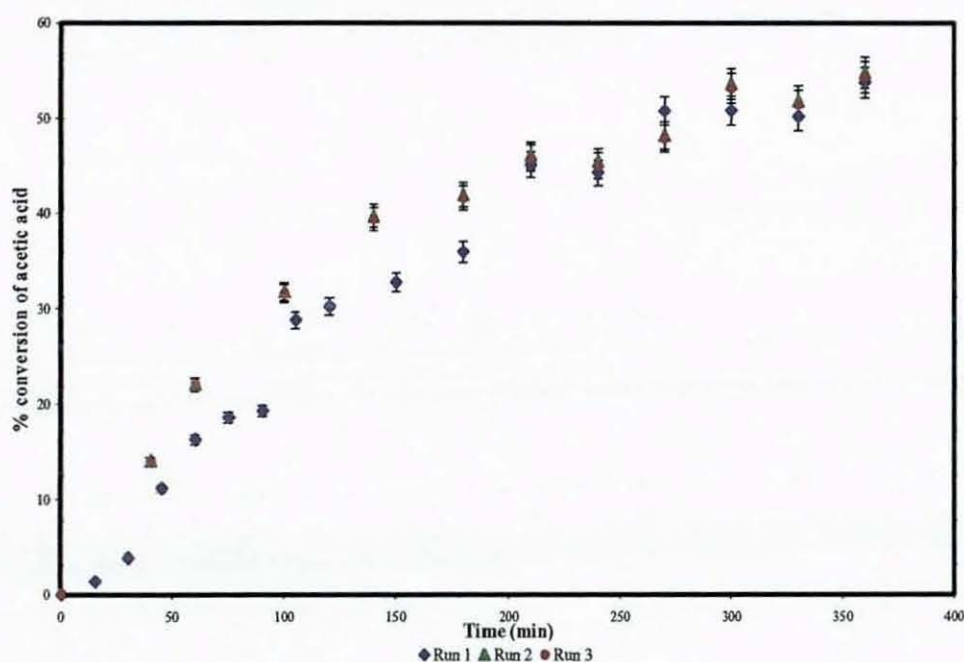


**Figure 3.34.** Effect of catalyst reusability on conversion of 30% (w/w) acetic acid at a catalyst loading of 10% (w/w); temperature, 358 K; feed mole ratio (*iso*-amyl alcohol to acetic acid), 2:1; catalyst, CT-175; stirrer speed, 500 rpm.

### 3.4.7. Comparison of different catalysts

The esterification rates of 30% (w/w) diluted acetic acid with *iso*-amyl alcohol at 358 K with initial feed molar ratio (*iso*-amyl alcohol to acetic acid) 2:1 were compared between 5% (w/w) of Purolite<sup>®</sup> CT-175 and Purolite<sup>®</sup> CT-275 at a stirrer speed of 500 rpm. Figure 3.35 shows a slightly faster reaction rate and higher acetic acid conversion with the use of Purolite<sup>®</sup> CT-175 catalyst as

compared to Purolite<sup>®</sup> CT-275 catalyst. As shown in Figure 3.11, Purolite<sup>®</sup> CT-175 ion exchange resins has larger pore volume as compared to Purolite<sup>®</sup> CT-275 ion exchange resins. This increases its ability to be accessed by the reagents, and henceforth leading to a slightly faster reaction rate and slightly higher conversion of acetic acid at a fixed contact time. The ion exchange capacity are very similar for both Purolite<sup>®</sup> CT-175 and Purolite<sup>®</sup> CT-275.

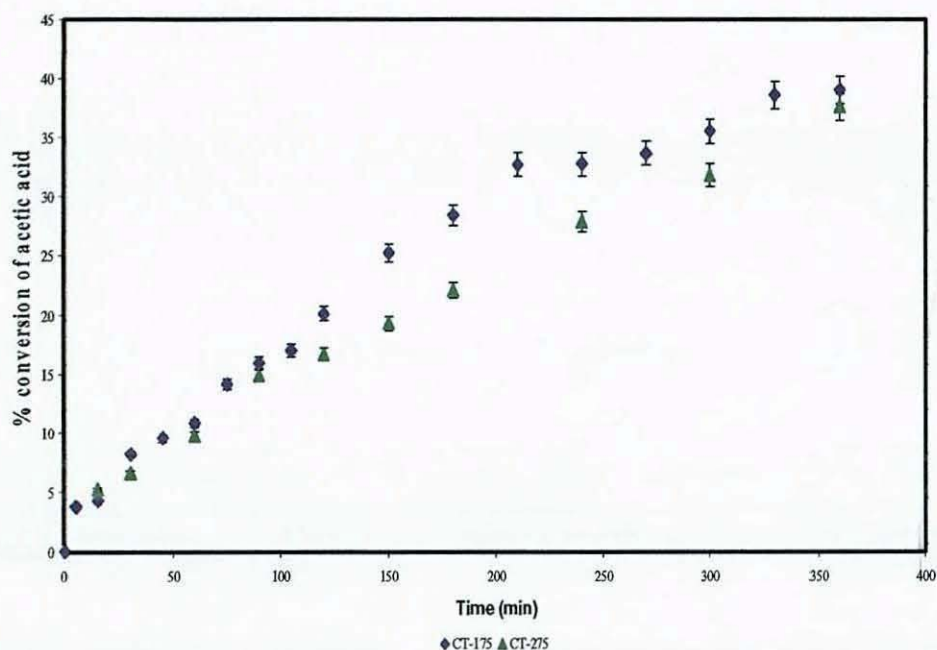


**Figure 3.35.** Effect of catalyst type on conversion of 30% (w/w) acetic acid at a catalyst loading of 5% (w/w); temperature, 358 K; feed mole ratio (*iso*-amyl alcohol to acetic acid), 2:1; stirrer speed 500 rpm.

### 3.5 CONCLUSIONS

The batch kinetic studies for the esterification of acetic acid with *iso*-amyl alcohol were investigated over a wide range of operating conditions including stirrer speed, catalyst particle size, reaction temperature, catalyst loading, feed mole ratio, acetic acid concentration, catalyst reusability and catalyst type.

The main conclusions for the batch kinetic studies are:

- (i) Internal mass transfer resistance is negligible in the particle size range used in this work.
- (ii) External mass transfer resistance is eliminated by carrying out all batch kinetic experiments at a stirrer speed of 500 rpm.

- (iii) The rate of conversion of acetic acid increases with an increase in temperature from 333 K to 363 K.
- (iv) The rate of conversion of acetic acid increases with an increase in catalyst loading from 2.5% (w/w) to 10% (w/w) with the equilibrium conversion remaining the same.
- (v) The conversion of acetic acid is higher at a fixed contact time using a higher feed mole ratio of *iso*-amyl alcohol to acetic acid under the conditions investigated.
- (vi) The reaction rate and overall conversion of acetic acid increase with an increase in the acetic acid concentration from 10% (w/w) to 99.8% (w/w).
- (vii) Purolite® CT-175 ion exchange resin catalyst can be used repeatedly without losing its catalytic capability.
- (viii) Purolite® CT-175 ion exchange resin catalyst shows slightly better catalytic performance as compared to Purolite® CT-275 ion exchange resin catalyst, and was subsequently used for the residue curve map and reactive distillation column experiments.

## 4. KINETIC MODELLING

### 4.1 INTRODUCTION

A kinetic rate expression would be useful towards the simulation of the dynamic behaviour of a reactive distillation column. The objective of this work is to obtain a suitable kinetic rate expression for the esterification of acetic acid with *iso*-amyl alcohol catalysed by Purolite® CT-175.

The non-ideality of the liquid phase was taken into account by using activities instead of the mole fractions. The UNIFAC group contribution method was used for the prediction of the activity coefficients. The UNIFAC method of determining the activity coefficients is presented.

This chapter presents derivation of the individual kinetic models including the Langmuir-Hinshelwood-Hougen-Watson (LHHW), Eley-Rideal (E-R), modified LHHW (M-L) and quasi-homogenous (Q-H) kinetic models. The kinetic models were subsequently used to correlate the experimental kinetic data under different operating conditions. The capabilities of the models were compared with one another, and the activation energy for the reaction was determined.

### 4.2 THE KINETIC MODELS

As all the experiments were conducted in the presence of a solid ion-exchange resin catalyst, the heterogeneous kinetic models including LHHW, E-R, M-L and Q-H models were applied for correlating the kinetic data available at different temperatures, catalyst loadings and acetic acid concentrations. In the case of this heterogeneously catalysed reaction, the batch equation (Levenspiel, 1999) was used. With reference to acetic acid (limiting reactant) for this reaction, the batch equation is as illustrated in Equation 4.1.

$$(-r_A)W = N_{AO} \left( \frac{dX_A}{dt} \right) \quad \text{Eq. 4.1}$$

where  $-r_A$  is the reaction rate of acetic acid ( $\text{mol g}^{-1} \text{min}^{-1}$ ),  $W$  is the weight of the catalyst (g),  $N_{A0}$  is the initial number of moles of acetic acid (mole),  $X_A$  is the conversion of acetic acid and  $t$  is the time of the reaction (min).

In accounting for the non-ideal mixing behaviour of the bulk liquid phase, the activity of the components was taken into account instead of the concentration of the components. Lee *et al.* (2000), Sanz *et al.* (2002) and Zhang *et al.* (2004) adopted the same approach by using the activities whilst taking into account the non-ideality of the liquid phase. Fredenslund *et al.* (1975) highlighted that the UNIFAC method for predicting the liquid phase activity coefficients was a useful tool towards the calculation of vapour-liquid equilibrium compositions in situations where no experimental information was available. Reid *et al.* (1987) reported that the UNIFAC group contribution method was used for the estimation of the activity coefficients. Fredenslund *et al.* (1975) and Skjold-Jørgensen *et al.* (1979) stated that the UNIFAC group contribution method was a useful method for the prediction of activity coefficients in non-electrolyte liquid mixtures at low to moderate pressures and at temperatures between 300 K and 425 K. The method is a combination of the solution of groups concept and a model for activity coefficients based on an extension of the quasi chemical theory of liquid mixtures. The solution of groups concept is based on considering a liquid mixture as a solution of groups instead of a solution of molecules. The groups are individual structural units e.g.  $\text{CH}_3$ ,  $\text{CH}_2$ ,  $\text{H}_2\text{O}$ , etc. which when added together form the parent molecules. The activity coefficients of the components are then determined by the properties of the groups rather than the properties of the molecules that made up the components. The resulting UNIFAC method provides a simple procedure for calculating activity coefficients ( $\gamma_i$ ) on the basis of constants reflecting the difference in sizes and surface area of the individual functional groups (combinatorial part,  $\gamma_i^C$ ) as well as parameters representing the energetic interactions between the functional groups (residual part,  $\gamma_i^R$ ). Smith *et al.* (1996) stated that the UNIFAC method of determining the activity coefficient could be obtained by Equation 4.2.

$$\ln \gamma_i = \ln \gamma_i^C + \ln \gamma_i^R \quad \text{Eq. 4.2}$$

A systematic procedure of determining the activity coefficients for the reacting system between acetic acid and *iso*-amyl alcohol through the UNIFAC group contribution method is highlighted to demonstrate its applications. It is for a quaternary mixture of acetic acid (A)/*iso*-amyl alcohol (B)/*iso*-amyl acetate (C)/water (D) at 358 K whereby  $x_A = 0.3024$ ;  $x_B = 0.6357$ ;  $x_C = 0.0310$  and  $x_D = 0.0310$ . The volume and area parameters of the functional groups and their interaction parameters are listed in Table 4.1 and Table 4.2, respectively.

**Table 4.1.** The volume and area parameters  $R_k$  and  $Q_k$  of the UNIFAC group for the acetic acid/*iso*-amyl alcohol/*iso*-amyl acetate/water system. (Skjold-Jørgensen *et al.*, 1979).

Functional group	Subgroup number (k)	Relative volume ( $R_k$ )	Relative surface area ( $Q_k$ )	$v_k^A$	$v_k^B$	$v_k^C$	$v_k^D$
CH <sub>3</sub>	1	0.9011	0.848	1	2	2	0
CH <sub>2</sub>	2	0.6744	0.540	0	2	2	0
CH	3	0.4469	0.228	0	1	1	0
OH	15	1.0000	1.200	0	1	0	0
H <sub>2</sub> O	17	0.9200	1.400	0	0	0	1
CH <sub>3</sub> COO	22	1.9031	1.728	0	0	1	0
COOH	43	1.3013	1.224	1	0	0	0

Where  $v_k^A$ ,  $v_k^B$ ,  $v_k^C$  and  $v_k^D$  are the numbers of each subgroup in each of the components.

**Table 4.2.** The interaction parameters,  $a_{mn}$ , of the UNIFAC group (m,n) for the acetic acid/*iso*-amyl alcohol/*iso*-amyl acetate/water system (Gmehling *et al.*, 1982)

n	m						
	CH <sub>3</sub>	CH <sub>2</sub>	CH	OH	H <sub>2</sub> O	CH <sub>3</sub> COO	COOH
CH <sub>3</sub>	0	0	0	986.5	1318	232.1	663.5
CH <sub>2</sub>	0	0	0	986.5	1318	232.1	663.5
CH	0	0	0	986.5	1318	232.1	663.5
OH	156.4	156.4	156.4	0	353.5	101.1	199.0
H <sub>2</sub> O	300.0	300.0	300.0	-229.1	0	14.42	-14.09
CH <sub>3</sub> COO	114.8	114.8	114.8	245.4	10000	0	660.2
COOH	315.3	315.3	315.3	-151.0	-66.17	-256.3	0

The properties of the components  $r_i$ ,  $q_i$ ,  $e_{ki}$ ,  $\beta_{ik}$ ,  $\theta_k$ ,  $s_k$  and  $\tau_{mk}$  could be calculated through Equations 4.3 to 4.9 (Smith *et al.*, 1996). The molecular properties ( $r_i$  and  $q_i$ ) are independent of composition.

$$r_i = \sum_k v_k {}^{(i)}R_k \quad \text{Eq. 4.3}$$

$$q_i = \sum_k v_k {}^{(i)}Q_k \quad \text{Eq. 4.4}$$

$$e_{ki} = \frac{v_k {}^{(i)}Q_k}{q_i} \quad \text{Eq. 4.5}$$

$$\tau_{mk} = \exp \frac{-a_{mk}}{T} \quad \text{Eq. 4.6}$$

$$\beta_{ik} = \sum_m e_{mi} \tau_{mk} \quad \text{Eq. 4.7}$$

$$\theta_k = \frac{\sum_i x_i q_i e_{ki}}{\sum_j x_j q_j} \quad \text{Eq. 4.8}$$

$$s_k = \sum_m \theta_m \tau_{mk} \quad \text{Eq. 4.9}$$

where  $i$  represents a component in the reacting system, and  $j$  is a dummy index running over all components.  $k$  is a representation of the subgroups, and  $m$  is a dummy index running over all subgroups.

$$r_A = 1(0.9011) + 1(1.3013)$$

$$= 2.2024$$

$$r_B = 2(0.9011) + 2(0.6744) + 1(0.4469) + 1(1.0000)$$

$$= 4.5979$$

$$r_C = 2(0.9011) + 2(0.6744) + 1(0.4469) + 1(1.9031)$$

$$= 5.5010$$

$$r_D = 1(0.9200)$$

$$= 0.9200$$

$$q_A = 1(0.848) + 1(1.224)$$

$$= 2.072$$

$$q_B = 2(0.848) + 2(0.540) + 1(0.228) + 1(1.200)$$

$$= 4.204$$

$$q_C = 2(0.848) + 2(0.540) + 1(0.228) + 1(1.728)$$

$$= 4.732$$

$$q_D = 1(1.400)$$

$$= 1.400$$

Substituting known values into Equation 4.5 give the values of  $e_{ki}$  which are presented in Table 4.3.

**Table 4.3.** Values of  $e_{ki}$

$e_{1A}$	0.4093	$e_{1B}$	0.4034	$e_{1C}$	0.3584	$e_{1D}$	0.0000
$e_{2A}$	0.0000	$e_{2B}$	0.2569	$e_{2C}$	0.2282	$e_{2D}$	0.0000
$e_{3A}$	0 0000	$e_{3B}$	0.0542	$e_{3C}$	0.0482	$e_{3D}$	0 0000
$e_{15A}$	0.0000	$e_{15B}$	0.2854	$e_{15C}$	0 0000	$e_{15D}$	0.0000
$e_{17A}$	0.0000	$e_{17B}$	0 0000	$e_{17C}$	0.0000	$e_{17D}$	1.0000
$e_{22A}$	0.0000	$e_{22B}$	0.0000	$e_{22C}$	0.3652	$e_{22D}$	0.0000
$e_{43A}$	0.5907	$e_{43B}$	0.0000	$e_{43C}$	0.0000	$e_{43D}$	0 0000

The substitution of the  $a_{mn}$  values from Table 4.2 into Equation 4.6 with  $T=358.15$  K give the values of  $\tau_{mk}$ , which are consolidated and presented in Tables 4.4(i) and 4.4(ii).

**Table 4.4(i)** Values of  $\tau_{mk}$

$\tau_{1,1}$	1.0000	$\tau_{2,1}$	1.0000	$\tau_{3,1}$	1.0000	$\tau_{15,1}$	0.6462
$\tau_{1,2}$	1.0000	$\tau_{2,2}$	1.0000	$\tau_{3,2}$	1.0000	$\tau_{15,2}$	0.6462
$\tau_{1,3}$	1.0000	$\tau_{2,3}$	1.0000	$\tau_{3,3}$	1.0000	$\tau_{15,3}$	0 6462
$\tau_{1,15}$	0.0636	$\tau_{2,15}$	0.0636	$\tau_{3,15}$	0.0636	$\tau_{15,15}$	1.0000
$\tau_{1,17}$	0.0252	$\tau_{2,17}$	0.0252	$\tau_{3,17}$	0.0252	$\tau_{15,17}$	0.3727
$\tau_{1,22}$	0.5231	$\tau_{2,22}$	0.5231	$\tau_{3,22}$	0.5231	$\tau_{15,22}$	0.7541
$\tau_{1,43}$	0.1568	$\tau_{2,43}$	0.1568	$\tau_{3,43}$	0.1568	$\tau_{15,43}$	0.5737

Table 4.4(ii) Values of  $\tau_{mk}$ 

$\tau_{17,1}$	0.4327	$\tau_{22,1}$	0.7258	$\tau_{43,1}$	0.4146
$\tau_{17,2}$	0.4327	$\tau_{22,2}$	0.7258	$\tau_{43,2}$	0.4146
$\tau_{17,3}$	0.4327	$\tau_{22,3}$	0.7258	$\tau_{43,3}$	0.4146
$\tau_{17,15}$	1.8959	$\tau_{22,15}$	0.5040	$\tau_{43,15}$	1.5244
$\tau_{17,17}$	1.0000	$\tau_{22,17}$	0.0000	$\tau_{43,17}$	1.2029
$\tau_{17,22}$	0.9605	$\tau_{22,22}$	1.0000	$\tau_{43,22}$	2.0455
$\tau_{17,43}$	1.0401	$\tau_{22,43}$	0.1583	$\tau_{43,43}$	1.0000

The substitution of the numerical values of  $e_{ki}$  from Table 4.3 and the numerical values of  $\tau_{mk}$  from Tables 4.4(i) and 4.4(ii) lead to the values of  $\beta_{ik}$  as tabulated in Table 4.5.

Table 4.5. Values of  $\beta_{ik}$ 

$\beta_{A,1}$	0.6542	$\beta_{B,1}$	0.8990	$\beta_{C,1}$	0.8999	$\beta_{D,1}$	0.4327
$\beta_{A,2}$	0.6542	$\beta_{B,2}$	0.8990	$\beta_{C,2}$	0.8999	$\beta_{D,2}$	0.4327
$\beta_{A,3}$	0.6542	$\beta_{B,3}$	0.8990	$\beta_{C,3}$	0.8999	$\beta_{D,3}$	0.4327
$\beta_{A,15}$	0.9266	$\beta_{B,15}$	0.3309	$\beta_{C,15}$	0.2244	$\beta_{D,15}$	1.8959
$\beta_{A,17}$	0.7209	$\beta_{B,17}$	0.1244	$\beta_{C,17}$	0.0160	$\beta_{D,17}$	1.0000
$\beta_{A,22}$	1.4224	$\beta_{B,22}$	0.5890	$\beta_{C,22}$	0.6972	$\beta_{D,22}$	0.9605
$\beta_{A,43}$	0.6549	$\beta_{B,43}$	0.2758	$\beta_{C,43}$	0.1574	$\beta_{D,43}$	1.0401

The substitution of the results in Equations 4.8 and 4.9 give values of  $\theta_i$  and  $S_i$  (Table 4.6)

Table 4.6. Values of  $\theta_i$  and  $S_i$ 

$\theta_1$	0.3976	$S_1$	0.8493
$\theta_2$	0.2064	$S_2$	0.8493
$\theta_3$	0.0436	$S_3$	0.8493
$\theta_4$	0.2186	$S_4$	0.4528
$\theta_5$	0.0124	$S_5$	0.2378
$\theta_6$	0.0154	$S_6$	0.7478
$\theta_7$	0.1061	$S_7$	0.3484

When UNIQUAC is applied to a solution of groups, the combinatorial part ( $\ln\gamma_i^C$ ) and residual part ( $\ln\gamma_i^R$ ) of the activity coefficient are expressed as in Equations 4.10 and 4.11, respectively (Smith *et al.*, 1996).

$$\ln\gamma_i^C = 1 - J_i + \ln J_i - 5q_i \left(1 - \frac{J_i}{L_i} + \ln \frac{J_i}{L_i}\right) \quad \text{Eq. 4.10}$$

$$\ln\gamma_i^R = q_i \left[ 1 - \sum_k (\theta_k \frac{\beta_{ik}}{s_k} - e_{ki} \ln \frac{\beta_{ik}}{s_k}) \right] \quad \text{Eq. 4.11}$$

The quantities  $J_i$  and  $L_i$  as part of Equation 4.10 are calculated using Equations 4.12 and 4.13 (Smith *et al.*, 1996).

$$J_i = \frac{r_i}{\sum_j r_j x_j} \quad \text{Eq. 4.12}$$

$$L_i = \frac{q_i}{\sum_j q_j x_j} \quad \text{Eq. 4.13}$$

The substitution of the values of the different parameters in Equations 4.12 and 4.13 give values of  $J_i$  and  $L_i$  (Table 4.7)

Table 4.7. Values of  $J_i$  and  $L_i$ 

$J_A$	0.5814	$L_A$	0.5939
$J_B$	1.2139	$L_B$	1.2049
$J_C$	1.4523	$L_C$	1.3563
$J_D$	0.2429	$L_D$	0.4013

The applications of Equations 4.10 and 4.11 lead to the values of  $\ln\gamma_i^C$  and  $\ln\gamma_i^R$  (Table 4.8).

Table 4.8. Values of  $\ln\gamma_i^C$  and  $\ln\gamma_i^R$ 

$\ln\gamma_A^C$	-0.1214	$\ln\gamma_A^R$	0.1112
$\ln\gamma_B^C$	-0.0195	$\ln\gamma_B^R$	0.0141
$\ln\gamma_C^C$	-0.0225	$\ln\gamma_C^R$	0.7269
$\ln\gamma_D^C$	0.0933	$\ln\gamma_D^R$	1.1232

The activity coefficient,  $\gamma_i$ , could hence be calculated from the values of  $\ln\gamma_i^C$  and  $\ln\gamma_i^R$  from Table 4.8 using Equation 4.2. The activity coefficient values for the different components are  $\gamma_A = 0.990$ ;  $\gamma_B = 0.995$ ;  $\gamma_C = 2.023$  and  $\gamma_D = 3.375$ .

However, the activity coefficients at different temperatures are obtained using the UNIFAC program (Cutlip, 1999). A representative set of activity coefficients are shown in Table 4.9.

**Table 4.9.** Activity coefficient values at 333 K as calculated by UNIFAC group contribution method.

Temperature	Liquid mole fraction				Activity coefficient			
333.15 K	0.333	0.667	0.000	0.000	1.021	0.983	2.035	3.143
	0.207	0.540	0.127	0.127	0.917	1.035	1.899	3.208
	0.199	0.532	0.134	0.134	0.911	1.040	1.894	3.209
	0.195	0.528	0.138	0.138	0.908	1.042	1.890	3.212
	0.190	0.524	0.143	0.143	0.891	1.050	1.865	3.235
	0.172	0.506	0.161	0.161	0.891	1.050	1.865	3.235
	0.172	0.506	0.161	0.161	0.891	1.051	1.867	3.232
	0.168	0.501	0.165	0.165	0.888	1.052	1.863	3.235
	0.148	0.482	0.185	0.185	0.873	1.057	1.841	3.258
	0.140	0.474	0.193	0.193	0.868	1.058	1.833	3.266
	0.128	0.462	0.205	0.205	0.859	1.066	1.820	3.278
	0.128	0.462	0.205	0.205	0.859	1.066	1.820	3.278

The equilibrium constant was calculated from the component concentrations at equilibrium through equation 4.14 (Liu and Tan, 2001; Lee *et al.*, 2002; Sanz *et al.*, 2002).

$$K_{eq} = \left( \frac{a_C a_D}{a_A a_B} \right)_{eq} = \left( \frac{x_C x_D}{x_A x_B} \right)_{eq} \left( \frac{\gamma_C \gamma_D}{\gamma_A \gamma_B} \right)_{eq} \quad \text{Eq. 4.14}$$

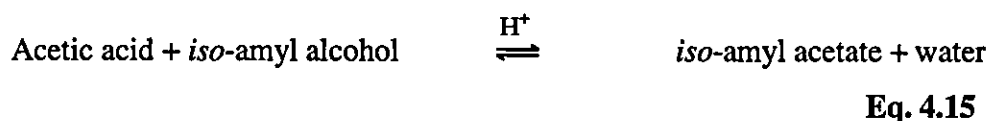
Where  $K_{eq}$  is the equilibrium constant of the reaction,  $a$  is the activity of the component,  $x$  is the liquid mole fraction of the component, and  $\gamma$  is the activity coefficient of the component. The subscripts  $A$ ,  $B$ ,  $C$  and  $D$  denote acetic acid, *iso*-amyl alcohol, *iso*-amyl acetate and water, respectively.

The rate expression,  $-r_A$ , as defined in equation 4.1 depends on the assumptions of the reaction mechanism. Four types of rate expressions, including the Langmuir-Hinshelwood-Hougen-Watson (LHHW), Eley-Rideal (E-R), modified LHHW (ML) and quasi-homogenous (Q-H) were adopted to correlate the kinetic data for the different experimental conditions.

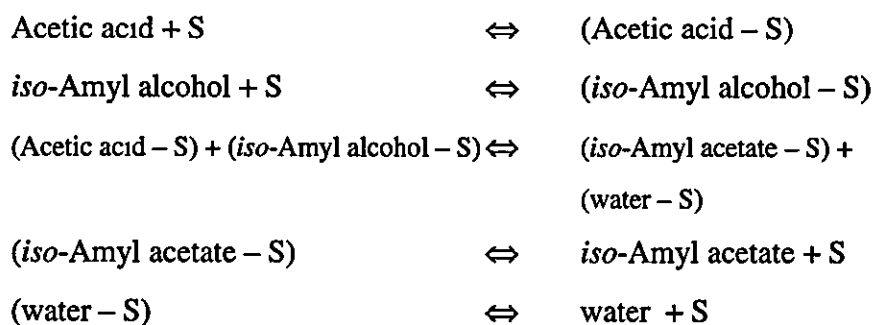
## 4.2.1 Langmuir-Hinshelwood Hougen-Watson (LHHW) model

The LHHW kinetic model is applicable whenever the rate-determining step is the surface reaction between the adsorbed molecules. In this model, all of the components were assumed in their adsorbed phases. The derivation of the LHHW kinetic model was presented in Carberry (1976). Several assumptions are made for the derivation of the LHHW model. The rate determining step is controlled by the surface reaction, the adsorption sites are uniformly energetic, a monolayer catalytic coverage is assumed and a dual site adsorption mechanism is being used for the reaction. With application to the reacting system between acetic acid and *iso*-amyl alcohol, the LHHW kinetic model is described.

The reversible reaction between acetic acid and *iso*-amyl alcohol is as illustrated in Equation 4.15:



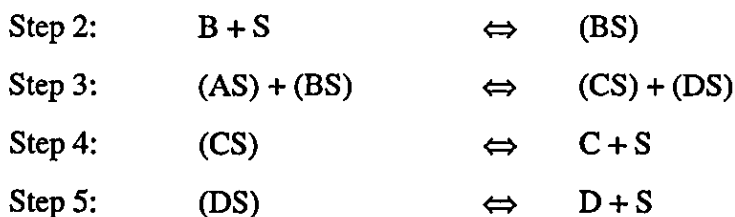
The assumed reaction sequence for the above reaction between acetic acid and *iso*-amyl alcohol based on the LHHW mechanism is:



where S denotes a vacant adsorption site.

The assumed reaction sequence for the reaction between acetic acid and *iso*-amyl alcohol based on the LHHW mechanism is simplified as follows:





Where A, B, C and D are acetic acid, *iso*-amyl alcohol, *iso*-amyl acetate and water.

Steps 1 and 2 are the adsorption steps of the reactant molecules onto the catalyst surface, Step 3 is the surface reaction between the adsorbed molecules, and Steps 4 and 5 are the desorption steps of the product molecules from the catalyst surface.

With the assumption that the bimolecular surface reaction (Step 3) is the rate determining step,

$$r = k_3(AS)(BS) - k_3(CS)(DS) \quad \text{Eq. 4.16}$$

where  $k_3$  is the rate constant for the forward reaction of the rate determining step, and  $k_3$  is the rate constant for the reverse reaction of the rate determining step. Implicit in the concept of a single rate determining step within a sequence of several steps as outlined above is the understanding that all steps except that for the rate controlling step exist in equilibrium, or perhaps more accurately, a steady state prevailing. This results in a ratio of reactant and product of constant value for all the steps except the rate controlling step (Step 3). The steady state ratios ( $K_1$ ,  $K_2$ ,  $K_4$  and  $K_5$ ) are expressed in Equations 4.17 to 4.20.

$$\text{Step 1:} \quad \frac{(AS)}{AS} = K_1 \quad \text{Eq. 4.17}$$

$$\text{Step 2:} \quad \frac{(BS)}{BS} = K_2 \quad \text{Eq. 4.18}$$

$$\text{Step 4:} \quad \frac{(CS)}{CS} = K_4 \quad \text{Eq. 4.19}$$

$$\text{Step 5:} \quad \frac{(DS)}{DS} = K_5 \quad \text{Eq. 4.20}$$

Substituting Equations 4.17 to 4.20 into Equation 4.16 and with the overall experimental equilibrium constant  $K_{eq}$  being defined as  $K_{eq}=k_3/k_{-3}$ ,

$$\begin{aligned} r &= k_3(AS)(BS) - k_{-3}(CS)(DS) \\ &= k_3ASK_1BSK_2 - k_{-3}CSK_4DSK_5 \\ &= k_3AB K_1 K_2 S^2 - \frac{k_{-3}}{K_{eq}} CDK_4K_5S^2 \\ \therefore r &= k_3 K_1 K_2 S^2 \left( AB - \frac{K_4K_5}{K_{eq}K_1K_2} CD \right) \quad \text{Eq. 4.21} \end{aligned}$$

Assuming ideality i.e. no active sites may be created *in situ* during the catalytic process, the total concentration of active catalytic sites for a given catalyst is designated as  $S_0$ . The concentration of unoccupied sites is  $S$ , and that occupied by the different adsorbed species is  $S_A$ ,  $S_B$ ,  $S_C$ ,  $S_D$ , etc.  $S_0$  is defined as follow:

$$S_0 = S + S_A + S_B + S_C + S_D + \dots \quad \text{Eq. 4.22}$$

$$S_0 = S + (AS) + (BS) + (CS) + (DS) + (IS) \quad \text{Eq. 4.23}$$

Where (IS) accounts for the catalytic sites occupied by inert i.e. non-reactive components e.g. nitrogen used as diluents in feed streams.

Substituting Equations 4.17 to 4.20 into Equation 4.23 whilst taking into account adsorption of any inert components,

$$S_0 = S + (AS) + (BS) + (CS) + (DS) + (IS)$$

$$\begin{aligned}
 &= S + SK_1A + SK_2B + SK_4C + SK_5D + SK_6I \\
 &= S(1 + K_1A + K_2B + K_4C + K_5D + K_6I) \\
 S &= \frac{S_0}{(1 + K_1A + K_2B + K_4C + K_5D + K_6I)} \quad \text{Eq. 4.24}
 \end{aligned}$$

Therefore, the fraction of total catalytic sites that are unoccupied is represented as in Equation 4.25.

$$\frac{S}{S_0} = \frac{1}{(1 + K_1A + K_2B + K_4C + K_5D + K_6I)} \quad \text{Eq. 4.25}$$

The sites occupied by acetic acid (A), *iso*-amyl alcohol (B), *iso*-amyl acetate (C), water (D) and inert components (I) are expressed in Equations 4.26 to 4.30.

$$\begin{aligned}
 \frac{(AS)}{S_0} &= \frac{SK_1A}{S_0} \\
 \therefore \frac{(AS)}{S_0} &= \frac{K_1A}{(1 + K_1A + K_2B + K_4C + K_5D + K_6I)} \quad \text{Eq. 4.26}
 \end{aligned}$$

$$\begin{aligned}
 \frac{(BS)}{S_0} &= \frac{SK_2B}{S_0} \\
 \therefore \frac{(BS)}{S_0} &= \frac{K_2B}{(1 + K_1A + K_2B + K_4C + K_5D + K_6I)} \quad \text{Eq. 4.27}
 \end{aligned}$$

$$\frac{(CS)}{S_0} = \frac{SK_4C}{S_0}$$

$$\therefore \frac{(CS)}{S_0} = \frac{K_4 C}{(1 + K_1 A + K_2 B + K_4 C + K_5 D + K_6 I)} \quad \text{Eq. 4.28}$$

$$\frac{(DS)}{S_0} = \frac{SK_5 D}{S_0}$$

$$\therefore \frac{(DS)}{S_0} = \frac{K_5 D}{(1 + K_1 A + K_2 B + K_4 C + K_5 D + K_6 I)} \quad \text{Eq. 4.29}$$

$$\frac{(IS)}{S_0} = \frac{SK_6 I}{S_0}$$

$$\therefore \frac{(IS)}{S_0} = \frac{K_6 I}{(1 + K_1 A + K_2 B + K_4 C + K_5 D + K_6 I)} \quad \text{Eq. 4.30}$$

Alternatively, the fraction of total catalytic sites that are unoccupied could be represented as in Equation 4.31.

$$\frac{S}{S_0} = 1 - \theta_{\text{total}} \quad \text{Eq. 4.31}$$

Where  $\theta_{\text{total}}$  represents the total coverage of the catalytic sites.

$$\theta_A = \frac{(AS)}{S_0}$$

$$\therefore \theta_A = \frac{K_1 A}{(1 + K_1 A + K_2 B + K_4 C + K_5 D + K_6 I)} \quad \text{Eq. 4.32}$$

Where  $\theta_A$  is the catalytic sites occupied by acetic acid (A).

Similarly, the catalytic sites occupied by *iso*-amyl alcohol (B), *iso*-amyl acetate (C), water (D) and inert components (I) are represented in Equations 4.33 to 4.36.

$$\theta_B = \frac{(BS)}{S_0}$$

$$\therefore \theta_B = \frac{K_2 B}{(1 + K_1 A + K_2 B + K_4 C + K_5 D + K_6 I)} \quad \text{Eq. 4.33}$$

$$\theta_C = \frac{(CS)}{S_0}$$

$$\therefore \theta_C = \frac{K_4 C}{(1 + K_1 A + K_2 B + K_4 C + K_5 D + K_6 I)} \quad \text{Eq. 4.34}$$

$$\theta_D = \frac{(DS)}{S_0}$$

$$\therefore \theta_D = \frac{K_5 D}{(1 + K_1 A + K_2 B + K_4 C + K_5 D + K_6 I)} \quad \text{Eq. 4.35}$$

$$\theta_I = \frac{(IS)}{S_0}$$

$$\therefore \theta_I = \frac{K_6 I}{(1 + K_1 A + K_2 B + K_4 C + K_5 D + K_6 I)} \quad \text{Eq. 4.36}$$

The total number of catalytic sites that are occupied can be expressed as in Equation 4.37.

$$\theta_{\text{total}} = \theta_A + \theta_B + \theta_C + \theta_D + \theta_I$$

$$= \frac{K_1 A + K_2 B + K_4 C + K_5 D + K_6 I}{(1 + K_1 A + K_2 B + K_4 C + K_5 D + K_6 I)}$$

$$= \frac{\sum K_i X_i}{1 + \sum K_i X_i} \quad \text{Eq. 4.37}$$

In Langmuir-Hinshelwood terms, Equation 4.16 could be written as

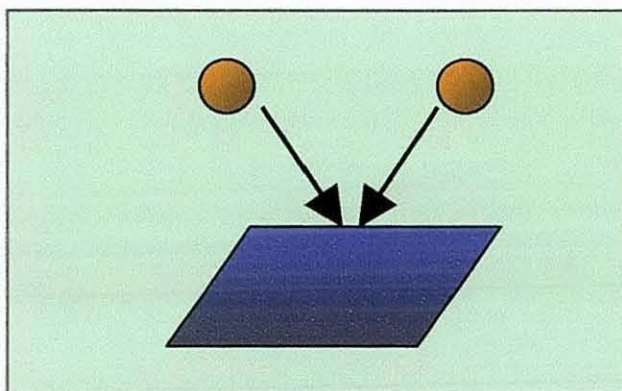
$$r = k'_3 \theta_A \theta_B - k_{-3} \theta_C \theta_D \quad k'_3 \neq k_3 \quad \text{Eq. 4.38}$$

Substituting for  $\theta$ 's from Equations 4.32 to 4.36, Equation 4.38 becomes

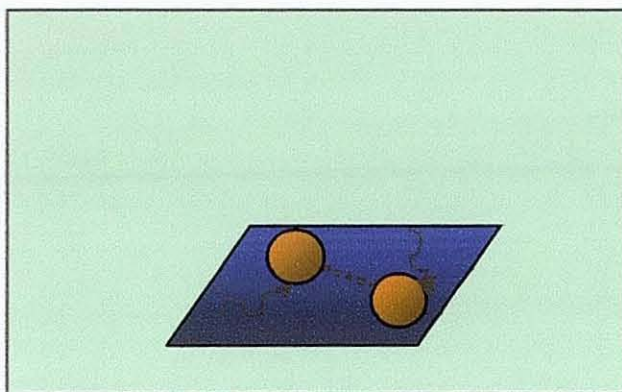
$$\begin{aligned} r &= k'_3 \frac{K_1 A}{(1 + K_1 A + K_2 B + K_4 C + K_5 D + K_6 I)} \frac{K_2 B}{(1 + K_1 A + K_2 B + K_4 C + K_5 D + K_6 I)} \\ &\quad - k_{-3} \frac{K_4 C}{(1 + K_1 A + K_2 B + K_4 C + K_5 D + K_6 I)} \frac{K_5 D}{(1 + K_1 A + K_2 B + K_4 C + K_5 D + K_6 I)} \\ &= k'_3 \frac{K_1 A K_2 B}{(1 + K_1 A + K_2 B + K_4 C + K_5 D + K_6 I)^2} - k_{-3} \frac{K_4 C K_5 D}{(1 + K_1 A + K_2 B + K_4 C + K_5 D + K_6 I)^2} \\ &= k'_3 K_1 K_2 \left[ \frac{AB - CD \left( \frac{K_4 K_5}{K_{eq} K_1 K_2} \right)}{(1 + K_1 A + K_2 B + K_4 C + K_5 D + K_6 I)^2} \right] \\ \therefore r &= k'_3 K_1 K_2 \left[ \frac{AB - \frac{CD}{K'_0}}{(1 + K_1 A + K_2 B + K_4 C + K_5 D + K_6 I)^2} \right] \quad \text{Eq. 4.39} \end{aligned}$$

A pictorial representation of the LHHW mechanism is illustrated in Figure 4.1. With reference to Figure 4.1, the proposed LHHW mechanism can be described as follows:

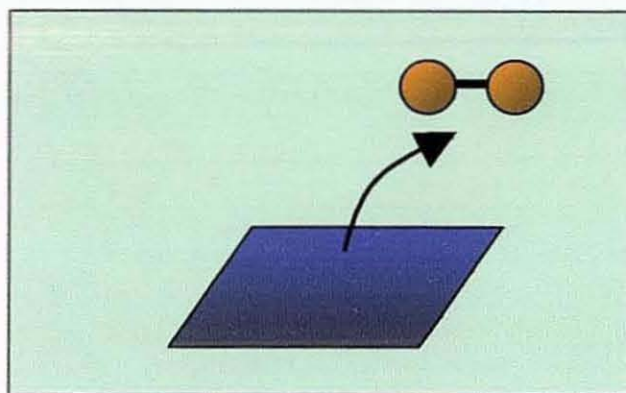
- (i) Two reactant molecules, acetic acid and *iso*-amyl alcohol, adsorb onto the catalyst surface (Figure 4.1a);
- (ii) The adsorbed reactant molecules diffuse across the catalyst surface and interact when they are close to each other (Figure 4.1b);
- (iii) Product molecules i.e. *iso*-amyl acetate and water, are formed which desorbs from the catalyst surface (Figure 4.1c).



(a)



(b)



(c)

**Figure 4.1.** Illustration of the LHHW mechanism (a) adsorption of reactant molecules (b) interaction between molecules (c) desorption of product molecules.

The general rate of reaction for the LHHW model can be written as follows:

$$\begin{aligned}
 -r_A &= \frac{A_f \exp\left(-\frac{E_0}{RT}\right)(a_A a_B - \frac{A_r}{A_f} a_C a_D)}{(1 + k_A a_A + k_B a_B + k_C a_C + k_D a_D)^2} \\
 &= k \frac{(a_A a_B - \frac{a_C a_D}{K_{eq}})}{(1 + k_A a_A + k_B a_B + k_C a_C + k_D a_D)^2}
 \end{aligned}
 \tag{Eq. 4.40}$$

Where  $-r_A$  is the reaction rate of acetic acid,  $E_0$  is the activation energy for the reaction,  $A_f$  and  $A_r$  are the pre-exponential factors for the forward and reverse reactions respectively,  $k$  represents the reaction rate constant,  $k_i$  represents the adsorption coefficient for component  $i$ ,  $a_i$  is the activity of each component and  $K_{eq}$  is the reaction equilibrium constant.

The adsorption coefficient ( $k_i$ ) of the respective component can be defined through the equation 4.41 (Zhang *et al.*, 2004)

$$k_i = \frac{c_{i-s}}{a_i c_s}
 \tag{Eq. 4.41}$$

Where  $c_{i-s}$  and  $c_s$  denote the concentration of component  $i$  at the catalyst surface and concentration of vacant site on the catalyst surface respectively.  $a_i$  is the activity for each component.

As the denominator of equation 4.40 is a multi-component complex, the unknown parameters cannot be regressed correctly on the basis of the experimental results. For this kinetic model, it was assumed that the adsorption of the molecules was very competitive on the same active site of the catalyst, and only those molecules that had the strongest adsorptions were taken into account in the simplified mechanisms. Helfferich (1962) reported that the adsorption of a polar component to the ion exchange resin from a solvent mixture has been found to be considerably stronger than the adsorption of the less polar components. Rihko and Krause (1995) and Sanz *et al.* (2002) offered differing opinions regarding which components had the strongest adsorption on the catalyst surface. Mazzotti *et al.* (1997) found that the affinity of Amberlyst 15 for the acetic acid, ethanol, ethyl acetate and water followed the sequential order of water > alcohol > acid > ester. Gonzalez and Fair (1997) assumed in the LHHW kinetic model that the reaction took place between the water molecule and isoamylene molecule, with both molecules adsorbed on two separate acid sites. Lee *et al.* (2002) suggested that the water affinity of Amberlyst 35 cation exchange resin was the strongest, and the adsorption terms of the other components in the investigated reacting system i.e. *n*-butanol, propionic acid as well as *n*-butyl propionate were neglected in the kinetic models as a result. Gangadwala *et al.* (2003) made the assumption in the LHHW kinetic model that all of the components were in their adsorbed phases for the esterification reaction between acetic acid and *n*-butanol. In this work, two mechanisms were tested to find out which one was more reliable. The first mechanism (mechanism A) assumes that water and *iso*-amyl alcohol are adsorbed much more strongly than the other components i.e. acetic acid and *iso*-amyl acetate in the esterification solution. As a result, the adsorption for both acetic acid and *iso*-amyl acetate are neglected. The equation according to mechanism A could be written as in Equation 4.42.

$$-r_A = k \frac{(a_A a_B - \frac{a_C a_D}{K_{eq}})}{(1 + k_B a_B + k_D a_D)^2} \quad \text{Eq. 4.42}$$

The second mechanism (mechanism B) assumes that water and acetic acid have the strongest adsorption in the esterification solution. As a result, the adsorption for both *iso*-amyl alcohol and *iso*-amyl acetate are neglected. The equation according to mechanism B could be written as in Equation 4.43.

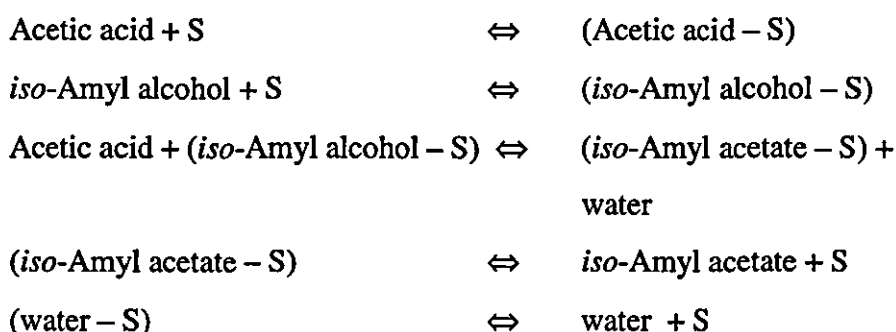
$$-r_A = k \frac{(a_A a_B - \frac{a_C a_D}{K_{eq}})}{(1 + k_A a_A + k_D a_D)^2} \quad \text{Eq. 4.43}$$

In mechanisms A and B, i.e. equations 4.42 and 4.43 respectively, there are three parameters to be estimated. In mechanism A (Equation 4.42), the parameters to be estimated are  $k$ ,  $k_B$  and  $k_D$ . In mechanism B (Equation 4.43), the parameters to be estimated are  $k$ ,  $k_A$  and  $k_D$ .

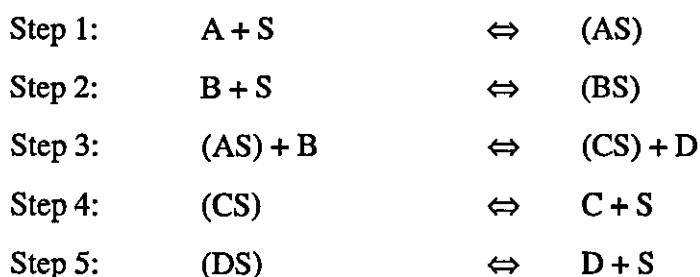
#### 4.2.2 Eley-Rideal (E-R) model

The E-R kinetic model is applicable if the surface reaction taking place between one adsorbed species and one non-adsorbed reactant from the bulk liquid phase is the rate-limiting step. Gangadwala *et al.* (2003) made the assumption that the esterification reaction takes place between adsorbed *n*-butanol and acetic acid species on the catalyst surface to give unadsorbed butyl acetate and adsorbed water molecules in the E-R kinetic model. In general, the assumptions made for the E-R derivation are the rate determining step is controlled by the surface reaction, the adsorption sites are uniformly energetic, monolayer coverage as well as a single site adsorption mechanism is being used for the reaction.

The assumed reaction sequence for the reaction between acetic acid and *iso*-amyl alcohol based on the E-R mechanism is as follow:



The assumed reaction sequence for the reaction between acetic acid and *iso*-amyl alcohol based on the E-R mechanism is simplified as follows:



where A represents acetic acid, B represents *iso*-amyl alcohol, C represents *iso*-amyl acetate and D represents water.

Steps 1 and 2 are the adsorption steps of the molecule onto the catalyst surface, Step 3 is the surface reaction between the one adsorbed molecule and one non-adsorbed molecule, and Steps 3 and 4 are the desorption steps from the catalyst surface.

With the assumption that the surface reaction between one adsorbed molecule and one non-adsorbed molecule (Step 3) is the rate determining step,

$$r = k_3(\text{AS})\text{B} - k_{-3}(\text{CS})\text{D} \quad \text{Eq. 4.44}$$

where  $k_3$  is the rate constant for the forward reaction and  $k_3$  is the rate constant for the reverse reaction of the rate determining step. Similarly to the derivation of the LHHW kinetic model, implicit in the concept of a single rate determining step within a sequence of several steps as outlined above is the understanding that all steps except that for the rate controlling exist in equilibrium, or perhaps more accurately, a steady state prevailing. This results in a ratio of reactant and product of constant value for all the steps except the rate controlling step (Step 3). The steady state ratios ( $K_1$ ,  $K_2$ ,  $K_4$  and  $K_5$ ) are expressed in Equations 4.45 to 4.48.

$$\text{Step 1:} \quad \frac{(AS)}{AS} = K_1 \quad \text{Eq. 4.45}$$

$$\text{Step 2:} \quad \frac{(BS)}{BS} = K_2 \quad \text{Eq. 4.46}$$

$$\text{Step 4:} \quad \frac{(CS)}{CS} = K_4 \quad \text{Eq. 4.47}$$

$$\text{Step 5:} \quad \frac{(DS)}{DS} = K_5 \quad \text{Eq. 4.48}$$

Substituting Equations 4.45 to 4.48 into Equation 4.44 and with the overall experimental equilibrium constant  $K_{eq}$  being defined as  $K_{eq}=k_3/k_{-3}$ ,

$$\begin{aligned} r &= k_3(AS)B - k_{-3}(CS)D \\ &= k_3ASK_1B - k_{-3}CSK_4D \\ &= k_3AB K_1S - \frac{k_{-3}}{K_{eq}} CD K_4S \\ \therefore r &= k_3K_1S(AB - \frac{K_4}{K_{eq}K_1} CD) \end{aligned} \quad \text{Eq. 4.49}$$

Assuming ideality i.e. no active sites may be created in situ over the course of the catalytic process, the total concentration of active catalytic sites for a given catalyst is designated as  $S_0$ . The concentration of unoccupied sites is  $S$ ,

and that occupied by the different adsorbed species is  $S_A$ ,  $S_B$ ,  $S_C$ ,  $S_D$ , etc.  $S_0$  is defined as follow:

$$S_0 = S + S_A + S_B + S_C + S_D + \dots \quad \text{Eq. 4.50}$$

$$S_0 = S + (AS) + (BS) + (CS) + (DS) + (IS) \quad \text{Eq. 4.51}$$

Where (IS) accounts for the catalytic sites occupied by inert i.e. non-reactive components e.g. nitrogen used as diluents in feed streams.

Substituting Equations 4.45 to 4.48 into Equation 4.51 whilst taking into account adsorption of any inert components,

$$\begin{aligned} S_0 &= S + (AS) + (BS) + (CS) + (DS) + (IS) \\ &= S + SK_1A + SK_2B + SK_4C + SK_5D + SK_6I \\ &= S(1 + K_1A + K_2B + K_4C + K_5D + K_6I) \\ S &= \frac{S_0}{(1 + K_1A + K_2B + K_4C + K_5D + K_6I)} \quad \text{Eq. 4.52} \end{aligned}$$

Therefore, the fraction of total catalytic sites that are unoccupied is represented as in Equation 4.53.

$$\frac{S}{S_0} = \frac{1}{(1 + K_1A + K_2B + K_4C + K_5D + K_6I)} \quad \text{Eq. 4.53}$$

The sites occupied by acetic acid (A), *iso*-amyl alcohol (B), *iso*-amyl acetate (C), water (D) and inert components (I) are expressed in Equations 4.54 to 4.58.

$$\frac{(AS)}{S_0} = \frac{SK_1A}{S_0}$$

$$\therefore \frac{(AS)}{S_0} = \frac{K_1A}{(1 + K_1A + K_2B + K_4C + K_5D + K_6I)} \quad \text{Eq. 4.54}$$

$$\frac{(BS)}{S_0} = \frac{SK_2B}{S_0}$$

$$\therefore \frac{(BS)}{S_0} = \frac{K_2B}{(1 + K_1A + K_2B + K_4C + K_5D + K_6I)} \quad \text{Eq. 4.55}$$

$$\frac{(CS)}{S_0} = \frac{SK_4C}{S_0}$$

$$\therefore \frac{(CS)}{S_0} = \frac{K_4C}{(1 + K_1A + K_2B + K_4C + K_5D + K_6I)} \quad \text{Eq. 4.56}$$

$$\frac{(DS)}{S_0} = \frac{SK_5D}{S_0}$$

$$\therefore \frac{(DS)}{S_0} = \frac{K_5D}{(1 + K_1A + K_2B + K_4C + K_5D + K_6I)} \quad \text{Eq. 4.57}$$

$$\frac{(IS)}{S_0} = \frac{SK_6I}{S_0}$$

$$\therefore \frac{(IS)}{S_0} = \frac{K_6I}{(1 + K_1A + K_2B + K_4C + K_5D + K_6I)} \quad \text{Eq. 4.58}$$

Alternatively, the fraction of total catalytic sites that are unoccupied could be represented as in Equation 4.59.

$$\frac{S}{S_0} = 1 - \theta_{\text{total}} \quad \text{Eq. 4.59}$$

where  $\theta_{\text{total}}$  represents the total coverage of the catalytic sites.

$$\theta_A = \frac{(AS)}{S_0}$$

$$\therefore \theta_A = \frac{K_1 A}{(1 + K_1 A + K_2 B + K_4 C + K_5 D + K_6 I)} \quad \text{Eq. 4.60}$$

where  $\theta_A$  is the catalytic sites occupied by acetic acid (A).

The catalytic sites occupied by *iso*-amyl alcohol (B), *iso*-amyl acetate (C), water (D) and inert components (I) are similarly represented in Equations 4.61 to 4.64.

$$\theta_B = \frac{(BS)}{S_0}$$

$$\therefore \theta_B = \frac{K_2 B}{(1 + K_1 A + K_2 B + K_4 C + K_5 D + K_6 I)} \quad \text{Eq. 4.61}$$

$$\theta_C = \frac{(CS)}{S_0}$$

$$\therefore \theta_C = \frac{K_4 C}{(1 + K_1 A + K_2 B + K_4 C + K_5 D + K_6 I)} \quad \text{Eq. 4.62}$$

$$\theta_D = \frac{(DS)}{S_0}$$

$$\therefore \theta_D = \frac{K_5 D}{(1 + K_1 A + K_2 B + K_4 C + K_5 D + K_6 I)} \quad \text{Eq. 4.63}$$

$$\theta_I = \frac{(IS)}{S_0}$$

$$\therefore \theta_I = \frac{K_6 I}{(1 + K_1 A + K_2 B + K_4 C + K_5 D + K_6 I)} \quad \text{Eq. 4.64}$$

The total number of catalytic sites that are occupied,  $\theta_{total}$ , can be expressed as in Equation 4.65.

$$\begin{aligned} \theta_{total} &= \theta_A + \theta_B + \theta_C + \theta_D + \theta_I \\ &= \frac{K_1 A + K_2 B + K_4 C + K_5 D + K_6 I}{(1 + K_1 A + K_2 B + K_4 C + K_5 D + K_6 I)} \\ &= \frac{\sum K_i X_i}{1 + \sum K_i X_i} \end{aligned} \quad \text{Eq. 4.65}$$

In Langmuir-Hinshelwood terms, Equation 4.44 could be written as

$$r = k'_3 \theta_A B - k'_{-3} \theta_C D \quad k'_3 \neq k_{-3} \quad \text{Eq. 4.66}$$

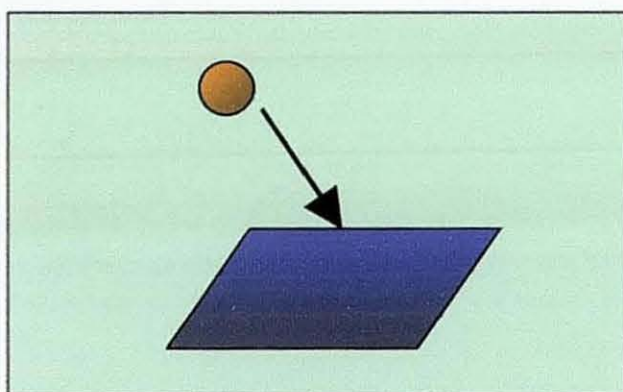
Substituting for  $\theta_A$  (Equation 4.60) and  $\theta_C$  (Equation 4.62), Equation 4.66 becomes

$$\begin{aligned} r &= k'_3 \frac{K_1 AB}{(1 + K_1 A + K_2 B + K_4 C + K_5 D + K_6 I)} - k'_{-3} \frac{K_4 CD}{(1 + K_1 A + K_2 B + K_4 C + K_5 D + K_6 I)} \\ &= k'_3 K_1 \left[ \frac{AB - CD \left( \frac{K_4}{K_{eq} K_1} \right)}{(1 + K_1 A + K_2 B + K_4 C + K_5 D + K_6 I)} \right] \end{aligned}$$

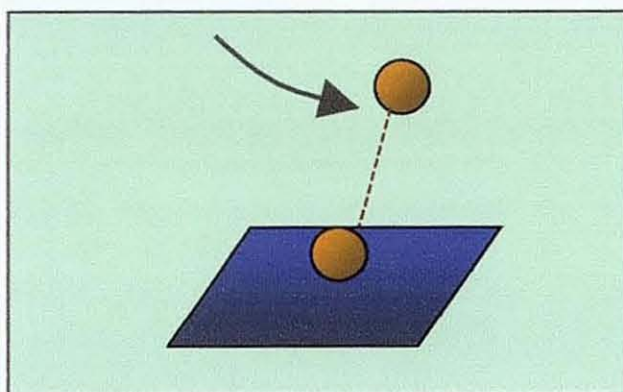
$$= k_3' K_1 \left[ \frac{AB - \frac{CD}{K_0'}}{(1 + K_1 A + K_2 B + K_4 C + K_5 D + K_6 I)} \right] \quad \text{Eq. 4.67}$$

A pictorial representation of the E-R mechanism is illustrated in Figure 4.2. With reference to Figure 4.2, the proposed E-R mechanism could be described as follow:

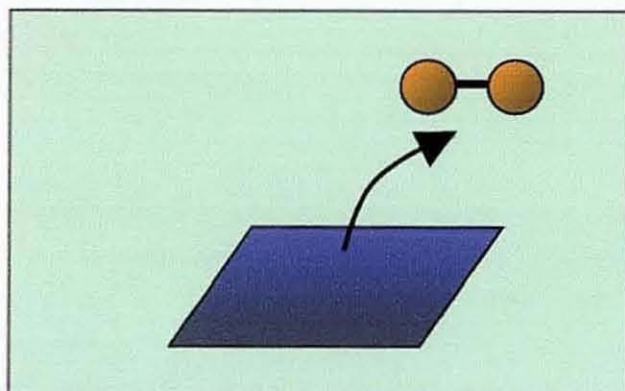
- (i) A reactant molecule, *iso*-amyl alcohol, is adsorbed onto the catalyst surface (Figure 4.2a);
- (ii) An unadsorbed reactant molecule, acetic acid, in the liquid phase passes by which interacts with the adsorbed *iso*-amyl alcohol molecule on the catalyst surface (Figure 4.2b);
- (iii) Product molecules, *iso*-amyl acetate and water, are formed which desorbs from the catalyst surface (Figure 4.2c).



(a)



(b)



(c)

**Figure 4.2.** Illustration of the Eley-Rideal mechanism (a) adsorption of a reactant molecule (b) interaction between molecules (c) desorption of product molecules.

The general rate of reaction for the E-R model can be rewritten as follows:

$$\begin{aligned}
 -r_A &= \frac{A_f \exp\left(-\frac{E_0}{RT}\right) (a_A a_B - \frac{A_r}{A_f} a_C a_D)}{(1 + k_A a_A + k_B a_B + k_C a_C + k_D a_D)} \\
 &= k \frac{(a_A a_B - \frac{a_C a_D}{K_{eq}})}{(1 + k_A a_A + k_B a_B + k_C a_C + k_D a_D)}
 \end{aligned}
 \tag{Eq. 4.68}$$

Where  $-r_A$  is the reaction rate of acetic acid,  $E_0$  is the activation energy for the reaction,  $A_f$  and  $A_r$  are the pre-exponential factors for the forward and reverse reactions respectively,  $k$  represents the reaction rate constant,  $k_i$  represents the adsorption coefficient for component  $i$ ,  $a_i$  is the activity of each component and  $K_{eq}$  is the reaction equilibrium constant.

### 4.2.3 Modified Langmuir-Hinshelwood Hougen-Watson (ML) model

Gonzalez and Fair (1997), Lee *et al.* (2000) Lee *et al.* (2001) and Gangadwala *et al.* (2003) reported that an empirical constant ( $\alpha$ ) can be introduced in the LHHW model to account for the non-linear distribution of water concentration in the resin phase. This gives an expression for the ML model (Equation 4.69)

$$-r_A = k \frac{(a_A a_B - \frac{a_C (a_D)^\alpha}{K_{eq}})}{(1 + k_A a_A + k_B a_B + k_C a_C + k_D a_D^\alpha)^2} \quad \text{Eq. 4.69}$$

Lee *et al.* (2000) reported that the ML model with  $\alpha = 3$  represented the kinetic behaviour of the catalytic esterification between acetic acid and amyl alcohol over Dowex whilst Lee *et al.* (2001) reported that the ML model with  $\alpha = 4$  represented the kinetic behaviour for the same reacting system over Amberlyst 15. Gangadwala *et al.* (2003) assumed a value of 2 for  $\alpha$  in the ML model and gained satisfactory results for the model correlation for the esterification of acetic acid with *n*-butanol.

### 4.2.4 Quasi-Homogenous (Q-H) model

In contrast to the LHHW and E-R mechanisms, the Q-H model does not allow for any adsorption of the reactant molecules onto the catalyst surface. The solid catalyst is assumed to act like a catalyst which is in the same phase i.e. liquid phase as the reactants. Sanz *et al.* (2002) stated that the Q-H model assumed complete swelling of the polymeric catalyst in contact with the polar solvents, leading to an easy access of the reacting components to the active catalytic sites. Xu and Chuang (1996) reported that the Q-H model is derived on the basis of the Langmuir-Hinshelwood formalism with the assumptions that the surface reaction is the controlling step and the adsorption is weak for all components.

With the above assumption that the adsorption is weak for all components in the Q-H model i.e. values of  $k_i$  are negligible, the denominator of Equation

4.40 on the right hand side approaches unity. Therefore, the general rate of reaction for the Q-H model can be written as expressed in Equation 4.70:

$$-r_A = k(a_A a_B - \frac{a_C a_D}{K_{eq}}) \quad \text{Eq. 4.70}$$

The four kinetic models described were solved using a non-linear regression method. A commercially available software package (Fogler, 1999) was used to carry out the regressions and to obtain values of the parameters for each of the kinetic models.

Sanz *et al.* (2002) reported that a two-stage optimisation procedure was adopted for the parameter evaluation. These procedures are indicators used in evaluating the quality of the model in relation to the prediction of the reaction rate. First, the estimation of the parameters for the different kinetic models was performed by minimising the sum of residual squares (SRS) between the experimental and calculated reaction rates through the simplex algorithm as illustrated in Equation 4.71.

$$\text{SRS} = \sum_N (r_{\text{exp}} - r_{\text{calc}})^2 \quad \text{Eq. 4.71}$$

where SRS is the minimum sum of residual squares resulting in the fitting procedure, N is a representation of all samples, and  $r_{\text{exp}}$  and  $r_{\text{calc}}$  represent the experimental and calculated reaction rates respectively.

The numerical integration method was used for integrating the calculated reaction rates with previously determined parameters to obtain the conversions. The experimental results were then compared with those of the model prediction through the values of the mean relative deviation (MRD) between the experimental ( $X_{\text{exp}}$ ) and calculated acid conversions ( $X_{\text{calc}}$ ) as denoted in Equation 4.72.

$$\text{MRD} = \frac{1}{N} \left( \sum_N \left| \frac{X_{\text{calc}} - X_{\text{exp}}}{X_{\text{exp}}} \right| \right) \times 100\% \quad \text{Eq. 4.72}$$

#### 4.2.5 Criteria for acceptance of kinetic models

The estimated rate constant and adsorption coefficient values from each individual kinetic model should be positive values. As the adsorption of the reactant molecules are assumed to have taken place for the different kinetic models (except in the case of the Q-H kinetic model), a negative value would therefore be meaningless. Gangadwala *et al.* (2003) found that the LHHW model for the esterification of acetic acid with *n*-butanol without modification (i.e. with  $\alpha = 1$ ) gave negative values of the adsorption coefficients, which gave an indication that the LHHW model was not suitable for the reacting system as reported.

### 4.3 RESULTS AND DISCUSSION OF BATCH KINETIC MODEL

The first part of the work towards correlating the batch kinetic model was to test the two assumed mechanisms on the LHHW model to find out which one was more reliable. The first mechanism (mechanism A) assumes that water and *iso*-amyl alcohol are adsorbed much more strongly than the other components i.e. acetic acid and *iso*-amyl acetate in the esterification solution. As a result, the adsorption for both acetic acid and *iso*-amyl acetate are neglected. The equation according to mechanism A was expressed as in Equation 4.42.

$$-r_A = k \frac{(a_A a_B - \frac{a_C a_D}{K_{\text{eq}}})}{(1 + k_B a_B + k_D a_D)^2}$$

The second mechanism (mechanism B) assumes that water and acetic acid have the strongest adsorption in the esterification solution. As a result, the adsorption for both *iso*-amyl alcohol and *iso*-amyl acetate are neglected. The equation according to mechanism B was expressed as in Equation 4.43.

$$-r_A = k \frac{(a_A a_B - \frac{a_C a_D}{K_{eq}})}{(1 + k_A a_A + k_D a_D)^2}$$

The regression results including the regression parameters, SRS and MRD at 333 K are represented in Table 4.10. The differences of the two mechanisms were compared through the values of SRS and MRD. From the regression results as presented in Table 4.10, the rate equation for mechanism A i.e. water and *iso*-amyl alcohol being adsorbed much more strongly than acetic acid and *iso*-amyl acetate in the esterification solution, represented the experimental data more accurately than that of mechanism B. This is in good agreement with the findings of Mazzotti *et al.* (1997) which found that the affinity of another ion exchange resin in the form of Amberlyst 15 for acetic acid, ethanol, ethyl acetate and water followed the sequential order of water > alcohol > acid > ester. Furthermore, similar mechanisms were applied for the esterification of acetic acid with methanol (Song *et al.*, 1998), esterification of acetic acid with amyl alcohol (Lee *et al.*, 2001), esterification of lactic acid with methanol (Sanz *et al.*, 2002) and the esterification of lactic acid with ethanol (Zhang *et al.*, 2004).

**Table 4.10.** Values of parameters for the kinetic equations based on mechanisms A and B.

Mechanism	Parameter	Value	SRS	MRD (%)
A	k	$2.9697 \times 10^{-6}$	$1.0321 \times 10^{-4}$	3.31
	$k_B$	1.522		
	$k_D$	0.384		
B	k	$4.1814 \times 10^{-6}$	$1.0486 \times 10^{-4}$	12.45
	$k_A$	3.161		
	$k_D$	0.968		

From the comparison of the mechanisms above through the SRS and more notably the MRD in Table 4.10, with the rate equation for mechanism A representing the experimental data much more favourably than the rate equation for mechanism B, the adsorption of the most polar molecules, water and *iso*-amyl alcohol, was considered to be stronger than the adsorption of acetic acid and *iso*-amyl acetate, which were considered negligible in comparison for the different kinetic models. Therefore, the rate expressions of each of the kinetic model used in this work are illustrated as follow:

(i) The LHHW model

$$-r_A = \frac{k \left( a_A a_B - \frac{a_C a_D}{K_{eq}} \right)}{(1 + k_B a_B + k_D a_D)^2} \quad \text{Eq. 4.73}$$

(ii) The E-R model

$$-r_A = \frac{k \left( a_A a_B - \frac{a_C a_D}{K_{eq}} \right)}{(1 + k_B a_B + k_D a_D)} \quad \text{Eq. 4.74}$$

(iii) The M-L model

$$-r_A = \frac{k \left( a_A a_B - \frac{a_C (a_D)^\alpha}{K_{eq}} \right)}{[1 + k_B a_B + k_D (a_D)^\alpha]^2} \quad \text{Eq. 4.75}$$

(iv) The Q-H model

$$-r_A = \frac{k \left( a_A a_B - \frac{a_C (a_D)}{K_{eq}} \right)}{K_{eq}} \quad \text{Eq. 4.76}$$

The adjustable parameters obtained for the LHHW, E-R and M-L ( $\alpha = 2$ ) kinetic models are presented in Table 4.11 along with the sum of residual squares and the mean relative deviation between the experimental and calculated acid conversion values. The Q-H model is excluded from the list as there are high errors while fitting the experimental data. This represents that the assumption for the Q-H model whereby there is no allowance for any adsorption of the reactant molecules onto the catalyst surface is not valid for the reacting system between acetic acid and *iso*-amyl alcohol. The consideration of the adsorption effect improves the accuracy of the data correlation.

**Table 4.11.** Adjustable parameters of the kinetic models for the catalysed esterification of acetic acid with *iso*-amyl alcohol.

Model	k	$k_B$	$k_D$	SRS	MRD (%)
LHHW	$2.9697 \times 10^6$	1.52184	0.384001	$1.03210 \times 10^{-4}$	3.312
E-R	$1.9341 \times 10^{-4}$	1.51519	0.383745	$1.03217 \times 10^{-4}$	4.814
M-L	$1.3679 \times 10^{-5}$	1.64075	0.400000	$1.05646 \times 10^{-4}$	13.765

As shown in Table 4.11 through the comparison of the SRS and MRD, the LHHW kinetic model best represents the experimental data obtained amongst the three kinetic models presented. The M-L model with an empirical parameter of 2 did not improve the data correlation. This meant that the non-linear distribution of water in the liquid and resin phase was not significant for this reaction. The activation energy for the reacting system between acetic acid and *iso*-amyl alcohol was thus obtained for the LHHW kinetic model through the Arrhenius plot and the value was  $48.0 \text{ kJ mol}^{-1}$ . No previous literature value was reported for this system. Liu and Tan (2001) reported an activation energy of  $59.0 \text{ kJ mol}^{-1}$  for the liquid phase esterification of propionic acid and *n*-butanol using the E-R kinetic model. Lee *et al.* (2002) reported an activation energy value of  $63.72 \text{ kJ mol}^{-1}$  for the reaction between propionic acid and *n*-butanol over Amberlyst 35 using the LHHW kinetic model while Gangadwala *et al.* (2003) reported an activation energy value of  $72.896 \text{ kJ mol}^{-1}$  for the esterification of acetic acid with *n*-butanol using the

M-L kinetic model . The high value of the activation energy lends support to the assumption that the overall process is controlled by the reaction at the surface of the catalyst. The kinetic model represented in the graphs (Figures 4.3 to 4.10) under the given conditions in this work is the LHHW model because it presented the lowest MRD among the different kinetic models tested. According to the LHHW mechanism, acetic acid adsorbed on one catalytic centre reacts with *iso*-amyl alcohol adsorbed on another catalytic centre to give *iso*-amyl acetate and water each adsorbed on one catalytic centre. The kinetic data and rate expression obtained would be useful for the simulation of the dynamic behaviour of a reactive distillation column for the removal of acetic acid from aqueous streams.

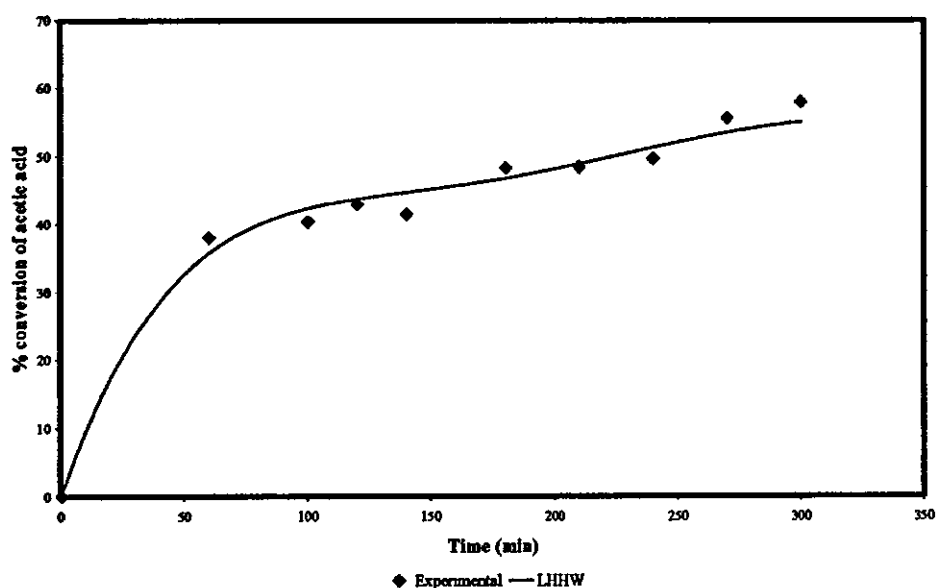


**Figure 4.3.** Conversion *versus* time for the esterification of concentrated acetic acid with *iso*-amyl alcohol at a catalyst loading of 5% (w/w); feed mole ratio (*iso*-amyl alcohol to acetic acid), 2:1, temperature, 333 K; stirrer speed, 500 rpm; catalyst, Purolite® CT-175.

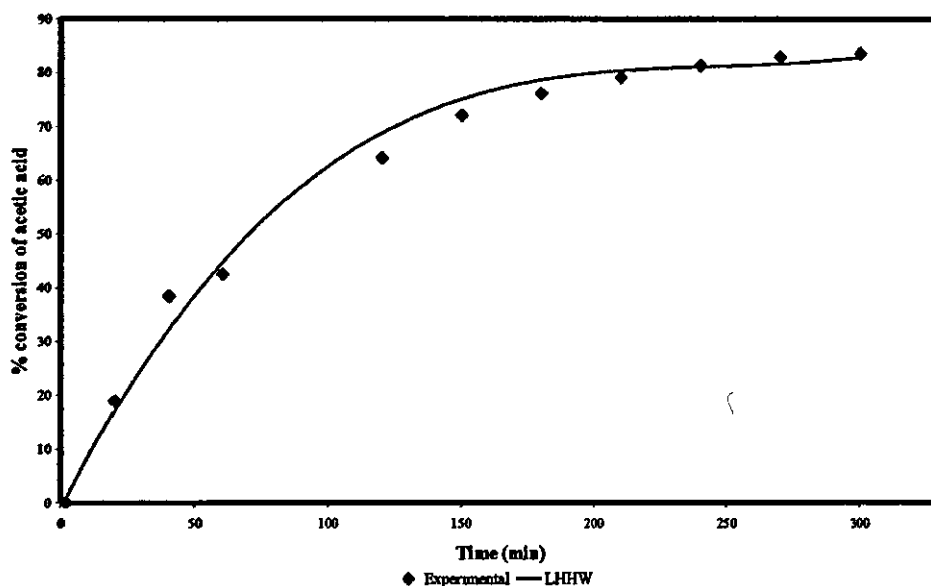


**Figure 4.4.** Conversion *versus* time for the esterification of concentrated acetic acid with *iso*-amyl alcohol at a catalyst loading of 5% (w/w); feed mole ratio (*iso*-amyl alcohol to acetic acid), 2:1, temperature, 343 K; stirrer speed, 500 rpm; catalyst, Purolite® CT-175.

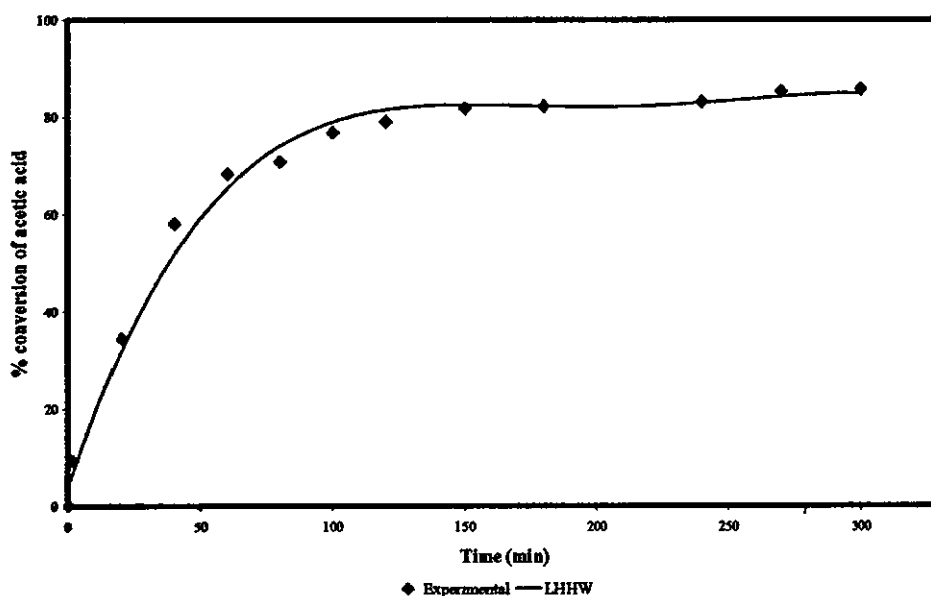


**Figure 4.5.** Conversion *versus* time for the esterification of concentrated acetic acid with *iso*-amyl alcohol at a catalyst loading of 5% (w/w); feed mole ratio (*iso*-amyl alcohol to acetic acid), 2:1; temperature, 358 K; stirrer speed, 500 rpm; catalyst, Purolite® CT-175.

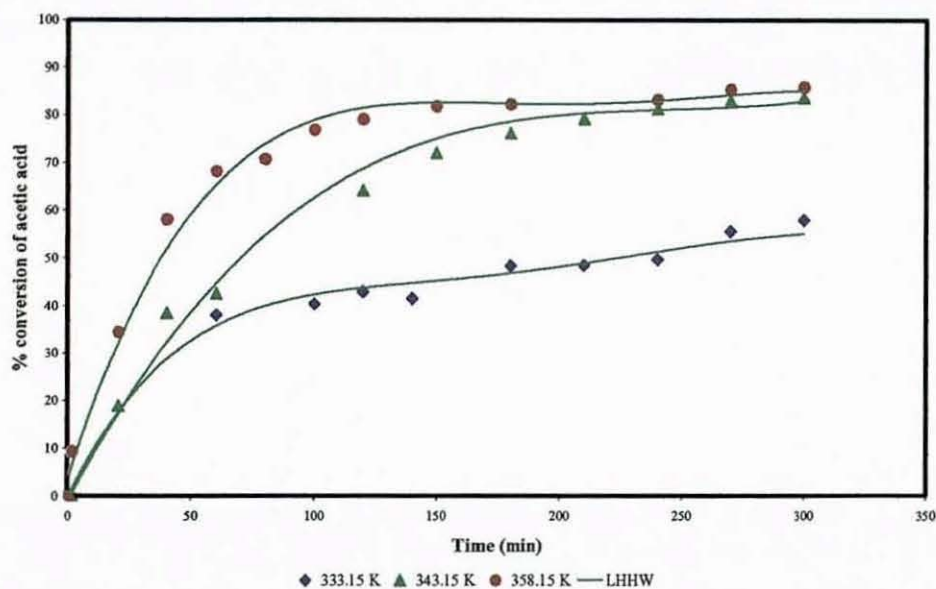


**Figure 4.6.** Conversion *versus* time for the esterification of concentrated acetic acid with *iso*-amyl alcohol at different temperatures over a catalyst loading of 5% (w/w); feed mole ratio (*iso*-amyl alcohol to acetic acid), 2:1; stirrer speed, 500 rpm; catalyst, Purolite<sup>®</sup> CT-175.

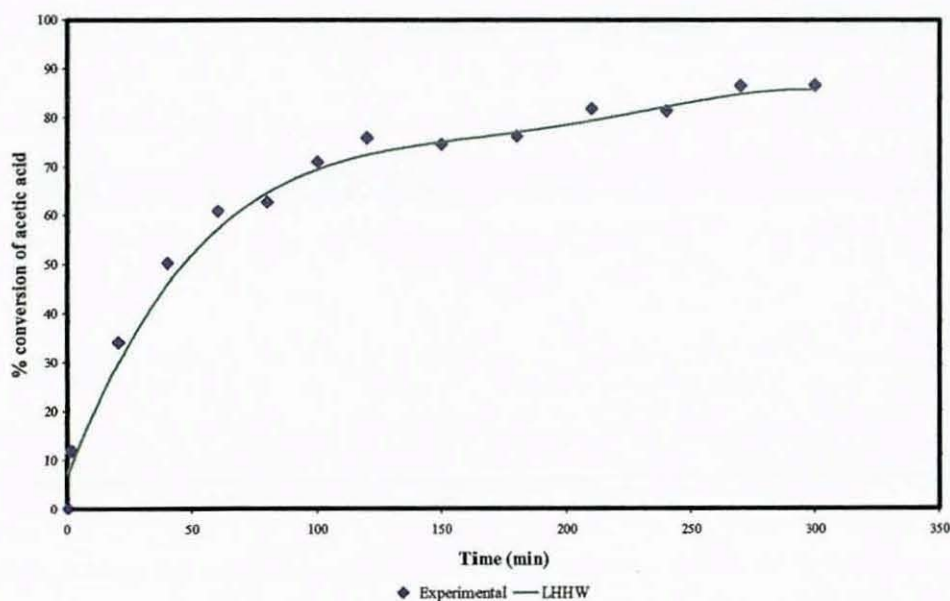


**Figure 4.7.** Conversion *versus* time for the esterification of concentrated acetic acid with *iso*-amyl alcohol at a catalyst loading of 2.5% (w/w); feed mole ratio (*iso*-amyl alcohol to acetic acid), 2:1; temperature, 358 K; stirrer speed, 500 rpm; catalyst, Purolite<sup>®</sup> CT-175.

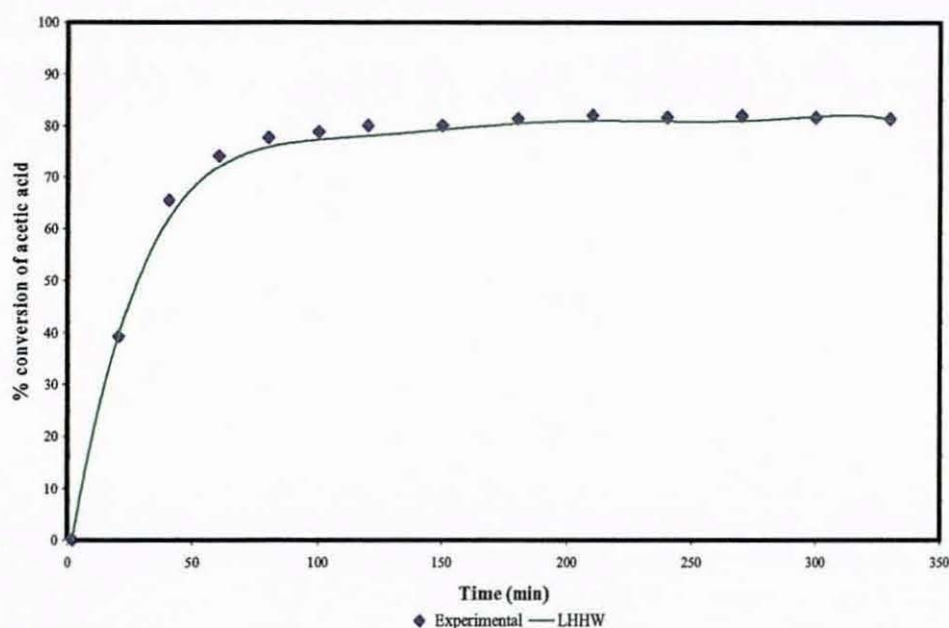


**Figure 4.8.** Conversion *versus* time for the esterification of concentrated acetic acid with *iso*-amyl alcohol at a catalyst loading of 10.0 % (w/w); feed mole ratio (*iso*-amyl alcohol to acetic acid), 2:1; temperature, 358 K; stirrer speed, 500 rpm; catalyst, Purolite<sup>®</sup> CT-175.

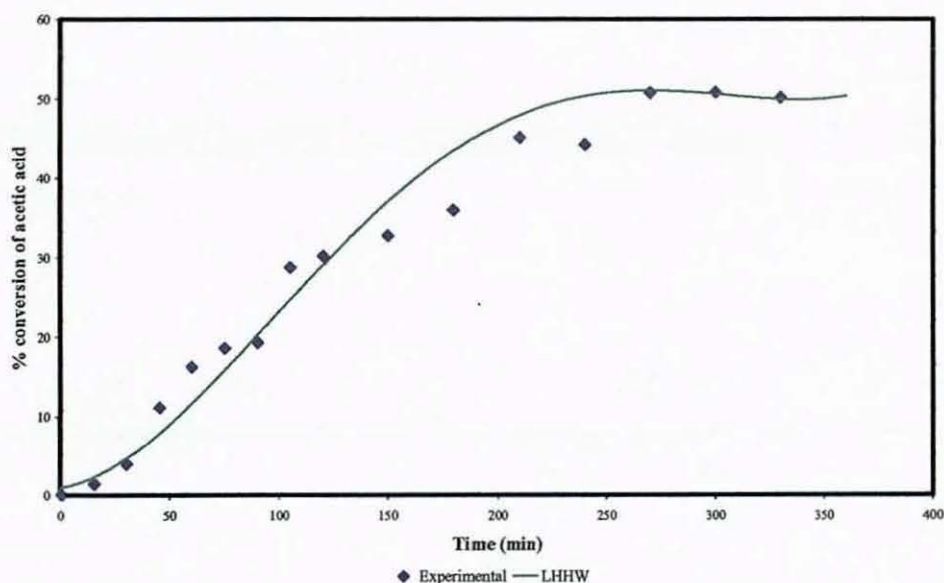


**Figure 4.9.** Conversion *versus* time for the esterification of 30% (w/w) acetic acid with *iso*-amyl alcohol at a catalyst loading of 10 % (w/w); feed mole ratio (*iso*-amyl alcohol to acetic acid), 2:1, temperature, 358 K; stirrer speed, 500 rpm; catalyst, Purolite<sup>®</sup> CT-175.

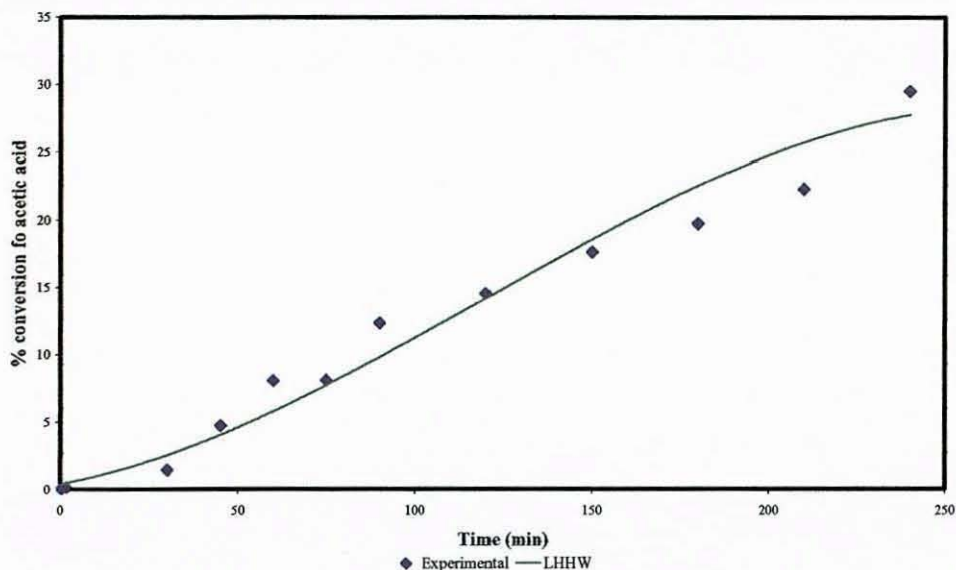


**Figure 4.10.** Conversion *versus* time for the esterification of 30% (w/w) acetic acid with *iso*-amyl alcohol at a catalyst loading of 5% (w/w); feed mole ratio (*iso*-amyl alcohol to acetic acid), 1:1, temperature, 358 K; stirrer speed, 500 rpm; catalyst, Purolite<sup>®</sup> CT-175.

#### 4.4 CONCLUSIONS

The main conclusions drawn from the kinetic modelling work are:

- (i) The LHHW kinetic model yielded the best representation of the experimental data over a wide range of temperatures and catalyst loadings as well as different acid concentrations for the esterification reaction between acetic acid and *iso*-amyl alcohol.
- (ii) The model results with the regressed kinetic parameters are in good agreement with the experimental data obtained.
- (iii) The high value of the activation energy supports the assumption that the reaction at the catalyst surface was the rate controlling step.

## 5. RESIDUE CURVE MAP DETERMINATION

### 5.1 INTRODUCTION

Although reactive distillation is highly regarded as a potential alternative process in replacing the conventional reaction-separation process, it is not always advantageous. A systematic method is required to analyse the feasibility and applicability of reactive distillation for a given reaction system. A residue curve map (RCM) is a suitable tool for the synthesis and analysis of reactive distillation.

This chapter presents results on the residue curve map obtained for the reacting system involving acetic acid, *iso*-amyl alcohol, *iso*-amyl acetate and water.

### 5.2 THEORY

Schreinemakers (1901) defined the residue curve as the locus of the liquid composition remaining from a simple distillation process. Doherty and Perkins (1978) stated that a residue curve is derived from a simple distillation process. Tapp *et al.* (2003) gave an illustration of the simple distillation process. With reference to Figure 5.1, a liquid mixture of known composition is heated in a single stage batch still at constant pressure without reflux. The components in the liquid will evaporate at different rates due to volatility differences, except at azeotropes. Over time, the liquid is vaporised, and the vapour is removed from contact with the liquid as it is formed. At this point, the vapour is in equilibrium with the remaining liquid. The vapour is withdrawn from the still as a distillate. As there is no additional feed and reflux of the distillate, the composition of the liquid remaining will be enriched in the less volatile component with time, with the vapour formed being always richer in the more volatile component than the liquid from which it is formed. The progression of the distillation process will result in the residue becoming more depleted in the more volatile component. Consequently, the distillate withdrawn would be richer in the most volatile component.

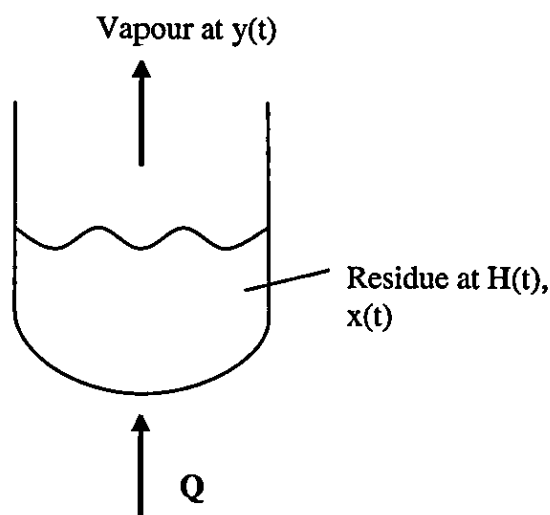


Figure 5.1. A simple batch still

Barbosa and Doherty (1988) stated that the residue curves are closely related to the composition profiles in continuous distillation processes, which is one of the main reasons for studying simple distillation. A collection of these residue curves for a given reacting system is called a residue curve map. Pham and Doherty (1990) outlined that the changing liquid composition is most conveniently described by following the trajectory of the overall composition of all the coexisting liquid phases, which is otherwise termed the residue curve. Ung and Doherty (1995) reported that a residue curve map contains the same information as the phase diagram for a mixture. Song *et al.* (1997) used the residue curve map in investigating the reacting system between acetic acid and isopropanol, and discovered a boiling state of constant composition and temperature. Huang *et al.* (2004) defined residue curve maps as a representation of the dynamic behaviour of the liquid phase composition in a simple batch reactive distillation process. Song *et al.* (1998) studied the residue curve maps towards methyl acetate synthesis, and found that the experimental residue curves compared well with the predictions generated by the model developed by Venimadhavan *et al.* (1994).

## Chapter 5. Residue Curve Map Determination

A residue curve map is made up of some key components (Seader and Henley, 1998) which are defined as follow:

Node	Residue curves begin and end at nodes.
Stable node	The component or azeotrope with the highest boiling point in the region. All the residue curves in the region terminate at this point (Figure 5.2a).
Unstable node	The component or azeotrope with the lowest boiling point in the region (Figure 5.2b).
Saddle	Residue curves move toward and then away from saddles. A saddle is a pure component or an azeotrope which has a boiling point in between the stable and unstable nodes (Figure 5.2c).

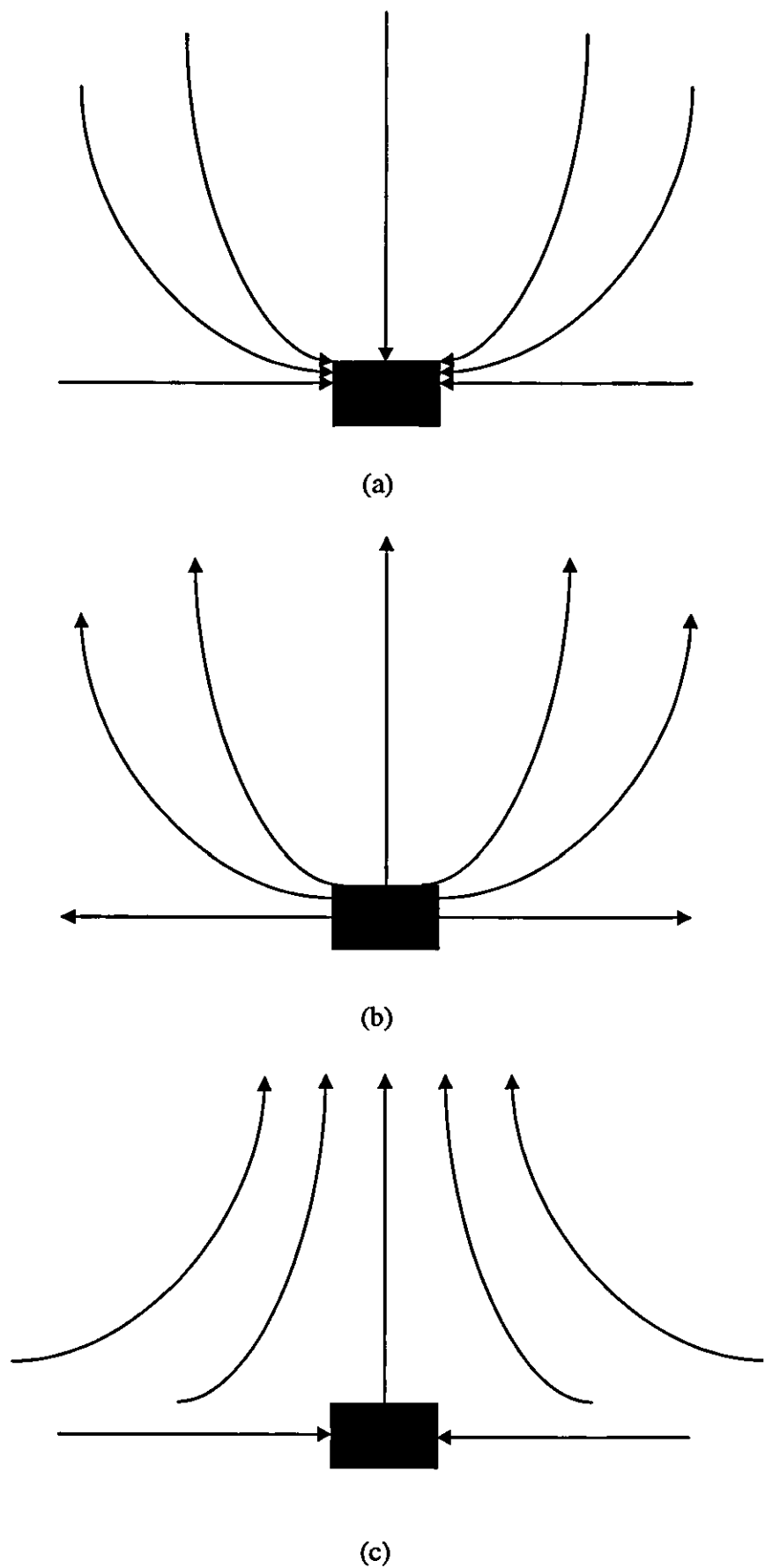


**Figure 5.2.** Classification of singular points in a residue curve map (a) a stable node; (b) an unstable node; (c) a saddle point (Fien and Liu, 1994).

## 5.3 EXPERIMENTAL

### 5.3.1 Materials

#### 5.3.1.1 Chemicals

*iso*-Amyl alcohol (99%) was purchased from Aldrich Chemical Company, Inc. Acetic acid (99.8%) and *iso*-amyl acetate (>99% purity) were supplied by Fisher Scientific, United Kingdom. The purity of the chemicals were verified by gas chromatographic analysis and they were used without further purification.

#### 5.3.1.2 Catalyst

A solid acidic resin in the form of Purolite<sup>®</sup> CT-175 (supplied courtesy of Purolite, United Kingdom) was used as the catalyst for the residue curve map experiments. Purolite<sup>®</sup> CT-175 ion exchange resin catalyst was used in the residue curve map experiments because it showed the most promising results among the catalysts tested in the batch kinetic experiments as reported in Chapter 3.

### 5.3.2 Experimental set-up

Figure 5.3 is a representation of the experimental set-up for the residue curve map measurements. The reaction flask was initially charged with the liquid mixture of desired initial compositions together with a measured amount of pre-treated ion exchange resin catalyst, Purolite<sup>®</sup> CT-175. With reference to Figure 5.3, while valve A of the distillation head was open and valve B was closed, a constant heat input was supplied to the continuously stirred reaction mixture, and the liquid was totally refluxed until the temperatures of both the liquid and the vapour phases of the reaction mixture were stabilised. The liquid and vapour temperatures were measured via the use of thermocouples. The experimental set-up was insulated with glass wool to provide insulation so as to minimise loss of heat to the surroundings, as well as to prevent vapour condensation into the reaction flask. At this juncture, valve A was closed and valve B was opened to allow the vapour phase to be removed continuously and

condensed into a collection flask. The liquid samples in the reaction flask were taken periodically during the distillation process, and analysed for their composition. The experimental run was eventually stopped when the amount of liquid residue in the reaction flask was small enough to preclude sampling. Subsequent experimental runs were carried out at compositions as close as possible to the measured end point of the previous experiment. This was to necessitate the plot of a significant portion of each residue curve.

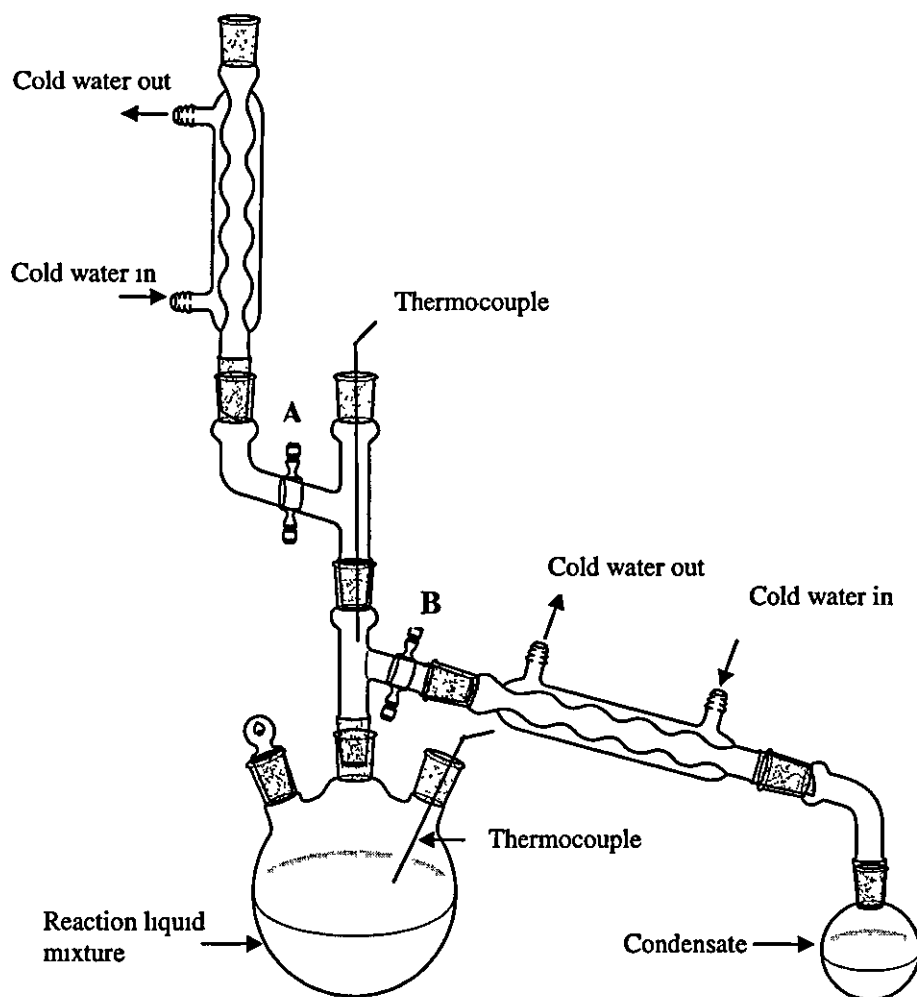


**Figure 5.3.** Experimental set-up for the measurement of residue curve map.

### 5.3.3 Method of Analysis

A Pye Unicam 104 Gas Chromatograph (GC) equipped with a thermal conductivity detector was used to analyse the composition of the samples from the liquid phase of the reacting mixture. The sample size for each gas chromatograph injection was 1  $\mu\text{L}$ . Both the oven and detector port temperatures were set isothermally at 523 K. The GC column was packed with Porapak Q, which was used to separate water, acetic acid, *iso*-amyl alcohol and *iso*-amyl acetate. The length and diameter of the column were 2.5 m and 0.00635 m, respectively. *n*-Butanol was used as the internal standard. High purity (>98%) helium gas was used as the carrier gas. The flow rate of the helium gas was 50 ml/min, and a complete GC run took about 12 minutes.

## 5.4 RESULTS AND DISCUSSION OF THE DEVELOPMENT OF RESIDUE CURVE MAP

Without chemical reaction, a mixture of acetic acid, *iso*-amyl alcohol, *iso*-amyl acetate and water has two binary azeotropes and a ternary azeotrope as listed in Table 5.1. Rowlinson (1969) defined azeotropic mixtures as mixtures that can be distilled or condensed without a change in composition.

**Table 5.1.** Azeotropes for non-reacting system at 1 atm (Horsley, 1952).

Boiling temperature (K)	Weight %			
	Acetic acid	<i>iso</i> -Amyl alcohol	<i>iso</i> -Amyl acetate	Water
366.6	0.00	31.2	24.0	44.8
366.8	0.00	0.00	63.7	36.3
368.15	0.00	50.4	0.00	49.6

In the investigation of the residue curve map for the catalysed esterification of 30% (w/w) acetic acid with *iso*-amyl alcohol, a series of nine experiments with different initial feed mole conditions were performed with each set of runs in a series representing one residue curve; successive runs were necessary in some cases to represent a significant portion of each residue curve.

In the four component mixture studied here, the transformed variable coordinate is used, which is a representation of the composition in terms of the total amount of acetic acid and *iso*-amyl alcohol. The transformed variables are also inclusive of the equivalent amounts of *iso*-amyl acetate and water. *iso*-Amyl acetate was chosen as the reference component in the determination of the transformed variables towards the plotting of the residue curve map. Song *et al.* (1997) showed that the transformed variables could be expressed as follow:

$$X_A = x_{\text{acetic acid}} + x_{\text{iso-amyl acetate}} \quad \text{Eq. 5.1}$$

$$X_B = x_{\text{iso-amyl alcohol}} + x_{\text{iso-amyl acetate}} \quad \text{Eq. 5.2}$$

$$X_C = x_{\text{water}} - x_{\text{iso-amyl acetate}} \quad \text{Eq. 5.3}$$

Where  $X_A$ ,  $X_B$  and  $X_C$  are the transformed variables and  $x$  is the liquid molar composition of the respective component as denoted by the subscript.

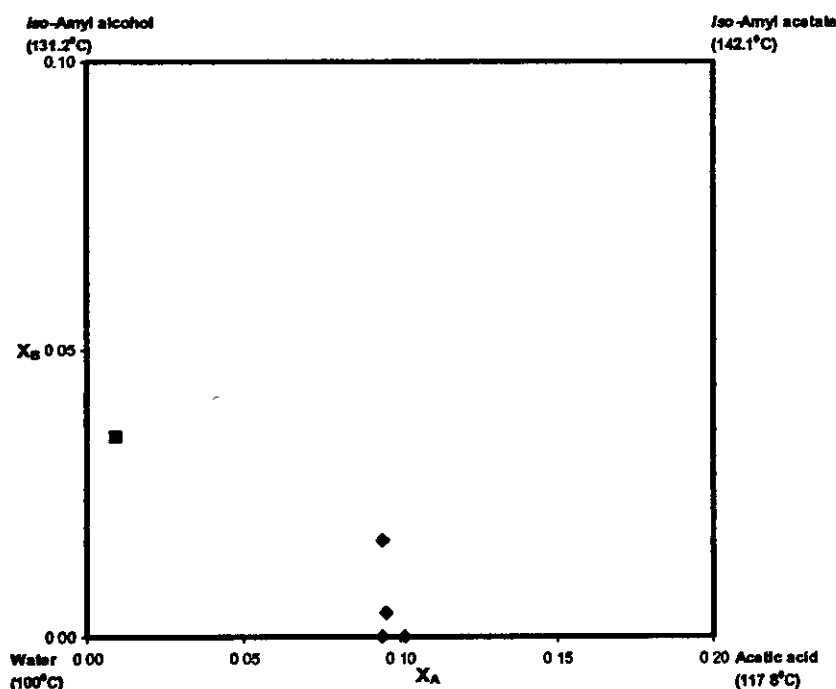


Figure 5.4. Residue curve for acetic acid-*iso*-amyl alcohol-*iso*-amyl acetate-water reacting system with initial feed mole ratio (*iso*-amyl alcohol/acetic acid), 0.5:1 at 1 atm.

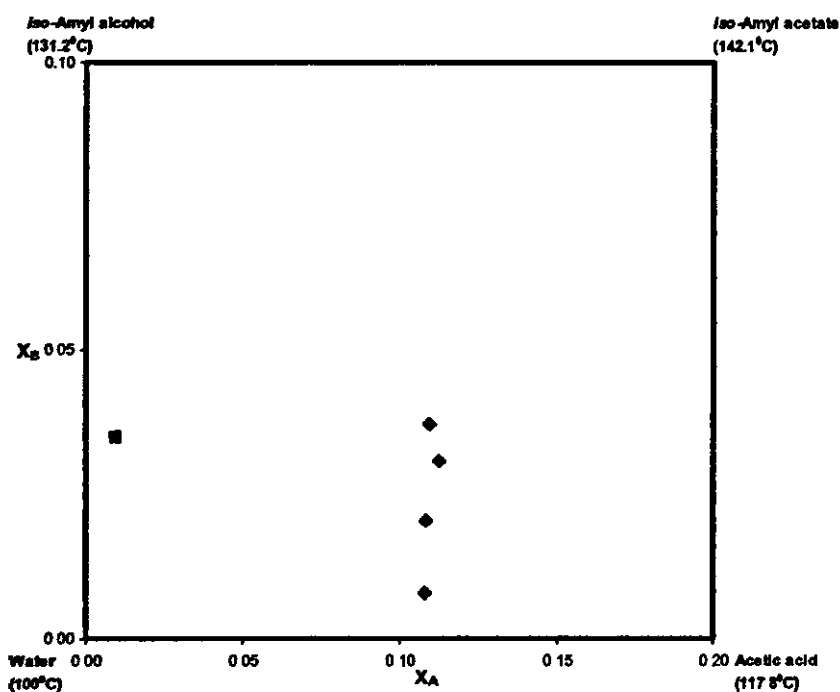


Figure 5.5. Residue curve for acetic acid-*iso*-amyl alcohol-*iso*-amyl acetate-water reacting system with initial feed mole ratio (*iso*-amyl alcohol/acetic acid), 0.7:1 at 1 atm.

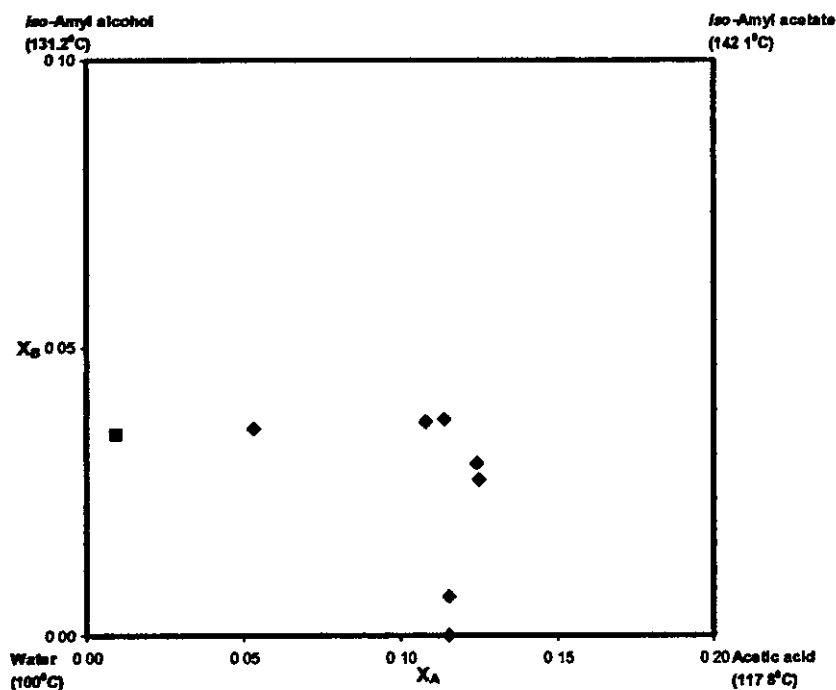
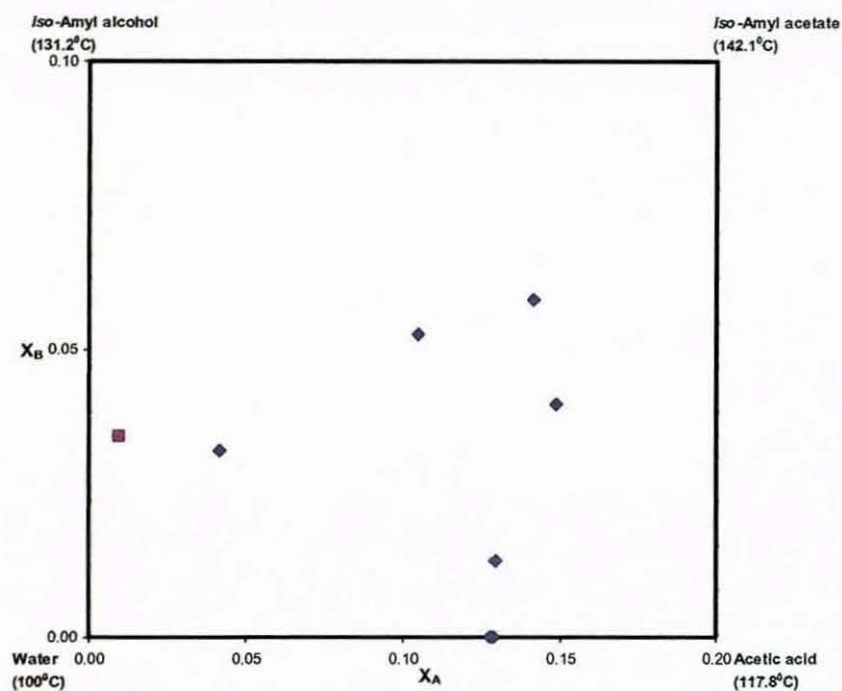
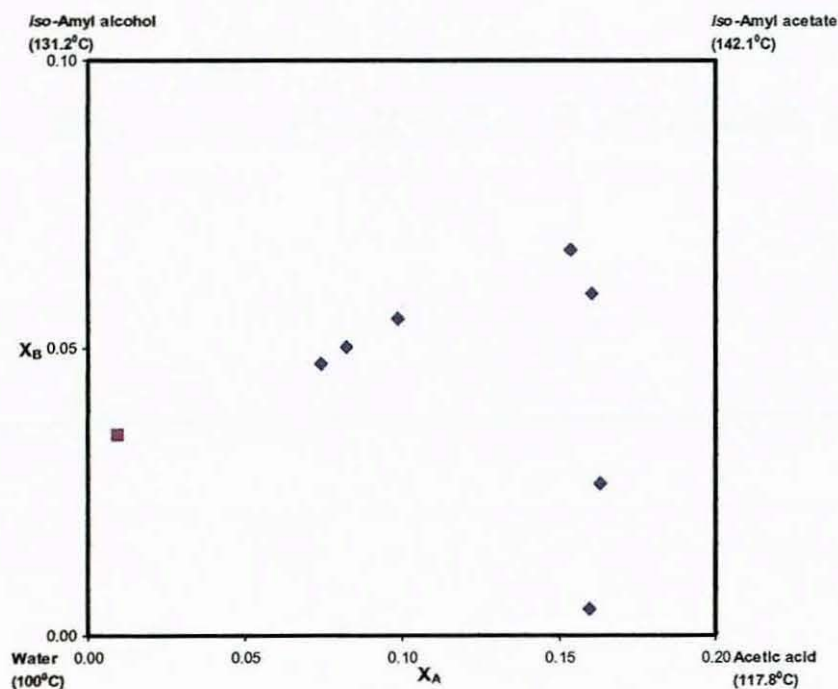


Figure 5.6. Residue curve for acetic acid-*iso*-amyl alcohol-*iso*-amyl acetate-water reacting system with initial feed mole ratio (*iso*-amyl alcohol/acetic acid), 0.9:1 at 1 atm.



**Figure 5.7.** Residue curve for acetic acid-*iso*-amyl alcohol-*iso*-amyl acetate-water reacting system with initial feed mole ratio (*iso*-amyl alcohol/acetic acid), 1:1 at 1 atm.



**Figure 5.8.** Residue curve for acetic acid-*iso*-amyl alcohol-*iso*-amyl acetate-water reacting system with initial feed mole ratio (*iso*-amyl alcohol/acetic acid), 1.3:1 at 1 atm.

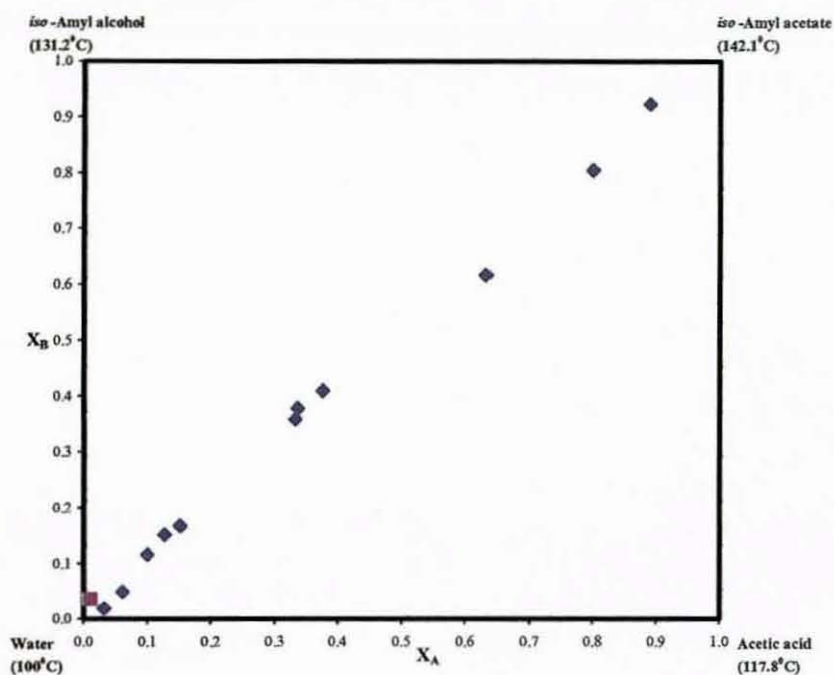


**Figure 5.9.** Residue curve for acetic acid-*iso*-amyl alcohol-*iso*-amyl acetate-water reacting system with initial feed mole ratio (*iso*-amyl alcohol/acetic acid), 1.5:1 at 1 atm.

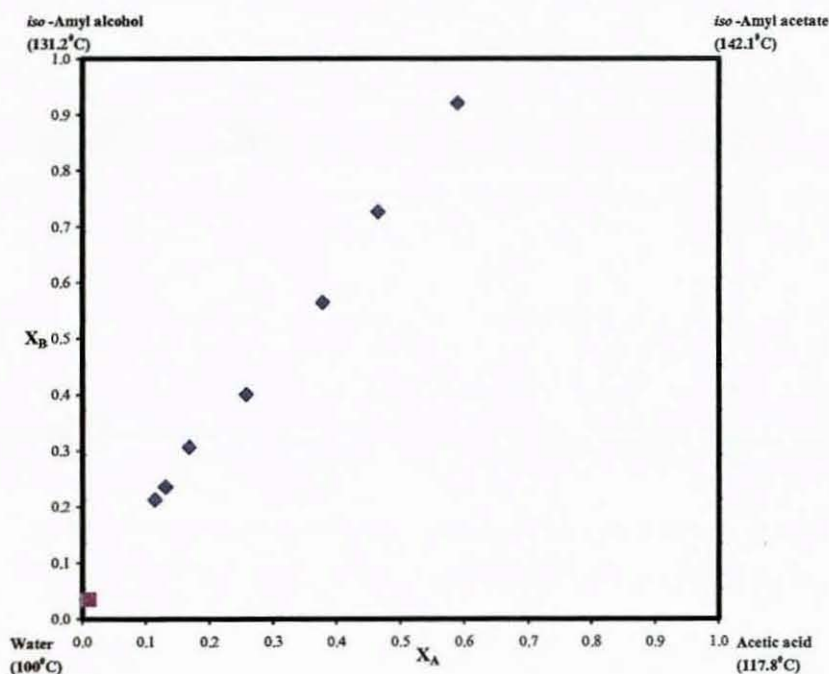


**Figure 5.10.** Residue curve for acetic acid-*iso*-amyl alcohol-*iso*-amyl acetate-water reacting system with initial feed mole ratio (*iso*-amyl alcohol/acetic acid), 2:1 at 1 atm.

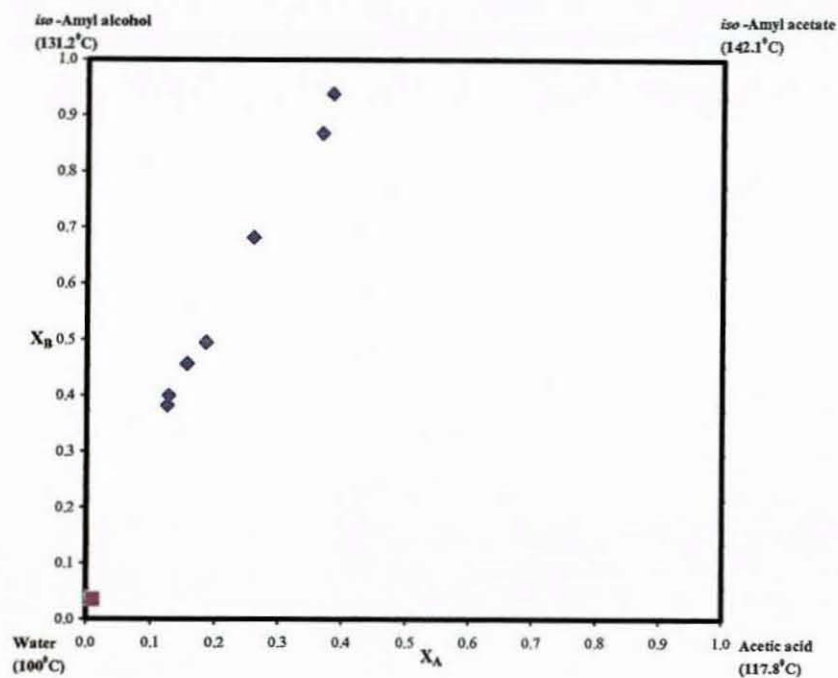


**Figure 5.11.** Residue curve for acetic acid-*iso*-amyl alcohol-*iso*-amyl acetate-water reacting system with initial feed mole ratio (*iso*-amyl alcohol/acetic acid), 3:1 at 1 atm.

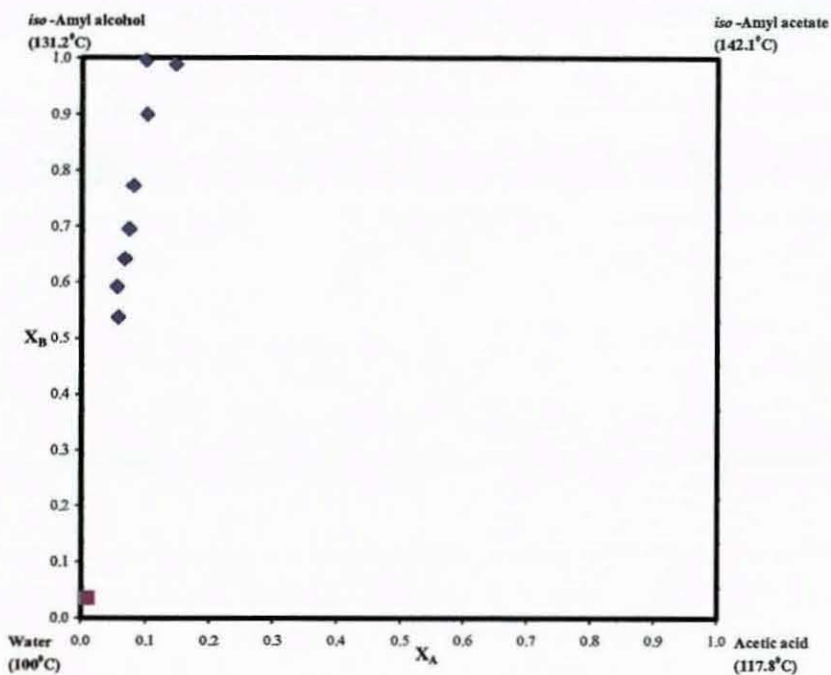


**Figure 5.12.** Residue curve for acetic acid-*iso*-amyl alcohol-*iso*-amyl acetate-water reacting system with initial feed mole ratio (*iso*-amyl alcohol/acetic acid), 8:1 at 1 atm

Figures 5.4 -5.12 show the individual residue curves for the reacting system of 30 % w/w acetic acid with *iso*-amyl alcohol under different initial feed mole conditions (Saha *et al.*, 2005b).

A combination of the residue curves from Figures 5.4-5.12 produce the feasible composition space otherwise known as the residue curve map (Figure 5.13). Each individual vertex i.e. corner of the square is a pure component; each edge is a non-reactive binary mixture and any point inside the square is a four-component reactive mixture. In addition, Figure 5.13 shows the residue curves, which are representations of the liquid composition paths under different feed molar conditions in an isobaric simple distillation experiment.

Figure 5.13 is a representation of the residue curve map for the reacting system between acetic acid and *iso*-amyl alcohol. The water pure component point is an unstable node; the acetic acid and *iso*-amyl alcohol pure component points are saddles and the *iso*-amyl acetate pure component point in the reacting system is a stable node. Initiating the reaction with the addition of the catalyst (Purolite® CT-175) allowed the binary azeotropes (*iso*-amyl alcohol/water and *iso*-amyl acetate/water) and ternary azeotrope (*iso*-amyl alcohol/*iso*-amyl acetate/water) as outlined in Table 5.1 to react into the four component mixture. The results showed that the catalysed chemical reaction eliminated the non-reactive azeotropes, which would otherwise limit the progression of the reaction or hinder the purity of the desired product, *iso*-amyl acetate. The experimental results obtained showed that it was feasible to obtain *iso*-amyl acetate (as denoted by the compositions moving towards the *iso*-amyl acetate stable node) through reactive distillation under certain conditions. The residue curve map results showed the formation of a four component reactive azeotrope between all reactants and products at 368 K (Figure 5.13). The measured molar composition of the reactive azeotrope was 0.45% acetic acid, 1.95% *iso*-amyl alcohol, 0.38% *iso*-amyl acetate and 97.21% water. The corresponding transformed mole compositions were  $X_A = 0.0084$  and  $X_B = 0.0233$ . Furthermore, the residue curve map results showed that the composition of the products was dependent on the feed molar ratio of the reactants. When very low molar ratios of *iso*-amyl alcohol to acetic acid

were used, the bottom product contained water and acetic acid. With reference to Figure 5.13, using feed molar conditions (*iso*-amyl alcohol to acetic acid) of 1.3:1 and less resulted in high concentrations of acetic acid and water obtained in the bottom product. However, the bottom products contained mainly of *iso*-amyl alcohol and some *iso*-amyl acetate when very high molar ratios of *iso*-amyl alcohol to acetic acid were utilised. With reference to Figure 5.13, using a feed mole ratio (*iso*-amyl alcohol to acetic acid) of 8:1 resulted in a high concentration of *iso*-amyl alcohol obtained in the top product, with the bottom product composition consisting mainly of *iso*-amyl alcohol along with some *iso*-amyl acetate. Therefore, the use of very high feed molar ratios of *iso*-amyl alcohol to acetic acid would not be feasible as *iso*-amyl acetate would be present in both the top and bottom product streams of a reactive distillation column. This would mean a requirement of two separation units (one for the top product stream and the other for the bottom product stream) to separate the ester from both streams. The residue curve map results (Figure 5.13) indicated that the optimal feed molar ratio (*iso*-amyl alcohol to acetic acid) was between 1.5:1 and 2:1, with high *iso*-amyl acetate obtained in the top product stream. The RCM preliminary studies provide the basis (in terms of feed mole conditions) for the optimisation of the process configurations of the RDC experiments (Chapter 6).

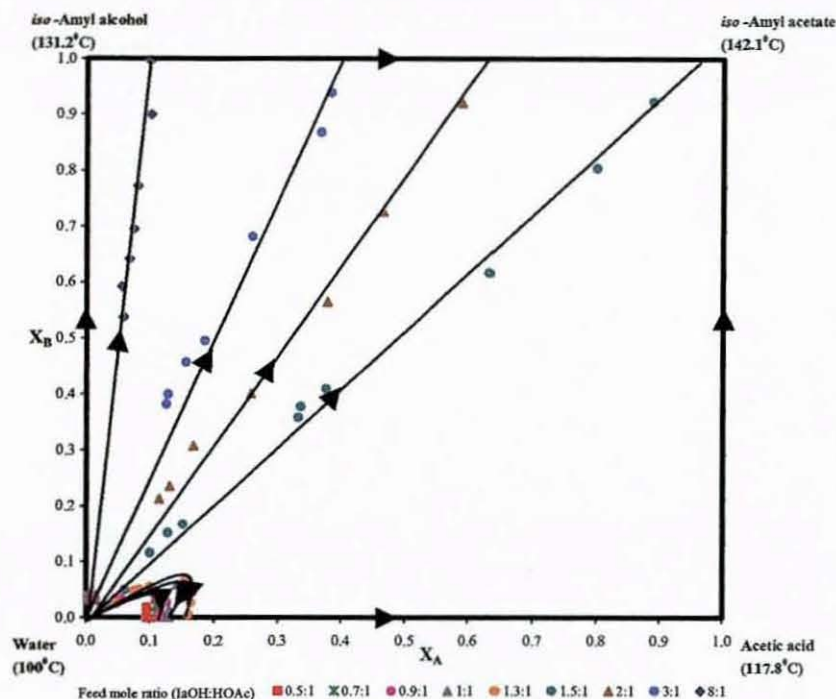


**Figure 5.13.** Residue curve map for acetic acid-*iso*-amyl alcohol-*iso*-amyl acetate-water reacting system at 1 atm.

## 5.5 CONCLUSIONS

A residue curve map could be used to elucidate the feasibility of reactive distillation for a reacting system. The main conclusions drawn from the residue curve map work are:

- (i) The non-reactive azeotropes are eliminated with the addition of the catalyst, Purolite<sup>®</sup> CT-175, into the reacting system.
- (ii) A minimum-boiling four component reactive azeotrope was formed at 368 K. The measured molar composition of the reactive azeotrope was 0.45% acetic acid, 1.95% *iso*-amyl alcohol, 0.38% *iso*-amyl acetate and 97.21% water.
- (iii) The residue curve map suggests the use of feed molar ratio (*iso*-amyl alcohol to acetic acid) in the range of 1.5:1 and 2:1 in the reactive distillation column so that the desired product, *iso*-amyl acetate, would only be present in the top product stream. Moreover, very little acetic acid would be obtained in the bottom product stream.

## 6. PILOT PLANT STUDIES (REACTIVE DISTILLATION COLUMN)

### 6.1 INTRODUCTION

This chapter presents the experimental results carried out in the reactive distillation column (RDC) with the aim of optimising the column configurations as well as process conditions for the synthesis of *iso*-amyl acetate. The parameters investigated included the effect of feed mole ratio of the reactants, the effect of reflux ratio of the organic phase, the effect of acetic acid feed position into the reactive distillation column, the effect of the reflux configuration and the effect of the acetic acid concentration in the feed stream.

### 6.2 EXPERIMENTAL

#### 6.2.1 Materials

##### 6.2.1.1 Chemicals

Acetic acid (99.8%) and *iso*-amyl alcohol (99%) were purchased from Sigma Aldrich Chemical Company, Inc and *iso*-amyl acetate (>99% purity) was supplied by Fisher Scientific, United Kingdom. The purity of the individual chemicals were verified by gas chromatographic analysis, and they were used without further purification. The acetic acid was mixed with water to its appropriate concentration for the reactive distillation column experiments.

##### 6.2.1.2 Catalyst

The catalyst used was Purolite® CT-175 supplied courtesy of Purolite International Limited, United Kingdom. The catalyst to be used was pre-treated by first washing several times with water until the supernatant liquid was colourless to remove impurities. The catalyst was subsequently washed with methanol to remove any water sorbed on the catalyst resin. This step aids in avoiding the collapse of the resin pore structure in the subsequent drying process. The washed catalyst was dried in a vacuum oven at 373 K for 6 hours. Drying at higher temperatures involves the risk of losing sulfonic acid sites in

the form of  $\text{SO}_3$  because of desulfonation of the polystyrene matrix of the catalyst (Fang, 1964; Petrus *et al.*, 1981; Teo and Saha, 2004).

### 6.2.2 Experimental set-up

The experiments were carried out in a packed reactive distillation column. The column consists of three distinct parts, a reactive section with Katamax<sup>®</sup> catalytic packings containing Purolite<sup>®</sup> CT-175 ion exchange resin catalyst, sandwiched in between a non-reactive rectifying section and a non-reactive stripping section (Figure 6.1). The diameter of each section of the column was 0.050 m. The reboiler was heated by two heating rods (800 W total capacity), and all sections of the column were coiled with heating tapes and insulated with Superwool 607<sup>™</sup> MAX Blanket. The temperatures in the column and reboiler were measured using type K thermocouples with the temperatures being monitored with the use of LabVIEW<sup>™</sup> program. The experimental set-up was completed with a decanter, a timer-controlled automatic reflux device and a water-cooled condenser. The reactants were fed through Viton<sup>®</sup> tubing (Fisher Scientific, United Kingdom) to the reactive distillation column through independently-controlled valves. Viton<sup>®</sup> tubing is made of synthetic fluoroelastomer, and could handle temperature in the range of 253 K – 473 K. Furthermore, Viton<sup>®</sup> tubing shows outstanding chemical resistance to strong acids and alcohols. In addition, Viton<sup>®</sup> tubing could be used for transferring corrosive liquids even at high temperatures. The flow rates of acetic acid and *iso*-amyl alcohol were controlled volumetrically using the metric pump and HPLC pump, respectively. The catalytic section of the column was filled with Purolite<sup>®</sup> CT-175 cation exchange resin (a macroreticular sulphonated styrene divinylbenzene resin), packed in Katamax<sup>®</sup> catalytic packing (Figure 6.3) supplied from Koch-Glitsch<sup>®</sup>, USA. Katamax<sup>®</sup> catalytic packings were used because they provided for excellent heat and mass transfer between the liquid and vapour phases, which arises from the catalytic packing's structure of ordered flow channels. These characteristics help to promote mixing and distribution of the ascending vapour and descending liquid phases. Besides, the design of the Katamax<sup>®</sup> packing allows for high hydraulic capacity and low pressure drop. These advantages of the packing lead to a better separation of products from reactants for equilibrium limited reactions such as the present

reacting system involving acetic acid and *iso*-amyl alcohol. The non-reactive packed enriching and stripping sections were filled with PRO-PAK<sup>®</sup> distillation packing. Figures 6.2a to 6.2f show representative sections and components of the RDC.

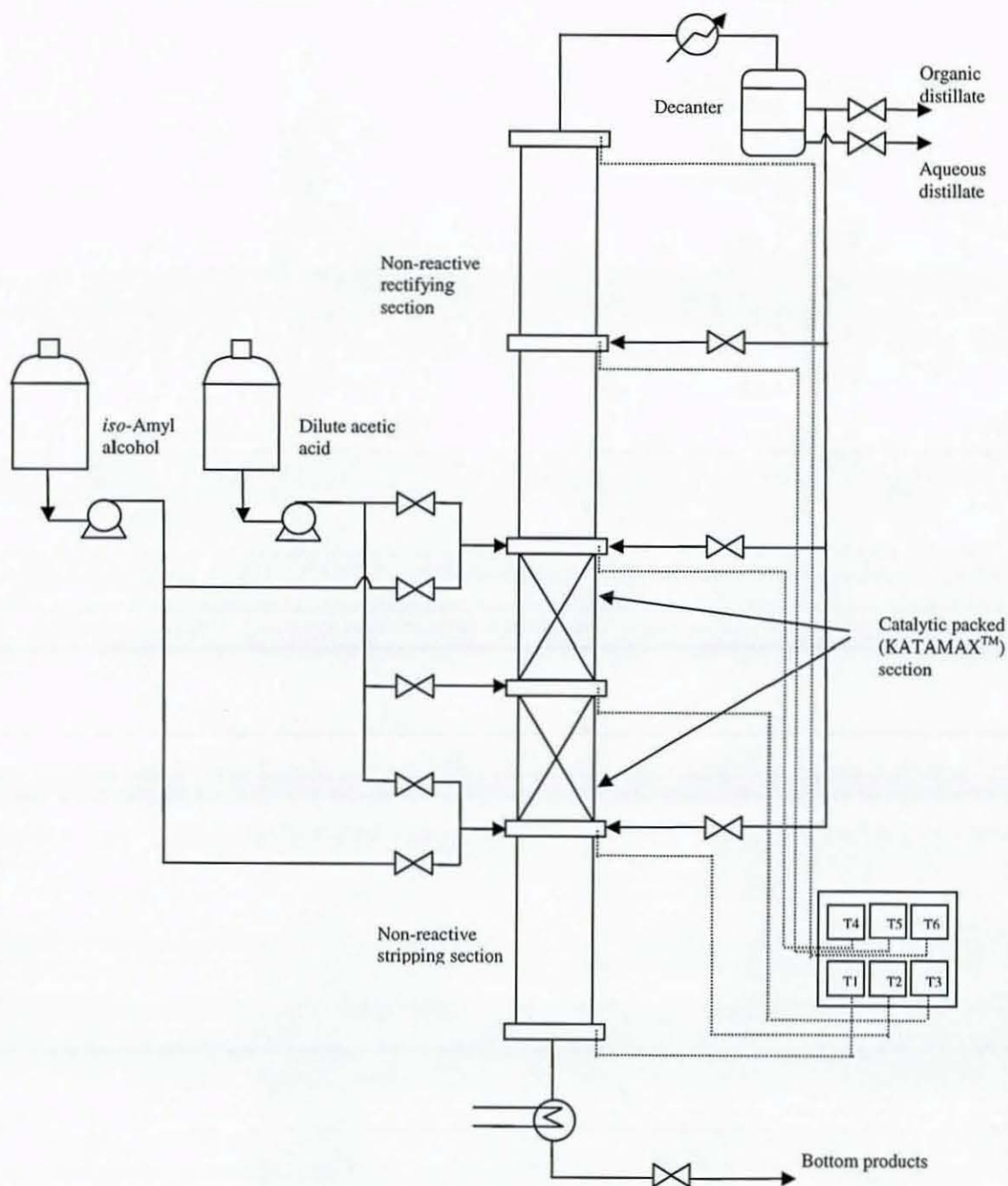
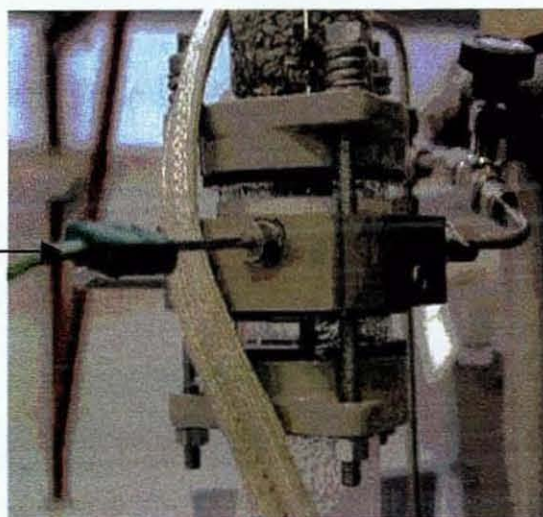


Figure 6.1. Diagram of reactive distillation column.



(a) Decanter

Type K  
thermocouple



(b) Thermocouple in RDC

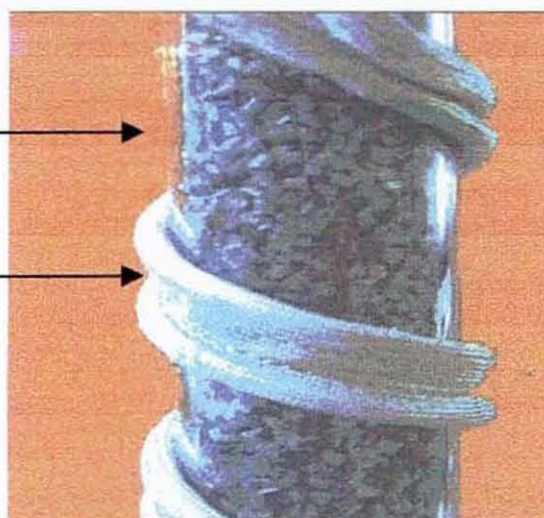


(c) LabVIEW<sup>TM</sup> software program for temperature monitoring

**Figure 6.2.** Different sections of RDC used for the present work.

PROPAK<sup>TM</sup>  
Distillation  
packing

Heating tape



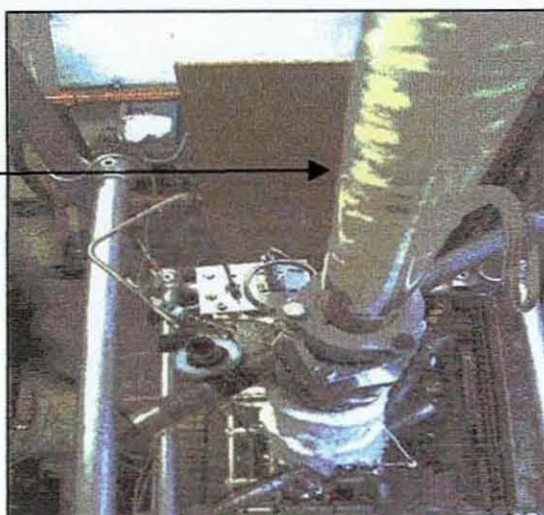
(d) PROPAK<sup>TM</sup> Distillation packing with heating tape

Water cooled  
condenser



(e) RDC

Water cooled  
condenser



(f) RDC (aerial view)

**Figure 6.2.** Different sections of RDC used for the present work.

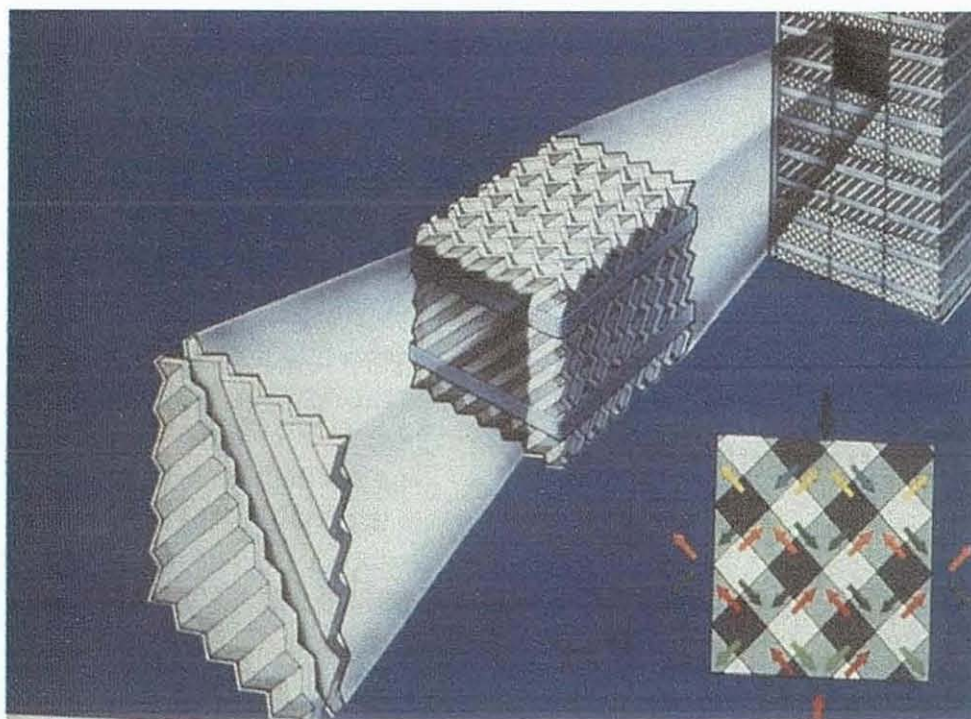


**Figure 6.3.** Katamax<sup>®</sup> packing (Kulprathipanja, 2001)

In a typical experimental run, acetic acid was introduced at the top of the reactive section and *iso*-amyl alcohol was fed at the bottom of the reactive section (except in the investigation of the effect of acid feed position). The temperature in each section of the reactive distillation column was monitored after starting the reaction, and steady state was achieved when the temperatures in the different sections of the column were stabilised. Thereafter, the top (inclusive of both organic and aqueous phases) and bottom products were continuously withdrawn. The sampling of the top and bottom products were done at 1 hour interval, and subsequently analysed for their composition.

The RDC experiments were carried out over a duration of 2 hours after steady state was attained. The key features of the reactive distillation column experimental set-up are presented in Table 6.1.

**Table 6.1.** Key features of the reactive distillation column.

Parameter	Details
Diameter, d (m)	0.050
Insulation	Heating blanket (Superwool 607 <sup>TM</sup> MAX Blanket)
<b>Rectifying section</b>	
Height, h (m)	1.500
Type of packing	PRO-PAK <sup>®</sup> (Sigma-Aldrich)
<b>Reactive section</b>	
Height, h (m)	1.000
Type of packing	Katamax <sup>®</sup> (Koch-Glitsch), USA
Catalyst type	Purolite <sup>®</sup> CT-175
<b>Stripping section</b>	
Height, h (m)	0.750
Type of packing	PRO-PAK <sup>®</sup> (Sigma-Aldrich)
Operating pressure	Atmospheric

### 6.2.3 Method of Analysis

Acetic acid, *iso*-amyl alcohol, *iso*-amyl acetate and water were analysed using gas chromatograph (Pye Unicam 104) which was equipped with a thermal conductivity detector. *n*-Butanol was used as the internal standard. The gas chromatograph column was packed with Porapak Q using helium gas as the carrier gas. The flow rate of the helium gas was  $6.25 \times 10^{-7} \text{ m}^3 \text{ s}^{-1}$  which was determined by the use of a calibrated flow meter (J and W Scientific). The injector and detector block temperatures were maintained at 523 K. The oven temperature was maintained isothermally at 523 K.

### 6.3 RESULTS AND DISCUSSION OF REACTIVE DISTILLATION COLUMN EXPERIMENTS

The experiments were carried out in order to achieve an optimum column configuration for the synthesis of *iso*-amyl acetate in a reactive distillation column. From the acetic acid recovery point of view, the optimal reactive distillation column configuration should give the highest conversion of acetic acid with minimum concentration of acetic acid at the top as well as minimum concentration of *iso*-amyl acetate at the bottom. Furthermore, it is desirable to withdraw only non-converted excess acetic acid at the bottom in order to avoid an additional purification step. The bottom stream could subsequently be recycled to the acetic acid feed stream.

#### 6.3.1 Effect of feed mole ratio of reactants

The feed mole ratio of the reactants has a key role in determining the conversion of acetic acid to *iso*-amyl acetate, the distillate purity as well as the relative weight compositions of the top and bottom product streams. The feed mole ratio of *iso*-amyl alcohol to acetic acid was investigated at 1.5:1, 1.9:1 and 3:1 (Saha *et al.*, 2005a). In all experimental runs, the organic phase of the top product was refluxed back into the top of the rectifying section at a reflux ratio of 10 while the aqueous phase of the top product was continually withdrawn through the use of a decanter.

With reference to Figure 6.4, the conversion of acetic acid increased from 24.8% to 53.5% when the feed mole ratio of *iso*-amyl alcohol to acetic acid was increased from 1.5:1 to 1.9:1. However, the conversion of acetic acid decreased to 44.7% when the feed mole ratio of *iso*-amyl alcohol to acetic acid was further increased to 3:1. The experimental results indicate that any further increase in feed mole ratio of *iso*-amyl alcohol to acetic acid under those specific reacting conditions would not improve the acetic acid conversion. It is therefore conclusive based on the experimental results that the feed mole ratio of *iso*-amyl alcohol to acetic acid of 1.9:1 is optimum for the adopted configuration. Further experimental runs were carried out at or very close to this feed mole ratio. Figure 6.5 illustrated that the decanter was effective in removing the aqueous phase from the organic phase, with the

contents of the top aqueous phase predominantly water and very slight traces of acetic acid. Figure 6.6 showed that there was no trace of acetic acid at the top organic phase of the reactive distillation column with a feed mole ratio (*iso*-amyl alcohol to acetic acid) of 1.9:1 whereas there were very slight traces of acetic acid, 1.8 wt% acetic acid and 1.9 wt% acetic acid in the top organic phases when the experiments were conducted at feed mole ratios (*iso*-amyl alcohol to acetic acid) of 1.5:1 and 3:1, respectively. Furthermore, *iso*-amyl acetate was not present in the bottom product stream when the feed mole ratio of 1.9:1 and other feed mole ratio configurations were carried out for the experimental runs (Figure 6.7).

The amount of *iso*-amyl alcohol in the bottom product was 2.9 wt% when the feed mole ratio of *iso*-amyl alcohol to acetic acid was 1.9:1. However, higher traces of *iso*-amyl alcohol (3.7 wt% and 6.9 wt%) were detected in the bottom product stream at feed mole ratios (*iso*-amyl alcohol to acetic acid) of 1.5:1 and 3:1, respectively. In addition, since *iso*-amyl alcohol forms a binary azeotrope with water at 368.3 K and a ternary azeotrope with both water and *iso*-amyl acetate at 366.8 K, it is expected that most of the *iso*-amyl alcohol available will form azeotropes and move upwards of the column. This explains the very low conversion of acetic acid with a feed mole ratio (*iso*-amyl alcohol to acetic acid) of 1.5:1 and 3:1, as the limited availability of *iso*-amyl alcohol to react with acetic acid in the catalytic reactive section through is further restricted by the relatively high compositions of *iso*-amyl alcohol in the bottom product. These findings further substantiate that the feed mole ratio (*iso*-amyl alcohol to acetic acid) of 1.9:1 is optimal, as it meant that more of the *iso*-amyl alcohol in the reboiler move up the reactive distillation column to react with the acetic acid and hence improve the acetic acid conversion. The optimal feed mole ratio as obtained corresponds well with findings from the residue curve map experiments (Chapter 5).

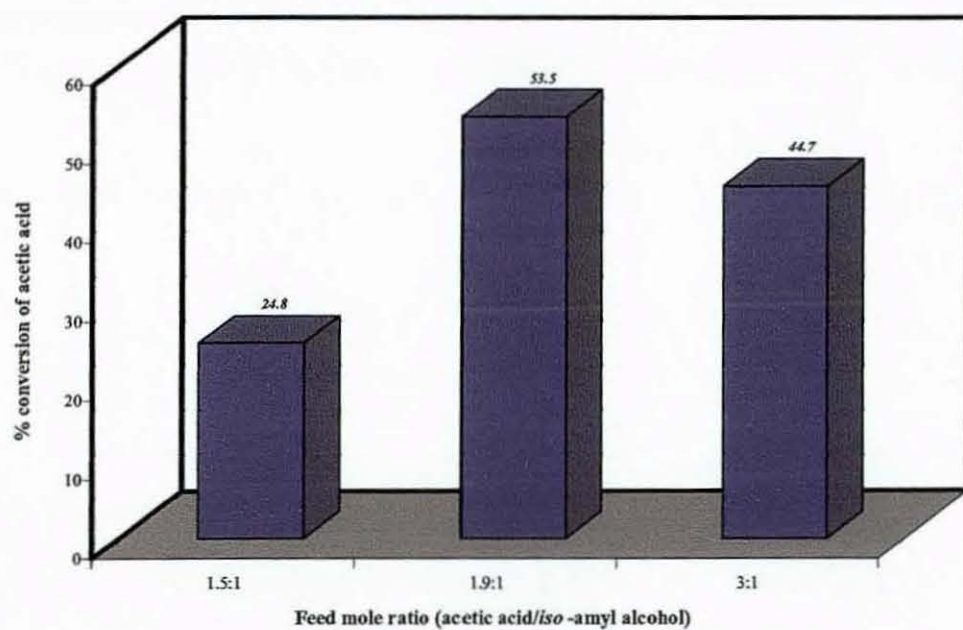


**Figure 6.4.** Effect of feed mole ratio (acetic acid to *iso*-amyl alcohol) on conversion of acetic acid.

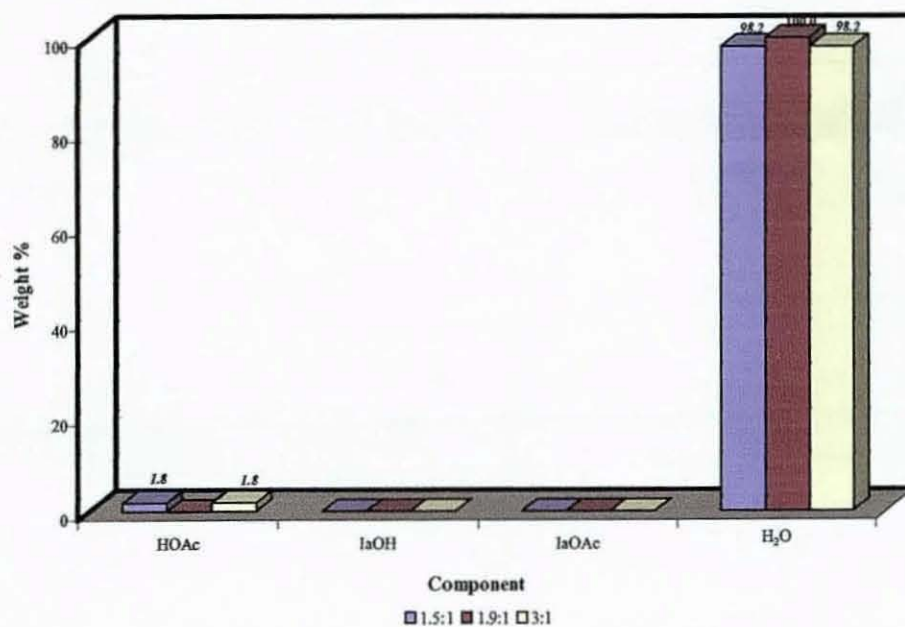


**Figure 6.5.** Effect of feed mole ratio (acetic acid to *iso*-amyl alcohol) on composition of top product (aqueous) in a reactive distillation column.

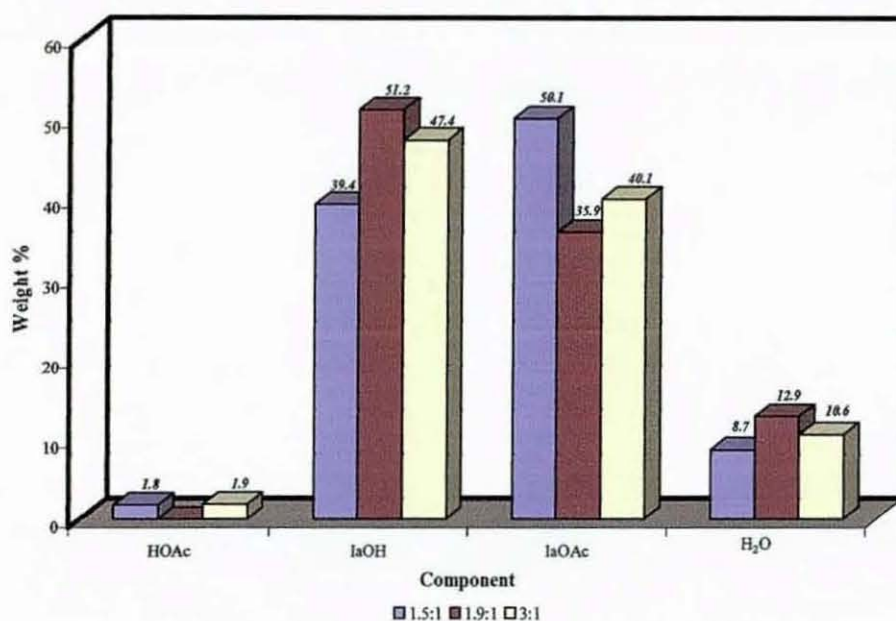


**Figure 6.6.** Effect of feed mole ratio (*iso*-amyl alcohol to acetic acid) on composition of top product (organic) in a reactive distillation column.

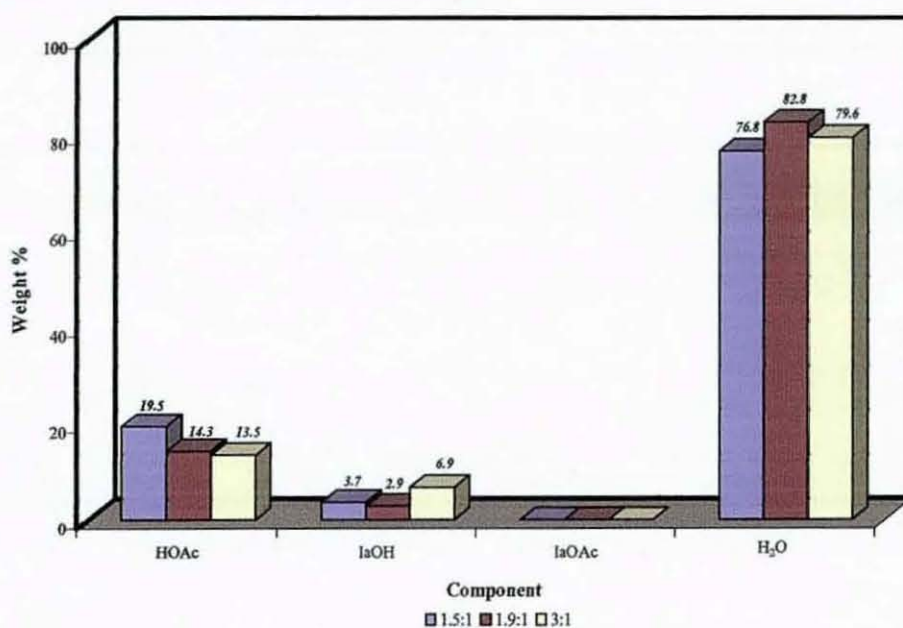


**Figure 6.7.** Effect of feed mole ratio (*iso*-amyl alcohol to acetic acid) on composition of bottom product in a reactive distillation column.

### 6.3.2 Effect of reflux ratio

The effect of the reflux ratio of the top organic phase product was investigated to determine how it would affect the conversion of acetic acid from its aqueous solution. Sharma and Mahajani (2003) reported that the reflux ratio played a crucial role. The reflux ratio not only influences the extent of reaction taking place in a column, but also dictates the capital cost and energy requirements. Sharma and Mahajani (2003) further reported that for the synthesis of methyl acetate, the separation was poor at low reflux ratios whereas the methanol reactant was separated through the azeotropes of methanol and methyl acetate at high reflux ratios. Baur *et al.* (2001) reported that the reflux ratio could affect the selectivity of the desired product. The selectivity of isobutene was affected by the formation of byproducts (*di-isobutene*, *di-methyl ether* and water) as the reflux ratio increases. The experiments were carried out under practical operating conditions in the reactive distillation column. Saha *et al.* (2000), Kloker *et al.* (2004) and Dhale *et al.* (2004) previously worked on reflux ratios that varied between 1 and 6.65. The experiments were conducted at time based reflux ratio values of 2, 5 and 10. It seemed impractical to carry out experimental runs at reflux ratio at a value higher than 10 in a reactive distillation column and hence no further experiments were carried out for reflux ratio value beyond 10. In all the experimental runs, the feed mole ratio of *iso*-amyl alcohol to acetic acid was kept at the optimum ratio value of 1.9:1 as previously determined, with acetic acid introduced at the top of the reactive section and *iso*-amyl alcohol introduced at the bottom of the reactive section. In addition, the organic phase of the top product was refluxed back into the top of the rectifying section while the aqueous phase of the top product was continually withdrawn from the reactive distillation column through the use of the decanter.

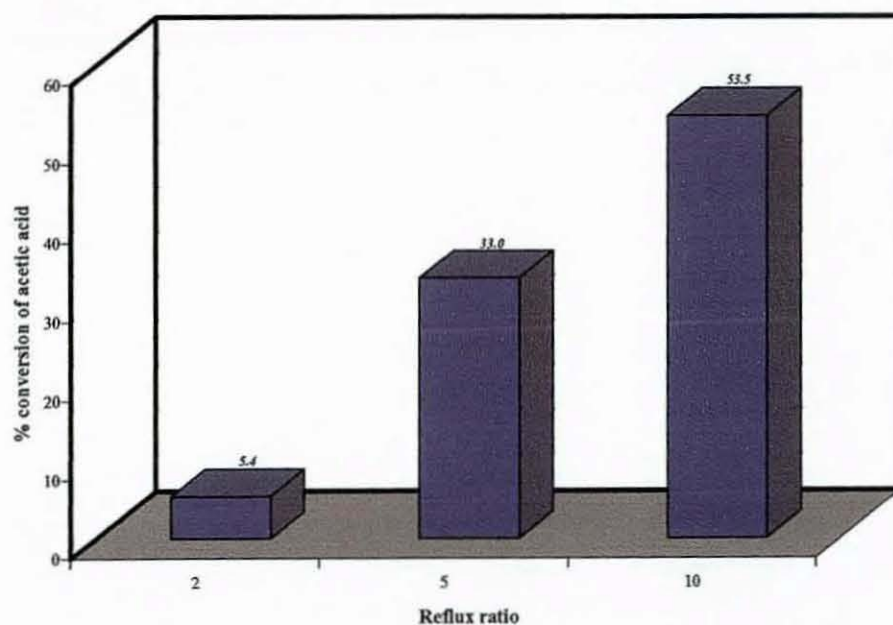


**Figure 6.8.** Effect of reflux ratio on conversion of acetic acid.

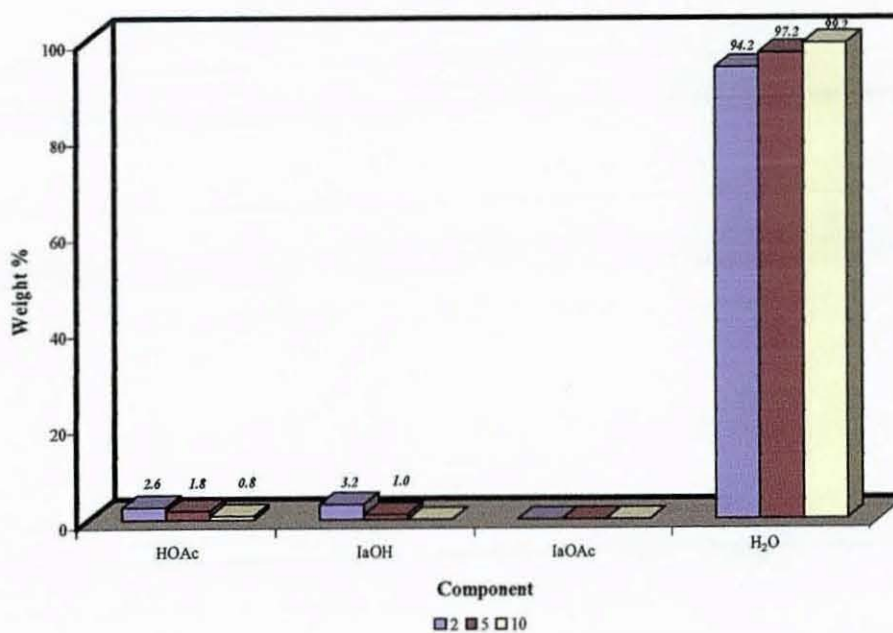


**Figure 6.9.** Effect of reflux ratio on composition of top product (aqueous) in a reactive distillation column.

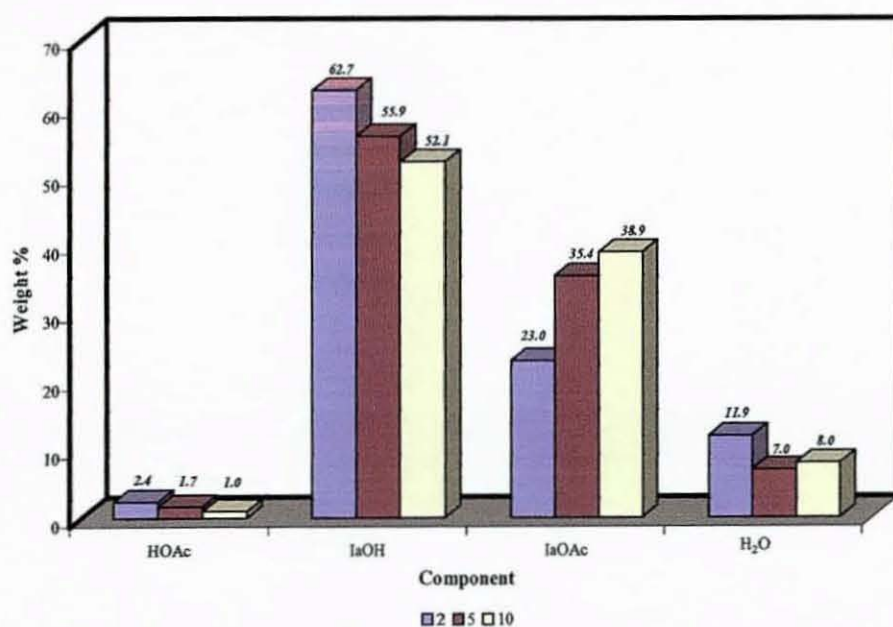


**Figure 6.10.** Effect of reflux ratio of composition of top product (organic) in a reactive distillation column.

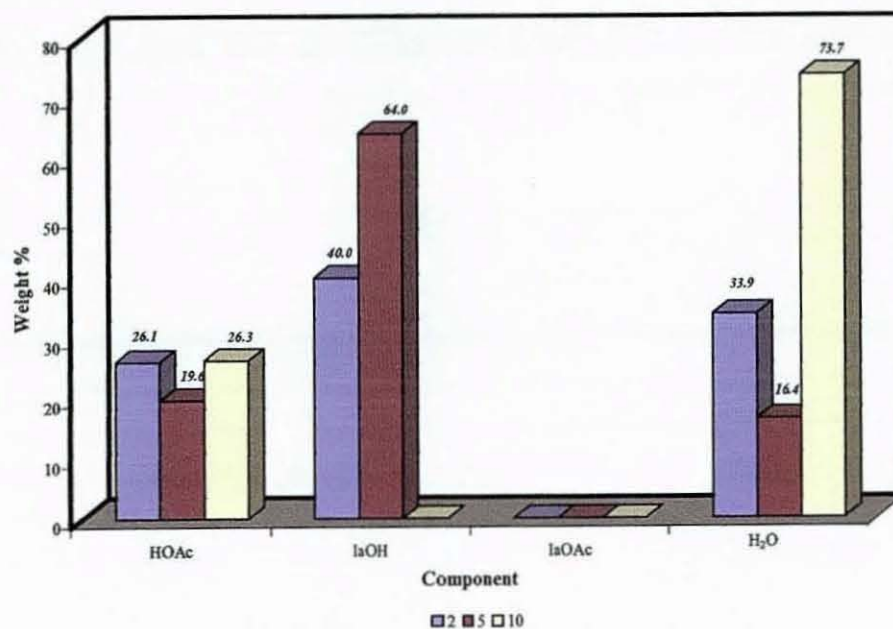


**Figure 6.11.** Effect of reflux ratio of composition of bottom product in a reactive distillation column.

With reference to Figure 6.8, there was an increase in the conversion of acetic acid from 5.4 % to 53.5 % when the reflux ratio was raised from 2 to 10. Figure 6.9 depicted that the decanter was effective in separating the aqueous and organic phases from the top product, with the contents of the top aqueous product made up mainly of water and traces of acetic acid and *iso*-amyl alcohol. Figure 6.10 illustrates that the amount of acetic acid in the top organic product decreases from 2.4 wt% to 1.0 wt% when the reflux ratio of the organic phase is increased from 2 to 10. Furthermore, the amount of *iso*-amyl acetate in the top organic product increase from 23.0 wt% to 38.9 wt% for the same experimental configuration. In addition, Figure 6.11 shows that the residual concentration of *iso*-amyl alcohol in the bottom product is non-existent by adopting a reflux ratio of 10. This finding is significant as it meant that the adoption of this experimental configuration allows for *iso*-amyl alcohol to move up the reactive distillation column to react with the acetic acid and hence improve the acetic acid conversion. Figure 6.11 further shows that *iso*-amyl acetate is not present in the bottom product regardless of the reflux ratio configuration. From the experiment findings, the optimal reflux ratio was found to be 10. Hence, all further experimental runs were carried out at this reflux ratio.

### 6.3.3 Effect of acid feed position

The feed positions of acetic acid and *iso*-amyl alcohol is a key parameter in the operation of the reactive distillation column. An important prerequisite is that the contact area between the reactants in the column is maximised, especially in the catalytic reactive zone. DeGarmo *et al.* (1992) highlighted that the contact of the reactants with the catalyst is as important as the mass transfer between the gas and liquid phases. This is to take advantage of the column's dual function as a reactor as well as a distillation unit. In the investigation of the effect of the acid feed position, the experiments were conducted at the optimal feed mole ratio (*iso*-amyl alcohol to acetic acid) of 1.9:1 and optimal reflux ratio of 10 as previously investigated. Acetic acid was introduced at the top of the reactive section while the *iso*-amyl alcohol was introduced at the bottom of the reactive section under the optimal conditions investigated thus far, and *vice versa*.

Both the experiments as outlined above were conducted to explore the effect of the acid feed position in the counter-current mode. Saha *et al.* (2000) carried out work for both co-current and counter-current, and found that the acetic acid conversion with *n*-butanol was higher when the operation was carried out in the counter-current mode. During the course of the experimental runs, the top distillate product was separated into the organic and aqueous phases with the decanter. The organic phase of the top distillate product was refluxed back into the top of the rectifying section while the aqueous phase of the top product was continually removed from the reactive distillation column.

It was found experimentally as illustrated from the results in Figure 6.12 that introducing the acetic acid at the top of the reactive section (52.0% acetic acid conversion) is more favourable as compared to introducing the acetic acid at the bottom of the reactive section (44.1% acetic acid conversion). Figure 6.13 shows that there was negligible amount of acetic acid in the top aqueous stream. Figure 6.14 illustrates that acetic acid was not present in the top organic products for both experimental configurations. In addition, the experimental results as presented in Figure 6.14 shows that when acetic acid was fed at the top of the reactive section, 55.9 wt% of *iso*-amyl alcohol was present in the top organic stream. However, when the acetic acid was introduced at the bottom of the reactive section, 74.1 wt% of *iso*-amyl alcohol was detected in the top organic stream. The latter result showed that the introduction of *iso*-amyl alcohol at the top of the reactive section led to a high *iso*-amyl alcohol content in the top organic stream. This inhibited the reaction of *iso*-amyl alcohol with acetic acid in the catalytic reactive zone and led to a reduction in the overall conversion of acetic acid. Furthermore, the amount of *iso*-amyl acetate in the top organic product reduced from 34.0 wt% to 14.9 wt% for the same set of experimental configurations. These findings show that the introduction of acetic acid at the top of the reactive section allows for more contact between the reactants i.e. acetic acid and *iso*-amyl alcohol in the catalytic reactive section which leads to increased acetic acid conversion.

Figure 6.15 shows that the amount of acetic acid increased from 14.0 wt% to 17.1 wt% whilst the amount of *iso*-amyl alcohol increased from 1.6 wt% to 4.8

wt% in the bottom product when the acetic acid feed position was changed from the top of the reactive section to the bottom of the reactive section. These findings further reiterate that introducing acetic acid at the bottom of the reactive section reduce the amount of reactants available to react in the catalytic reactive zone, leading to lower conversions of acetic acid to *iso*-amyl acetate. Figure 6.15 further shows that *iso*-amyl acetate was not present in the bottom product.

The experimental results showed that introducing acetic acid at the top of the reactive zone of the reactive distillation column and *iso*-amyl alcohol at the bottom of the reactive zone was more advantageous than the arrangement carried out *vice-versa*. All further experimental runs were thus carried out with the acetic acid being introduced at the top of the reactive zone with the *iso*-amyl alcohol being introduced at the bottom of the reactive zone in the reactive distillation column.

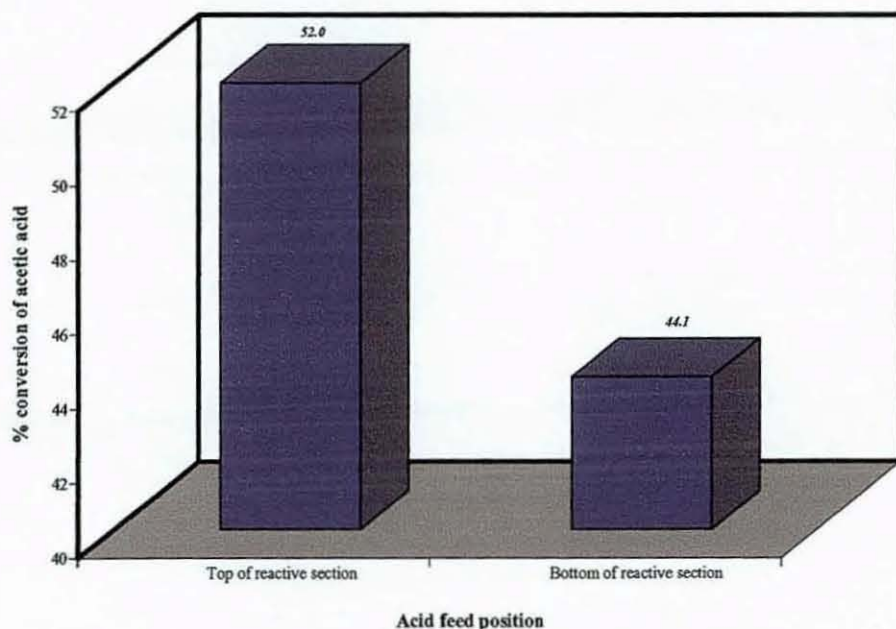


**Figure 6.12.** Effect of acid feed position on conversion of acetic acid.

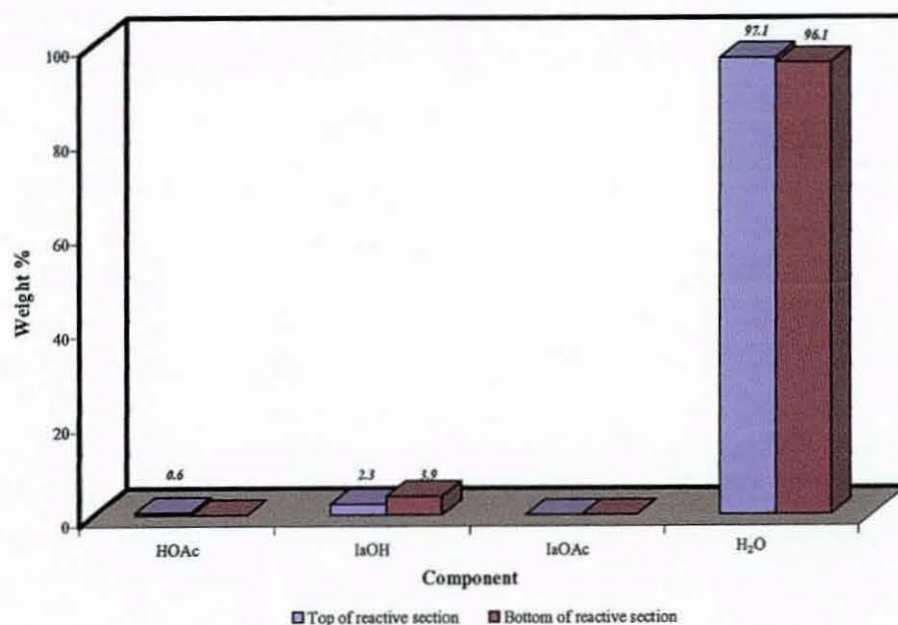


**Figure 6.13.** Effect of acid feed position on composition of top product (aqueous) in a reactive distillation column.

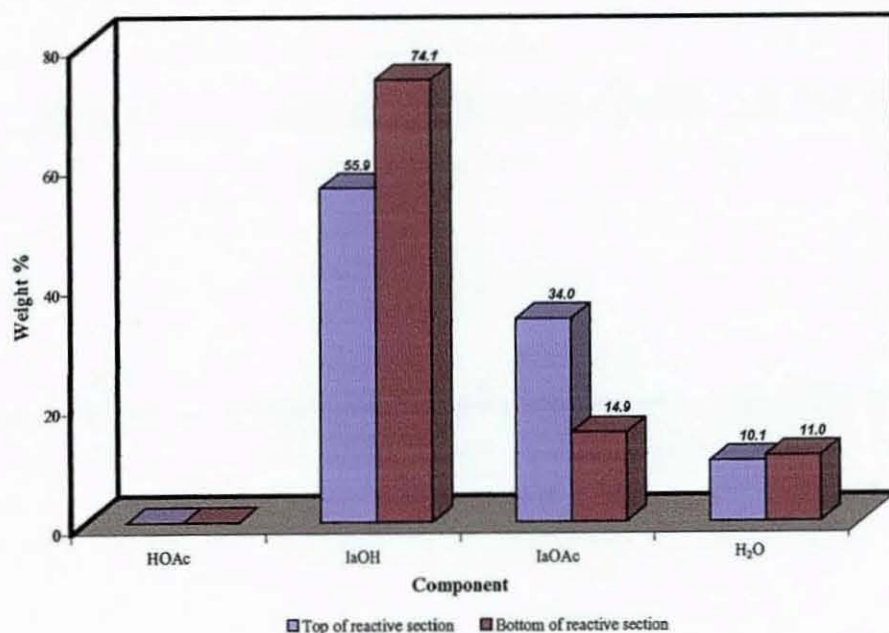


**Figure 6.14.** Effect of acid feed position on composition of top product (organic) in a reactive distillation column.

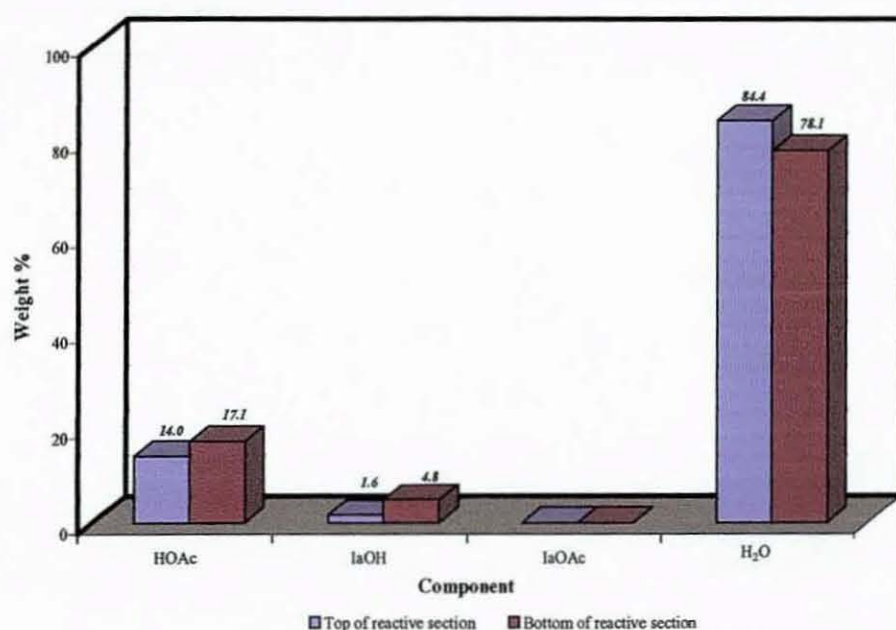


**Figure 6.15.** Effect of acid feed position on composition of bottom product in a reactive distillation column.

#### 6.3.4 Effect of reflux configuration

The effect of reflux configuration was investigated to increase the conversion of acetic acid from its aqueous solutions. In the investigation of the reflux configuration, the experimental runs were carried out under the optimal feed mole ratio (*iso*-amyl alcohol to acetic acid) of 1.9:1, optimal reflux ratio of 10 and the optimal acetic acid feed position at the top of the reactive section in the reactive distillation column as previously investigated. The top distillate product was separated into the aqueous and organic phases with the use of a decanter of which the aqueous phase was continually removed from the column while the organic phase was partially refluxed into the reactive distillation column via the top of the rectifying section. Further experiments were carried out under similar experimental conditions as outlined with the exception of the organic phase of the top product being partially refluxed into the reactive distillation column via the top and bottom of the reactive zone of the RDC.

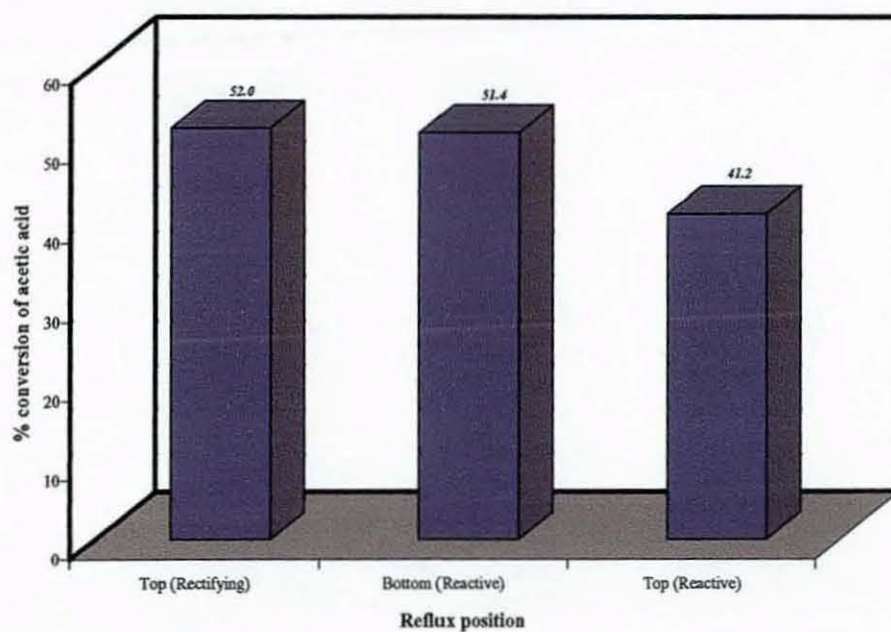


Figure 6.16. Effect of reflux position on conversion of acetic acid.

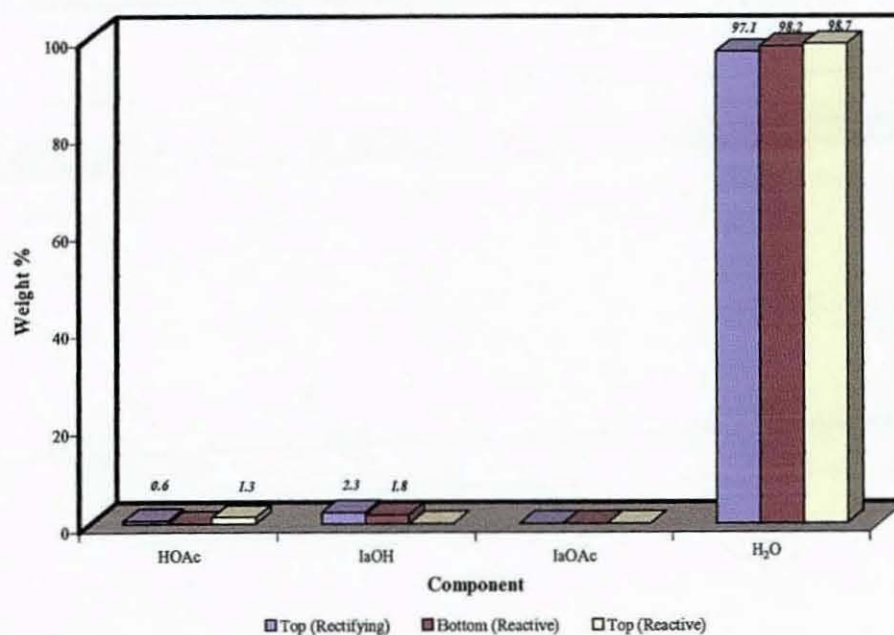
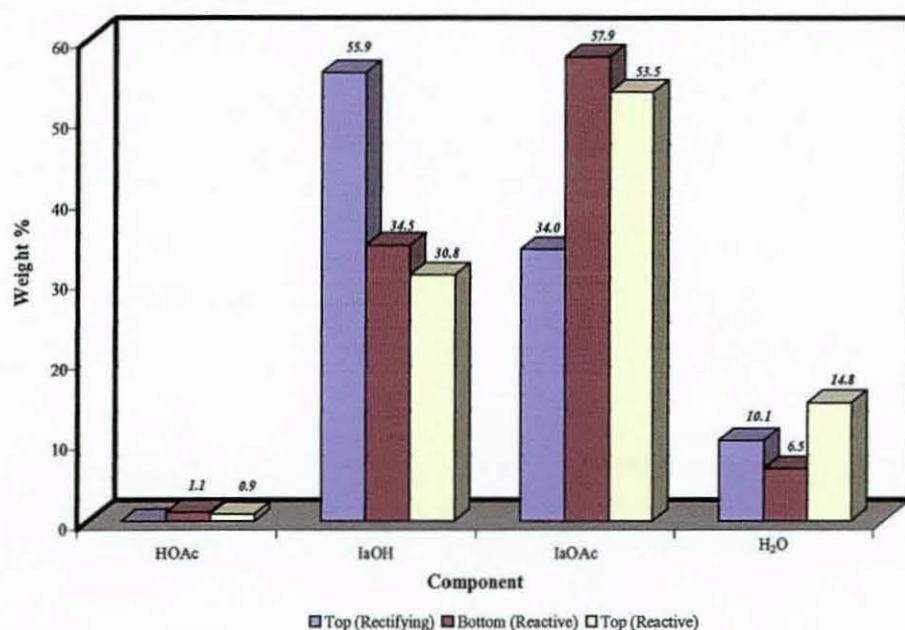
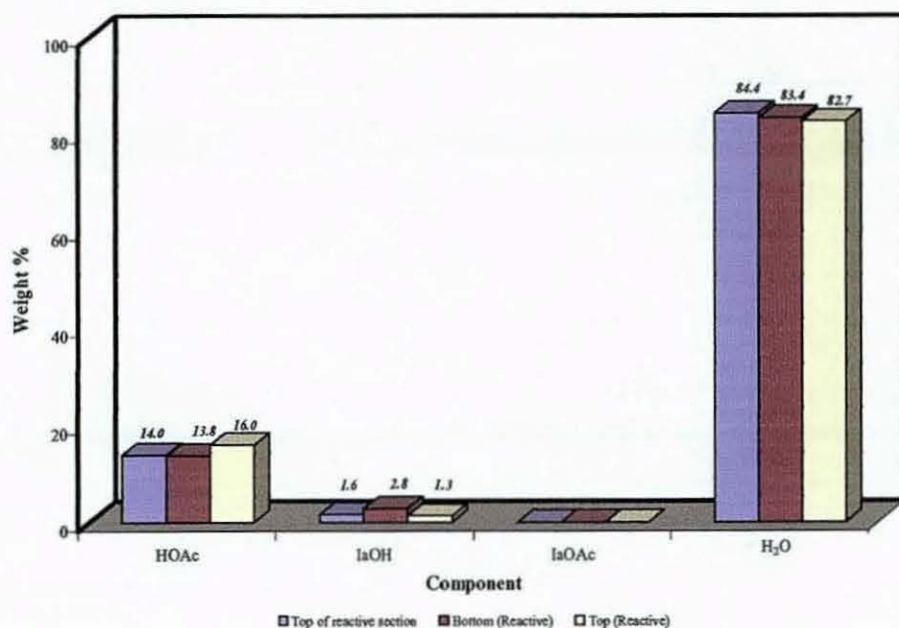


Figure 6.17. Effect of reflux position on composition of top product (aqueous) in a reactive distillation column.



**Figure 6.18.** Effect of reflux position on composition of top product (organic) in a reactive distillation column.



**Figure 6.19.** Effect of reflux position on composition of bottom product in a reactive distillation column.

The experimental results as illustrated in Figure 6.16 shows that partially refluxing the organic phase into the top of the rectifying section in the reactive distillation column yield the best conversion of acetic acid at 52.0%. Figure 6.17 shows that there were negligible amounts of acetic acid and *iso*-amyl alcohol in the aqueous phase of the top product. Figure 6.18 shows that there was a significant increase in the amount of *iso*-amyl acetate from 34.0 wt% to 57.9 wt% when the reflux feed position was changed from the top of the rectifying section to the bottom of the reactive section. *iso*-Amyl alcohol–*iso*-amyl acetate–water form lower boiling azeotropes at 366.6 K. Acetic acid does not form any azeotrope in this reacting system, which makes it the highest boiling component at 390 K. Therefore, the distillate at the top of the RDC contained small amount of acetic acid (~1 wt%) (Figure 6.18). The water content in the organic phase being refluxed to the bottom of the reactive section could be the contributing factor towards the higher amount of *iso*-amyl acetate in the top product. Water being the lowest boiling component of the organic reflux would lift the reacting components upwards of the column and into the reactive zone, resulting in higher conversion of acetic acid into *iso*-amyl acetate. Figure 6.19 shows that the amount of acetic acid in the bottom product was the least at 13.8 wt% when the top organic product was partially refluxed into the bottom of the reactive section in the reactive distillation column. Furthermore, *iso*-amyl acetate was not detected in the bottom product in all experimental configurations.

### 6.3.5 Effect of acetic acid concentration in the feed stream

The effect of acetic acid concentration was investigated to determine how the reactive distillation column would perform with the introduction of different acetic acid concentrations in the feed stream. In the investigation of this parameter, the experimental runs were carried out under the optimal experimental conditions obtained thus far i.e. feed mole ratio (*iso*-amyl alcohol to acetic acid) of 1.9:1, reflux ratio of the top organic product of 10, introducing the acetic acid feed at the top of the reactive section and refluxing the organic phase of the top product into the bottom of the reactive section.

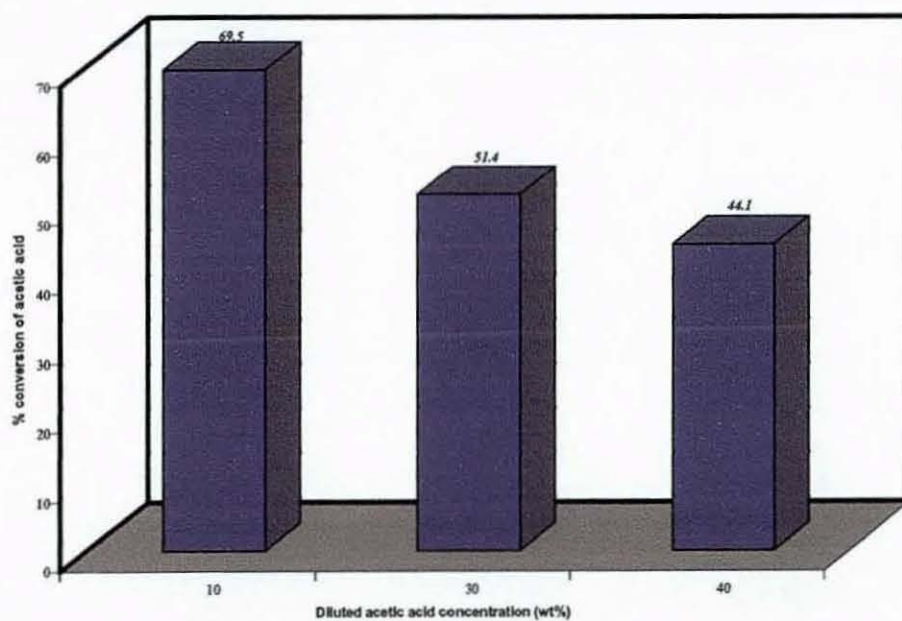


**Figure 6.20.** Effect of acetic acid concentration on conversion of acetic acid.

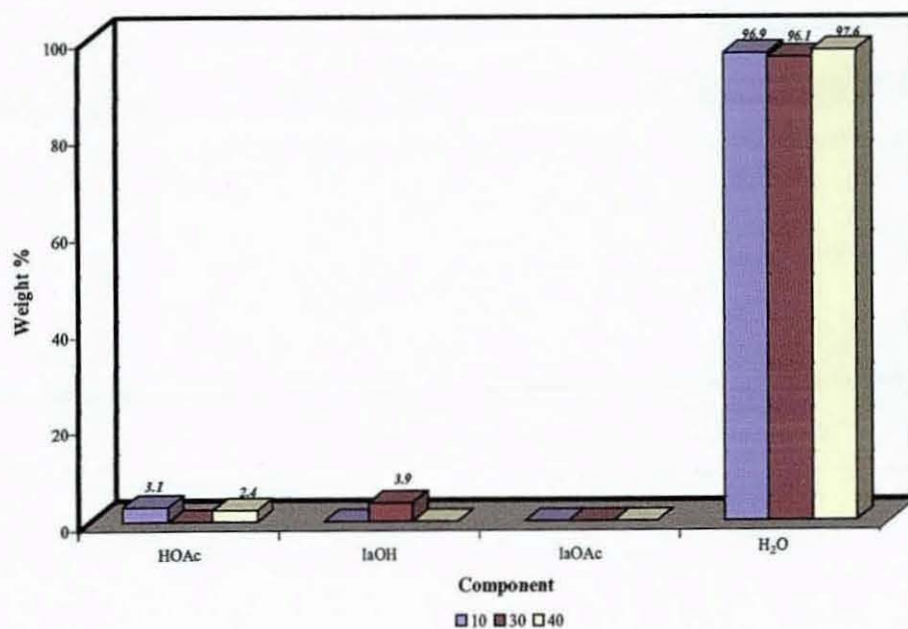


**Figure 6.21.** Effect of acetic acid concentration on composition of top product (aqueous) in a reactive distillation column.

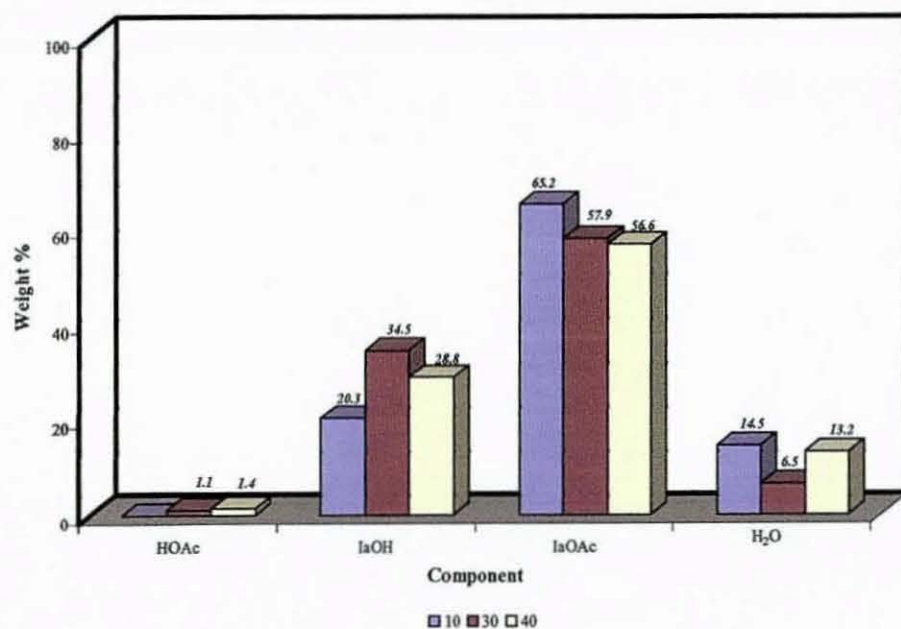


**Figure 6.22.** Effect of acetic acid concentration on composition of top product (organic) in a reactive distillation column.

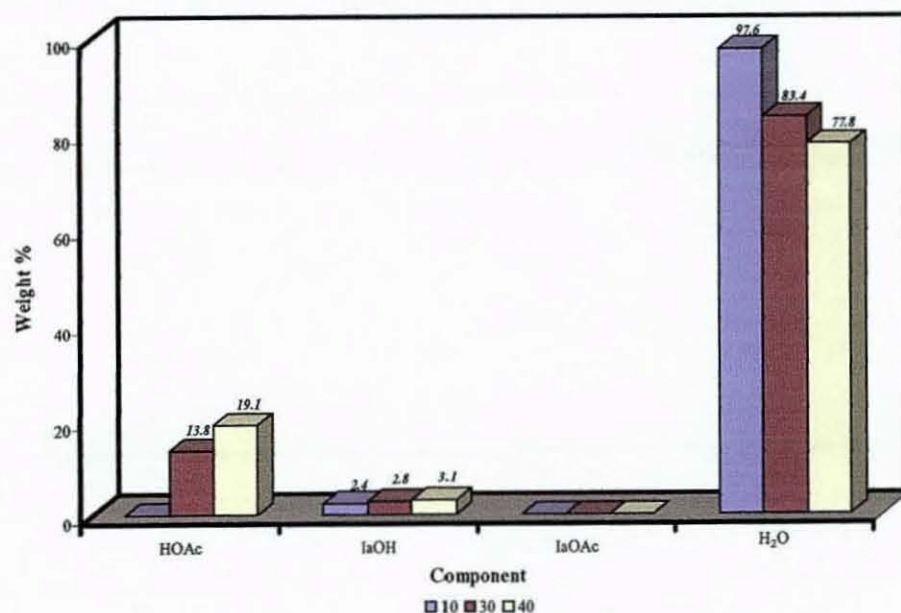


**Figure 6.23.** Effect of acetic acid concentration on composition of bottom product in a reactive distillation column.

The experimental results as illustrated in Figure 6.20 shows that there was an increase in conversion of acetic acid from 44.1% to 69.5% when the acetic acid concentration was reduced from 40 wt% to 10 wt%. Figure 6.21 shows that the decanter was effective in separating the top product from into the aqueous and organic phases. There were traces of acetic acid and *iso*-amyl alcohol detected in the aqueous phase. Figure 6.22 shows the amount of *iso*-amyl acetate increases from 56.6 wt% to 65.2 wt% when the acetic acid concentration was reduced from 40 wt% to 10 wt%. Figure 6.23 shows that the amount of acetic acid in the bottom product decreases from 19.1 wt% to 0 wt%. The amount of *iso*-amyl alcohol obtained in the bottom product increased from 3.1 wt% to 35.6 wt% when the diluted acetic acid concentration was reduced from 40 wt% to 10 wt% in the feed stream. Furthermore, *iso*-amyl acetate was not detected in the bottom product under all experimental configurations investigated.

### 6.4 CONCLUSIONS

The synthesis of *iso*-amyl acetate through the recovery of diluted acetic acid by esterification with *iso*-amyl alcohol was performed by reactive distillation using a macroreticular cation exchange resin Purolite<sup>®</sup> CT-175 packed within Katamax<sup>®</sup> catalytic packing. The main conclusions drawn from the RDC work are:

- (i) The optimal feed mole ratio of *iso*-amyl alcohol to acetic acid is 1.9:1;
- (ii) The optimal reflux ratio of the top organic product is 10;
- (iii) The optimal feed position for the acetic acid feed is at the top of the reactive section of the reactive distillation column;
- (iv) The optimal reflux feed position is at the bottom of the reactive section of the reactive distillation column;
- (v) The reactive distillation column could cope with different acetic acid concentrations.
- (vi) The implementation of reactive distillation for the recovery of 10% (w/w) acetic acid improved the acetic acid conversion from 18.2% (batch kinetic studies) to 69.5%.

It can be further concluded that reactive distillation with Purolite<sup>®</sup> CT-175 catalyst and Katamax<sup>®</sup> catalytic packing can be conveniently used for the recovery of dilute acetic acid and to produce a value added ester in the form of *iso*-amyl acetate.

## 7. CONCLUSIONS AND FUTURE WORK

### 7.1. CONCLUSIONS

The objective of this research was to implement a reactive distillation process using ion exchange resins as catalysts for the recovery of dilute acetic acid from aqueous waste streams, which was a by-product from petrochemical and fine chemical industries. The characteristics of the ion exchange resins have been determined to elucidate the relationship between the catalytic performance and the structure of the ion exchange resins.

The literature review presented a wide range of applications for the reactive distillation process but not much attention was dedicated to the recovery of acetic acid from industrial waste streams. No previous kinetic data for the catalysed esterification of acetic acid with *iso*-amyl alcohol was presented in the literature. The kinetics of the reacting system was investigated extensively under batch conditions at different stirrer speeds, catalyst particle sizes, reaction temperatures, acetic acid concentrations, feed mole ratio, catalyst loading, catalyst type and catalyst reusability. Thereafter, a suitable kinetic rate expression has been obtained to represent the kinetic behaviour of the reacting system over a range of operating conditions. This rate expression would be useful in the simulation of the dynamic behaviour of the reactive distillation column.

From the representative residue curve map experiments carried out, it was determined that the non-reactive azeotropes could be eliminated with the addition of the catalyst into the reacting system and the desired product for the reacting system i.e. *iso*-amyl acetate could be obtained successfully over time. Furthermore, the residue curve map suggested the use of a low feed molar ratio of *iso*-amyl alcohol to acetic acid in the reactive distillation column so that *iso*-amyl acetate would only be present in the top product stream. This finding has been subsequently backed up by results gathered during the optimisation of the reactive distillation column process configurations.

A reactive distillation column has been specially designed and built as part of this research, which is one of the major tasks of this project. The reactive distillation column experiments were subsequently carried out by using the more promising ion exchange resin catalyst, Purolite® CT-175, which was assessed from the results of the batch kinetic studies. An experimental methodology towards the optimisation of the process conditions and column configurations was established, after which it was found from experimental findings that the optimal process configuration was at a feed mole ratio of acetic acid to *iso*-amyl alcohol of 1:1.9, a reflux ratio of the organic phase of 10, introduction of the acetic acid feed at the top of the reactive section while introducing the reflux into the bottom of the reactive section. Furthermore, the implementation of reactive distillation for the recovery of 10% (w/w) acetic acid improved the acetic acid conversion from 18.2% in batch kinetic studies to 69.5% in the continuous reactive distillation column.

The ion exchange resins employed as catalysts in this work have shown promising results towards the recovery of acetic acid through the reaction with *iso*-amyl alcohol in a reactive distillation column whilst producing a value added ester in the form of *iso*-amyl acetate. The preliminary cost evaluation for the reactive distillation process built towards the synthesis of *iso*-amyl acetate is estimated at £11,500 for the investment costs and £26,000 towards the annual operating costs. The *iso*-amyl acetate product could be sold at a price of £227 for a barrel of 20L capacity. The work carried out in this research thus far provides a good platform for future work to be carried out along similar lines.

### 7.2. FUTURE WORK

- The batch kinetic studies could be expanded with the use of more catalysts e.g. zeolites and other suitable ion exchange resins. The characteristics of the ion exchange resins could be tailored specially to meet the requirements towards the implementation of reactive distillation for other esterification reactions. During the preparation of the catalysts, the ion exchange resins may be tailored in terms of  $H^+$

ion exchange capacity, particle size, pore volume, surface area and swelling capability in solvents.

- In the model assumption section, it was concluded through the comparison of two different mechanisms that water and *iso*-amyl alcohol were adsorbed more strongly than the other components i.e. acetic acid and *iso*-amyl acetate, in the reaction solution. Fourier Transform Infrared (FTIR) analysis could be carried out to test and confirm the component adsorbing strength on the catalyst surface. The FTIR technique measures the absorption of various infrared light wavelengths by the material of interest, in this case the reaction solution.
- The optimisation of the reactive distillation process configurations could be extended into investigation of the effects of the length of the reactive packed section as well as the reflux of water.
- A detailed cost evaluation for the implementation of reactive distillation for the recovery of acetic acid could be developed.
- The results obtained in this research work were based on simulated acetic acid solutions of appropriate weight concentrations. Effluent water from the industrial waste streams could be used as feed solution for the RDC experiments
- Modelling and simulation work on the RDC could be carried out. The experimental results obtained could be used to validate the model.

## 8. REFERENCES

Abella, L. C., Gaspillo, P. D., Itoh, H. and Goto, S., 1999, Dehydration of *tert*-butyl alcohol in reactive distillation. *Journal Chemical Engineering of Japan*, 32, pp. 742-746.

Adams, J., Groten, W. and Nemphos, S., 2003, Process for vinyl acetate. United States Patent 6,620, 465.

Agreda, V. H. and Partin, L. R., 1984, Reactive distillation process for the production of methyl acetate. United States Patent 4,435, 595.

Agreda, V. H., Partin, L. R. and Heise, W. H., 1990, High purity methyl acetate via reactive distillation. *Chemical Engineering Progress*, 86, pp. 40-46.

Agreda, V. H. and Zoeller, J. R., 1993, Acetic acid and its derivatives, Marcel Dekker, New York.

Al-Arfaj, M. A. and Luyben, W. L., 2002, Comparative control study of ideal and methyl acetate reactive distillation. *Chemical Engineering Science*, 57, pp. 5039-5050.

Althouse, J. W. and Tavlarides, L. L., 1992, Analysis of organic systems for acetic acid removal for calcium magnesium acetate production. *Industrial and Engineering Chemistry Research*, 31, pp. 1971-1981.

Altiookka, M. R. and Citak, A., 2003, Kinetics study of esterification of acetic acid with *iso*-butanol in the presence of amberlite catalyst. *Applied catalysis A: General*, 239, pp. 141-148.

Armor, I. N., 1991, New catalytic technology in the USA during the 1980s. *Applied Catalysis*, 78, pp. 141-173.

Backhaus, A. A., 1921, Continuous process for the manufacture of esters. United States Patent 1,400,849.

Backhaus, A. A., 1922, Apparatus for producing high grade esters. United States Patent 1,425,624.

Backhaus, A. A., 1923, Process of producing high grade esters. United States Patent 1,454,462.

Bao, J., Gao, B. L. , Wu, X. Q., Yoshimoto, M. and Nakao, K., 2002, Simulation of industrial catalytic-distillation process for production of methyl *tert*-butyl ether by developing user's model on Aspen plus platform. *Chemical Engineering Journal*, 90, pp. 253-266.

Banno, K., Sakura, K. and Kamioka, T., 2002, Sulfonated cation exchange resin fibers as catalysts and preparation of bisphenol A using the catalysts. Japan Patent No. 2,363,116.

Barbosa, D. and Doherty, M. F., 1988, The simple distillation of homogenous reactive mixtures. *Chemical Engineering Science*, 43, pp. 541-550.

Baur, R., Higler, A. P., Taylor, R. and Krishna, R., 2000, Comparison of equilibrium stage and non-equilibrium stage models for Reactive Distillation. *Chemical Engineering Journal*, 76, pp. 33-47.

Baur, R. and Krishna, R., 2004, Distillation column with reactive pumps around: an alternative to reactive distillation *Chemical Engineering and Processing*, 43, pp. 435-445.

Baur, R. and Krishna, R., 2002, Hardware selection and design aspects for reactive distillation columns. A case study on synthesis of TAME. *Chemical Engineering and Processing*, 41, pp. 445-462.

- Baur, R., Taylor, R. and Krishna, R., 2003, Bifurcation analysis for TAME synthesis in a reactive distillation column: Comparison of pseudo-homogeneous and heterogeneous reaction kinetic models. *Chemical Engineering and Processing*, 42, pp. 211-221.
- Baur, R., Taylor, R. and Krishna, R., 2001, Dynamic behaviour of reactive distillation columns described by a non-equilibrium stage model. *Chemical Engineering Science*, 56, pp. 2085-2102.
- Beckmann, A., Nierlich, F., Pöphen, T., Reusch, D., von Scala, C. and Tuchslenki, A., 2002, Industrial experience in the scale-up of reactive distillation with examples from C<sub>4</sub>-chemistry. *Chemical Engineering Science*, 57, pp. 1525-1530.
- Berg, L. and Yeh, A., 1986, The breaking of ternary acetate-alcohol-water azeotropes by extractive distillation. *Chemical Engineering Communications*, 48, pp. 93-101.
- Bianchi, C. L., Ragaini, V., Pirola, C. and Carvoli, G., 2003, A new method to clean industrial water from acetic acid via esterification. *Applied Catalysis B: Environmental*, 40, pp. 93-99.
- Bisowarno, B. H. and Tade, M. O., 2002, The comparison of disturbance properties of the point control schemes for ETBE reactive distillation. *Chemical Engineering Communications*, 189, pp. 85-100.
- Bisowarno, B. H., Tian, Y. C. and Tade, M. O., 2004, Application of side reactors on ETBE reactive distillation. *Chemical Engineering Journal*, 99, pp. 35-43.
- Bock, H., Wozny, G. and Gutsche, B., 1997, Design and control of a reaction distillation column including the recovery system. *Chemical Engineering and Processing*, 36, pp. 101-109.

## Chapter 8. References

- Bond, G. C., 1987, *Heterogeneous Catalysis: Principles and Applications*, 2<sup>nd</sup> Edition, Claredon Press, Oxford.
- Buchholz, M., Pinaire, R. and Ulowetz, M. A., 1995, Structure and method for catalytically reacting fluid streams in mass transfer apparatus. European Patent 448884B1.
- Carey, F., 1996, *Organic Chemistry* 3<sup>rd</sup> Edition, McGraw-Hill Book Company Inc., New York.
- Carberry, J. J., 1976, *Chemical and Catalytic Reaction Engineering*, 2<sup>nd</sup> Edition, McGraw-Hill Book Company Inc., New York, pp. 382-385.
- Cardona, C. A., Marulanda, V. F. and Young, D., 2004, Analysis of the environmental impact of butyl acetate process through the WAR algorithm. *Chemical Engineering Science*, 59, pp. 5839-5845.
- Chakrabati, A. and Sharma, M. M., 1993, Cationic ion exchange resins as catalyst. *Reactive Polymers*, 20, pp. 1-45.
- Chen, F., Huss, R. S., Doherty, M. F. and Malone, M. F., 2002, Multiple steady states in reactive distillation: Kinetic effects. *Computers and Chemical Engineering*, 26, pp. 81-93.
- Chiang, S. F., Kuo, C. L., Yu, C. C. and Wong, D. S. H., 2002, Design alternatives for the amyl acetate process: coupled reactor/column and reactive distillation. *Industrial and Engineering Chemistry Research*, 41, pp. 3233-3246.
- Choi, J. I. and Hong, W. H., 1999, Recovery of lactic acid by batch distillation with chemical reactions using ion exchange resins. *Journal of Chemical Engineering of Japan*, 32, pp. 184-189.

- Choi, J. I., Hong, W. H. and Chang, H. N., 1996, Reaction kinetics of lactic acid with methanol catalysed by acid resins. *International Journal of Chemical Kinetics*, 28, pp. 37-41
- Chopade, S. P., 1999, Ion-exchange resin-catalysed ketalization of acetone with 1,4- and 1,2-diols: use of molecular sieve in reactive distillation. *Reactive and Functional Polymers*, 42, pp. 201-212.
- Chopade, S. P. and Sharma, M. M., 1997a, Acetalization of ethylene glycol with formaldehyde using cation-exchange resins as catalysts: batch versus reactive distillation. *Reactive and Functional Polymers*, 34, pp. 37-45.
- Chopade, S. P. and Sharma, M. M., 1997b, Reaction of ethanol and formaldehyde: use of versatile cation-exchange resins as catalyst in batch reactors and reactive distillation columns *Reactive and Functional Polymers*, 32, pp. 53-65.
- Ciric, A. R. and Gu, D., 1994, Synthesis of non-reactive equilibrium reactive distillation processes via mixed integer non-linear programming. *AIChEJ.*, 40, pp.1479-1487.
- Ciric, A. R. and Miao, P., 1994, Steady state multiplicities in an ethylene glycol reactive distillation column. *Industrial and Engineering Chemistry Research*, 33, pp. 2738-2748.
- Cloete, F. L. D. and Marais, A. P., 1995, Recovery of very dilute acetic acid using ion exchange. *Industrial and Engineering Chemistry Research*, 34, pp. 2464-2467.
- Cohen, J. D., Fergusson, S. B., Marchildon, E. K., Marks, D. N. and Mutel, A. T., 2002, Process for the production of nylon 6. United States Patent 6,437,209.

Corte, H., Meier, E. and Seifert, H., 1957, Cation exchange resins prepared by non-branching polymerisation of cross-linked polymers. German Patent 1,113,570.

Cunill, F., Iborra, M., Fité, C., Tejero, J. and Izquierdo, J. F., 2000, Conversion, selectivity, and kinetics of the addition of isopropanol to isobutene catalyzed by a macroporous ion-exchange resin. *Industrial and Engineering Chemistry Research*, 39, pp.1235-1241.

Cunill, F., Tejero, J., Fité, C., Iborra, M., and Izquierdo, J. F., 2005, Conversion, selectivity, and kinetics of the dehydration of 1-pentanol to di-*n*-pentyl ether catalyzed by a microporous ion-exchange resin, *Industrial and Engineering Chemistry Research*, 44, pp. 318-324.

Cutlip, M. B. and Shacham, M., 1999, *Problem Solving in Chemical Engineering with Numerical Methods*. Prentice Hall.

Dassy, S., Wiame, H. and Thyron, F. C., 1994, Kinetics of the liquid phase synthesis and hydrolysis of butyl lactate catalysed by cation exchange resin, *Journal of Chemical Technology and Biotechnology*, 59, pp. 149-156.

DeGarmo, J. L., Parulekar, V. N. and Pinjala, V., 1992, Consider reactive distillation. *Chemical Engineering Progress*, 88, pp.43-50.

Dhale, A. D., Myrant, L. K., Chopade, S. P., Jackson, J. E. and Miller, D. J., 2004, Propylene glycol and ethylene glycol recovery from aqueous solutions via reactive distillation. *Chemical Engineering Science*, 59, pp. 2881-2890.

DiGuilio, R. M. and McKinney, M. W., 2000, Selective production of diethanolamine. United States Patent 6,075,168.

Dimian, A. C., Omota, F. and Blik, A., 2004, Entrainer-enhanced reactive distillation. *Chemical Engineering and Processing*, 43, pp. 411-420.

## Chapter 8. References

- Dirk-Faitakis, C. B. and Chuang, K. T., 2004, Simulation studies of catalytic distillation for removal of water from ethanol using a rate-based kinetic model. *Industrial and Engineering Chemistry Research*, 43, pp. 762-768.
- Doherty, M. F. and Buzad, G., 1992, Reactive distillation by design. *Trans IChemE*, 70, pp. 448-458.
- Doherty, M. F. and Perkins, J. D., 1978, On the dynamics of distillation process-I; The simple distillation of multicomponent non-reacting, homogenous liquid mixtures. *Chemical Engineering Science*, 33, pp. 281-301.
- Espinosa, J., Aguirre, P., Frey, T. and Stichlmair, J., 1999, Analysis of finishing reactive distillation columns. *Industrial and Engineering Chemistry Research*, 38, pp. 187-196.
- Fang, F. T., 1964, in: Proceedings of the Third International Congress on Catalysis, Amsterdam, The Netherlands, 2, pp. 90.
- Fang, Y. J. and Xiao, W. D., 2004, Experimental and modelling studies on a homogeneous reactive distillation system for dimethyl carbonate synthesis by transesterification. *Separation and Purification Technology*, 34, pp. 255-263.
- Feathers, R. E. and Mansell, J. D., 1992, Chlorinated benzenes. United States Patent 5,149,892.
- Fernholz, G., Engell, S., Kreul, L. U. and Gorak, A., 2000, Optimal operation of a semi-batch reactive distillation column. *Computers and Chemical Engineering*, 24, pp. 1569-1575.
- Fien, G. A. F. and Liu, Y. A., 1994, Heuristic synthesis and shortcut design of separation processes using residue curve maps: a review. *Industrial and Engineering Chemistry Research*, 33, pp. 2505-2522.
- Fogler, H. S., 1999, *Elements of Chemical Reaction Engineering*, 3<sup>rd</sup> Edition, Prentice Hall, Inc.

Frank, S., Zhiwen, Q. and Sundmacher, K., 2002, Synthesis of cyclohexanol by three phase reactive distillation: influence of kinetics on phase equilibria. *Chemical Engineering Science*, 57, pp. 1511-1520.

Fredenslund, A., Jones, R. L. and Prausnitz, J. M., 1975, Group-contribution estimation of activity coefficients in nonideal liquid mixtures. *AIChE Journal*, 21, pp. 1086-1099.

Furumoto, M. and Jimi, K., 1993, Method for modification of cation exchange resin catalysts in the preparation of bisphenols. Japan Patent No. 5,294, 876.

Gangadwaga, J., Mankar, S. and Mahajani, S., 2003, Esterification of acetic acid with butanol in the presence of ion-exchange resins as catalysts. *Industrial and Engineering Chemistry Research*, 42, pp. 2146-2155.

Gangadwala, J., Kienle, A. Stein, E. and Mahajani, S., 2004, Production of butyl acetate by catalytic distillation: process design studies. *Industrial and Engineering Chemistry Research*, 43, pp. 136-143.

Gelbard, G., 2005, Organic synthesis by catalysis with ion exchange resins. *Industrial and Engineering Chemistry Research*. In Press.

Gelbein, A. P., 2002, Three stage propylene oxide process. United States Patent 6,337,412.

Gildert, G. R., 2001, Hydrogenation of benzene to cyclohexane. United States Patent 6,187,980.

Gildert, G. R., Hearn, D. and Putman, H. M., 1998, Hydrogenation of unsaturated cyclic compounds. United States Patent 5,773,670.

Gildert, G. R. and Loescher, M. E., 2001, Catalytic distillation process for the production of C<sub>8</sub> alkanes. United States Patent 6,274,783.

## Chapter 8. References

Glasser, D., Hildebrandt, D. and Hausberger, B., 2000, 'Costing' distillation systems from residue curve based designs. *Computers and Chemical Engineering*, 24, pp. 1275-1280.

Gmehling, J., Rasmussen, P. and Fredenslund, P., 1982, Vapour-liquid equilibria by UNIFAC group contribution method. Revision and Extension 2. *Industrial and Engineering Chemistry Process Design and Development*, 21, pp.118-127.

González, J. C. and Fair, J. R., 1997, Preparation of tertiary amyl alcohol in a reactive distillation column. Reaction kinetics, chemical equilibrium and mass transfer issues. *Industrial and Engineering Chemistry Research*, 36, pp. 3833-3844.

Götze, L., Bailer, O., Moritz, P. and von Scala, C., 2001, Reactive distillation with KATAPAK®. *Catalysis Today*, 69, pp. 201-208.

Grob, R. L., 1995, *Modern Practice of Gas Chromatography*, 3<sup>rd</sup> Edition. Wiley and Sons, New York.

Groten, W. A. and Loescher, M. E., 2002, Process for the production of an ultra low sulphur. United States Patent 6,416,659.

Groten, W. A., Booker, D. and Crossland, C. S., 1998, Catalytic distillation structures. United States Patent 5,730,843.

Hanika, J., Kolena, J. and Smejkal, Q., 1999, Butyl acetate via reactive distillation: modeling and experiments. *Chemical Engineering Science*, 54, pp. 5205-5209.

Hanika, J., Smejkal, Q. and Kolena, J., 2001, 2-methylpropylacetate synthesis via catalytic distillation, *Catalysis Today*, 66, pp. 219-223.

Harmer, M. A. and Sun Q., 2001, Solid acid catalysis using ion-exchange resins. *Applied Catalysis A*, 221, pp. 45-62.

## Chapter 8. References

- Hauan, S., Hertzberg, T. and Lien, K. M., 1997, Multiplicity in reactive distillation of MTBE. *Computers and Chemical Engineering*, 21, pp. 1117-1124.
- Hayashi, K., 2002, Method for manufacture of bisphenols with high catalyst activity. Japan Patent No. 69,023.
- Hearn, D., 1993, Catalytic distillation machine. United States Patent 5,266,546.
- Helfferrich, F., 1962, *Ion Exchange*, McGraw-Hill Book Company Inc., pp. 511-512.
- Higler A. P., Taylor R. and Krishna R., 1999, Nonequilibrium modelling of reactive distillation: Multiple steady states in MTBE synthesis *Chemical Engineering Science*, 54, pp. 1389-1395.
- Hiwale, R. S., Bhate, N. V., Mahajan, Y. S. and Mahajani, S. M., 2004, Industrial applications of reactive distillation. *International Journal of Chemical Reactor Engineering*, 2, R1, pp. 1-54.
- Ho, W. S. W., 2002, Combined supported liquid membrane/strip dispersion process for the removal and recovery of penicillin and organic acids. United States Patent 6,433,163.
- Horsley, L. H., 1952, *Azeotropic Data*, American Chemical Society, Washington, D. C.
- Huang, C., Ng, F. T. T. and Rempel G. L., 2000, Application of catalytic distillation for the aldol condensation of acetone: the effect of mass transfer and kinetic rates on the yield and selectivity. *Chemical Engineering Science*, 55, pp. 5919-5931.

Huang, Y. S., Sundmacher, K., Qi, Z. W. and Schlönder, E. U., 2004, Residue curve maps of reactive membrane separation. *Chemical Engineering Science*, 59, pp.2863-2879.

Ingale, M. N. and Mahajani, V. V., 1994, Recovery of acetic acid and propionic acid from aqueous waste streams. *Separations Technology*, 4, pp. 123-126.

Isla, M. A. and Irazoqui, H. A., 1996, Modeling, analysis, and simulation of a methyl *tert*-butyl ether reactive distillation column. *Industrial and Engineering Chemistry Research*, 35, pp. 2696-2708.

Ito, M. and Ishikawa, H., 2004, Strong acidic cation exchange resin for catalyst reaction. Japan Patent No. 250,619.

Iwahara, M., 2001, Process for producing bisphenol-A. WO Patent No. JP9405.

Jiménez L., Garvín, A. and Costa-López J., 2002, The production of butyl acetate and methanol via reactive and extractive distillation. I. Chemical equilibrium, kinetics, and mass transfer issues. *Industrial and Engineering Chemistry Research*, 41, pp. 6663-6669.

Johnson, K. H., 1993, Catalytic distillation structure. United States Patent 5,348,710.

Johnson, K. H. and Dallas, A. B., 1994, Catalytic distillation structure. United States Patent 5,348,710.

Kenig, E. Y., Bader, H., Górak, A., Beßling, B., Adrian, T. and Schoenmakers, H., 2001, Investigation of ethyl acetate reactive distillation process. *Chemical Engineering Science*, 56, pp. 6185-6193.

Keyes, D. B., 1932, Esterification processes and equipment. *Industrial and Engineering Chemistry*, 24, pp. 1096-1103.

Kim, S. D. and Lee, K. H., 1993, Control of regioselectivity by cation-exchanged sulfonic acid resin catalysts. *Journal of Molecular Catalysis*, 78, pp. 237-248.

Kirk, R. E. and Othmer, D. F., 1980. *Encyclopedia of Industrial Chemistry*, 3<sup>rd</sup> Edition, 3, Wiley and Sons, New York, pp. 365-368.

Kissinger, G. M., 1989, Process for preparation and purification of bisphenols. United States Patent No. 4,876,391.

Kissinger, G. M., Shafer, S. J., Acharya, H. R., Peemans, R. F. A. J. and Schlarmann, E. H., 2002, Combination ion exchange resin bed for the synthesis of bisphenol A. United States Patent No. 6,486,222.

Klöker, M., Keing, E. Y., Górak, A., Markusse, A. P., Kwant, G. and Moritz, P., 2004, Investigation of different column configurations for the ethyl acetate synthesis via reactive distillation. *Chemical Engineering and Processing*, 43, pp. 791-801.

Knifton, J. F., Anantaneni, P. R., Eugene Dai, P. E. and Stockton, M. E., 2003, Reactive distillation for sustainable high 2-phenyl LAB production. *Catalysis Today*, 79-80, pp. 77-82.

Knifton, J. F., Sanderson, J., Ronald, S. and Melvin, E., 1998, Use of reactive distillation in the dehydration of tertiary butyl alcohol. United States Patent 5,811,620.

Kolodziej, A., Jaroszyński, M., Hoffmann, A. and Górak, A., 2001, Determination of catalytic packing characteristics for reactive distillation. *Catalysis Today*, 69, pp. 75-85.

## Chapter 8. References

- Kolah, A. K., Qi, Z. W. and Mahajani, S. M., 2001, Dimerized isobutene: An alternative to MTBE. *Chemical Innovation*, pp. 15-21.
- Kolah A. K. and Sharma, M. M., 1995, Removal of formaldehyde from aqueous solutions. *Separations Technology*, 5, pp. 13-22.
- Krishna, R., 2002, Reactive separations: more ways to skin a cat. *Chemical Engineering Science*, 57, pp. 1491-1504.
- Kulprathipanja, S., 2001, *Reactive Separation Processes*, New York: Taylor and Francis.
- Kuo, Y., Munson, C.L., Frierman, M. and King C.J., 1987, Use of adsorbents for recovery of acetic acid from aqueous solutions. *Reactive Polymers, Ion Exchangers, Sorbents*, 6, pp. 52.
- Kürüm, S. and Fonyo, Z., 1996, Comparative study of recovering acetic acid with energy integrated schemes. *Applied Thermal Engineering*, 16, pp. 487-495.
- Kyle, B. G., 1999, *Chemical and Process Thermodynamics*, Prentice Hall, Inc.
- Lee, J. W., 2002, Feasibility studies on quaternary reactive distillation systems. *Industrial and Engineering Chemistry Research*, 41, pp. 4632-4642.
- Lee, L. S., Chen, W. C. and Huang, J. F., 1996, Experiments and correlations of phase equilibria of ethanol-ethyl acetate-water ternary mixture. *Journal of Chemical Engineering of Japan*, 29, pp. 427-438.
- Lee, M. J., Chiu, J. Y. and Lin, H. M., 2002, Kinetics of catalytic esterification of propionic acid and *n*-butanol over Amberlyst 35. *Industrial and Engineering Chemistry Research*, 41, pp. 2882-2887.

- Lee, L. S. and Kuo, M. Z., 1996, Phase and reaction equilibria of the acetic acid-isopropanol-isopropyl acetate-water system at 760 mmHg. *Fluid Phase Equilibria*, 123, pp. 147-165.
- Lee, J. W. and Westerberg, A. W., 2001, Graphical design applied to MTBE and methyl acetate reactive distillation processes. *AIChE Journal*, 47, pp. 1333-1345.
- Lee, M. J., Wu, H. T., Kang, C. H. and Lin, H. M., 2001, Kinetics of catalytic esterification of acetic acid with amyl alcohol over Amberlyst 15. *Journal of Chemical Engineering of Japan*, 34, pp. 960-963.
- Lee, M. J., Wu, H. T. and Lin, H. M., 2000, Kinetics of catalytic esterification of acetic acid and amyl alcohol over Dowex. *Industrial and Engineering Chemistry Research*, 39, pp. 4094-4099.
- Leemann, M., Hildrebrandt, V., Thiele, H. and Espig, S., 2002, Production of polyamides by reactive distillation. United States Patent 6,358,373.
- Levenspiel, O., 1999, *Chemical Reaction Engineering*, 3<sup>rd</sup> Edition, John Wiley and Sons, New York.
- Levin, D. and Santiesteban, J. G., 2002, Production of phenol using reactive distillation. United States Patent 6,410,804.
- Leyes, C. E. and Othmer, D. F., 1945, Esterification of butanol and acetic acid. *Industrial and Engineering Chemistry*, 37, pp. 968-977.
- Li, Y. H., Yu, S. B. and Yuan, X. G., 2002, The etherification of methanol and isobutene in a catalytic distillation column packed with zeolite-beta-coated catalytic packings. *Industrial and Engineering Chemistry Research*, 41, pp. 4936-4940.

Lilja, J., Aumo, J., Salmi, T., Murzin, D. Y., Mäki-Arvela, P., Sundell, M., Ekman, K., Peltonen, R. and Vainio, H., 2002, Kinetics of esterification of propanoic acid with methanol over a fibrous polymer-supported sulphonic acid catalyst. *Applied Catalysis A: General*, 228, pp. 253-267.

Lilja, J., Murzin, D. Y., Salmi, T., Aumo, J., Mäki-Arvela, P. and Sundell, M., 2002, Esterification of different acids over heterogeneous and homogeneous catalysts and correlation with the Taft equation. *Journal of Molecular Analysis A: Chemical*, 182-183, pp. 555-563.

Lim, S. Y., Park, B., Hung, F., Sahimi, M. and Tsotsis, T. T., 2002, Design issues of pervaporation membrane reactors for esterification. *Chemical Engineering Science*, 57, pp. 4933-4946.

Liu, H., Qu, Y. and Wang, W., 2002, Simulation of hydration process of water and ethylene oxide by reactive distillation to produce glycol. *Beijing Huagong Daxue Xuebao*.

Liu, W. T. and Tan C. S., 2001, Liquid phase esterification of propionic acid with *n*-butanol. *Industrial and Engineering Chemistry Research*, 40, pp. 3281-3286.

Liu, K., Tong, Z. F., Liu, L. and Feng, X. S., 2005, Separation of organic compounds from water by pervaporation in the production of *n*-butyl acetate via esterification by reactive distillation. *Journal of Membrane Science*, 256, pp.193-201.

Lorette, N. B., Howard, W. L. and Brown, J. H., 1959, Preparation of ketone acetals from linear ketones and alcohols. *Journal of Organic Chemistry*, 24, pp. 1731.

Lundquist, E. G., 2002, Sulfonated polystyrene-divinylbenzene copolymer-based catalyst for manufacture of bisphenol-A. European Patent No. 1,222,960.

## Chapter 8. References

- Lundquist, E. G. and Bigwood, M. P., 1995, Producing bisphenols of low colour. European Patent No. 671,376.
- Luo, H. P. and Xiao, W. D., 2001, A reactive distillation process for a cascade and azeotropic reaction system: Carbonylation of ethanol with dimethyl carbonate. *Chemical Engineering Science*, 56, pp. 403-410.
- Luyben, W. L., 2000, Economic and dynamic impact of the use of excess reactant in reactive distillation systems. *Industrial and Engineering Chemistry Research*, 39, pp. 2935-2946.
- Luyben, W. L., Pszalgowski, K. M., Schaefer, M. R. and Siddone, C., 2004, Design and control of conventional and reactive distillation processes for the production of butyl acetate. *Industrial and Engineering Chemistry Research*, 43, pp. 8014-8025.
- Mahajani, S. M. , 2000, Reactions of glyoxylic acid with aliphatic alcohols using cationic exchange resins as catalysts, *Reactive and Functional Polymers*, 43, pp. 253-268.
- Mahajani, S. M., 1999, Design of reactive distillation columns for multicomponent kinetically controlled reactive systems. *Chemical Engineering Science*, 54, pp. 1425-1430.
- Mahajani, S. M., 1999, Kinetic azeotropy and design of reactive distillation columns. *Industrial and Engineering Chemistry Research*, 38, pp. 177-186.
- Mahajani, S. M. and Kolah, A. K., 1996, Some design aspects of reactive distillation columns. *Industrial and Engineering Chemistry Research*, 35, pp. 4587-4596.
- Malone M. F. , Doherty M. F., 2000, Reactive distillation. *Industrial and Engineering Chemistry Research*, 39, pp. 3953-3957.

## Chapter 8. References

- Mazzotti, M., Neri, B., Gelosa, D., Kruglov, A. and Morbidelli, M., 1997, Kinetics of liquid phase esterification catalysed by acidic resins. *Industrial and Engineering Chemistry Research*, 36, pp. 3-10.
- McKetta, J. J., 1976, *Encyclopaedia of Chemical Processing and Design*, 1, Marcel Dekker Inc., New York.
- Mehrabani, A., Akbarnejad, M. M. and Hosseini, H., 2002, Structural catalytic packing for reaction-distillation columns. *Industrial and Engineering Chemistry Research*, 41, pp. 5842-5847.
- Mendiratta, A. K., 1983, Ion exchange catalysed bisphenol synthesis. United States Patent 4,400,555.
- Miller, C. and Kaibel, G., 2004, Packings for fixed bed reactors and reactive distillation. *Chemical Engineering Science*, 59, pp. 5373-5379.
- Monroy-Loperena R. and Alvarez-Ramirez J., 1999, On the steady state multiplicities for an ethylene glycol reactive distillation column. *Industrial and Engineering Chemistry Research*, 38, pp. 451-455.
- Mukherjee, U. and Louie, W., 2003, Hydrocracking of vacuum gas and other oils using post-treatment reactive distillation system. United States Patent 6,547,956.
- Neier, W., 1991, Ion exchangers as catalysts, in : Dorfner, K. (Editor), *Ion Exchangers*, Walter de Gruyter, pp. 981.
- Netzer, D., 2001, Method for producing ethyl benzene. United States Patent 6,252,126.
- Neumann, R. and Sasson, Y., 1984, Recovery of dilute acetic acid by esterification in a packed chemorectification column. *Industrial and Engineering Chemistry, Process Design and Development*, 23, pp. 654-659.

## Chapter 8. References

- Noeres, C., Dadhe, K., Gesthuisen, R., Engell, S. and Górak, A., 2004, Model-based design, control and optimisation of catalytic distillation processes. *Chemical Engineering and Processing*, 43, pp. 421-434.
- Noeres, C., Hoffmann, A. and Górak, A., 2002, Reactive distillation: non-ideal flow behaviour of the liquid phase in structured catalytic packings. *Chemical Engineering Science*, 57, pp. 1545-1549.
- Noeres, C., Keing, E. Y. and Górak, A., 2003, Modelling of reactive separation processes: reactive adsorption and reactive distillation. *Chemical Engineering and Processing*, 42, pp. 157-178.
- O'Brien, D. J. and Senske, G. E., 1989, Separation and recovery of low molecular weight organic acids by emulsion liquid membranes. *Separation Science and Technology*, 24, pp. 617-628.
- Okasinski, M. J. and Doherty, M. F., 2000, Prediction of heterogeneous reactive azeotropes in esterification systems. *Chemical Engineering Science*, 55, pp. 5263-5271.
- Okur, H. and Bayramoglu, M., 2001, The effect of the liquid phase activity model on the simulation of ethyl acetate production by reactive distillation. *Industrial and Engineering Chemistry Research*, 40, pp. 3639-3646.
- Olivier, J. P., 1998, Improving the models used for calculating the size distribution of micropore volume of activated carbons from adsorption data. *Carbon*, 36, pp. 1469-1472.
- Omota, F., Dimian, A. C. and Bliek, A., 2003a, Fatty acid esterification by reactive distillation. Part 1: equilibrium-based design. *Chemical Engineering Science*, 58, pp. 3159-3174.
- Omota, F., Dimian, A. C. and Bliek, A., 2003b, Fatty acid esterification by reactive distillation. Part 2: kinetics based design for sulphated zirconia catalysts. *Chemical Engineering Science*, 58, pp. 3175-3185.

## Chapter 8. References

Peng, J., Lextrait, S., Edgar, T. F. and Eldridge, R. B., 2002, A comparison of steady state equilibrium and rate based models for packed reactive distillation columns. *Industrial and Engineering Chemistry Research*, 41, pp.2735-2744.

Petrus, L., Stamhuis, E. J. and Joosten, G. E. H., 1981, Thermal deactivation of strong-acid ion-exchange resins in water. *Industrial and Engineering Chemistry Product Research and Development*, 20, pp. 366-371.

Pham H. N. and Doherty, M. F., 1990, Design and synthesis of heterogeneous azeotropic distillations-II. Residue curve maps. *Chemical Engineering Science*, 45, pp. 1837-1843.

Podrebarac, G. G., Ng F. T. T. and Rempel, G. L., 1998, The production of diacetone alcohol with catalytic distillation Part I: Catalytic distillation experiments. *Chemical Engineering Science*, 53, pp. 1067-1075.

Pöpken, T., Gotze, L. and Gmehling, J., 2000, Reaction kinetics and chemical equilibrium of homogenously and heterogeneously catalysed acetic acid esterification with methanol and methyl acetate hydrolysis. *Industrial and Engineering Chemistry Research*, 39, pp. 2601-2611.

Pöpken, T., Steinigeweg, S. and Gmehling, J., 2001, Synthesis and hydrolysis of methyl acetate by reactive distillation using structured catalytic packings: experiments and simulation, *Industrial and Engineering Chemistry Research*, 40, pp. 1566-1574.

Qi, Z. W. and Zhang, R., 2004, Alkylation of benzene with ethylene in a packed reactive distillation column. *Industrial and Engineering Chemistry Research*, 43, pp. 4105-4111.

Qi, Z. W., Sundmacher, K., Stein, E., Kienle, A. and Kolah, A., 2002, Reactive separation of isobutene from C<sub>4</sub> crack fractions by catalytic distillation processes. *Separation and Purification Technology*, 26, pp. 147-163.

## Chapter 8. References

- Reid, R. C., Prausnitz, J. M. and Poling, B. E., 1987, *The properties of gases and liquids*, 4<sup>th</sup> Edition, McGraw Hill, New York.
- Reisinger, H. and King, C. J., 1995, Extraction and sorption of acetic acid at pH above  $pK_a$  to form calcium magnesium acetate. *Industrial and Engineering Chemistry Research*, 34, pp. 845-852.
- Ricker, N. L., Pittman, E. F. and King, C. J., 1980, Solvent extraction with amines for recovery of acetic acid from dilute aqueous industrial streams. *Journal of Separation Process and Technology*, 1, pp. 23-30.
- Rihko, L. K. and Krause, A. O. I., 1995, Kinetics of heterogeneously catalysed *tert*-amyl methyl ether reactions in the liquid phase. *Industrial and Engineering Chemistry Research*, 34, pp. 1172-1180.
- Rihko, L. K., Kiviranta-Pääkkönen, P. K. and Krause, A. O. I., 1997, Kinetic model for the etherification of isoamylenes with methanol. *Industrial and Engineering Chemistry Research*, 36, pp. 614-621.
- Rihko-Struckmann, L. K., Karinen, R. S., Krause, A. O. I., Jakobsson, K. and Aittamaa, J. R., 2004, Process configurations for the production of the 2-methoxy-2,4,4-trimethylpentane – a novel gasoline oxygenate, *Chemical Engineering and Processing*, 43, pp. 57-65.
- Rönneback, R., Salmi, T., Vuori, A., Haario, H., Lehtonen, J. Sundqvist, A. and Tirronen, E., 1997, Development of a kinetic model for the esterification of acetic acid with methanol in the presence of a homogenous acid catalyst. *Chemical Engineering Science*, 52, pp. 3369-3381.
- Rowlinson, J. S., 1969, *Liquids and Liquids Mixtures*, 2<sup>nd</sup> Edition, Butterworth, London.
- Saari K., Tirronen, E., Vuori, A. and Lahtinen M., 2002, Method for preparing formic acid. United States Patent 6,429,333.

## Chapter 8. References

- Saayman, N., Kinderman, S. and Lund, G. J., 2003, Process for production of MIBK using catalytic distillation technology. United States Patent 6,518,462.
- Saha, B. and Sharma M. M., 1996, Esterification of formic acid, acrylic acid and methacrylic acid with cyclohexene in batch and distillation column reactors: ion exchange resins as catalysts. *Reactive and Functional Polymers*, 28, pp. 263-278.
- Saha, B. and Sharma M. M., 1997, Reaction of dicyclopentadiene with formic acid and chloroacetic acid with and without cation exchange resins as catalysts. *Reactive and Functional Polymers*, 34, pp. 161-173.
- Saha, B., Chopade, S. P. and Mahajani, S. M., 2000, Recovery of dilute acetic acid through esterification in a reactive distillation column. *Catalysis Today*, 60, pp. 147-157.
- Saha, B., Iglesias, M., Cumming, I.W. and Streat, M., 2000, Sorption of trace heavy metals by thiol containing chelating resins. *Solvent Extraction and Ion Exchange*, 18(1), pp 133-167.
- Saha, B., Teo, H. T. R. and Alqahtani, A., 2005a, *iso*-Amyl acetate synthesis by catalytic distillation. *International Journal of Chemical Reactor Engineering*, 3, Article A11.
- Saha, B., Alqahtani, A. and Teo, H. T. R., 2005b, Production of *iso*-amyl acetate: Heterogeneous kinetics and techno-feasibility evaluation for catalytic distillation. *International Journal of Chemical Reactor Engineering*, 3, Article A30.
- Sanz, M. T., Murga, R., Beltran, S., Cabezas, J. L. and Coca, J., 2002, Autocatalyzed and ion exchange resin catalyzed esterification kinetics of lactic acid with methanol. *Industrial and Engineering Chemistry Research*, 41, pp. 512-517.

Saruwatari, T., 2001, Process for producing bisphenol-A. WO Patent No. JP11037.

Schmitt, M., Hasse, H., Althaus, K., Schoenmakers, H., Götze, L. and Moritz, P., 2004, Synthesis of *n*-hexyl acetate by reactive distillation. *Chemical Engineering and Processing*, 43, pp. 397-409.

Schmitt, M., von Scala, C., Moritz, P. and Hasse, H., 2005, *n*-Hexyl acetate pilot plant reactive distillation with modified internals. *Chemical Engineering and Processing*, 44, pp. 677-685.

Schoenmakers, H. G. and Bessling, B., 2003, Reactive and catalytic distillation from an industrial perspective. *Chemical Engineering and Processing*, 42, pp. 145-155.

Schopmeyer, H. H. and Arnold, C. R., 1944, Lactic acid purification. United States Patent 2,350,370.

Schreinemakers, F. A. H., 1901, Dampfdrucke ternärer Gemische, *Zeitschrift fuer Physikalische Chemie*, 36, pp. 257-289 and pp. 413-449.

Seader, J. D. and Henley, E. J., 1998, *Separation Process Principles*. John Wiley and Sons, Inc.

Sennewald, K., Gehrmann, K. and Schafer, S., 1971, Column for carrying out organic chemical reactions in contact with fine particulate catalysts. United States Patent 3,579,309.

Sharma, M. M., 1995, Some novel aspects of cationic ion exchange resins as catalysts. *Reactive and Functional Polymers*, 26, pp. 3-23.

Sharma, M. M. and Mahajani, S. M., 2003, Industrial applications of reactive distillation, in *Reactive Distillation* by Sundmacher K. and Kienle A., Wiley VCH, Germany, pp. 1-29.

Shi, Y. H., Fan, M. H., Li, N., Brown, R. C. and Sung, S. W., 2005, The recovery of acetic acid with sulphur dioxide. *Biochemical Engineering Journal*, 22, pp. 207-210.

Shinohara, C., Kawakami, S., Moriga, T., Hayashi, H., Hodoshima, S., Saito, Y. and Sugiyama, S., 2004, Local structure around platinum in Pt/C catalysts employed for liquid-phase dehydrogenation of decalin in the liquid-film state under reactive distillation conditions. *Applied Catalysis A: General*, 266, pp. 251-255.

Shinya, H., Arai, H., Takaiwa, S. and Saito, Y., 2003, Catalytic decalin dehydrogenation/naphthalene hydrogenation pair as a hydrogen source for fuel-cell vehicle. *International Journal of Hydrogen Energy*, 28, pp.1255-1262.

Shoemaker J. D. and Jones, Jr. E. M., 1987, Cumene by catalytic distillation. *Hydrocarbon Processing*, 66 (6), pp.57-58.

Siirola, J. J., 1995, An industrial perspective on process synthesis. *AIChE Journal*, 91, pp. 222-233.

Simons, R. M., 1983, Esterification. *Encyclopedia of Chemical Processing and Design*, Marcel Dekker, New York.

Singh, A., Hiwale, R., Mahajani, S. M., Gudi, R. D., Gangadwala, J. and Kienle, A., 2005, Production of butyl acetate by catalytic distillation. Theoretical and experimental studies. *Industrial and Engineering Chemistry Research*, 44, pp. 3042-3052.

Skjold-Jørgensen, S., Kolbe, B., Ghemling J. and Rasmussen, P., 1979, Vapour-liquid equilibria by UNIFAC group contribution. Revision and extension. *Industrial and Engineering Chemistry Process Design and Development*, 18, pp. 714-722.

Smejkal, Q, Hanika, J. and Kolena, J., 2001, 2-methylpropylacetate synthesis in a system of equilibrium reactor and reactive distillation column. *Chemical Engineering Science*, 56, pp. 365-370.

Smejkal, Q. and Šo6š, M., 2002, Comparison of computer simulation of reactive distillation using ASPEN PLUS and HYSYS software. *Chemical Engineering and Processing*, 41, pp. 413-418.

Smith, J. M., Van Ness, H. C. and Abbot, M. M., 1996, *Introduction to Chemical Engineering Thermodynamics*, 5<sup>th</sup> Edition. McGraw Hill Book Company. Singapore.

Smith, Jr., L. A., 1980, Catalyst system for separating isobutene from C<sub>4</sub> streams. United States Patent 4,215,011.

Smith, Jr., L. A., 1981, Catalytic distillation process. United States Patent 4,307,254.

Smith, Jr., L. A., 1985, Catalytic distillation process and catalyst. European Patent 008860B1.

Smith, Jr., L. A., 1984, Catalytic distillation structure. United States Patent 4,443,559.

Smith, Jr., L. A., 1990, Method for the preparation of methyl tertiary butyl ether. United States Patent 4,978,807.

Smith, Jr., L. A., 1993, Method for operating a catalytic distillation process. United States Patent 5,221,441.

Sneesby, M. G. and Tade, M. O., 2000, A multi-objective scheme for an ETBE reactive distillation column. *Chemical Engineering Research and Design*, 78, pp. 283-292.

- Solokhin, A. V. and Blagov, S. A., 1996, Reactive distillation is an advanced technique of reaction process operation. *Chemical Engineering Science*, 51, pp. 2559-2564.
- Solomons, T. W. G. and Fryhle, C. B., 2000, *Organic Chemistry*, 7<sup>th</sup> Edition, Wiley, New York, pp. 829.
- Song, W., Huss, R. S., Doherty, M. F. and Malone, M. F., 1997, Discovery of a reactive azeotrope. *Nature*, 388, pp. 561-563.
- Song, W., Venimadhavan, G., Manning, J. M., Malone, M. F. and Doherty, M. F., 1998, Measurement of residue curve maps and heterogeneous kinetics in methyl acetate synthesis. *Industrial and Engineering Chemistry Research*, 37, pp. 1917-1928.
- Stankiewicz, A., 2003, Reactive separations for process intensification: an industrial perspective. *Chemical Engineering and Processing*, 42, pp. 137-144.
- Steinigeweg, S. and Gmehling, J., 2003, Esterification of a fatty acid by reactive distillation. *Industrial and Engineering Chemistry Research*, 42, pp. 3612-3619.
- Steinigeweg, S. and Gmehling, J., 2002, *n*-butyl acetate synthesis via reactive distillation: thermodynamic aspects, reaction kinetics, pilot plant experiments and simulation studies. *Industrial and Engineering Chemistry Research*, 41, pp. 5483-5490.
- Steinigeweg, S. and Gmehling, J., 2004, Transesterification processes by combination of distillation with pervaporation. *Chemical Engineering and Processing*, 43, pp. 447-456.
- Steyer, F., Qi, Z. W., Sundmacher, K., 2002, Synthesis of cyclohexanol by three-phase reactive distillation: influence of kinetics on phase equilibria. *Chemical Engineering Science*, 57, pp. 1511-1520.

## Chapter 8. References

Subawalla, H. and Fair, J. R., 1999, Design guidelines for solid catalyzed reactive distillation systems. *Industrial and Engineering Chemistry Research*, 38, pp. 3696-3709.

Sugawara, T., Watanabe, M., Sumitani, N., Shirasaki, M., Suzuki, T., 1995, Modified sulfonic acid ion exchange resins for catalysts for reaction of phenols with ketones. European Patent No. 676,237.

Sundmacher, K. and Hoffman, U., 1996, Development of a new catalytic distillation process for fuel ethers via a detailed non-equilibrium model. *Chemical Engineering Science*, 51, pp 2359-2368.

Tadé, M. O. and Tian, Y. C., 2000, Conversion inference for ETBE reactive distillation. *Separation and Purification Technology*, 19, pp.85-91.

Tapp, M., Kauchali, S., Hausberger, B., McGregor, C., Hildebrandt, D. and Glasser, D., 2003, An experimental simulation of distillation column concentration profiles using a batch apparatus. *Chemical Engineering Science*, 58, pp. 479-486.

Taylor, R. and Krishna, R., 2000, Modelling reactive distillation. *Chemical Engineering Science*, 55, pp. 5183-5229.

Tejero, J., Cunill, F., Izquierdo, J. F., Iborra, M., Fité, C. and Parra, D., 1996, Scope and limitations of mechanistic inferences from kinetic studies on acidic macroporous resins: The MTBE liquid-phase synthesis case. *Applied Catalysis A: General*, 134, pp. 21-36.

Teo, H. T. R. and Saha, B., 2004, Heterogeneously catalysed esterification of acetic acid with *iso*-amyl alcohol: kinetic studies. *Journal of Catalysis*, 228, pp. 174-182.

Teralak K., Trybula, S., Majchrzak, M., Ott, M. and Hasse, H., 2005, Pilot plant formaldehyde distillation: experiments and modelling. *Chemical Engineering and Processing*, 44, pp. 671-676.

## Chapter 8. References

- Thiel, C., Sundmacher, K. and Hoffman, U., 1997, Residue curve maps for heterogeneously catalysed reactive distillation of fuel ethers MTBE and TAME. *Chemical Engineering Science*, 52, pp. 993-1005.
- Thiel, C., Sundmacher, K. and Hoffman, U., 1997, Synthesis of ETBE: Residue curve maps for the heterogeneously catalysed reactive distillation process. *Chemical Engineering Journal*, 66, pp. 181-191.
- Tian, Y., Zhao, F., Bisowarno, B. H. and Tadé, M. O., 2003, Pattern-based predictive control for ETBE reactive distillation. *Journal of Process Control*, 13, pp. 57-67.
- Tischmeyer, M. and Arlt, W., 2004, Determination of binary vapour-liquid equilibria (VLE) of three fast reacting esterification systems. *Chemical Engineering and Processing*, 43, pp. 357-367.
- Toukoniitty, B., Mikkola, J. P., Eranen, K., Salmi, T. and Yu. Murzin, D., 2005, Esterification of propionic acid under microwave irradiation over an ion-exchange resin. *Catalysis Today*, 100, pp. 431-435.
- Towler, G. P. and Frey, S. J., 2000, Reactive distillation. In Kulprathipanja, S. (Ed.), *Reactive Separation Processes*, New York: Taylor and Francis.
- Tuchlenski, A., Beckmann, A., Reusch, D., Dussel, R., Weidlich, U. and Janowsky, R., 2001, Reactive distillation – industrial applications, process design and scale-up. *Chemical Engineering Science*, 56, pp. 387-394.
- Tung, P., 2002, Dimensions in reactive distillation technology. United States Patent 6,500,309.
- Tustin, G. C., Colberg, R. D. and Zoeller, J. R., 2000, Synthesis of vinyl acetate monomer from synthesis gas. *Catalysis Today*, 58, pp. 281-291.

Ung, S. and Doherty, M. F., 1995, Calculation of residue curve maps for mixtures with multiple equilibrium chemical reactions. *Industrial and Engineering Chemistry Research*, 34, pp. 3195-3202.

Van Brunt, V., 1992, Process for recovering acetic acid from aqueous acetic acid solutions. United States Patent 5,175,357.

Vargas-Villamil, F. D., Marroquín, J. O., de la Paz, C. and Rodríguez, E., 2004, A catalytic distillation process for light gas oil hydrodesulfurisation. *Chemical Engineering and Processing*, 43, pp. 1309-1316.

Venimadhavan, G., Buzad, G., Doherty, M. F. and Malone, M. F., 1994, Effect of kinetics on residue curve maps for reactive distillation. *AIChE Journal*, 40, pp. 1814-1824.

Venimadhavan, G., Malone, M. F. and Doherty, M. F., 1999, A novel distillate policy for batch reactive distillation with application to the production of butyl acetate. *Industrial and Engineering Chemistry Research*, 38, pp. 714-722.

Vermijs, H. J. A. and Kramers, H., 1954, Liquid-liquid extraction in a "rotating disc contactor". *Chemical Engineering Science*, 3, pp. 55-64.

Viveros-García, T., Ochoa-Tapia, J. A., Lobo-Oehmichen, R., Reyes-Heredia, J. A. and Pérez-Cisneros, E. S., 2005, Conceptual design of a reactive distillation process for ultra-low sulphur diesel production. *Chemical Engineering Journal*, 106, pp. 119-131.

Vora, N. and Daoutidis, P., 2001, Dynamics and control of an ethyl acetate reactive distillation column. *Industrial and Engineering Chemistry Research*, 40, pp. 833-849.

Voss, B., 2001, Acetic acid reactive distillation based on DME/methanol carbonylation. United States Patent 6,175,039.

- Wainwright, L., 1949, Extraction Apparatus. United States Patent 2,682,452.
- Wang, S. J., Wong, D. S. H. and Lee, E. K., 2003, Effect of interaction multiplicity on control system design for a MTBE reactive distillation column. *Journal of Process Control*, 13, pp. 503-515.
- Wang, H. J., Yang, B. L., Wu, J., Zhao, G. S. and Tao, X. H., 2005, Multi-fields synergy in the process of reactive distillation coupled with membrane separation. *Chemical Engineering and Processing*, 44, pp. 1207-1215.
- Wasykiewicz, S. K., Kobylka, L. C. and Castillo, F. J. L., 2003, Synthesis and design of heterogeneous separation systems with recycle streams. *Chemical Engineering Journal*, 92, pp. 201-208.
- Webb, J. L. and Spivack, J. L., Method for producing bisphenol catalysts and bisphenols. United States Patent No. 6,534,686.
- Wise, D. L. and Augenstein, D., 1988, An evaluation of the bioconversion of woody biomass to calcium acetate deicing salt. *Solar Energy*, 41, pp. 453-463.
- Xiao, J., Liu, J. Q., Li, J. T., Jiang, X. H. and Zhang, Z. B., 2001, Increase MeOAc conversion on PVA production by replacing the fixed bed reactor with a catalytic distillation column. *Chemical Engineering Science*, 56, pp. 6553-6562.
- Xu, Z. P. and Chuang, K. T., 1997, Effect of internal diffusion on heterogeneous catalytic esterification of acetic acid. *Chemical Engineering Science*, 52, pp. 3011-3017.
- Xu, Z. P. and Chuang, K. T., 1996, Kinetics of acetic acid esterification over ion exchange catalysts. *The Canadian Journal of Chemical Engineering*, 74, pp. 493-500.

Yadav, G. D. and Joshi, A. V., 2001, Etherification of *tert*-amyl alcohol with methanol over ion exchange resin", *Organic Process Research and Development*, 5, pp. 408-414.

Yadav, G. D. and Thathagar, M. B., 2002, Esterification of maleic acid with ethanol over cation exchange resin catalysts. *Reactive and Functional Polymers*, 52, pp. 99-110.

Yang, Z. C., Cui, X. B. and Jing, G., 1998, Esterification-distillation of butanol and acetic acid. *Chemical Engineering Science*, 53, pp 2081-2088.

Yu, L. X., Guo, Q. F., Hao, J. H. and Jiang, W. J., 2000, Recovery of acetic acid from dilute wastewater by means of bipolar membrane electrodialysis. *Desalination*, 129, pp. 283-288.

Zhang, H., Mahajani, S. M., Sharma, M. M. and Sridhar, T., 2002, Hydration of cyclohexene with solid acid catalysts. *Chemical Engineering Science*, 57, pp. 315-322.

Zhang, Y., Ma, L. and Yang J. C., 2004, Kinetics of esterification of lactic acid with ethanol catalyzed by cation-exchange resins. *Reactive and Functional Polymers*, 61, pp. 101-114.

Zheng, Y., Ng. F. T. T. and Rempel, G. L., 2003, Process analysis for the production of diacetone alcohol via catalytic distillation. *Industrial and Engineering Chemistry Research*, 42, pp. 3962-3972.

Zundel, G., 1969, Hydration and intramolecular interaction: Infrared investigations with polyelectric membranes. Academic Press, New York.

## APPENDIX A

The work done has led to journal publications, of which the publication list is presented as follows:

1. Teo, H.T.R. and Saha, B., "Heterogeneous catalysed esterification of acetic acid with iso-amyl alcohol: kinetic studies", *Journal of Catalysis*, 228 , 2004, 174-182, ISSN 0021-9517.
2. Saha, B., Teo, H.T.R. and Alqahtani, A., "iso-Amyl acetate synthesis by catalytic distillation", *International Journal of Chemical Reactor Engineering*, 3 (A 11), 2005, ISSN 1542-6580.
3. Saha, B., Alqahtani, A. and Teo, H.T.R., "Production of iso-amyl acetate: heterogeneous kinetics and techno-feasibility evaluation for catalytic distillation", *International Journal of Chemical Reactor Engineering*, 3 (A 30), 2005, ISSN 1542-6580.

The work done has also led on to contributions in conference proceedings, of which the list is as follows:

4. Teo, H.T.R. and Saha, B., "Kinetics of cation exchange resin catalysed esterification of acetic acid with iso-amyl alcohol", *17th International Symposium on Chemical Reaction Engineering (ISCRE 17)*, Hong Kong, China, 2002, [CD-ROM].
5. Teo, H.T.R. and Saha, B., "Kinetics of catalytic esterification of acetic acid with iso-amyl alcohol over cation exchange resins", *International Symposium of Multifunctional Reactors (ISMR-3) Colloquium on Chemical Reaction Engineering (CCRE-18)*, University of Bath, UK, 2003, 117-120.
6. Teo, H.T.R., Alqahtani, A. and Saha, B., "Reactive distillation for synthesis of iso-amyl acetate", *7<sup>th</sup> World Congress of Chemical Engineering*, Glasgow, 2005, Paper 82458 (1-10 pages), [CD-ROM].
7. Alqahtani, A., Teo, H.T.R. and Saha, B., "Esterification of dilute acetic acid with iso-amyl alcohol: heterogeneous kinetics and measurement of residue curve map", *7<sup>th</sup> World Congress of Chemical Engineering*, Glasgow, 2005, Paper 82453 (1-10 pages), [CD-ROM].

## Appendices

8. Saha, B., Alqahtani, A. and Teo, **H.T.R.**, "Production of *iso*-amyl acetate: heterogeneous kinetics and techno-feasibility evaluation for catalytic distillation", ECI Conference on *CRE X - Innovations in Chemical Reactor Engineering*, Zacatecas, Mexico, 2005, Paper – 86 [CD-ROM].
9. Saha, B., Teo, **H.T.R.** and Alqahtani, A., "*iso*-Amyl acetate synthesis by catalytic distillation", ECI Conference on *CRE X - Innovations in Chemical Reactor Engineering*, Zacatecas, Mexico, 2005, Paper – 87 [CD-ROM].

## APPENDIX B

The other methods of analysing gas chromatography results are normalisation, normalisation with response factor, external standard and internal standard. Each of the analysis methods are detailed as follows:

### 1 Normalisation (Area %)

Calibration calculation:

None

Analysis calculation:

$$\%Conc_i = \frac{Area_i}{\sum_{i=1}^n Area_i} \times 100\%$$

Advantages:

- No calibration required.
- Simple calculation.
- Results independent of injection volume.

Disadvantages:

- All detected components are included in the calculation
- There is no allowance made for the response of each component to the detector.
- The results are expressed as a percentage of all components detected and not as absolute concentration.

## 2 Normalisation with response factor

Calibration calculation:

$$RF_i = \frac{Conc_i}{Area_i} \times \frac{Area_{REF}}{Conc_{REF}}$$

Analysis calculation:

$$\%Conc_i = \frac{(Area_i \times RF_i)}{\sum_{i=1}^n (Area_i \times RF_i)} \times 100\%$$

Advantages:

- Allowance made for the response of each component to the detector.
- Results independent of injection volume.

Disadvantages:

- All detected components are included in the calculation. Therefore, the calibration mixture must contain all components.
- The results are expressed as a percentage of all components detected and not as absolute concentration.

## Appendices

### 3 External standard

Calibration calculation:

$$R_i = \frac{Area_i}{Conc_i}$$

Analysis calculation:

$$Conc_i' = \frac{Area_i'}{R_i}$$

Advantages:

- Simple calculation.
- The results are expressed as absolute concentration i e. the units are the same as  $conc_i$  for calibration.
- The external standard is often used for gas analysis.

Disadvantages

- Injection volume must be constant.

#### 4 Internal standard

Calibration calculation:

$$RF_i = \frac{Conc_i}{Area_i} \times \frac{Area_{IS}}{Conc_{IS}}$$

Analysis calculation:

$$Conc_i = \frac{Area_i \times RF_i \times Conc_{IS}}{Area_{IS}}$$

Advantages:

- There is allowance made for the response of each component to the detector.
- The results are independent of injection volume.
- The results are expressed as absolute concentration.

Disadvantage:

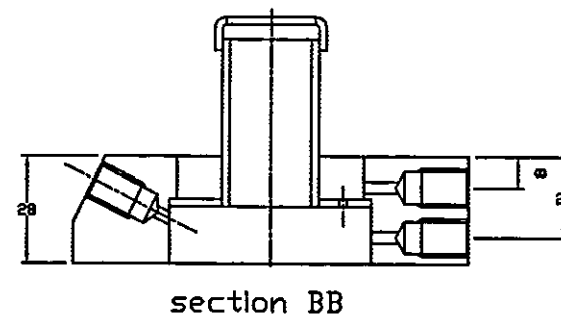
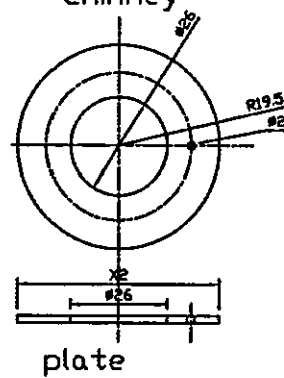
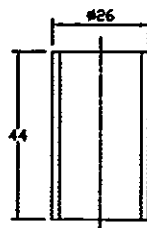
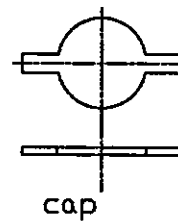
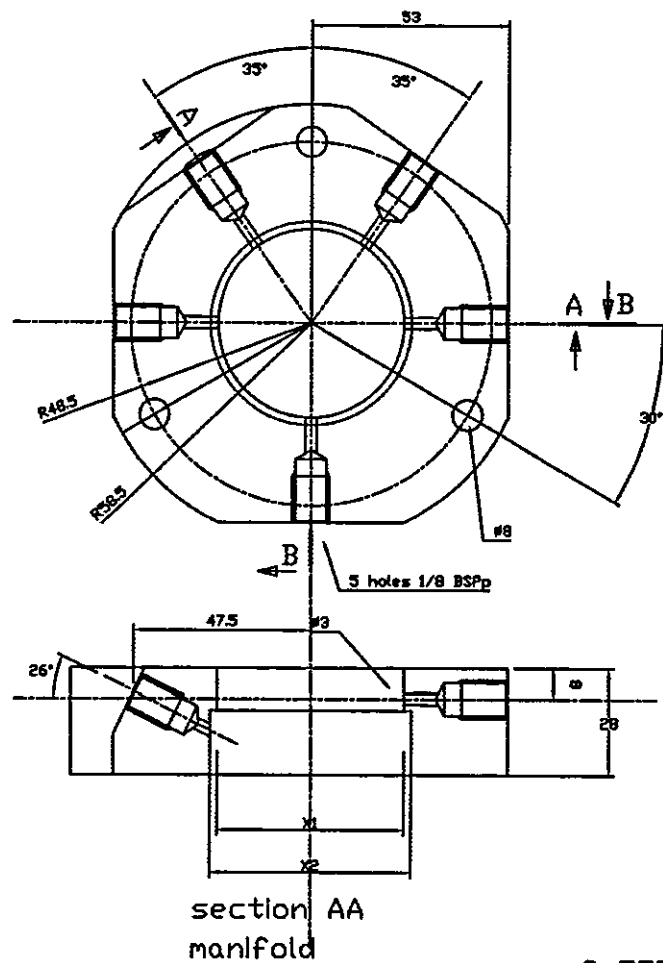
- The technique is not readily usable with gaseous samples.
- This technique requires the selection of a suitable internal standard.

**Appendix C: Cost estimation of RDC equipment**

Item	Unit cost (£)	Quantity	Cost
Glass vessel			432.76
PROPAK Distillation Packing (£/L)	83.40	5	417.00
KATAMAX	100.00	6	600.00
Purolite CT-175	0.00	0	0.00
LabVIEW software	500.00	1	500.00
Pumps	500.00	2	1000.00
Heating Tape	300.00	1	300.00
Total cost of RDC			3249.76
<b>Total purchase cost of major equipment item (PCE)</b>			3249.76
	<b>Factor</b>		
Equipment erection	0.45		
Piping	0.45		
Instrumentation	0.15		
Electrical	0.10		
Buildings, process	0.00		
Utilities	0.00		
Storages	0.20		
Site development	0.00		
<b>Total physical plant cost (PPC)</b>			7636.94
Design and Engineering	0.30		
Contractors' fee	0.00		
Contingencies	0.10		
Fixed capital			10691.71
Working capital (5% of fixed capital)			534.59
<b>Total investment required for RDC project</b>			11226.30
Annual operating costs			
Operating time	347		
Operating time (hours)	1734		

## Appendices

VARIABLE COSTS			
	Cost (£)	Quantity	Cost (£)
Raw material (acetic acid waste)	0		0.00
<i>iso</i> -amyl alcohol	8.75	540.93	4733.14
Miscellaneous materials (10% of maintenance)			53.46
Utilities			
Cooling water at 15p/ton for 10 kg/h	0.15	10	2.60
Power at 1.2p/MJ for 20 kWh	0.012	20	1497.96
Shipping and packaging			0.00
<b>Variable costs</b>			<b>6287.157</b>
FIXED COSTS			
Maintenance (5% of fixed capital)			534.59
Operating labour			10000.00
Plant overheads (50% of operating labour)			5000.00
Laboratory (30% of operating labour)			3000.00
Capital charges (10% of fixed capital)			1069.17
Insurance (1% of fixed capital)			106.92
Local Taxes			0 00
Royalties			0 00
<b>Fixed costs</b>			<b>19710.67</b>
<b>Direct production costs</b>			<b>25997.83</b>
Annual operating cost (rounded)			26000
<b>Summary</b>		<b>Actual</b>	<b>Rounded</b>
Investment costs (rounded)		11226.30	11500
Annual operating cost (rounded)		25997.83	26000
<b>Total</b>			<b>37500</b>



8 OFF STAINLESS STEEL

